University of Alberta

An Experimental and Theoretical Study of the Rate of Adsorption in Porous Media

by

Alistair S. Kirk

A thesis submitted to the Faculty of Graduate Studies and Research
in partial fulfillment of the requirements for the degree of

Master of Science

Department of Mechanical Engineering

Abstract

In the development of a numerical model for the water cycle on Mars, adsorption of water vapour in the Martian regolith acts as a significant sink and retards the transport of mass. Adsorption on Mars cannot be studied directly, so a numerical model was created, and a diffusion sorption experiment was devised using silica gel beads and water vapour to validate the model. In literature, the Local Instantaneous Equilibrium Adsorption (LIEA) assumption is often invoked, and here it is compared to a non-instantaneous form of the mass conservation equation, that uses a concentration dependent flux term to model the rate of adsorption. An analysis of the Damköhler number proves to be a reliable predictor of whether the LIEA assumption is appropriate. Adsorption is also shown to be strongly dependent on the porosity, and bulk density of the medium, as well as the temperature of the system.

Acknowledgements

The author would like to gratefully acknowledge the assistance of Dr. Zaher Hashisho and Dr. Masoud Jahandar Lashaki in obtaining the sorption data for the silica gel beads, Dr. Doug Schmitt and Randy Koffman for the use of their helium pycnometer and assistance with the solid density experiment, and the entirety of the Mechanical Engineering machine shop for all their hard work and instrumental advice. The author would especially like to thank Dr. Carlos Lange for his dedication as a supervisor and positive attitude throughout this work, and Dr. Marc Secanell Gallart and Dr. Janet Elliott for graciously donating their time and useful feedback during the defence.

Contents

List of Tables

List of Tables

List of Figures

List of Symbols

Latin symbols

C_f	Local Fluid Concentration	kg/m^3
C_{sat}	Fluid Concentration at Saturation	kg/m^3
d	Molecular Diameter	m
D_{ab}	Binary Diffusion Coefficient	m^2/s
D_{Kn}	Knudsen Diffusion Coefficient	m^2/s
Dm	Damköhler Number	1
J	Molecular Flux	kg/m^2-s
K	Permeability Coefficient	m^2
Kn	Knudsen Number	1
k_B	Boltzmann Constant = 1.380648 x 10^{-23}	J/K
L_C	Characteristic Length of a Porous Medium	m
M_i	Molar Mass	g/mol
p	Pressure	atm

p_c	Critical Pressure	atm
Pe	Péclet Number	1
p_{sat}	Saturation Pressure of Water Vapour in Air	Pa
p_{vap}	Partial Pressure of Water Vapour in Air	Pa
R_g	Universal Gas Constant = 8.3144621	J/K-mol
RH	Relative Humidity	1
T	Temperature	K
T_0	Reference Temperature = 273.15	K
T_c	Critical Temperature	K
$\vec{V}$	Velocity Vector	m/s
V_D	Darcy Velocity	m/s
w_{equi}	Equilibrium Adsorbed Mass Ratio	kg/kg
w_s	Time Dependent Adsorbed Mass Ratio	kg/kg

Greek symbols

α_{sf}	Fluid to Solid Phase Mass Transfer Coefficient	1/s
Γ	Langmuir Steady State Adsorbed Mass Coefficient	kg/kg
κ	Langmuir Coefficient	m^3/kg
λ	Mean Free Path	m
μ	Dynamic Viscosity	kg/m-s
ϕ	Total Porosity	m^3/m^3

List of Figures

ϕ_{inter}	Inter-particle Porosity	m^3/m^3
ρ_{α}	Component Mass Concentration	kg/m^3
ρ_{bulk}	Adsorbate Bulk Density	kg/m^3
ρ_{solid}	Solid Density	kg/m^3
τ	Tortuosity Factor	1
θ	Tortuosity	1

1

Introduction

1.1 Historical background

Humanity continually seeks to better understand the nature of the universe and its place in it, and inevitably this curiosity raises the question of whether life exists elsewhere. To begin trying to answer this question, one requires an understanding of the fundamental processes that govern not only the development of life on Earth but ostensibly the rest of the planets in our solar system and beyond. So far the strongest requirement for all known forms of life is the presence of liquid water, and naturally the exploration of our nearest celestial neighbours includes the search for the conditions and elements necessary for the development and sustainability of life.

Mars is the closest neighbouring planet that has been theorized to be capable of supporting life under certain conditions. The exploration of Mars has been accomplished with both orbiting and landed interplanetary probes, the most recent of landed probes being the Phoenix Lander Mission and the Mars Curiosity Rover. The Phoenix mission carried a Wet Chemistry Lab that performed aqueous analysis of Martian soil near the northern Martian pole. The presence of perchlorate salts, calcium carbonate, and aqueous minerals were detected with the instrument, and the formation of these compounds likely required the presence of liquid water[1, 2].

Today water exists primarily in the form of water-ice below the surface of Mars. The Martian polar ice caps while initially assumed to be pure water ice are now known to be a combination of CO_2 and water ice whose composition varies depending on the seasons and amount of CO_2 and particulate dust in the atmosphere. The Mars Odyssey Orbiter's Thermal Emission Imaging System monitored the seasonal sublimation of CO_2 ice for two years over large areas of the planet, and concluded from the thermal inertia and albedo that water ice is indeed present and stable for much longer terms than the CO_2 ice[3].

Subsurface water ice of 15 to 18 cm depth was found near the northern Martian pole by the Phoenix Lander robotic arm. The arm dug several small trenches in the local soil and the presence of water ice was inferred from the sublimation rate observed over several days, and later confirmed to be water when heated in the onboard mass spectrometer. Although the atmospheric pressure on Mars is near the triple point for water, it was concluded that the combination of salts, water ice, and percholrates as detected by the Wet Chemistry Lab meet the criteria for habitability during certain seasonal cycles either currently or in recent geological history [4].

Geological formations such as gullies and drainage patterns additionally suggest that liquid water existed in the Martian past [5, 6]. It has also been speculated that with water and volcanic activity in early Martian history, the planet could have been more conducive to early forms of life. When compared with current theories and evidence regarding planetary formation and the beginning of microbial life on Earth, the shallow seas and warm, CO_2 rich atmosphere, which was supplied with the necessary compounds from erupting volcanos could have provided an ideal environment for life to form on Mars.

Nisbet et al. [7] asserts that independent of whether life began on Earth, Mars, or some other nearby protoplanetary object, heavy meteorite bombardment during the first approximately 800 million years after the formation of the Moon, would have caused ejecta to have crossed to other inner planets promoting the evolution of life elsewhere. The conclusion that conditions on Mars in the past may have been amenable to life raises further questions about the type of life we would expect to find and how it would function in the current environment.

1.2 Motivation

The pervasive nature of life has become more evident recently with the search for extremophiles, organisms that thrive in extreme environments, here on Earth. Rothschild [8] covers a range of possible niches for life on Mars by analogy with Earth based organisms living in dry desert conditions, in frozen conditions near the polar caps, near oceanic hydrothermal vents, and endolithic organisms that live inside rock or porous minerals. Popa et al. [9] introduce the organism *Pseudomonas* sp. HerB which uses ferrous iron Fe(II) from the minerals olivine and pyroxene in its biological processes. The organism functions well in a low oxygen environment in the rock-ice interface in basalt on Earth, and because the surface of Mars is primarily composed of igneous rock similar to Earth basalt, the organism is an ideal candidate for an analogous Martian life form. On Earth, the rock-ice interface creates a zone of liquid water under certain environmental conditions.

The requirement for liquid water raises the question of where it would most likely be found on Mars, which necessitates an understanding of the physical processes involved in the Martian soil and the atmosphere. The presence of water vapour has been detected in the Martian atmosphere[10], indicating sublimation of the subsurface water ice, and the diffusion of water vapour through the fine top layer of soil known as regolith, and its eventual release into the atmosphere. There is also evidence that the water vapour condenses when the atmospheric temperature reaches its dew point and forms fog or light snow [11]. The water vapour can then diffuse back into the soil and lead to diurnal and seasonal change in the depth of the subsurface ice sheet.

Möhlmann [12] has shown from thermodynamic principles that a thin layer of water could exist sandwiched between the grain and mineral surfaces in the regolith, and the ice layers that build up in the porous soil structure. This finding is significant because the liquid layer is analogous to the interface seen in Earth basalt, where life has previously been found. By analogy, it is desirable to understand the conditions on Mars under which the liquid water could exist in the regolith, to find similar types of lifeforms.

Any understanding would require knowledge of the physical properties of the Martian regolith and ice-atmosphere interface, which may then be used in a model for the transport and phase change of water. Unfortunately the access to physical data on Mars is severely restricted to a limited number of sites and instruments, and it then becomes important to use well understood principles and analogous physical data on Earth to accurately model the transport of water vapour between the subsurface ice, the regolith and the basal atmospheric boundary layer. A sufficiently accurate model would be used to predict when and where liquid water may exist on Mars, and aid in the search for life in future missions.

1.3 The history and role of adsorption on Mars

In addition to the well known transport processes of advection and diffusion of water vapour in a porous medium, evidence from experiments performed on Earth and measurements made with the various interplanetary probes suggest that the physical process known as adsorption plays a significant role in the transport and storage of water vapour through the regolith. Adsorption is a process by which the working fluid, or adsorbate, adheres to the porous solid matrix, or adsorbent, through intermolecular forces and reaches an equilibrium with the local fluid concentration. The adsorbate is released by the process of desorption when the local fluid concentration is reduced or the local temperature increases.

Adsorption was conjectured to play a major role in the storage of water and CO_2 on Mars during seasonal and diurnal atmospheric processes, and the first estimates of the adsorbed quantites on a global scale were made using analogous Martian conditions and sorption data for both CO_2 and water vapour in pulverized basalt [13, 14]. Further preliminary investigations into adsorption were made after the Viking orbiter and probe missions measured seasonal variations in the concentration of atmospheric water vapour. Jakosky and Farmer [15] suspected a seasonal reservoir of water vapour for which the sorption process was responsible, but this conclusion could only be inferred from the existing data.

The early investigation of adsorption was on a global scale, and further research was required to understand the local water vapour concentrations in the diurnal basal atmospheric boundary layer as measured by the Phoenix Lander. Jakosky et al. [16] developed a soil-atmosphere interaction model which was quantitatively consistent with the exchange of a significant amount of water vapour between the regolith and the atmosphere, but highlighted the need for measurements and models for the near surface which depend on the local water vapour density and diffusive and adsorptive properties of the regolith. Work was then proceeded by others that continued to develop soil-atmosphere interaction models [10, 17–19].

Sears and Moore [20] attempted to further define the water vapour exchange process in terms of the sublimation rate of water from ice samples in a CO_2 chamber that replicated the atmospheric pressure on Mars. The chamber measured temperature, pressure and humidity at discrete points in the experiment by using thermocouples, transducers and hygrometers. The sublimation rate of the samples through simulated Martian regolith was also measured by using a mass balance. The results appeared to agree with previous investigations of sublimation rates under Martian conditions, only differing in the method used to account for the decreased buoyancy due to the reduced gravity on Mars.

The experimental setup and results were later used in Chittenden et al. [21] in an attempt to account for the increased sublimation rate due to advection expected by the winds on the Martian surface. While the experiments and models from these works acknowledged the dependence of the sublimation rate on temperature, regolith depth and wind speed, the semi empirical approaches were only applicable under similar conditions. The models could only be used to predict the steady state sublimation rate typically assumed in a horizontally homogeneous, or one dimensional system.

Chevrier et al. [18] continued the development of the sublimation models and investigated the dependence of water vapour transport on not only atmospheric conditions but also the structure of the regolith including the depth of the surface layers, the porosity of the medium and the average grain size. A similar experimental setup to Sears and Moore [20] was used, however the mass difference of the regolith was also measured before and after the experiment by baking the vacuum chamber in an oven with the intent of understanding the sorption processes. The mass difference confirmed the significant effect of water vapour adsorption in the simulated Martian regolith and also suggested that the simultaneous adsorption of CO_2 could interfere with the adsorption of water as the available adsorption sites in the regolith would be occupied by the CO_2.

The adsorption theories originally proposed by Langmuir [22] and later improved by Brunauer et al. [23] provide a means of describing the adsorptive capacity of porous materials. The steady state capacity of an adsorbent is typically determined over a range of discrete local fluid concentrations, where each point represents the adsorbed concentration as it exists in equilibrium with the local fluid concentration. The equilibrium condition is analogous to the law of mass action in Chemistry, where the rates of adsorption and desorption are equal over a long enough time average. The molecular forces are usually many orders of magnitude stronger than any other molecular transport processes, and sorption may be considered instantaneous when the local fluid is in sufficiently close proximity to the adsorbent surface [24–26].

These static systems work well for describing the steady state conditions of adsorbate/adsorbent pairs, when the adsorbate is proximal to the adsorbent, however in most porous media the adsorbate must travel to the adsorption sites in the adsorbent. The time dependent, or kinetic rates of adsorption, were not accounted for in the early sublimation models for Mars. Chevrier et al. [18] and others [10, 17] present a one dimensional model that incorporates the kinetic effects of adsorption using rate constants that were found by using experimental data under Martian conditions.

While the model of Chevrier et al. [18] appeared to agree with the experiment, the empirical rate constants convey little understanding of the physical processes involved with adsorption, and the one-dimensional formulation is limited in application. Their experiment also only considered a fine grained montmorillonite clay to simulate the Martian regolith. The empirical rate constants and adsorptive capacities were then specific to that combination of adsorbent/adsorbate pair, and temperature.

The most recent kinetic adsorption model given by Beck et al. [17] measured six different sets of simulated regolith at a temperature of 243 K. The experiment consisted of an environmental chamber to monitor adsorption and diffusion of water vapour through each regolith sample under expected Martian atmospheric conditions. The water vapour source was an ultra pure, demineralized, and carefully out-gassed volume of liquid water at a controlled temperature of 293 K. The vapour concentration at the upper surface of the regolith was measured using a bidirectional reflectance spectrometer.

Beck et al. [17] found kinetic rate constants for adsorption using Langmuir adsorption theory, and large variations in the rates were found between samples, which implied a strong dependence on the geological properties of the regolith. The influence of sample depth was also investigated and showed that even for thin samples, diffusive transport through the soil affected the adsorption rates. Therefore, consideration must be given to the physical properties of the adsorbate, and the simultaneous transport mechanisms involved in porous media, which can affect the net rate and quantity of adsorbed water vapour in the regolith on Mars.

1.4 Present work

The CFD Lab at the University of Alberta is attempting to create a numerical model of the Martian water cycle for the regolith/atmosphere interface, with recent work by Chen [27] focusing on the momentum transport of water vapour due to dust devils on Mars and its effect on transport in the regolith, and that of Zubik [11] who developed a numerical model to account for the effect of thermo-diffusion of water vapour in regolith, and to model the sublimation and deposition of water vapour in the form of fog, immediately above the regolith.

The work of Chen [27] and predecessors [28] used an experiment with a vortex generator situated above a porous polyurethane foam, where the foam overlayed a vat of distilled water. A vortex was generated under standard Earth atmospheric conditions, and temperature and relative humidity sensors were used to monitor the water vapour transport through the foam. The experiment was used to validate their numerical models of the advective and diffusive transport of water vapour through a porous medium, which would later be used to model the effects under Martian conditions.

The data from these experiments showed an appreciable resistance to the diffusion of water vapour through the porous foam which was attributed to adsorption. The effect was not accounted for in their final numerical models, and was avoided by allowing the foam to reach equilbrium with the water source before the experiment began.

The long term goal of the CFD Lab is to produce a numerical model that simulates all significant physics and transport processes for water on Mars. The consideration of adsorption is crucial to completing a comprehensive model that will eventually be used to predict the locations that are most conducive to life, either under present Martian atmospheric conditions or perhaps also under those found in its geologic past. This work will attempt to further the understanding of the adsorption process and to incorporate the effect in a three dimensional, time dependent numerical framework.

2

Theory

The following Chapter outlines the theory behind species transport and adsorption in porous media. The development of a time dependent numerical model of water vapour transport and adsorption in porous media builds from a static theory of adsorption. The theory of adsorption under equilibrium conditions is introduced, followed by a discussion of geometry in porous media, and its importance for dynamic models of adsorption. Finally, transport mechanisms in porous media are reviewed and a numerical model is proposed which combines a dynamic theory of adsorption and species transport in porous media.

2.1 Adsorption

2.1.1 Overview

The phenomenon known as adsorption is a process in which an adsorbate molecule adheres to the surface of an adsorbent host. The adherence is theorized to be the result of the equilibration of molecular forces between the adsorbate and adsorbent. These forces may be described in terms of the potential energy of the interacting molecules, which is dependent on the system's molecular interaction parameters and the distance between molecules[29], and according to the principle of minimization of total potential energy, the additive potential energies in a closed system are minimized when the system is in equilibrium.

Discrete sources of potential energy can be both positive and negative and may be added to find the total potential energy of a given system. The sources may be categorized as the result of attractive, or London dispersion forces, and the repulsive electrostatic forces arising from dipoles, quadrapoles, and induced polarization between adsorbent and adsorbate molecules. When adsorbent and adsorbate molecules interact, the pairwise addition of all potential energies is lower than the initial condition, which results in a minimized or equilibrium state.

The reduction in total potential energy necessitates a loss of energy in the form of heat as entropy is increased. The process of adsorption has been shown experimentally and through thermodynamic principles to be exothermic, and can be explained as a reduction in the degrees of freedom of movement for the adsorbate molecules. The heat is then dissipated through the adsorbate, and adsorbent [25], and this loss of energy is termed the isosteric heat of adsorption[29]. It is important to note that any chemical reactions between adsorbate and adsorbent are typically neglected when defining adsorption, and it is then understood to be a purely physical process.

2.1.2 Langmuir Static Adsorption Theory

The investigation of adsorption historically began in the early 20th century with Langmuir [22], where the adsorption of a gas phase on a planar surface was extrapolated from the theory of ideal gases. Simple mechanisms were proposed that related the local gas concentration to the adsorbed concentration. The equilibrium theory proposed by Langmuir [22] rests on the assumption that a monolayer of adsorbate molecules forms on the surface of the adsorbate with the following corollaries[26]:

- The adsorbed molecules do not interact with other adsorbed members
- The energy of adsorption is equal over the entire surface and no preferential adsorption sites exist.
- Once the molecules have adsorbed there is no migration to other sites.

For low concentrations of adsorbate in the surrounding local fluid the behaviour of adsorption could be described by the well known linear relationship known as Henry's Law for liquid and gas equilibrium[26]:

$$w_{equi} = K\frac{C_f}{C_{sat}} \tag{2.1.1}$$

where the equilibrium adsorbed mass ratio w_{equi} is related to the local fluid concentration C_f by the linear coefficient K. However Langmuir [22] discovered through his experiments that for increased local fluid concentrations the equilibrium relationship described by 2.1.1 was inaccurate and proposed the following non-linear relationship to model a larger range of local fluid concentrations:

$$w_{equi} = \Gamma\frac{\kappa C_f}{1+\kappa C_f} \tag{2.1.2}$$

where Γ is a coefficient that represents the adsorbed concentration when all adsorption sites have been filled, and along with the coefficient κ, is obtained from linear regression of adsorption equilibrium data. The equilibrium data are generated by measuring the steady state mass of an adsorbent in a temperature controlled chamber at different adsorbate concentrations in the surrounding fluid.

In a typical experiment to generate equilibrium data, the adsorbate concentration in the chamber is maintained at a specific level until the mass increase of the adsorbent has stabilized. At this point the adsorbent has adsorbed as much of the adsorbate as permitted by the system. The adsorbate concentration is then increased and held constant in the surrounding fluid in the chamber, and the process is repeated until the local fluid has reached saturation of the adsorbate. The equilibrium data is then fitted with a curve whose constants are used in an isotherm equation such as 2.1.2. Alternative isotherm fitting curves may be applied for more complex adsorption behaviour, such as multilayer adsorption and surface diffusion which violate the basic assumptions of the Langmuir isotherm[25] [26].

The general form of Equation 2.1.2 has been normalized and graphed for varying values of κ and Γ in Figure 2.1. The abscissa is normalized by the maximum local fluid concentration for a given system, and may alternately be represented by a partial pressure normalized with the saturated vapour pressure in the case of adsorption of a given gas on an adsorbent. The ordinate is normalized by the mass of adsorbent in the sample.

In analogy to Le Chatelier's principle of chemical equilibrium, the temperature of the adsorbate/adsorbent system must remain constant while in equilibrium, as an increase in temperature would reduce the activation energy required for the molecules to desorb from the surface, resulting in new constants to describe

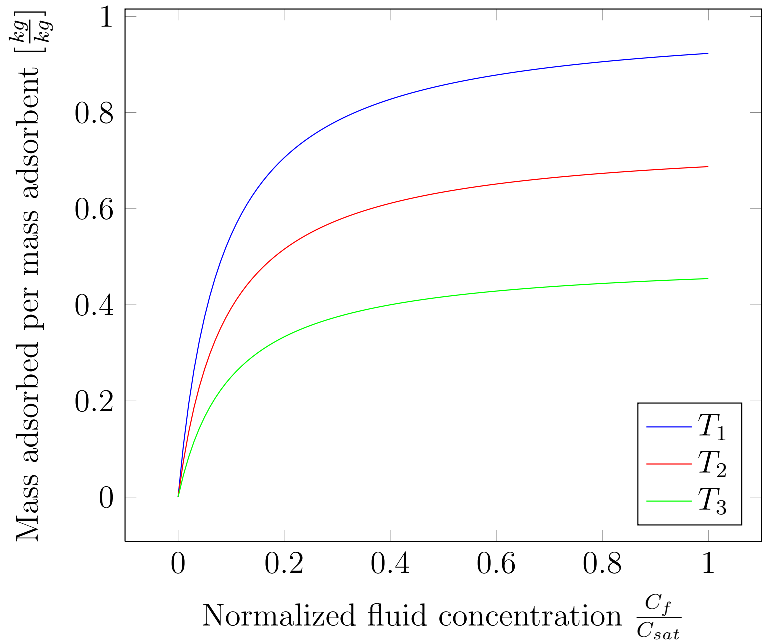

Figure 2.1: *Typical isotherms for a given adsorbent/adsorbate pair*

the state of equilibrium. The generic Langmuir isotherms in Figure 2.1 show that for an increase in temperature the quantity adsorbed for a given local fluid concentration is reduced as the steady state temperature is increased. The temperatures are related as $T_3 > T_2 > T_1$.

Due to the isosteric heat of adsorption, no adsorbent/adsorbate system is ever completely isothermal. However if the timescales of mass transport are much larger than those for heat transfer, such as in a steady state, temperature controlled system, then the effects of non-isothermal behaviour on the adsorbed quantities may be neglected. This approach is valid for the static study of adsorption where the steady state adsorbed concentration may be predicted from empirically generated isotherms given the temperature and local fluid concentration[25].

2.1.3 Extended Static Adsorption Isotherms

The assumption in Langmuir adsorption theory that only a monolayer of adsorbate may form on an adsorbent is generally applicable only for highly adsorbing materials and then only up to a certain local fluid concentration. The work of Brunauer et al. [23] expanded on Langmuir's static adsorption theory to include the adsorption of additional layers, known colloquially by the authors' initials as BET adsorption theory. In Figure 2.1 the adsorption isotherms display a concave curve with respect to the abscissa, in the low to middle concentration region, indicating asymptotic filling of the available adsorption sites. However Brunauer et al. [23] discovered that at higher concentrations a convex curve would then occur, which they proposed was due to capillary condensation in micropores that were impenetrable at lower concentrations, and to the buildup of multiple layers of adsorbate. BET adsorption theory thus allowed the modelling of more complex adsorption isotherms over Langmuir static adsorption theory, even though they restricted themselves to a qualitative interpretation.

BET theory allowed the classification of different types of isotherms encountered with common adsorbate/adsorbent pairs. Brunauer et al. [30] formalized the classification of adsorption isotherms as shown in Figure 2.2, where the historic Langmuir isotherm is known as Type I. The Type II isotherm was the form derived by BET theory and illustrates the effect of capillary condensation in the micropores, which occurs after the adsorption sites with stronger affinity have been occupied by adsorbate, and multiple layers of adsorbate have accumulated. The Type III isotherms may be interpreted as predominantly due to capillary condensation in micropores, and either weak interaction forces between adsorbent and adsorbate, or that the adsorbate is primarily composed of micropores [30].

Type IV and V isotherms address multilayer adsorption and enhanced capillary

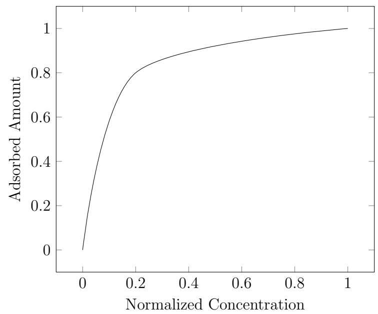

(a) *Type I*

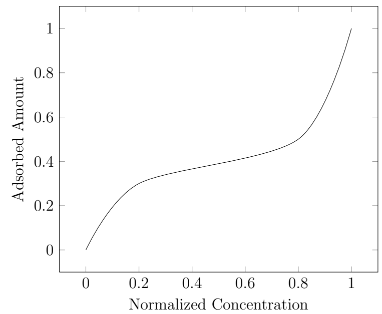

(b) *Type II*

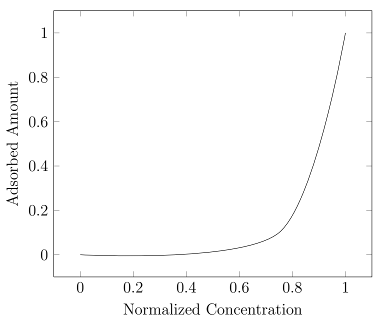

(c) *Type III*

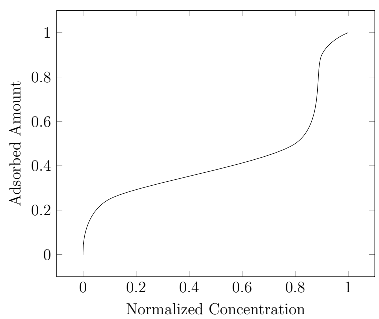

(d) *Type IV*

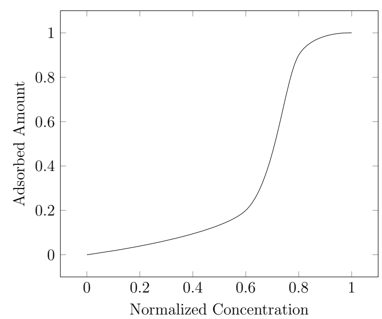

(e) *Type V*

Adapted with permission from Brunauer et al. [30]. Copyright 1940 American Chemical Society

Figure 2.2: *BET Classification of Isotherms*

condensation in the micropores. The plateau in adsorption at the high end of local fluid concentration is theorized to be caused by the completion of filling of micropores, and the absence of macropore filling. The binding energy of the final layers of adsorbate in a micropore are higher than those that preceded it due to the additional interaction with other adsorbate molecules in a filled capillary. The higher binding energy makes it more difficult for the molecules to desorb back into the gas phase[25].

Burgess et al. [31] asserts that capillary condensation occurs when multiple layers of adsorbate have built up during adsorption, and the top most layers develop fluid behaviour and exhibit surface tension. The capillary filling of the pores may then take place with a dependence on relative sizes between

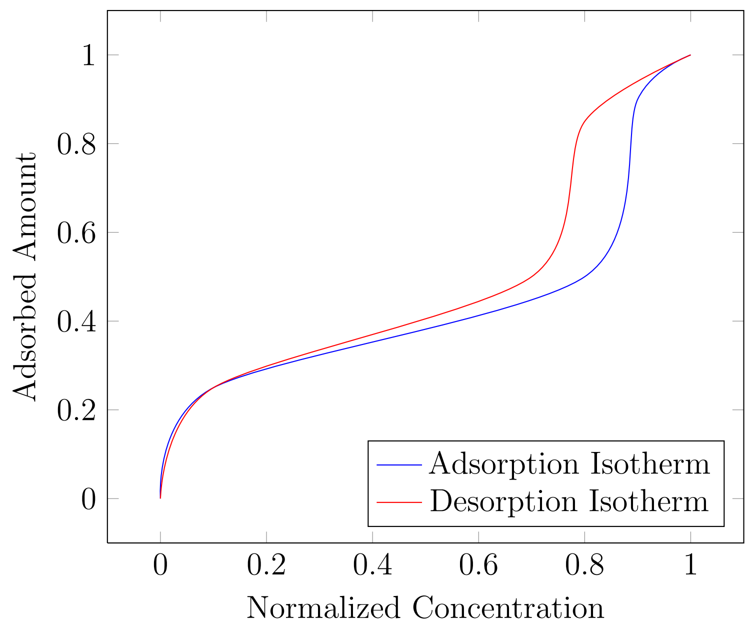

Figure 2.3: *Adsorption/Desorption Hysteresis*

adsorbate and pore width. The temperature of the adsorbate also affects the capillary condensation, whereby if the local fluid temperature surpasses a critical temperature, the distinction between liquid and vapour is non-existent and the surface tension, and thus the capillary filling mechanism, is eliminated.

The enhanced binding energy of surface layers of adsorbate in micropores, and the presence of surface tension in a liquid like state leads to an important consequence. During a desorption process, where the local fluid concentration is reduced from saturation and a desorption isotherm is created in the same manner as an adsorption isotherm, hysteresis may occur and the new adsorbed mass at equilibrium for a given local fluid concentration is higher than that predicted by the adsorption isotherm. This phenomenon is illustrated in Figure 2.3.

To develop any kinetic model where the local fluid concentration may both increase and decrease, an understanding of the mechanisms of the adsorption and desorption over the entire range of local fluid concentration is required.

The mechanisms of static adsorption and desorption are directly related to pore geometry and thus the isotherms generated from static equilibration experiments give insight to the structure of the porous medium and its effects on adsorption.

2.2 Pore Geometry

The pore geometry in a given porous medium serves as a basis for understanding the transport mechanisms within. The pore shape and width can be used to estimate void volume and available surface area, and to provide an estimate of the flux components from first principles. A simple geometry is assumed to represent the pores and is dependent on the type of analysis used to estimate volume and surface area, and also on the model of the underlying atomic structure.

A cylindrical pore shape may be selected for activated oxides and the pore width then refers to the diameter of the cylinder. In the case of activated carbon and clays, a slit structure is typically assumed where the pore width is measured as the distance between infinitely parallel sheets of adsorbent. Aggregate media, such as zeolites and silica gel, have pore spaces that result from the void between solid spheres or other particles that constitute the aggregate. In reality the pore geometry in complicated structures may be difficult to define as the connections between pores, and closed or dead end pores are neglected in the simplified pore models, and a given medium could consist of a range of pore widths. Concepts such as tortuosity, fractal geometry, and percolation theory[32] have been introduced to the simplified models to better approximate the complexity of porous media found in nature [33].

As a unified starting point in the discussion of pore sizes and their distributions, Rouquerol et al. [33] defined the IUPAC classification of pore sizes corresponding to the following regimes:

- Micropore width less than 2 nm
- Mesopore width between 2 nm and 50 nm
- Macropore width greater than 50 nm

The pore size distribution (PSD) for meso and micro porous materials can be measured by analyzing the adsorption of nitrogen at its boiling point of 77 K. The isotherm for nitrogen adsorption is assembled from equilibrium mass measurements at discrete intervals of pressure, where the quantity of nitrogen involved in filling of the pore is estimated from the assumed pore geometry and a constitutive equation to describe the filling process. The constitutive equation may be a simplified relation such as the modified Kelvin equation[34], or an empirical relation such as those given in the Dubinin et al. experiments reviewed by Do [25], which describe the concept of micropore filling well but perform poorly in the low pressure range.

The development of quantum mechanics and non-local density functional theory (DFT) has led to the creation of PSD's using nitrogen adsorption data which is favoured for its accuracy in describing mesopore capillary condensation, and the transition to micropore continuous filling. Non-local DFT can assume a slit pore configuration for carbonaceous materials, or cylindrical/-spherical for siliceous materials such as silica gel and porous glass. The assumed geometry is used with the nitrogen adsorption isotherm data by fitting a correlation function to the isotherm. The correlation function is dependent on pore width and allows the generation of a pore size distribution[35]. Automated machines manufactured by Quantachrome (*Boynton Beach, USA*) use non-local DFT to generate the PSD data, and estimate the incremental pore volume change due to nitrogen filling.

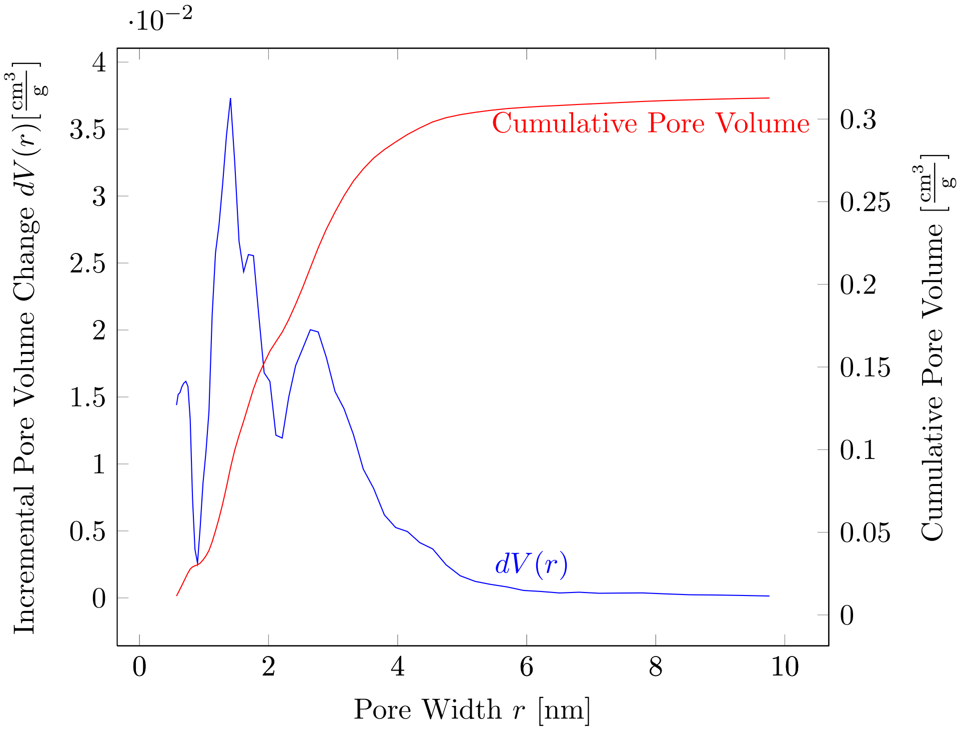

Figure 2.4: *Typical Pore Size Disribution derived from N_2 adsorption*

A typical PSD curve generated by the Quantachrome nitrogen adsorption analysis of silica gel, is shown in Figure 2.4. There is a prevalence of micropores in the sample of silica gel, with an average width on the order of 1-2 nm, and a similar quantity of mesoporous volume for pore widths greater than 2 nm. The geometry of the pores aides in applying the appropriate flux mechanisms when modelling transport, for example the ratio of microporous to mesoporous volume may be used to estimate the tortuosity and effective diffusion coefficients in the consolidated porous media[36].

Other experimental methods may be used to determine the PSD, such as mercury intrusion porosimetry, which is commonly used only in the macro and meso porous regimes. León y León [37], however, recommends to use mercury porosimetry to further characterize porous media beyond its common application, such as to produce estimates of the tortuosity, fractal dimension, surface area and compressibility.

Mercury intrusion is limited however to materials that do not collapse under high pressure. The calculated lower limit of resolvable pore sizes in mercury porosimetry is on the order of 3 nm and would not be applicable for microporous PSD generation.

Gas adsorption using helium may also be used to characterize the micropore regime due to its inert nature, and the virtue of its small van der Waals radius and ability to penetrate smaller geometry. A PSD from helium adsorption data may be combined with data from mercury intrusion porosimetry to develop a complete picture of a given porous medium[37][33].

The intrinsic nature of the porous media, and thus transport mechanisms, may be interpreted from the PSD even if the underlying assumptions about the geometry are not entirely accurate. Lastoskie et al. [35] gives a comprehensive discussion on the limitations of non-local DFT, and the sensitivity of the results to the underlying assumptions in developing the theory. It is the intent of this work to develop a preliminary understanding of the internal pore geometry of the silica gel adsorbent used in the experiment, from which a numerical model of species transport may be made.

2.2.1 Consolidated vs. Unconsolidated Porous Media

Porous media may be broadly considered as either consolidated or unconsolidated material, where consolidated material consists of rigid bodies with an average pore dimension many orders of magnitude smaller than the macro scale media. Some examples of which are sediment such as sandstone, zeolite particles, and clays where the pores are a result of imperfect crystalline structure. Unconsolidated media may be considered as a packed aggregate of particles. The particles in an aggregate may also be porous, however the larger pore volume available for species transport in unconsolidated media can lie in the inter-particle void space. The understanding of relative scale between the solid media and the pores is important for understanding adsorption and the dominant transport mechanisms in a given medium[33].

Due to the lack of qualitative measurements of the properties of the regolith on Mars, substitute materials have been used on Earth to simulate the regolith. Seiferlin et al. [38] describes the analogous porous media found on Earth commonly used as simulants for Martian regolith. The earliest simulant known as JSC (Mars-1) was developed from raw material mined from a cinder cone in Hawaii, and was selected due to its spectral and chemical similarity to Martian regolith. Recently another regolith simulant known as Salten Skov used by European planetary researchers serves as an analogue of Martian dust, due to its high level of red iron oxides and similar grain size. Seiferlin et al. [38] notes that while some properties of the Martian regolith are replicated with the simulants, properties such as porosity, grain size, and bulk density differ significantly between measurements obtained from the Viking lander probes and the soil simulants.

Bell et al. [39] analyzed spectral signatures of soils on Mars from the Pathfinder probe and suggests that the regolith is composed of poorly crystalline ferric oxides, mixed with coarser grained, and slightly compacted silicates high in magnesium and iron. The physical nature of the Martian regolith is that of a fine grained aggregate of sand or dust particles, and the regolith may be considered an unconsolidated porous medium. The aggregate particles may also be porous due to their poor crystalline structure.

Silica gel is a common desiccant composed of silicon dioxide and is used in the food and packaging industry to regulate humidity. During manufacturing the silica gel is pressed into beads to form consolidated porous media with pore widths in the micro and meso pore regimes, and an image of the beads may be seen in Figure 2.5. The beads may then be stacked together to form

Figure 2.5: *Silica gel bead dessicant*

an unconsolidated aggregate porous media that consists of inter-particle and intra-particle void space.

A 20x magnified view of the surface of a silica gel bead in Figure 2.6 shows the consolidated porous media that constitutes the bead, and the inter-particle void space between two beads on the right of the image. The combination of consolidated and unconsolidated porous media of the stacked silica gel beads are physically analogous to the Mars regolith albeit at a different scale, and serve as a starting point in understanding the transport and adsorption of porous media to be used in future research.

When modelling transport of species in this particular porous media, the mass is expected to move through the inter-particle void space, and also into and through the various pore regimes in each silica gel bead. The transport of mass into the porous bead is a source of significant resistance and must be considered when developing a transient numerical model for mass transport

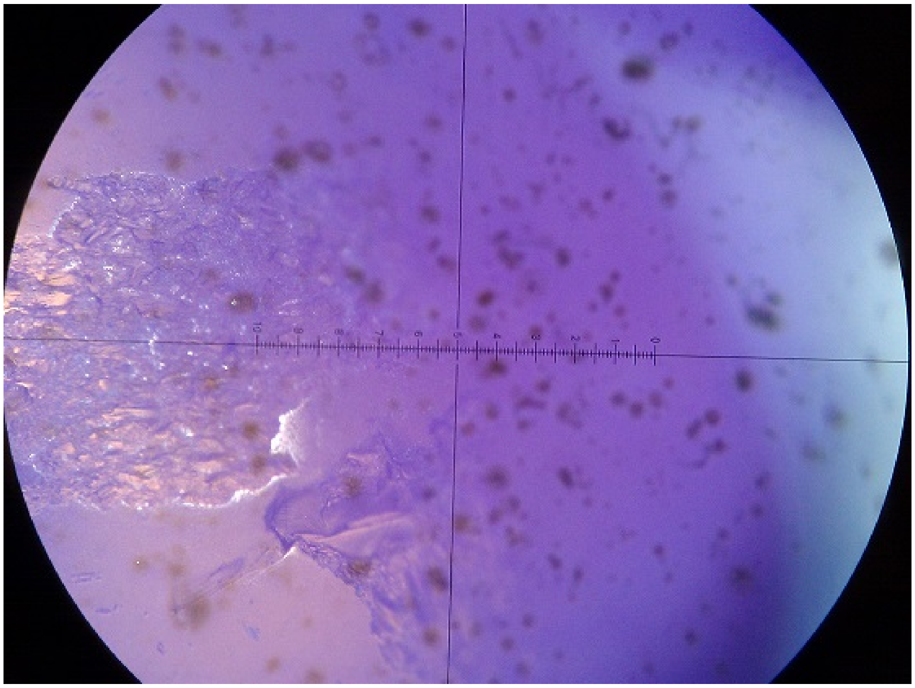

Figure 2.6: *Magnified view of silica gel beads*

through this type of porous medium.

It should be noted that the alternative storage mechanism known as *ab*sorption, may be encountered when using silica gel beads. The water vapour may diffuse into the silica gel solid structure, in addition to adsorption on surfaces and as a liquid in the pore space. The term *sorption* as used in this work henceforth acknowledges the potential for *ab*sorption to occur in silica gel, in addition to *ad*sorption.

2.2.2 Porosity

Porosity is defined as the volumetric fraction of pore space relative to the total volume:

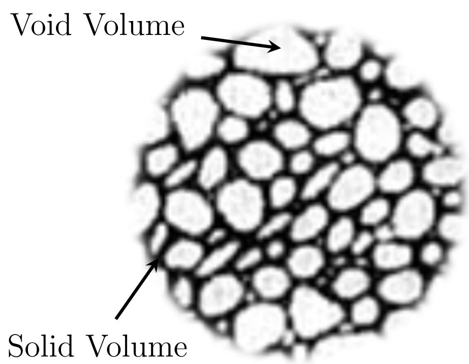

(a) *True consolidated media*

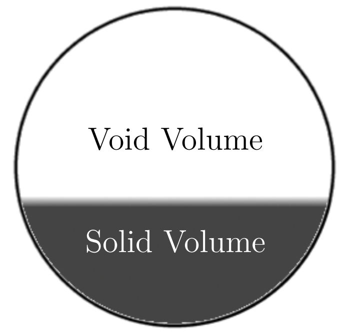

(b) *Simplified model*

Figure 2.7: *Porosity in consolidated media*

$$\phi = \frac{V_{pores}}{V_{total}} \tag{2.2.1}$$

where V_{pores} is the volume of the void space, and V_{total} is the total control volume, and ϕ is the total porosity. The porosity of consolidated porous media can be visualized with a simplified model as shown in Figure 2.7, which aides in understanding the relative volumes in unconsolidated media.

In unconsolidated porous media as found in the Martian regolith and silica gel beads, the aggregate particles may individually be considered consolidated porous media with an internal or intra-particle void volume. The intra-particle void volume adds to the inter-particle void volume to define the total void volume. The total void volume may then be used in Equation 2.2.1 to define the total porosity. The distinction between volumes is shown in Figure 2.8.

The total porosity may alternatively be defined by:

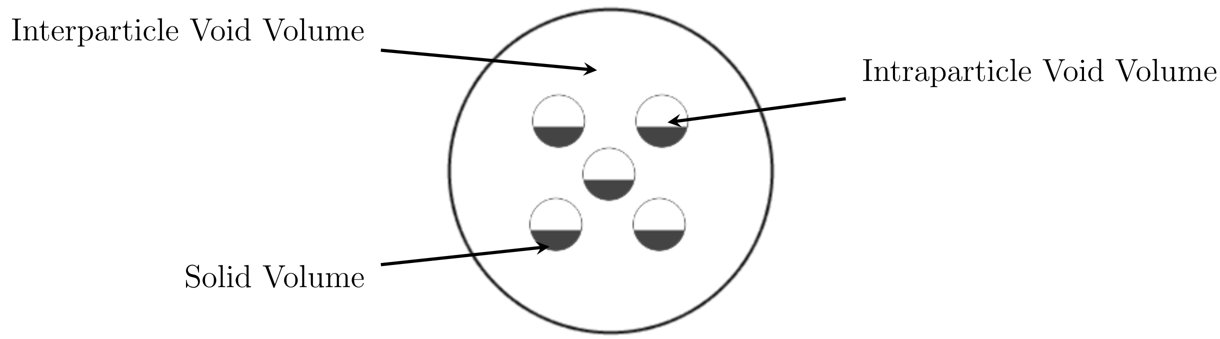

Figure 2.8: *Porosity in unconsolidated media composed of aggregate particles*

$$\phi = 1 - \frac{\rho_{bulk}}{\rho_{solid}} \tag{2.2.2}$$

where ρ_{bulk} is the bulk density of the porous media, and ρ_{solid} is the density of the solid material. The bulk density can be estimated by measuring the mass of the media in a container of known volume, and the solid density can be estimated from fluid displacement measurements, also known as pycnometry.

The measurement of solid density by helium displacement is often used, and it is assumed that the helium does not adsorb on the surface of the sample being measured, and also that any closed pores which are inaccessible by the helium do not significantly contribute to the total pore volume[33]. Malbrunot et al. [40] discusses the effect of adsorption in helium pycnometry for a variety of adsorbents including silica gel, and suggests that adsorption of helium in silica gel at room temperature can be a significant source of error when used to calculate the solid density. They recommend performing helium pycnometry analysis at the adsorbent regeneration temperature to eliminate the effect of adsorption.

By measuring the bulk density and solid density of any porous medium, an estimate can be made of the total porosity. The porosity found with this method includes both the intra-particle and inter-particle void volume, and is used to modify the coefficients used in transport equations. Dead end and closed/inaccessible pores, and the adsorption of helium in the pycnometry method are sources of error that are typically ignored in the case of silica gels[41, 42], but are noted for future reference and discussion.

2.2.3 Tortuosity

The tortuosity is a concept that describes the ratio of the average pore length in a parallel capillary model, to the length of the porous medium in the direction of transport. Epstein [43] explains the derivation of the tortuosity starting from the Hagen-Poiseuille equation for laminar flow in a parallel capillary, and notes an important corollary: that there is considerable confusion in the literature when distinguishing between the foundation of the tortuosity concept, and the use of a tortuosity factor when modifying transport coefficients.

The tortuosity factor τ is the square of the tortuosity θ, and is used with the porosity to account for the deviation of the transport path in a pore from the straight line capillary by modification of the free diffusion coefficient D_{ab}, to create an effective diffusion coefficient D_{eff}:

$$\frac{\phi}{\theta^2} D_{ab} = \frac{\phi}{\tau} D_{ab} = D_{eff} \tag{2.2.3}$$

The diffusion coefficient is used in Fick's law of diffusion to describe diffusive flux as explained later in Section 2.3.2.

Due to the structural complexity of natural porous media, the tortuosity is often an empirically estimated parameter that provides a bridge between the simple parallel capillary flux model and the true complex pore networks in porous media.

Boudreau [44] reviewed several common, empirically derived relationships to estimate the tortuosity factors in fine grained un-lithified sediments using only the porosity as an input parameter, and proposed a new relation which shows good agreement between the estimate and measured tortuosity values. The tortuosity factor may be initially estimated with the following relationship:

$$\tau = 1 - \ln(\phi^2) \tag{2.2.4}$$

Equation 2.2.4 provides a better estimate of the tortuosity in fine grained sediment than the relations proposed by other researchers, however the empirical relation lacks a theoretical basis[44]. The tortuosity can also be obtained by measuring the effective diffusive flux, D_{eff}, in a steady state system and using the porosity in 2.2.3 to isolate the tortuosity factor τ, as seen in Prieto [28], Hudson [45].

2.3 Transport Mechanisms in Porous Media

Mass transport models can be developed using known transport mechanisms and assumed pore structure, with appropriate modifications to account for the complexity of the pore geometry. In general, the flux of a species through a control volume can be due to diffusion or advection, and the mathematical models used to simulate the effect in a porous medium depend on the fluid properties, energy of adsorption, and the relative size of the pores to the fluid mean free path.

2.3.1 Knudsen Diffusion

The mean free path of a molecule in an ideal gas, λ, is the average distance travelled between collisions and can be described by following relation[46]:

$$\lambda = \frac{k_B T}{\sqrt{2}\pi d^2 p} \tag{2.3.1}$$

where k_B is the Boltzmann constant, d is the diameter of non-attractive molecules, at absolute temperature T and pressure p. The kinetic theory of gases can then be used to describe the motion of molecules through a parallel capillary, when the mean free path is much larger than the pore width and the diffusion of the molecules is dominated by collisions with the walls and not other gas molecules. The non-dimensional Knudsen number provides a description of whether transport due to Knudsen diffusion is active in a porous medium and is given by[25]:

$$\mathrm{Kn} = \frac{\lambda}{d_{pore}} \tag{2.3.2}$$

If the Knudsen number is much less than unity, molecular collisions dominate and Knudsen diffusion is inactive. This regime, which is usually limited to Kn< 0.1, can be described using continuum mechanics, Fickian diffusion, and fluid viscosity.

If the Knudsen number is on the order of unity then the velocity at the walls is non-zero and is in the so called viscous slip regime, where continuum mechanics requires the application of correction factors to the viscosity when modelling gas flow and transport processes[47].

Finally, if the Knudsen number is much greater than unity, then wall collisions dominate and the kinetic theory of gases needs to be applied to model the flux.

Do [25] derived an equation to model the flux due to Knudsen diffusion in a porous medium, which assumes that the pore takes the shape of a long cylindrical capillary:

$$J_{\mathrm{Kn}} = -D_{\mathrm{Kn}} \nabla C \tag{2.3.3}$$

where the Knudsen Diffusion Coefficient D_{Kn} is defined in terms of the molar mass of the diffusing gas species M_i, the radius of the capillary r, the universal gas constant R_g, and absolute temperature T:

$$D_{Kn} = \frac{2r}{3}\sqrt{\frac{8R_gT}{\pi M_i}} \tag{2.3.4}$$

An evaluation of the Knudsen number using the mean free path λ and the assumed pore diameter d_{pore} can provide an estimate of the contribution of Knudsen diffusion to the transport of mass in porous media. It is expected to be significant in low pressure, or small pore systems. The atmospheric pressure on Mars is significantly lower than on Earth, and Knudsen diffusion can be the dominant transport mechanism in consolidated porous media[11].

2.3.2 Fick's Law of Diffusion

Diffusion of a chemical species A in another species B can be described by Fick's first law of diffusion, which relates the flux J of a binary chemical mixture to the spatial concentration gradient ∇C by an effective diffusion coefficient D_{ab}[46]:

$$J = -D_{ab}\nabla C \tag{2.3.5}$$

The diffusion coefficient for a binary mixture D_{ab} is known to be a function of temperature, and pressure. The coefficient can be obtained from empirical datasets, or estimated from kinetic theory and corresponding states such as the relation given by Bird et al. [46]:

$$\frac{pD_{ab}}{(p_{cA}\,p_{cB})^{\frac{1}{3}}\,(T_{cA}\,T_{cB})^{\frac{5}{12}}\left(\frac{1}{M_A}+\frac{1}{M_B}\right)^{\frac{1}{2}}} = a\left(\frac{T}{\sqrt{T_{cA}T_{cB}}}\right)^{b} \tag{2.3.6}$$

where the coefficients $a = 3.64 \cdot 10^{-4}$ and $b = 2.33$ for a polar species, such as H_2O, diffusing in a non-polar species, such as nitrogen, oxygen, or CO_2. The relation in Equation 2.3.6 fits experimental data at atmospheric pressure within 8%, and works well for low pressures[46]. The relation shows the dependence of the diffusivity on the reduced pressures p_{ci} and reduced temperatures T_{ci}, the corresponding pressure p [atm], temperature T [K], and the molar masses $M_i[\frac{\mathrm{g}}{\mathrm{mol}}]$. The relation yields D_{ab} with units of $[\frac{\mathrm{cm}^2}{\mathrm{s}}]$.

Equation 2.3.6 can be used to estimate the diffusion coefficient between two chemical species under the prescribed conditions, however multicomponent gases, such as the diffusion of water vapour in air, require additional consideration. Massman [48] performed a comprehensive comparison of estimating the diffusivity of common gases in air, and provides the following relation for the diffusivity of H_2O in air given the temperature, and atmospheric pressure of 1 atm:

$$D_{WA} = 0.2178\left(\frac{T}{T_0}\right)^{1.81} \tag{2.3.7}$$

where $D_{WA}[\frac{\text{cm}^2}{\text{s}}]$ is the diffusivity of water vapour in air, at the temperature T [K], and $T_0 = 273.15$ [K]. Equation 2.3.7 fits experimental data within 7% uncertainty in the temperature range of $0 < T < 100$°C with a coefficient of regression $R^2 = 0.975$[48].

Using the appropriate relation to estimate the diffusion coefficient, the diffusive flux of a chemical species in free space, i.e. outside of a porous medium, can be modelled using Fick's law of diffusion.

2.3.3 Advection

Advection is the transport of a species due to the momentum imparted on the fluid, and arises due to a gradient in pressure. The advective flux can be modelled with the following equation:

$$J_{adv} = C_f \vec{V} \tag{2.3.8}$$

where the flux J_{adv} of the local fluid concentration C_f is directly proportional to the velocity vector $\vec{V}$, and is a consequence of the conservation of momentum. To determine if the advective flux is significant for mass transport in porous media, an analysis of the Péclet number is necessary. The Péclet number, Pe, is the ratio of the advective flux to the diffusive flux. If Pe is less than unity then diffusion is dominant.

In general the Péclet number can be described as:

$$\text{Pe} = \frac{V_{\mathit{eff}} L_C}{D_{ab}} \tag{2.3.9}$$

where the effective velocity V_{eff} through the porous medium, as defined below, is multiplied by a characteristic length L_C.

Huysmans and Dassargues [49] provide a review of various interpretations of the Péclet number, and assert that the parameters used to define Pe are not consistent in the literature and suggest the use of diffusion accessible porosity instead of the effective total porosity to determine the relative importance of diffusive and convective flux. They propose one form of Pe as:

$$\mathrm{Pe} = \frac{V_D \sqrt{K}}{\phi_{diff} D_{ab}} \tag{2.3.10}$$

The Darcy velocity V_D is also known as the Darcy flux and does not represent the true velocity of the species through a porous medium but can be modified by the diffusion accessible porosity ϕ_{diff} to reclaim the effective velocity V_{eff} as in Equation 2.3.9. The characteristic length here is given by the square root of the permeability coefficient K.

To estimate the effective velocity in porous media, the advective flux can be modelled as laminar or creeping flow at steady state in a capillary under a constant pressure gradient ∇p. The flux incorporates an obstruction factor, which is composed of the permeability K and viscosity μ. The final form is also known as the Darcy equation[25]:

$$V_D = \frac{K}{\mu} \nabla p \tag{2.3.11}$$

The permeability K is a purely geometric quantity that can be estimated empirically, or by using relations that are dependent on measurable properties of the medium such as the porosity, and mean grain diameter, as originally proposed by Hazen and Kozeny-Carman[50]. Barr [51] discusses the simplicity of Hazen, and extends the use of the Kozeny-Carman equation in estimating the permeability coefficient by accounting for surface roughness. Use of grain diameter, porosity, surface area, and surface roughness coefficient shows better agreement than the original methods:

$$K = \frac{1}{C_C C_s^2 S_O^2} \frac{\phi_{inter}^3}{(1 - \phi_{inter})^2} \tag{2.3.12}$$

where the factor C_C has been shown by Carrier III [50] to be approximately 5, and they show that C_C is within 3% of the experimentally derived value. C_s is a coefficient that accounts for surface roughness and takes a value of 1 for smooth sphere particle shape, and approximately 1.35 for rough grains. The nominal surface area for packed spheres, S_O, is related to the average grain radius r, is derived from geometric arguments and is equal to $\frac{3}{r}$. In unconsolidated porous media, such as randomly packed silica gel beads, ϕ_{inter} can be considered the inter-particle porosity, and is the volume that is available for advective transport. For the purposes of this study, the value of ϕ_{inter} will be conservatively chosen as the total porosity ϕ.

The permeability K can be used with a known pressure gradient in Equation 2.3.11 to provide an estimate of the effective velocity and resulting advection in a porous medium. Further, an estimate of the relative importance of advection in porous media transport may be made using the Péclet number. If the Péclet number is much less than unity, then diffusion is the dominant form of transport and advective flux can be neglected from the total species transport equation.

2.3.4 Dispersion

Dispersion is an irreversible diffusive effect caused by advection and acts in addition to macroscale diffusion as modelled by Fick's Law. Bear and Cheng [24] propose an additional diffusive flux term to account for the enhanced mixing of a solute due to turbulence and subsequent mechanical mixing of high velocity flow through porous media:

$$J_{disp} = -D_{disp}\nabla C \tag{2.3.13}$$

where the dispersion coefficient D_{disp} can be found by matrix multiplication of an $[m \times m]$ matrix of coefficients of dispersion, $\vec{a}$, with the local $[m \times 1]$ velocity vector, $\vec{V}$, where each element in the dispersion matrix have units of length:

$$D_{disp} = \vec{a}\,\vec{V} \tag{2.3.14}$$

In an isotropic porous medium, $\vec{a}$ can be reduced to a diagonal vector with two coefficients, a_T and a_L, for the transverse and longitudinal directions, respectively. The longitudinal and transverse directions are relative to the net velocity vector in the representative volume. The coefficients of dispersion are related to the characteristic length scales for the fluid in the medium, and are of the magnitude of pore width.

$$\vec{a} = \begin{bmatrix} a_L & 0 & 0 \\ 0 & a_T & 0 \\ 0 & 0 & a_T \end{bmatrix} \tag{2.3.15}$$

For low velocity flows, or where diffusion dominates the transport, as in the present study, the dispersion effect is minimal and will not be discussed further, but is provided for future reference[24].

2.3.5 Surface Diffusion

When modelling species transport in consolidated porous media, surface diffusion can play a significant role. Surface diffusion is a mechanism by which adsorbed molecules move randomly by 'hopping' along the adsorbent surface area. The energy used in hopping is due to thermal fluctuations, and the adsorbate molecules are not removed from the surface, because the energy required to diffuse to another free adsorption site is much less than the energy required for complete desorption. Surface diffusion is an important transport mechanism in adsorbents with high surface area and pore width in the micro regime, and it is shown to be proportional to temperature and to the adsorbed quantity[25].

Flux due to surface diffusion in the intra-particle region can be modelled as a function of the surface concentration gradient, and the energy of activation required to jump to an adjacent site:

$$J_{surf} = -D_S \nabla C_{surf} \tag{2.3.16}$$

The surface diffusion coefficient D_S can be represented by an Arrhenius type function that models the dependence on the energy of activation E_s:

$$D_S = D_{S0}\, e^{\frac{E_s}{RT}} \tag{2.3.17}$$

where the pre-factor D_{S0} is typically found experimentally by measuring the total diffusive flux in the consolidated medium, and subtracting other known fluxes due to Knudsen diffusion, and continuum diffusion as modelled by Fick's first law[26].

In this work, the total diffusive flux from the inter-particle volume into consolidated media, such as the silica gel beads, could be established in terms of the Knudsen, surface, and continuum diffusion components. However, an alternative approach will be developed using a combined mass transfer coefficient to simplify the numerical model of mass transport into the silica gel beads. The concept of surface diffusion is included for the completeness of understanding the various transport mechanisms inside consolidated porous media, and will not be discussed further.

2.4 Species Conservation Equation

The generalized mass conservation equation for a component of a gaseous mixture is given by[46]:

$$\frac{\partial \rho_\alpha}{\partial t} = -\left(\nabla \cdot \rho_\alpha \vec{V}\right) - (\nabla \cdot J) + \Sigma f \tag{2.4.1}$$

where the mass density ρ_α of a component α is conserved in a control volume by the net rates of the advective flux $\nabla \cdot \rho_\alpha \vec{V}$ and diffusive flux $\nabla \cdot J$, and any sources/sinks denoted by the variable f, which may be chemical reactions, or other physical processes such as adsorption.

It follows that the total mass, which is the addition of all component equations, must be conserved to yield the equation of continuity for the mixture:

$$\frac{\partial \rho}{\partial t} = -\left(\nabla \cdot \rho \vec{V}\right) \tag{2.4.2}$$

If the assumption of incompressibility, or constant total mass density is made for the complete mixture, then Equation 2.4.2 can be reduced:

$$\left(\nabla \cdot \vec{V}\right) = 0 \tag{2.4.3}$$

In a mixture of humid air at 25°C and atmospheric pressure, the relative mass density of the water component to the air components is approximately 2% [52], and the advective flux will be shown to be much less than the diffusive flux, therefore the assumption of constant total mass density is acceptable in the experiment studied in this work.

The first term on the right hand side of Equation 2.4.1 can be expanded by the chain rule:

$$\nabla \cdot \rho_\alpha \vec{V} = \nabla \rho_\alpha \cdot \vec{V} + \rho_\alpha \left(\nabla \cdot \vec{V}\right) \tag{2.4.4}$$

where, by using the identity in Equation 2.4.3, the last term on the right hand side is zero, and thus the incompressible mass conservation equation for a component in a mixture, with the application of the dot product commutative rule, becomes:

$$\frac{\partial \rho_\alpha}{\partial t} = -\left(\vec{V} \cdot \nabla \rho_\alpha\right) - (\nabla \cdot J) + \Sigma f \tag{2.4.5}$$

To avoid confusion with the bulk density of porous medium, ρ_{bulk}, the mass density ρ_α in Equation 2.4.5 will be replaced by the symbol C_f, which stands for the volumetric mass concentration of the transported species (water vapour) in the gas phase only, yielding the incompressible mass conservation equation for water vapour:

$$\frac{\partial C_f}{\partial t} = -\left(\vec{V} \cdot \nabla C_f\right) - (\nabla \cdot J) + \Sigma f \tag{2.4.6}$$

where the total effective diffusive flux J is the sum of all active diffusive flux components, as described in Section 2.3.

2.4.1 Conservation Equations in Porous Media

The incompressible water vapour conservation equation 2.4.6 can be modified to represent the concentration in the fluid phase of a porous medium, C_f, by introducing the total porosity, as seen in Bear and Cheng [24]:

$$\phi \frac{\partial C_f}{\partial t} = -\phi \left(\vec{V} \cdot \nabla C_f \right) - \nabla \cdot (-D_{eff} \nabla C_f) - f \tag{2.4.7}$$

where ϕ is the total porosity, D_{eff} $[\frac{\mathrm{m}^2}{\mathrm{s}}]$ is the effective binary diffusion coefficient of C_f $[\frac{\mathrm{kg}}{\mathrm{m}^3}]$ that incorporates the effect of porosity and tortuosity. The velocity $\vec{V}$ $[\frac{\mathrm{m}}{\mathrm{s}}]$ is the average effective velocity of the fluid in the pore space, and in a purely diffusive process $\vec{V} = 0$ and the advection term may be neglected. f is a negative sink term and will be used to model the effect of sorption, and thus the removal of water vapour from the system.

An additional equation is required to track the time dependent adsorbed concentration that is extracted from the fluid phase in a porous medium through the sink term f. If the time dependent adsorbed mass ratio w_s is assumed to remain immobile once adsorbed, the flux components in the solid adsorbed phase are zero, and the adsorbed component conservation equation becomes:

$$(1 - \phi) \frac{\partial w_s}{\partial t} = f \tag{2.4.8}$$

The solid phase volume ratio $(1 - \phi)$ is the counterpart to the porous fluid phase. For convenience the time dependent adsorbed mass ratio w_s is defined on a unit adsorbate mass basis: $\left[\frac{mass\ adsorbed}{mass\ adsorbate}\right]$, which is consistent with adsorption literature, and can be multiplied by the bulk density of the adsorbate, ρ_{bulk} $\left[\frac{\mathrm{kg}}{\mathrm{m}^3}\right]$, to obtain the time dependent adsorbed mass on a unit volume basis.

2.4.2 Local Instantaneous Equilibrium Adsorption

The rate of change of adsorbed mass can be considered instantaneous when the rate of transport of mass through the fluid phase of a porous medium is much less than the rate of transport from the fluid phase to the adsorbate surface phase. This phenomenon can occur in low porosity consolidated media, such as limestone or sandstone, or in very fine grained unconsolidated media, such as dust or silt, where the specific surface area readily available for adsorption is much greater than that for large grains. The adsorbed concentration is then assumed to reach equilibrium with the local fluid phase instantaneously.

Bear and Cheng [24] discuss the use of the non-dimensional Damköhler number, Dm, to evaluate the relative rates of advection, diffusion, and reaction, such as adsorption. The characteristic rate of the reaction, $\lambda_c\,[\frac{1}{\mathrm{s}}]$, is inversely proportional to the characteristic time for a change in concentration, and is included in the denominator of the Damköhler number:

$$\mathrm{Dm} = \frac{L_c^2/D_{\mathit{eff}}}{1/\lambda_c} = \frac{t_{c,diffusion}}{t_{c,reaction}} \tag{2.4.9}$$

Equation 2.4.9 is the second type of Damköhler number, since the mass transport through the fluid phase of the porous medium is diffusion dominated. The characteristic length L_c is associated with the domain's dimensions and, for the intent of analysis in unconsolidated porous media, may be chosen as the particle or grain radius.

If Dm is much greater than unity, then the reaction rate is relatively fast and the local instantaneous equilibrium adsorption assumption can be used. Conversely if Dm is much less than unity, there is significant resistance to the mass transfer from the fluid phase to the adsorbent surface. In this case, the instantaneous equilibrium assumption is not valid and the mass transfer of adsorbate to the adsorption site must be modelled with an appropriate rate equation.

Bear and Cheng [24] propose that the adsorption sink term f in Equation 2.4.7 take the form of the time derivative of the equilibrium adsorbed concentration on a volumetric basis, $(\rho_{bulk}\, w_{equi})$, when the instantaneous adsorption equilibrium assumption is invoked:

$$f = f_{instant} = \frac{\partial \left(\rho_{bulk}\, w_{equi}\right)}{\partial t} \tag{2.4.10}$$

The equilibrium adsorbed concentration can be described either by the product of the local fluid concentration C_f and a scalar value (in the case of linear isothermal behaviour analogous to Henry's law), or by a non-linear function of the local fluid concentration. The non-linear function can be represented by an isotherm equation, such as the Langmuir isotherm given in Equation 2.1.2. When using the Langmuir isotherm equation for w_{equi}, Equation 2.4.10 can be expanded using the chain, and quotient rule of derivation:

$$f_{instant} = \rho_{bulk} \frac{\partial}{\partial t}\left(\Gamma \frac{\kappa C_f}{1+\kappa C_f}\right) = \rho_{bulk}\left(\Gamma \frac{\kappa}{\left(1+\kappa C_f\right)^2}\right)\frac{\partial C_f}{\partial t} \tag{2.4.11}$$

Equation 2.4.11 is then inserted into the fluid phase conservation equation 2.4.7, and moved to the left hand side to form what is known as the 'retardation coefficient' in adsorption literature[24]:

$$\left(\phi + \rho_{bulk}\left(\Gamma \frac{\kappa}{\left(1+\kappa C_f\right)^2}\right)\right)\frac{\partial C_f}{\partial t} = -\phi\left(\vec{V}\cdot\nabla C_f\right) - \nabla\cdot\left(-D_{eff}\nabla C_f\right) \tag{2.4.12}$$

Equation 2.4.12 only tracks the local fluid phase concentration. However, since the local instantaneous adsorption equilibrium assumption is used, the time dependent adsorbed mass ratio is equivalent to the equilibrium adsorbed mass ratio, which is obtained by inserting C_f into the isotherm equation:

$$w_s = w_{equi} = \left(\Gamma \frac{\kappa C_f}{1 + \kappa C_f} \right) \tag{2.4.13}$$

2.4.3 Kinetic Sorption

In the case where the Damköhler number indicates a slow rate of reaction for sorption relative to the bulk transport, the sink term f must be represented by a non-equilibrium rate equation to accurately model transport of adsorbent through an adsorbate. In general, the rate can be represented by a reversible mass transfer flux that depends on the concentration gradient between the equilibrium adsorbed mass ratio, and the current adsorbed mass ratio[24]:

$$f = \alpha_{sf} \left(w_{equi} - w_s \right) \tag{2.4.14}$$

where $\alpha_{sf}[\frac{1}{\mathrm{s}}]$ is the mass transfer coefficient between the fluid and solid phases. In the case of unconsolidated porous media, the mass transfer coefficient represents the combined effects of Knudsen, continuum, and surface diffusive flux from the inter-particle fluid phase *into* the consolidated particles where the mass is adsorbed.

The mass ratio w_{equi} is the mass of the sorbed fluid per unit mass of adsorbent when the solid phase is in equilibrium with the fluid phase. The Langmuir isotherm equation as given in 2.1.2 is a non-linear, empirical relationship that is often used for its simplicity in equilibrium sorption modelling. The Langmuir equation can be implemented in the rate equation 2.4.14, and combined with the fluid phase conservation equation 2.4.7 to model transport of a component through porous media with kinetic, or time dependent sorption:

$$\phi\frac{\partial C_f}{\partial t} = -\phi\left(\vec{V}\cdot\nabla C_f\right) - \nabla\cdot\left(-D_{eff}\nabla C_f\right) - \rho_{bulk}\alpha_{sf}\left(\Gamma\frac{\kappa C_f}{1+\kappa C_f} - w_s\right) \tag{2.4.15}$$

The rate equation for sorption has been multiplied by the bulk density to be dimensionally consistent with the rest of the conservation equation. The conservation equation for the immobile, time dependent adsorbed mass ratio w_s is also formulated with the Langmuir isotherm to complete the system of transport equations:

$$(1-\phi)\frac{\partial w_s}{\partial t} = \alpha_{sf}\left(\Gamma\frac{\kappa C_f}{1+\kappa C_f} - w_s\right) \tag{2.4.16}$$

The rate constant α_{sf} has been implicitly assumed as identical for both adsorption and desorption, which may not be applicable in the higher fluid phase concentration range due to the hysteresis phenomenon arising from capillary filling in micro porous adsorbents. This work only considers the modelling of transport and adsorption of water vapour on silica gel beads, and an empirical adsorption rate constant will be used.

3

Preliminary Experiments

This chapter describes the experiments that were performed to evaluate the physical properties of silica gel beads, which were used in the main adsorption experiment. An experiment to find the solid density for the beads using helium pycnometry is described, followed by a bulk density experiment to determine the porosity of the bulk medium. The equilibrium adsorption experiment for water vapour on silica gel under isothermal conditions is also described, for which a Type I Langmuir isotherm is generated from linear regression of the data. The adsorption data was also used to derive an expression for the mass transfer coefficient α_{sf}.

Figure 3.1: *Quantachrome Manual Multipycnometer*

3.1 Solid Density by Helium Pycnometry

This section describes the determination of the solid density of silica gel beads by measuring the differential displacement of helium using a multipycnometer. The silica gel beads were obtained from Adsorbent Industries, LLC. (*Harrisburg, NC, USA*) and are of the orange indicating type.

3.1.1 Experimental Setup and Procedure

The helium multipycnometer (*Quantachrome, Boynton Beach, FL, USA*) is a device used to measure the volume displaced by powders, and other similar solid materials when compared to a calibrated reference volume. The volume can then be used to find the solid or 'skeletal' density by dividing the sample mass by the volume. The manual helium pyncometer used in this experiment can be seen in Figure 3.1.

The multipycnometer sample volume is limited to the range between 5 and 135 cm^3, and provides a measured volume between 2 and 135 cm^3 with a published accuracy of at least 0.2% when properly calibrated and under isothermal conditions. The device performs experiments at room temperature with no active temperature control.

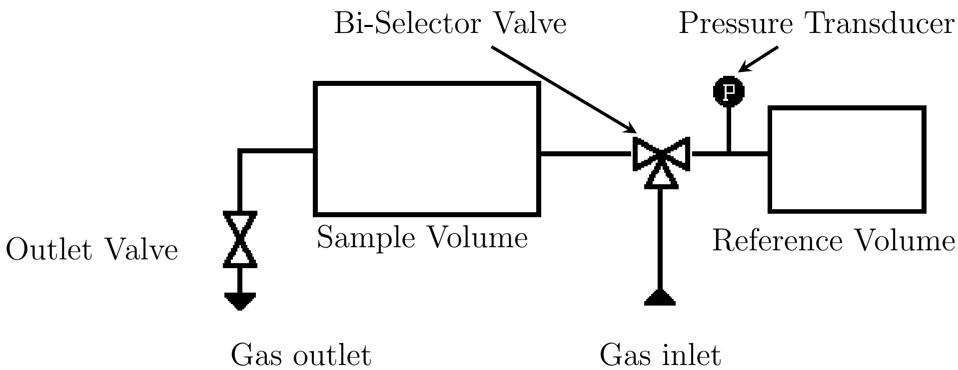

Figure 3.2: *Schematic Diagram of Helium Pycnometer*

In general the multipycnometer has an integrated reference volume cell and another sample containment cell where the solid to be measured is inserted, and a schematic diagram can be seen in Figure 3.2. The reference cell contains a volume of inert gas, such as helium, at a measured pressure. The reference cell gas is vented to the sample cell and the pressure change is measured by a pressure transducer. The volume in the sample cell can be found by using Boyle's Law which asserts that an ideal gas under isothermal conditions yields the following relationship between two states:

$$P_1 V_1 = P_2 V_2 \tag{3.1.1}$$

where P_1 and P_2 are the measured pressures at state 1 and state 2 respectively. State 1 corresponds to the pressurized reference volume only, and after the bi-selector valve is switched, the gas in the reference volume is vented to the sample volume, and upon equilibration is considered to be state 2. The volume of the sample can be found as the difference between the empty sample cell volume and the volume in the second state when the pressure differences are known.

The equation used to solve for the sample volume is given as:

$$V_{sample} = V_{empty} - V_{ref}\left(\frac{P_1}{P_2} - 1\right) \tag{3.1.2}$$

where the reference volume V_{ref} is found by measuring two additional pressure states P_1' and P_2', which are measured when the sample cell is empty. These pressures are used in a differential version of Equation 3.1.2, along with the pressure states $P1_{cal}$ and $P2_{cal}$, which are measured when using a steel calibration sphere with a known volume V_{sphere} of 56.5592 cm^3 in the sample cell:

$$V_{ref} = \frac{V_{sphere}}{((\frac{P_1'}{P_2'} - 1) - (\frac{P1_{cal}}{P2_{cal}} - 1)} \tag{3.1.3}$$

The empty sample cell volume can then be found by rearranging Equation 3.1.2 and solving for V_{empty} using the known reference volume and calibration sphere pressure states:

$$V_{empty} = V_{sphere} + V_{ref}(\frac{P1_{cal}}{P2_{cal}} - 1) \tag{3.1.4}$$

The manufacturer recommends using a sample with greater than 75% of the nominal empty cell volume to ensure greater than 0.2% accuracy in determining the sample volume. The pressure transducers in the reference cell have a resolution of 0.001 psi. A complete step by step description of the calibration and measurement process can be found in Appendix A.

Prior to measuring the volume of the silica gel beads, the beads were evacuated in a vacuum oven at 60°C for 90 minutes to ensure complete desorption of any contaminants or water vapour in the sample, and was then allowed to cool to room temperature while still under vacuum.

V_{sample} Average [cm^3]	Std. Dev.	Sample Mass [g]	Solid Density [$\frac{g}{cm^3}$]
14.041	0.016	29.704	2.116

Table 3.1: *Silica Gel Solid Density from Helium Pycnometry*

3.1.2 Results

The multipycnometer was calibrated in accordance with the guidelines using the largest sample cell and calibration sphere. The large calibration sphere had a true volume of 56.5592 cm^3, and the measured pressure differences were taken as an average over six runs for the empty sample cell case, and the large calibration sphere case.

To estimate the accuracy after calibration, a test measurement was made of two small steel calibration spheres in the sample cell. After six repeated runs the sample sphere volumes were found to be an average of 2.207 cm^3 with a standard deviation 0.035. The two calibration spheres have a total true volume of $1.073 * 2 = 2.146$ cm^3. The error in volume measurement for the two calibration spheres was then 2.84%. The measurement error is attributable to the fact that the sample spheres were much less than 75% of the sample cell empty volume.

After the calibration, the volume measurement of a silica gel sample was completed for ten runs. The average of the sample volume for all runs was used as the final sample volume, and the result is presented in Table 3.1. The calibration data and silica gel solid volume measurements are recorded in Appendix A for future reference.

It should be noted that the helium pycnometry was carried out at room temperature for the silica gel beads, and not at the adsorbent regeneration temperature of approximately 110°C, due to the inability to control the temperature of the sample in the manual multipycnometer. The solid density for silica gel as found in this experiment is expected to be higher than the true value, as the solid density reported by Malbrunot et al. [40] for their brand of silica gel (*Kieselgel 60,MERK,Germany*) was 1.71 $\frac{\mathrm{g}}{\mathrm{cm}^3}$ when measured by helium pycnometry at 400°C.

However, Woignier and Phalippou [41] shows that the solid density of silica gel is affected by the manufacturing process and report densities in the range of 1.85 to 2.2 $\frac{\mathrm{g}}{\mathrm{cm}^3}$ by the helium pycnometry method at room temperature. The solid density for silica gel in this work, is less than that of amorphous silica (2.2 $\frac{\mathrm{g}}{\mathrm{cm}^3}$), and in close agreement with those reported by literature[40, 41]. The uncertainty due to helium adsorption is noted, and the value of 2.116 $\frac{\mathrm{g}}{\mathrm{cm}^3}$ will be used in the following experiments and models.

3.2 Bulk Density Measurement

This section describes the bulk density measurement experiment for the silica gel beads used in the main adsorption experiment. The bulk density and the solid density from the helium pycnometry experiment were then used to calculate the porosity of the randomly poured silica gel beads, with no compaction.

3.2.1 Experimental Setup and Procedure

A cubic measurement cell was created using laser cut pieces from a 3 mm thick acrylic sheet, fastened together with acrylic solvent (*Weld-On 3, IPS Corp., CA, USA*). The cubic measurement cell was constructed to have an internal volume of approximately $5 \times 5 \times 4.25 = 105$ cm^3. The volume was selected to represent the cross section of beads to be found in the main adsorption experiment (5×5 cm^2).

The cubic cell was filled with distilled water at room temperature, and the mass of the water was measured with a calibrated microbalance (*Explorer, OHaus, Parsippany, NJ, USA*). The microbalance was calibrated with four specialized calibration spheres with masses of $2, 10, 100, 150$ g, and the balance was accurate to within 0.001 g. The meniscus of the water was observed to ensure a constant fill level. After the measurement of mass of water in the cubic cell, the temperature of the water was determined using an alcohol thermometer. This mass measurement process was repeated ten times. The true volume of the cubic cell was then found by using the measured mass of water, and the density of water from published data[53].

The silica gel beads were regenerated by heating in an oven for one hour, set at approximately 110°C for which the temperature was monitored with a T-type thermocouple attached to a temperature display (*CN77000, Omega, Stamford, CN, USA*) with a resolution of 1°C. Prior to measuring the oven temperature, the thermocouple was calibrated by using an alcohol thermometer at the boiling point of water. The temperature of the oven fluctuated during it's default heating/cooling cycles between approximately 80°C and 120°C. It was recommended by the manufacturer of the silica gel beads not to heat above 120°C to avoid damaging the indicating type silica gel, which would affect the consistency of adsorption.

The silica gel beads were allowed to cool to room temperature in a sealed plastic container to prevent any adsorption of atmospheric water vapour. Once cool the beads were poured into the cubic measurement cell in a random fashion to emulate the loading procedure to be found in the main adsorption experiment. The cubic cell was filled to the top edge and the beads were not compacted. The mass of the beads was then measured using the microbalance, and the beads were removed from the cell. The filling and mass measurement process was repeated ten times.

Using the average true volume of the sample cell and the average mass of the

	V_{cell} [cm^3]	Mass of Beads [g]	Bulk Density ρ_{bulk} [$\frac{g}{cm^3}$]
Average	105.913	87.234	0.824
Std. Dev.	0.286	0.637	0.006

Table 3.2: *Silica Gel Bulk Density Measurement*

randomly poured beads, the bulk density ρ_{bulk} of the beads was then calculated. The bulk density and the solid density ρ_{solid} were then used to calculate the porosity of the bulk porous medium. All recorded measurement data can be found in Appendix B.

3.2.2 Results and Total Porosity

The average values, and corresponding standard deviation for the measured cubic cell volume, mass of randomly poured beads, and the resulting bulk density are shown in Table 3.2.

The bulk density of the randomly poured silica gel beads was then used with the solid density to define the total porosity using Equation 2.2.2:

$$\phi = 1 - \frac{\rho_{bulk}}{\rho_{solid}} = 1 - \frac{0.824}{2.116} = 0.611 \tag{3.2.1}$$

3.3 Equilibrium Sorption

This section describes the equilibrium sorption of water vapour on a sample of silica gel beads at discrete partial pressures of water vapour, using an automated sorption analyzer. The sorbed mass of water vapour was inferred from the change in sample mass at each equilibrium point given the partial pressure of water vapour, from which a Langmuir Type I isotherm was fitted using linear regression. The mass transfer coefficient was also estimated and shows a non-linear dependence on the partial pressure of water vapour surrounding the silica gel beads.

3.3.1 Experimental Setup and Procedure

The sorption analyzer (*VTI-SA, TA Instruments, New Castle, DE, USA*) is an automated instrument that provides a continuous flow of controlled vapour in a nitrogen carrier gas, for use over a temperature range of 5°C to 150°C. The temperature is typically fixed for a desired isotherm, and is controlled to within 0.1°C.

The concentration of water vapour in the nitrogen carrier gas is controlled using a closed loop chilled mirror dew-point analyzer with an accuracy of 1% relative humidity. The adsorbate sample is held in a hemispherical sample tray that is connected to a mass balance with a published accuracy of 0.1%.

In general, the sorption analyzer was prepared, and the silica gel sample weighing approximately 20 mg was inserted into the sample tray. The sample was dried by flushing with dry nitrogen, which was heated up to 120°C over 120 minutes. After cooling the sample, the relative humidity in the carrier gas was increased over discrete intervals at the fixed temperature of 25 °C, and increased only when equilibrium was reached between the sample and the carrier gas water vapour concentration.

The step by step procedure conducted for this experiment, and the resulting sorption equilibrium data for the silica gel beads can be found in Appendix C. The experiment's equilibrium conditions and discrete relative humidity equilibration points are summarized in Table 3.3.

Condition	Value
Drying Temp.	120°C
Heating Rate	1 °C/min
Max Drying Time	120 min
Experiment Temp.	25°C
Equilibration Criteria	Less than 0.0050 wt% increase over 5.00 min
Relative Humidity Steps	0.05, 0.1, 0.2, 0.3, 0.4, 0.5, 0.6, 0.7, 0.8, 0.9
Data Logging Interval	2.00 min or 0.01 wt % change

Table 3.3: *VTI-SA Sorption Analyzer Settings*

3.3.2 Sorption Isotherm

The equilibrium data points found using the VTI-SA sorption analyzer describe the steady state sorbed mass of water vapour on silica gel beads given the fixed water vapour concentration in the pure nitrogen carrier gas. The water vapour concentration in the carrier gas is synonymous with the local fluid concentration, C_f. It is assumed that the steady state sorption of water vapour from a pure nitrogen carrier gas is equivalent to the sorption of water vapour from air, due to nitrogen being the primary constituent of atmospheric air on Earth, and that the other components of air do not significantly interact with the silica gel beads. To clearly interpret the data from the sorption analyzer, some additional theory is required, and will serve as a basis for construction of the Langmuir Type I isotherm.

Equation of State

The local fluid concentration can be described in terms of relative humidity (RH) of the water vapour in air, which is defined as the ratio of partial pressure of water vapour in air p_{vap}, to the saturation pressure p_{sat}:

$$RH = \frac{p_{vap}}{p_{sat}} \tag{3.3.1}$$

The partial pressure of water vapour can then be found by multiplying the relative humidity RH by the saturation vapour pressure, which is a strong function of temperature. The saturation vapour pressure for water in air as seen in the CIPM-2007 Revised formula for the density of moist air by Picard et al. [54]:

$$p_{sat} = 1\,\mathrm{Pa} \cdot \ e^{\left(A \cdot T^2 + B \cdot T + C + \frac{D}{T}\right)} \tag{3.3.2}$$

where the coefficients are defined as:

- A: $1.2378847 \cdot 10^{-5}\ \mathrm{K}^{-2}$
- B: $-1.9121316\ \cdot 10^{-2}\ \mathrm{K}^{-1}$
- C: 33.93711047
- D: $-6.3431645 \cdot 10^{3}\ \mathrm{K}$

Using the ideal gas law as the equation of state, the partial pressure of water vapour can be converted to the mass concentration of water vapour in air C_f:

$$C_f = \frac{p_{vap} M_{H_2O}}{R_g T} \tag{3.3.3}$$

The use of the ideal gas law as an equation of state is acceptable because the compressibility factor Z, which describes the deviation of real gases from the ideal gas law, is very close to 1 and yields an error in mass concentration of less than 0.42%. An analysis of the Z compressibility factor using the method of Picard et al. [54] can be seen in Appendix G.

Equilibrium Sorption and Langmuir Linear Regression

The Type I isotherm can be represented by Equation 2.1.2, for which Langmuir [22] performs a linear regression of sorption data by recasting the equation in the following form:

$$\frac{C_f}{w_{equi}} = \frac{C_f}{\Gamma} + \frac{1}{\kappa\Gamma} \tag{3.3.4}$$

The equilibrium adsorbed mass ratio w_{equi} is defined as the mass adsorbed per unit mass of adsorbate, which is equivalent to the fractional increase of mass of adsorbate measured by the VTI-SA sorption analyzer under equilibrium conditions. Additionally, each relative humidity equilibrium point seen in Table 3.3 as a percentage, can be converted to the local fluid concentration of water vapour, C_f, using the ideal gas relationship of Equation 3.3.3.

The local fluid concentration C_f, and the adsorbed mass ratio w_{equi} can then be used in Equation 3.3.4 to plot the linearized form of the sorption isotherm, where the coefficients $\frac{1}{\Gamma}$ and $\frac{1}{\kappa\Gamma}$ are respectively the slope and intercept for the linear relationship. The slope and intercept coefficients were found by the method of least squares regression, and the resulting linear relationship has been plotted overlaying the original adsorption equilibrium data points in Figure 3.3.

The coefficients found from the least squares regression are shown in Table 3.4, and the coefficient of determination R^2 indicates a good agreement between the data and the equation found from linear regression. The coefficients can be rearranged to solve for the desired Langmuir Type I Isotherm coefficients

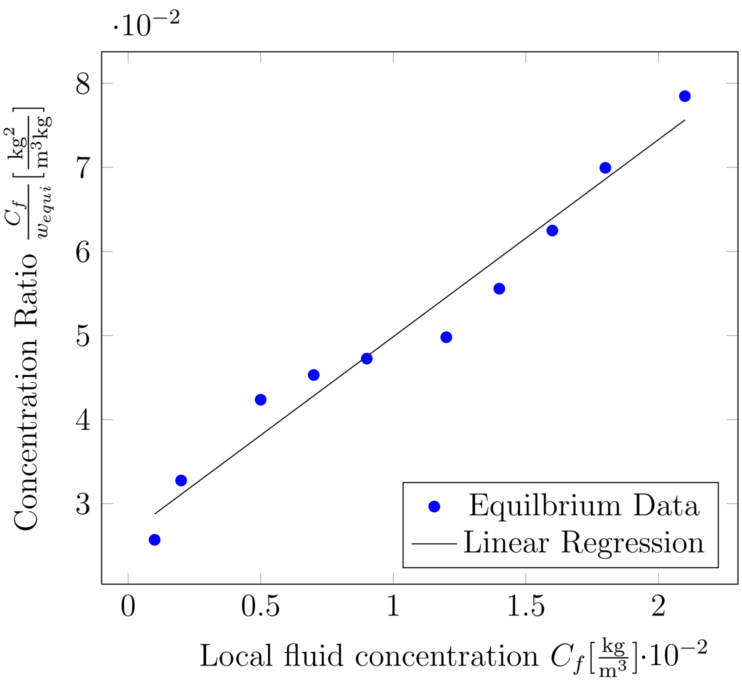

Figure 3.3: *Linearized Sorption Equilibrium Data; Water Vapour on Silica Gel*

Slope $\frac{1}{\Gamma}$	Intercept $\frac{1}{\kappa\Gamma}$	R^2	Γ	κ
2.344	0.026	0.964	0.426	88.728

Table 3.4: *Results of Linear Regression of Sorption Equilibrium Data*

Γ and κ, and are also included in the table.

Type I Langmuir Isotherm

The Langmuir Type I isotherm coefficients Γ and κ were found using linear regression, and are used in Equation 2.1.2 to plot the continuous Langmuir sorption isotherm in Figure 3.4. The equilibrium data points from the VTI-SA sorption isotherm experiment are shown in the same plot for comparison, and the abscissa is normalized by the concentration at saturation.

Although the underlying assumptions of Langmuir theory incorrectly describe

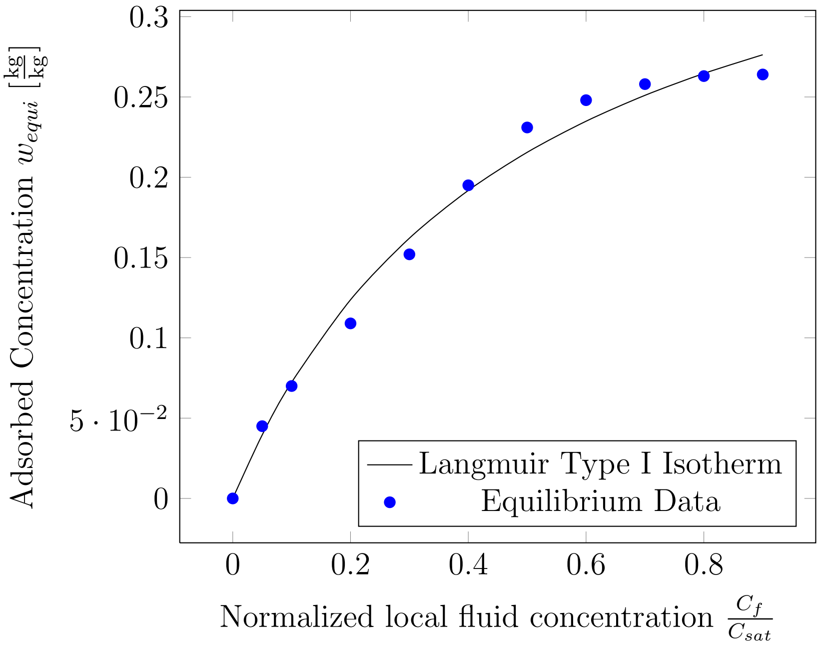

Figure 3.4: *Comparison between Sorption Equilibrium Data and Langmuir Type I Isotherm for Water Vapour on Silica Gel at* 25°C

the process of sorption, the equilibrium sorption isotherm fits the data sufficiently well over the entire local concentration range for this adsorbate/adsorbent pair, and due to the simplicity of the sorption isotherm equation, the Langmuir Type I isotherm has been selected to model equilibrium adsorption in this work.

3.3.3 Mass Transfer Coefficient

The mass transfer coefficient, α_{sf} $[\frac{1}{s}]$, describes the kinetic rate of mass transfer of the local fluid concentration to the internal surfaces of adsorbate. In this work, the mass transfer of water vapour into the silica gel is impeded by the internal structure of each bead, and it is assumed that the process can be described by a linear driving force model that is dependent on the local fluid concentration.

Li et al. [55] investigated the effects of water vapour transport into silica gel beads and proposed a method of using adsorption equilibrium data, and a linear driving force model to estimate the mass transfer coefficient. The linear driving force model predicts an asymptotic relationship between the adsorbate mass at time t, m_t, and final adsorbate mass, m_f:

$$\frac{m_t}{m_f} = 1 - e^{-kt} \tag{3.3.5}$$

where the time constant k is the mass transfer coefficient for a final local fluid concentration. The equation can be re-arranged to isolate the time constant:

$$\ln\left(1 - \frac{m_t}{m_f}\right) = -kt \tag{3.3.6}$$

The slope of the plot of $\ln\left(1 - \frac{m_t}{m_f}\right)$ vs. time provides an estimate of the mass transfer coefficient k. The mass of silica gel was tracked over time for each increment of local fluid concentration in the VTI-SA sorption analyzer experiment and was plotted using Equation 3.3.6. A linear regression was then performed on each data set to determine the slope.

For example, in the case of incrementing RH from 5% to 10%, the local fluid concentration was set to 10% RH, and the mass of silica gel beads increased over time. The example data set is plotted in Figure 3.5. The data was linearized using Equation 3.3.6 and a linear regression was performed to estimate the slope of the line. Both the linearized kinetic adsorption data and linear regression are plotted in Figure 3.6. In the final minutes of equilibration the linear driving force model is no longer appropriate and significant noise appears. The data used for linear regression is then only selected up to the point where significant noise begins.

The linear regression was performed for each increment of relative humidity

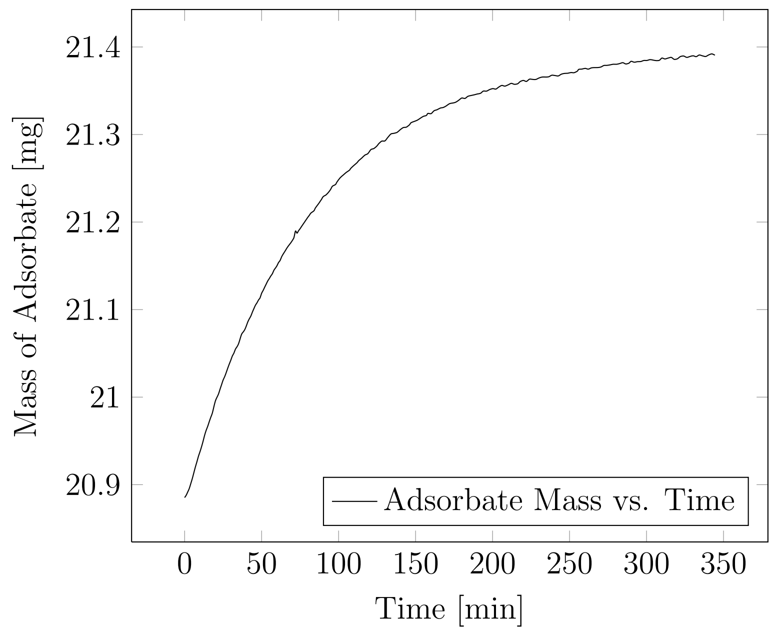

Figure 3.5: *Adsorbate Mass vs. Time for Increment of Relative Humidity from 5% to 10%*

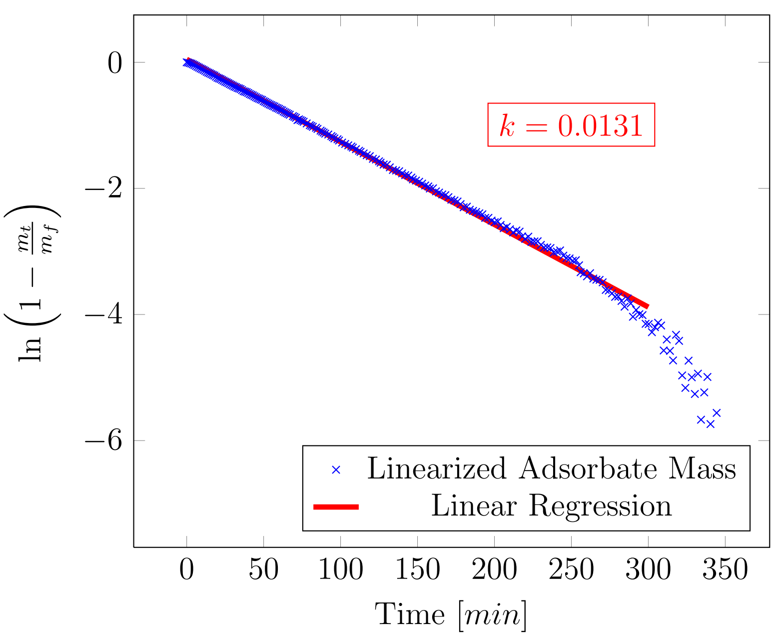

Figure 3.6: *Linearized Adsorbate Mass vs. Time for Increment of Relative Humidity from 5% to 10%*

RH Interval (%):	5-10	10-20	20-30	30-40	40-50	50-60	60-70	70-80	80-90
Slope (k):	0.0131	0.0138	0.0146	0.0173	0.0215	0.0452	0.1048	0.0791	0.1612

Table 3.5: *Mass Transfer Coefficients from Linear Regression of Sorption Equilibrium Kinetic Data*

and the slope, or effective mass transfer coefficient, for each interval was estimated. The mass transfer coefficients k are reported in Table 3.5, and the data, plots and coefficients of regression for each interval are included in Appendix D for reference.

The data in Table 3.5 suggests that the mass transfer coefficient is proportional to the local fluid concentration, and is qualitatively consistent with the results of Li et al. [55]. A continuous relationship was desired for the mass transfer coefficient as a function the local fluid concentration, so the mass transfer rates were plotted against the relative humidity ranges, and an exponential best fit was made for the data, where both are plotted in Figure 3.7. The coefficient of determination for the exponential fit was $R^2 = 0.903$.

It should be noted that the measured mass transfer coefficient k at relative humidities greater than the 50-60% range, were estimated from a shrinking data set because the late term noise appeared at an earlier time. The proposed reason for this is due to the mass vs. time measurement being made over a 10% increase, e.g. 70% to 80%, instead of from 0% to 80% as found in Li et al. [55], where the latter case would have presented a larger, more consistently linear data set. This is a source of error that is acknowledged, and can be eliminated in the future by conducting additional experiments using the VTI-SA sorption analyzer, and ensuring re-generation of the adsorbate sample between each RH final value.

The exponential best fit provides a continuous function for the mass transfer coefficient α_{sf}, which will be used in the conservation of mass equations 2.4.15 and 2.4.16. The relative humidity is expressed in terms of the local fluid

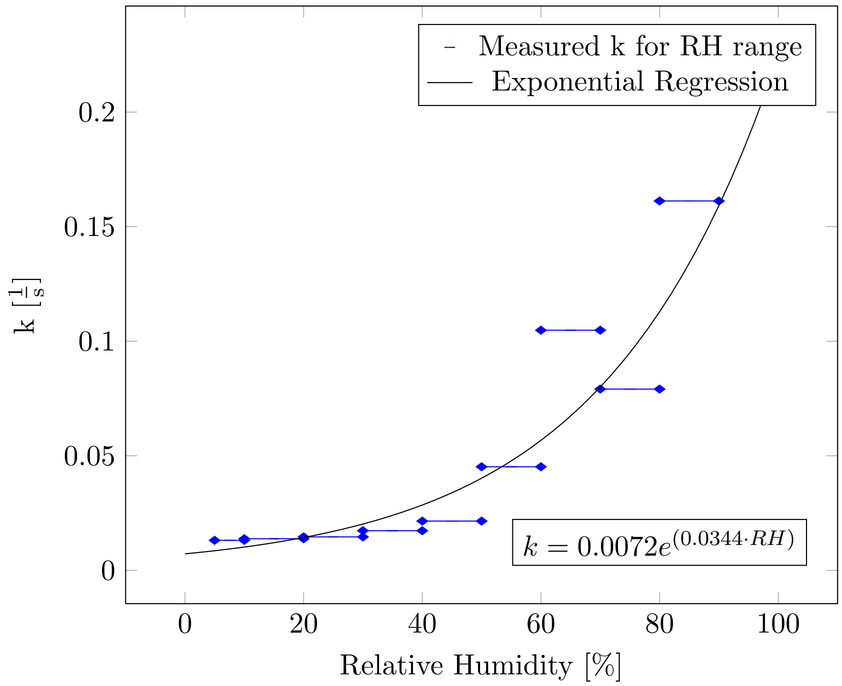

Figure 3.7: *Exponential Fit for Empirical Mass Transfer Coefficient*

concentration C_f for consistency:

$$\alpha_{sf} = 0.0072 \, e^{\left(0.0344 \, \frac{C_f}{C_{sat}}\right)} \tag{3.3.7}$$

4

Main Sorption Experiment

This chapter describes the creation and execution of the main sorption experiment. The construction of the diffusion sorption apparatus, and calibration of the relative humidity and temperature sensors are both discussed. Finally a description of the experimental procedure is included.

4.1 Experiment Background

The intent of the main experiment was to investigate the effect of sorption on the transport of water vapour through a porous medium. The apparatus was designed to isolate and quantify the sorption process by using only diffusion as the primary transport mechanism for the mass of water vapour. The mass concentration of water vapour in the inter-particle fluid phase was then measured using relative humidity and temperature sensors at specific probe points.

In general, the diffusion-sorption experiment consists of two chambers connected in vertical alignment by a 5 cm channel which was filled with a porous medium. An approximately cubic bottom chamber with 10 cm side length, was constructed to house a source of water vapour, and a manually operated door was connected between the source chamber and the porous medium channel which was to be opened once the bottom chamber had reached saturation.

Another approximately cubic top chamber with 10 cm side length, was constructed to house a large source of desiccant which acted as a sink for the water vapour. The concentration difference between the two opposite ends of the porous channel was then known and the water vapour transport through the medium can be modelled using Fick's first law and the porosity and tortuosity, which are purely physical properties of the porous media.

The concentration of water vapour was monitored using seven Sensirion SHT˜75 relative humidity and temperature sensors, one sensor was placed in the bottom source chamber, one in the top sink chamber, and three were placed at equal distance in the porous medium. The sensors inside the medium tracked the progression of the water vapour as it moved through the channel from the source to the sink. Two additional sensors were placed outside of the apparatus to monitor the conditions in the room.

Three trials were run for this experiment, where the first trial was the longest experiment with a total running time of approximately 15 days. The first trial did not reach steady state conditions and was shut down after the 15 days because a substantial quantity of data was obtained for each sensor, and further measurement would not have added any value. The second and third trials were each run for one week, to demonstrate the repeatability of the diffusion sorption experiment. This work will focus on the first trial run for analysis as it is the largest data set.

The trials were conducted in a small insulated room to prevent interference from the heating and ventilation systems. The recording computer, and sensor interface were kept outside of the insulated room, to minimize heating of the experiment from the electrical components.

4.2 Construction of the Apparatus

The diffusion sorption apparatus was designed in a modular fashion using sheets of 3 mm thick acrylic (*PG Plastics, AB. Canada*). All parts were first designed in Solidworks CAD software, and connected in a virtual assembly, or 3D model, to check for interference and that the dimensions were reasonable. Each component of the apparatus, such as the door mechanism, channel, and chambers, were made individually by joining laser cut acrylic parts together with Weld-On 3 acrylic glue, and finally attached together with fasteners, rubber washers and custom gaskets to ensure an air tight seal.

Solidworks was used to map the parts onto a 2D drawing file which was then converted to the input format required for guiding a 50 W CNC automated laser cutting and etching tool (*Versa Laser, NSW Australia*). An image of the laser cutter is shown in Figure 4.1, and the procedure for using the laser cutter was supplied by Bayans [56]. The CAD drawing files for each component are included in Appendix E.

The holes in each part were made to fit 6-32 thread screws with EPDM rubber washers, and the custom made EPDM rubber gaskets were also placed between all mating faces of the components. The apparatus assembly and an isolated view of the manual sliding door mechanism are shown in Figure 4.2. The assembly is shown without fasteners for clarity.

On each of the top and bottom chambers, one face was constructed with a porthole and detachable door with gasket in order to access the inside of the apparatus at the beginning of the experiment for loading purposes. Additionally, holes were created in the top and bottom chamber, and the channel component to allow the SHT˜-75 temperature and humidity sensors to be inserted. The sensor holes were patched with silicone on the outside to create an air tight seal.

4.3 Sensor Type and Calibration

The relative humidity and temperature sensor (*SHT-75, Sensirion, ZH, Switzerland*), as seen in Figure 4.3, is an integrated circuit dual sensor probe that communicates through a serial interface. A capacitive sensor is used for the relative humidity, and the temperature is measured using a band-gap semiconductor sensor. Both internal sensors are connected to an on-chip 14-bit analog to digital converter that transmits to a custom made interface card when the sensor is prompted for output. The minimum time between prompts is recommended as one second by the manufacturer to prevent overheating of the sensors, thus the interface card was programmed with a four second delay.

4.3.1 Saturated Salt Solution

The sensors were calibrated before the experiment at five calibration points using an airtight cylindrical glass flask, in a 25°C temperature controlled and

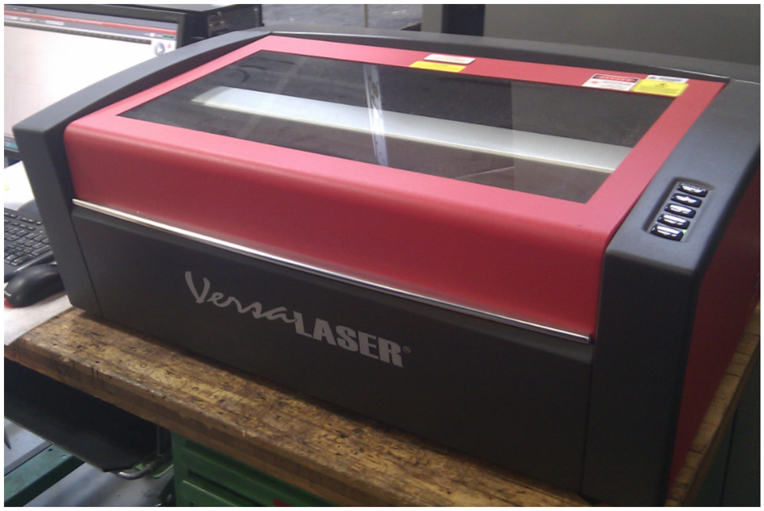

(a) *Outside view*

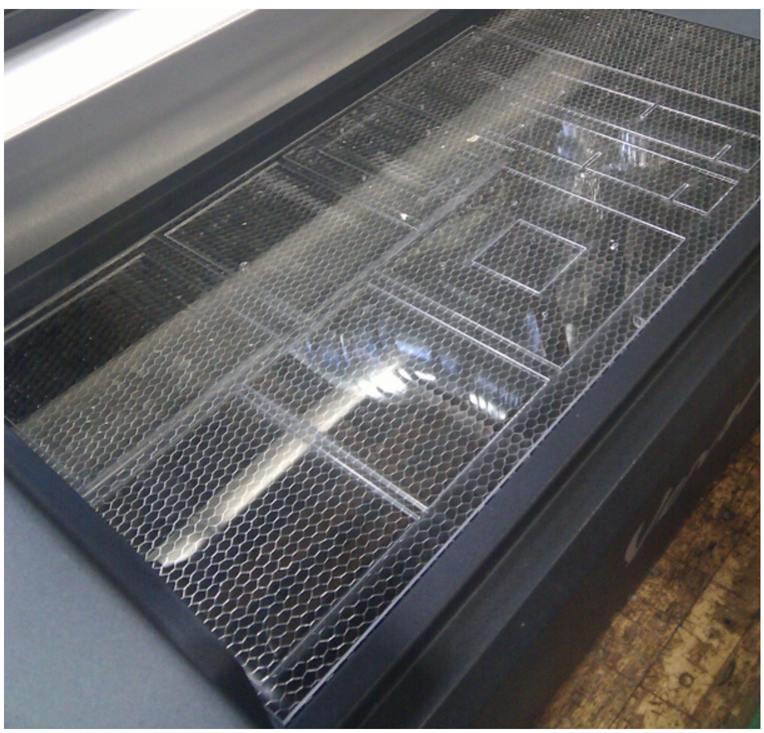

(b) *Acrylic sheet after laser cutting*

Figure 4.1: *Versa Laser Cutter*

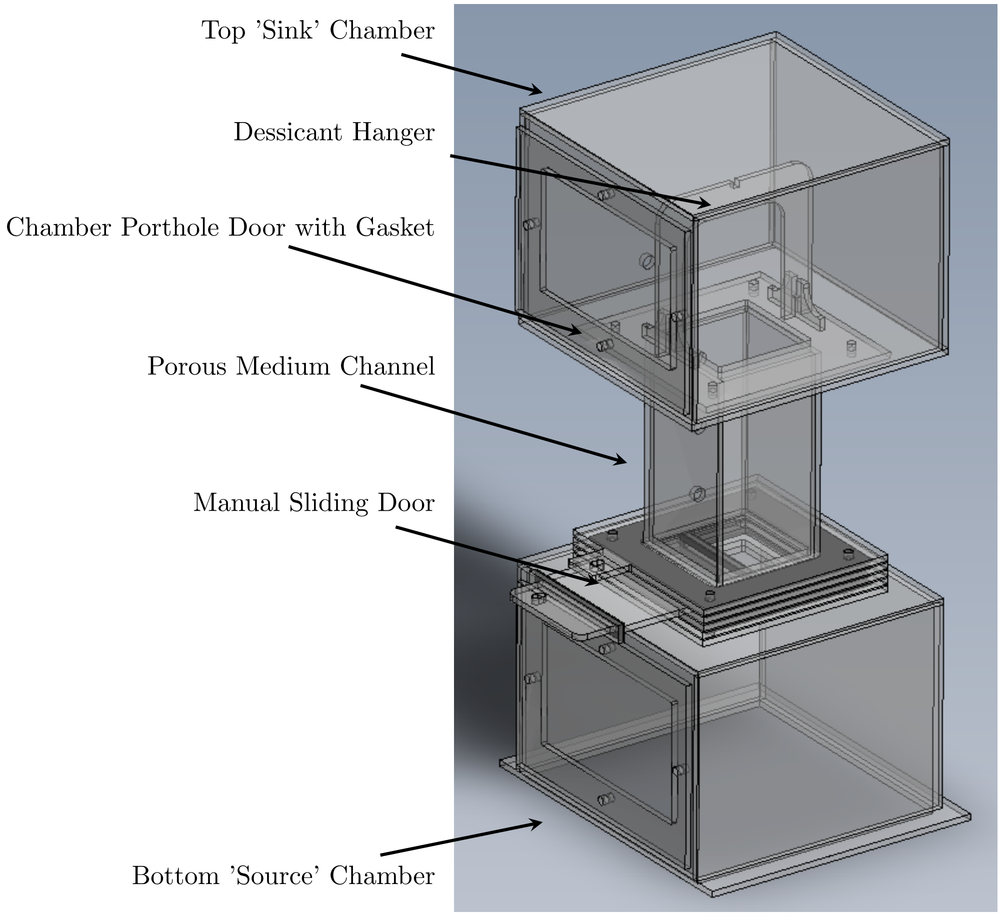

(a) *Full assembly*

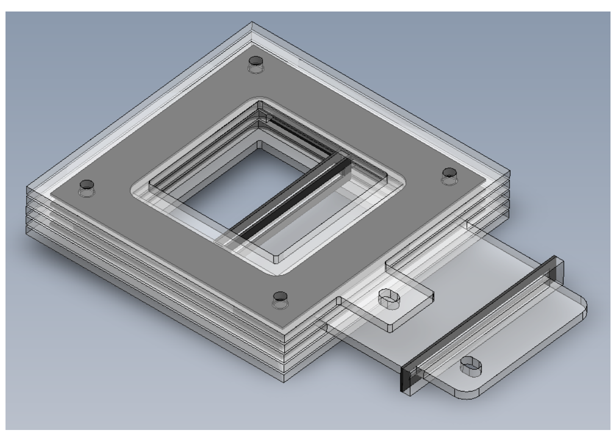

(b) *Isolated view of manual sliding door with gaskets*

Figure 4.2: *Diffusion Sorption Apparatus CAD Model*

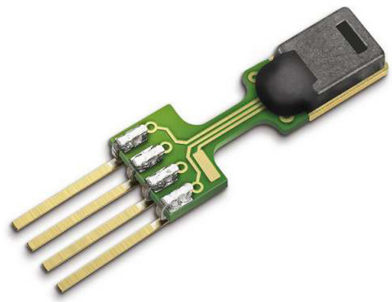

Figure 4.3: *Sensirion SHT-75 Relative Humidity and Temperature Sensor*

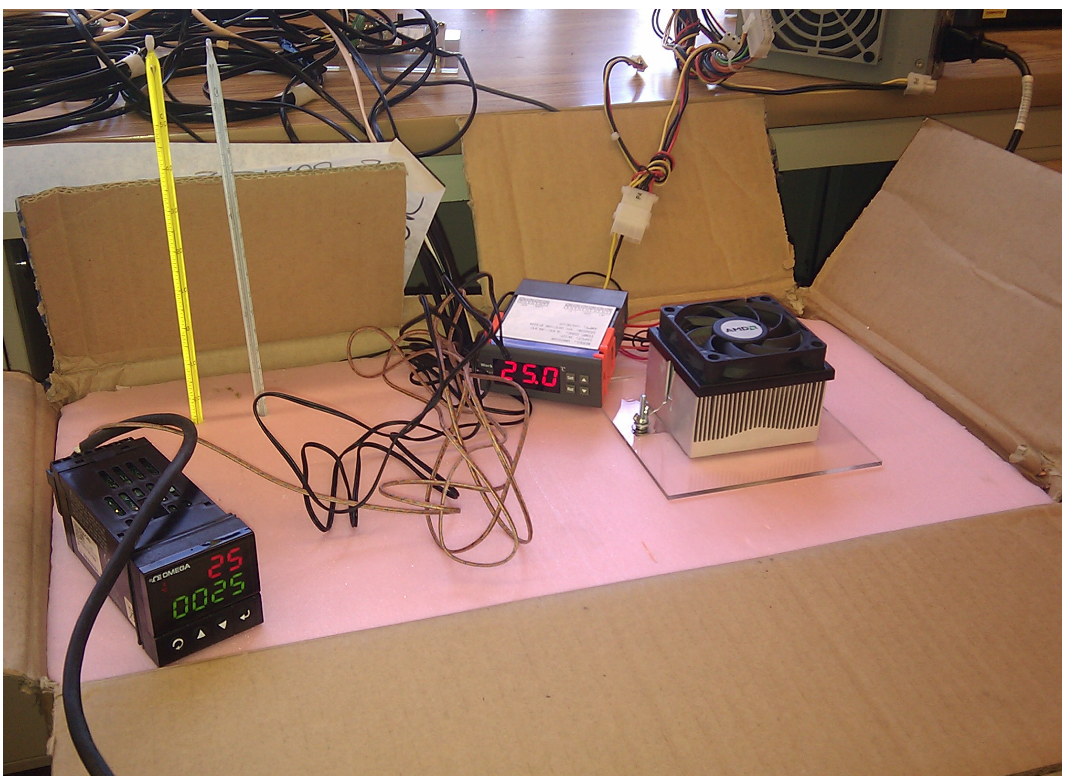

Figure 4.4: *Calibration of Relative Humidity and Temperature Sensors*

Flask Contents	Expected Relative Humidity [%]
Dessicated	0
Saturated Lithium Chloride	11.30 ± 0.27
Saturated Potassium Carbonate	43.16 ± 0.39
Saturated Sodium Chloride	75.29 ± 0.12
Pure Distilled Water	100

Table 4.1: *Calibration Flask Contents and Expected Relative Humidity*

1.27 cm ($\frac{1}{2}$ in) thick polystyrene foam insulated box. The temperature was kept constant using a 12 V DC, 60 W thermoelectric Peltier device (*TEC1-12706, Wellentech, China*), connected to a control unit with 0.1°C accuracy. The temperature control unit was calibrated at 25°C using two mercury thermometers with 0.1°C gradation. The relative humidity in the flask was monitored for a sufficient amount of time to allow equilibrium of temperature and relative humidity to occur in the flask. The calibration setup is shown in Figure 4.4.

According to Raoult's Law, the vapour pressure of a saturated salt solution is equal to the product of the mole fraction of solvent, and the vapour pressure of pure solvent. However Raoult's Law is only applicable for extremely dilute or ideal solutions, and the true vapour pressure above a saturated salt solution is typically found empirically[57].

Three saturated salt solutions were used as calibration points in the mid range of the relative humidity spectrum. Additionally a dessicated flask, using silica gel beads, was used as a 0% RH calibration point, and conversely pure distilled water was used as a 100% RH calibration point. The salt types used for calibration, and expected relative humidity for each are reported in Table 4.1[58].

	T1	T2	T3	T4	T5	T6	T7
T_{offset}	-0.454	-0.299	-0.478	-0.391	-0.234	-0.528	-0.453
Coeff.	RH1	RH2	RH3	RH4	RH5	RH6	RH7
c_3	-4.088E-05	-5.329E-05	-4.337E-05	-4.107E-05	-4.987E-05	-3.779E-05	-3.695E-05
c_2	7.457E-03	8.585E-03	7.342E-03	6.890E-03	7.925E-03	6.721E-03	6.187E-03
c_1	6.885E-01	6.735E-01	7.091E-01	7.341E-01	7.101E-01	7.304E-01	7.873E-01
b	-3.178E-02	1.258E-02	-4.152E-01	2.777E-01	-1.242E-01	-6.046E-01	-1.207E+00
R^2	1	0.999	1	1	0.999	1	1

Table 4.2: *Temperature Offset and RH Cubic Polynomial Calibration Coefficients*

Both the temperature and relative humidity were taken as a time average at their equilibrium conditions for each sensor. The criteria for the time average data set was at least 15 minutes of equilibrium conditions for both temperature and RH, and the averages were performed for each of the flask contents listed in Table 4.1. It should be noted that a single point calibration was used for the temperature, where the scalar offset value was the average of the temperatures at all five calibration points for a given sensor.

A single point scalar offset was used for the temperature because the main sorption experiment was intended to run at 25°C and the sensors are most accurate at that temperature. The measured relative humidities were recorded for each sensor and plotted against the expected relative humidities, for which a cubic regression was performed, and the coefficients of regression for each sensor are shown in Table 4.2.

The cubic polynomial used to convert the relative humidities from sensor i to calibrated values takes the form:

$$RHi_{calibrated} = c_3 \cdot RHi^3_{measured} + c_2 \cdot RHi^2_{measured} + c_1 \cdot RHi_{measured} + b \quad (4.3.1)$$

where the coefficients are used from Table 4.2. The coefficients of regression show a very good fit for the conversion of relative humidity in each sensor, and

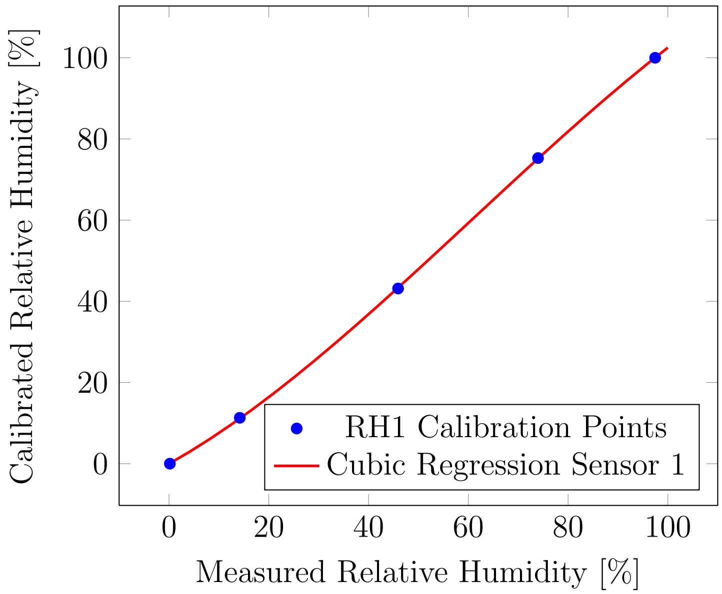

Figure 4.5: *Calibration plot using cubic polynomial regression for RH on Sensor 1*

the deviation from linearity is only in the extremities of the relative humidity spectrum, which is expected because the manufacturer's data sheets show increasing uncertainty at the extremes.

The phenomenon of non-linearity is visualized when plotting the calibration data and cubic polynomial regression as seen in Figure 4.5. It should be noted that the calibrated relative humidity was artificially kept in the range of 0 to 100%, to prevent unphysical results. The calibration data for each sensor, and plots of equilibrium for each calibration point can be found in Appendix F.

4.4 Experimental Procedure

4.4.1 Adsorbent Preparation

The silica gel adsorbent was prepared for each experiment by baking on an aluminum foil tray in a toaster oven (*Black and Decker CTO-4300BC*) for at least one hour to remove all sorbed water vapour. The oven temperature was set at approximately 110°C, however the temperature fluctuated between 80°C and 120°C over its duty cycle, when monitored with a calibrated thermocouple. After regenerating the silica gel beads, they were allowed to cool to room temperature in a sealed container before transferring to the diffusion-sorption apparatus.

4.4.2 Leak Test and Saturation Conditions

After the diffusion-sorption apparatus was assembled, and the sensors were fixed in place, a sample of water was placed in the bottom source chamber and the manual sliding door was kept closed. The system was monitored for a period of 24 hours to ensure that the water vapour could reach saturation conditions in the bottom chamber and not leak through the sliding door or to the outside. As seen in Figure 4.6, the sensor in the source chamber (C_1) rises to saturation within 2 hours and fluctuates relative to the temperature in the chamber.

4.4.3 Setup, Execution and Final Weighing

After the saturation leak test, the positions of all sensors were measured in the vertical direction relative to a datum, and the locations were recorded for use in the numerical model as probe points. The datum for Sensor 1 was the top outer face of the bottom chamber, and the datum for sensors 2 to 5 was the inner bottom face of the top chamber. A schematic diagram of the sensor locations that were measured in the apparatus during the first trial are shown in Figure 4.7.

After cooling to room temperature the regenerated silica gel beads were poured through a funnel in the top chamber porthole door to fill the channel section.

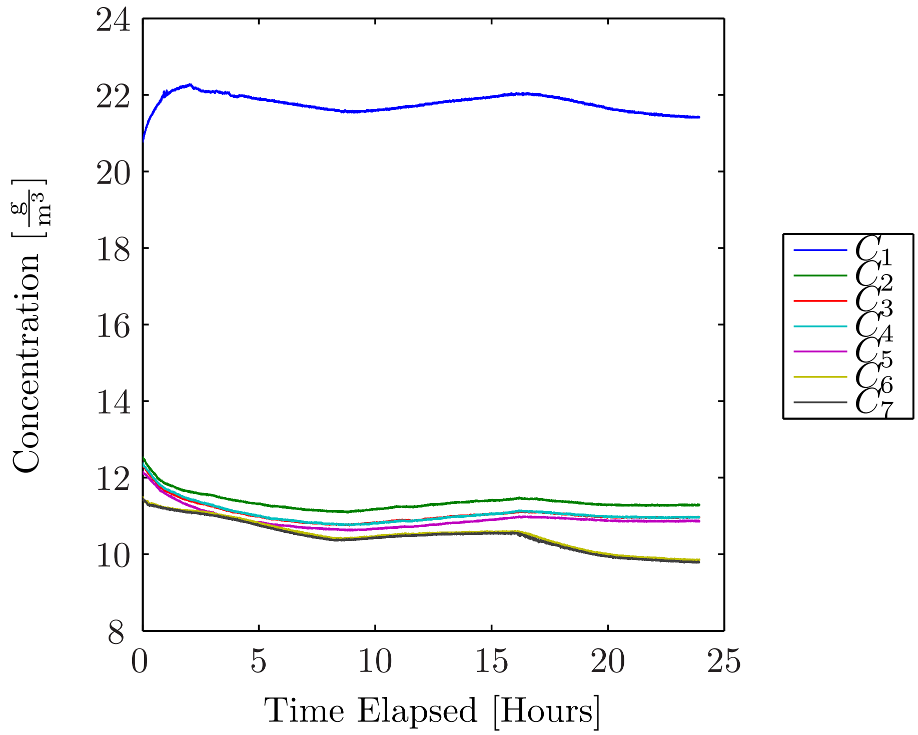

Figure 4.6: *24 Hour Leak Test*

At the bottom of the channel section, a porous metal sieve with 2 mm square gaps was previously installed to keep the beads from falling into the bottom chamber. Although care was taken to minimize disruption of the inserted sensors during the pouring process, as the falling beads were capable of moving the flexible sensors, the measured sensor locations in Figure 4.7 remain a source of uncertainty.

Approximately 30 g of silica gel beads were wrapped in a paper coffee filter and placed in the top chamber to act as a sink for the water vapour. The top chamber porthole was then sealed with a rubber gasket and fasteners. A polystyrene container with 104.3 g of water was again placed in the bottom chamber to act as a source of water, and the manually operated sliding door was kept closed to prevent any exposure to the channel and top chamber. The bottom chamber was then sealed with a rubber gasket and fasteners.

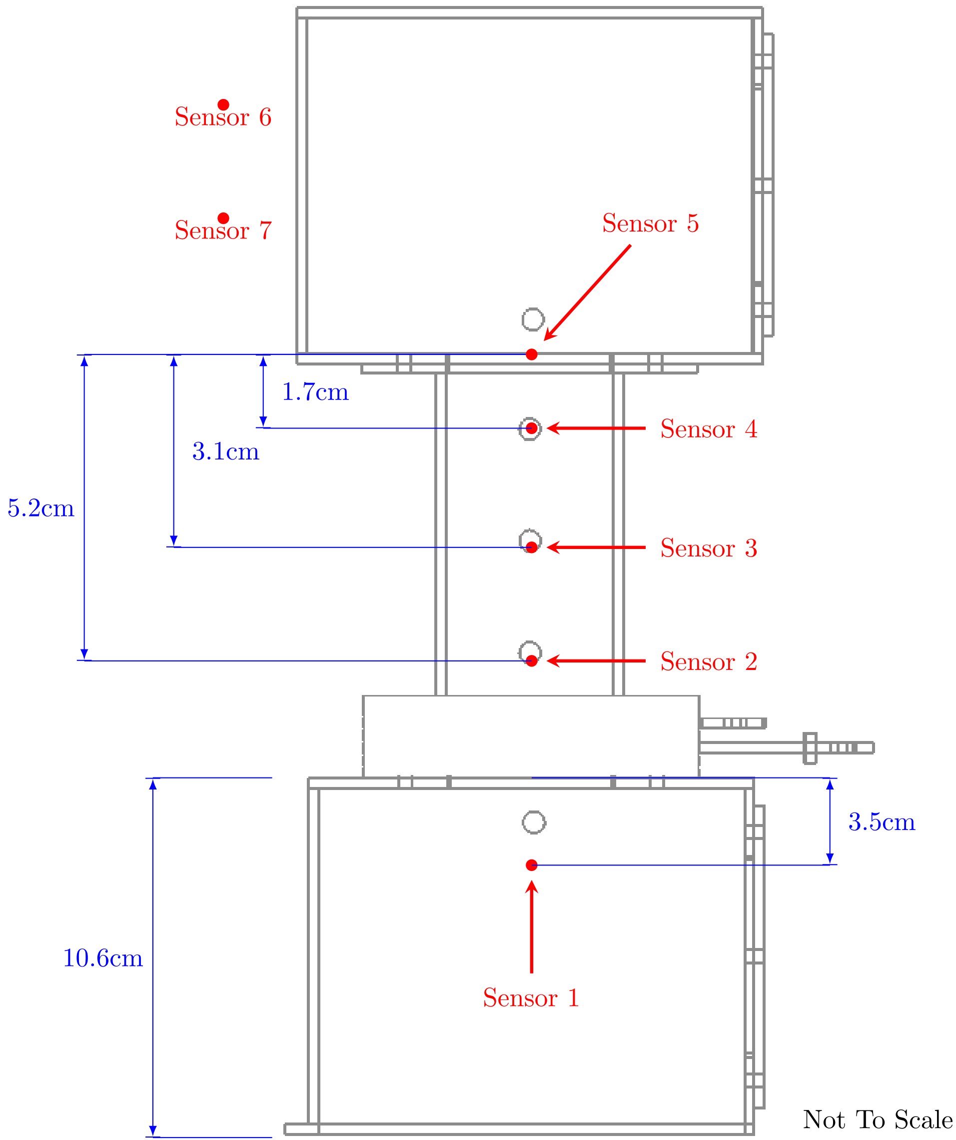

Figure 4.7: *Schematic Diagram of Apparatus with Sensor Locations.*

The closed system was monitored and left for approximately two hours to allow the water vapour to reach saturation in the bottom chamber, after which the manual sliding door was opened and the experiment had officially begun. As the water vapour moved through the porous media over two weeks, the indicating silica gel changed its colour from orange (dessicated) to green (saturation).

After sufficient data had been collected the trial was stopped, and the sliding door was closed to seal off the porous media from the source chamber. The apparatus was carefully dismantled, and the silica gel beads in the channel were quickly extracted to a dry polystyrene container, and their final sorbed mass was recorded.

The same container of beads was then transferred to an aluminum sheet, and regenerated in the oven using the same settings as before the experiment. After approximately one hour the beads were removed from the oven, and their mass was measured again to find the dry mass of the beads. This procedure assumes that the sorption and regeneration process did not alter the solid bead mass, and only affected the sorbed water vapour.

Using the dry mass and the sorbed mass of the silica gel beads, an estimate of the water vapour sorbed mass was made for comparison to the final sorbed mass predicted in the numerical model. Figure 4.8 shows the experiment in operation.

The above procedure was repeated for the second and third trial, however the duration of the later trials was limited to approximately ten days each due to time constraints. The second and third trial data were used to validate the repeatability of the diffusion sorption experiment, and to compare the true sorbed mass of water vapour at a given time to that predicted by the numerical model.

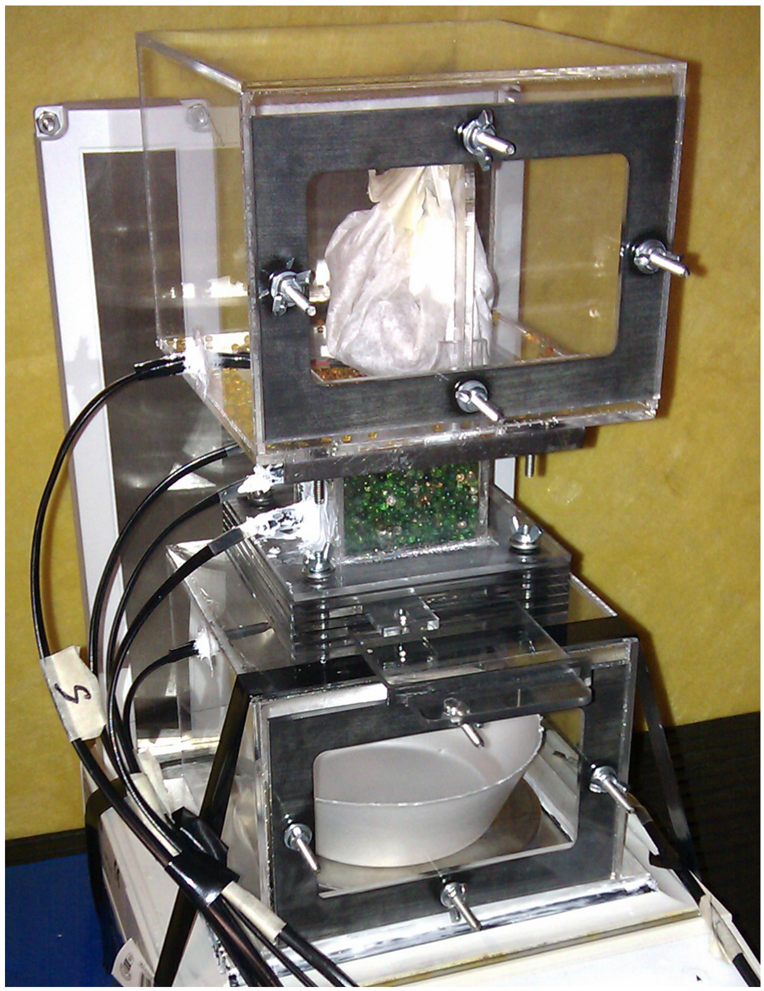

Figure 4.8: *Diffusion Sorption Experiment During Trial 1*

5

Numerical Model and Simulation

This chapter describes the development of the numerical model using COMSOL, a commercial finite element package. It begins with a description of the procedure used to estimate the effective diffusion coefficient of water vapour through silica gel beads, followed by a justification for the elimination of advection from the mass transport equations, and the use of the kinetic rate equation for sorption. Finally a two dimensional, time dependent, numerical model of the diffusion sorption apparatus is described.

5.1 Conservation Equations

Recalling the conservation equations for the local fluid concentration, C_f, and the time dependent adsorbed mass ratio, w_s, including the kinetic rate of sorption (Equations 2.4.15 and 2.4.16 respectively), the advection term includes the effective velocity of the local fluid concentration, and can be eliminated under appropriate conditions.

5.1.1 Diffusion Coefficient

To begin the analysis, the diffusion coefficient must be established. The diffusion coefficient for water vapour in air at 1 atm, can be evaluated at the average external temperature (23.7°C) found in the diffusion sorption experiment by using Equation 2.3.7:

$$D_{WA} = 0.2178\left(\frac{T}{T_0}\right)^{1.81} = 0.2178\left(\frac{296.85}{273.15}\right)^{1.81} = 2.532 \cdot 10^{-1}\ \frac{\text{cm}^2}{\text{s}} \quad (5.1.1)$$

The average external temperature, is defined as the average of all temperatures from sensors 6 and 7, taken over the entire trial time in the diffusion sorption experiment. The average external temperature was used to evaluate the diffusion coefficient because the maximum temperature deviation for any sensor i in the first trial, (ΔT_i), from the average external temperature was approximately 3°C, as indicated by sensor 2 in Figure 5.1.

It should be noted that the deviation in sensor 2 decreased as the experiment progressed, which is attributed to the heat of adsorption dissipating in the medium, and eventually synchronized with the other temperatures. Figure 5.1 shows the absolute deviation of the each sensor's temperature from 23.7°C.

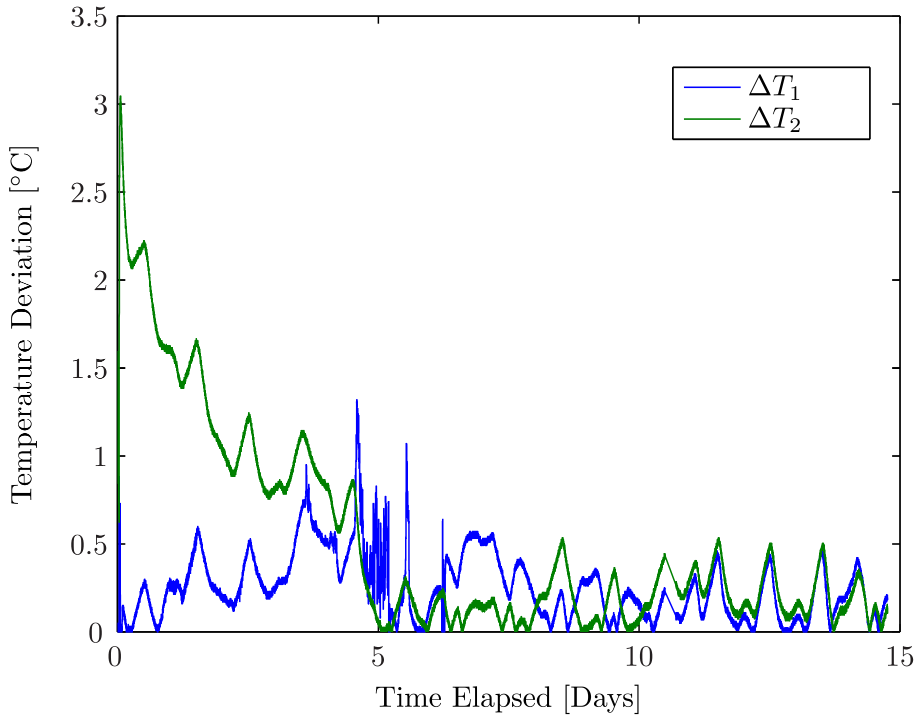

Figure 5.1: *Diffusion Sorption Trial 1 - Deviation of Sensor i's Temperature (ΔT_i) From Average External Temperature of* 23.7°C

When using Equation 2.3.7 again with the maximum deviation temperature, 26.7°C, the resulting diffusion coefficient is $2.578 \cdot 10^{-1} \frac{\text{cm}^2}{\text{s}}$, which is well within the 7% error expected for Equation 2.3.7. Therefore, the use of an isothermal diffusion coefficient given by the average external temperature is justified.

5.1.2 Péclet Number

The Péclet Number as described by Equation 2.3.10, may be evaluated by combining the relation given in Equation 2.3.11 to find the effective velocity using the Darcy flux:

$$\text{Pe} = \frac{\nabla p \sqrt{K^3}}{\mu \, \phi \, D_{WA}} \tag{5.1.2}$$

The permeability K is found with Equation 2.3.12, by using the total porosity ϕ as found in Equation 3.2.1. The silica gel beads were assumed to be approximately smooth on the surface, and the average grain radius was measured for 50 beads (Appendix B), and found to be 0.156 cm:

$$K = \frac{1}{C_C C_s^2 S_O^2} \frac{\phi^3}{(1-\phi)^2} = \frac{1}{5 \cdot 1^2 (\frac{3}{0.156[\text{cm}]})^2} \frac{0.611^3}{(1-0.611)^2} = 8.152 \cdot 10^{-4} \text{ cm}^2 \tag{5.1.3}$$

The viscosity, μ, of saturated humid air was reported by Kestin and Whitelaw [59] for a temperature of 25°C as $1.84 \cdot 10^{-4} \frac{\text{g}}{\text{cm} \cdot \text{s}}$, and changes less than 0.4% for air with low relative humidity. The viscosity can then be considered approximately constant for this study. At the beginning of the diffusion sorption experiment, a hissing sound could be heard briefly when the manually operated door was opened indicating that the pressure inside the whole apparatus was quickly equalized. The Péclet number can be evaluated using Equation 2.3.10 for the equalized pressure of 0 Pa:

$$\text{Pe} = \frac{\frac{0[\text{Pa}]}{5[\text{cm}]} \sqrt{(8.152 \cdot 10^{-4} \, [\text{cm}^2])^3}}{1.84 \cdot 10^{-4} [\frac{\text{g}}{\text{cm s}}] \cdot 0.611 \cdot 2.532 \cdot 10^{-1} \left[\frac{\text{cm}^2}{\text{s}}\right]} = 0 \tag{5.1.4}$$

The Péclet number found using the zero pressure gradient indicates that the system is diffusion dominant and the advection term may be neglected from the conservation equations. The initial effect of pressure equalization was not accounted for in the numerical model and is noted as a source of error in this study.

5.1.3 Tortuosity

The tortuosity is used with the porosity to modify the diffusion coefficient for water vapour in air, D_{WA}, to become the effective diffusion coefficient, D_{eff}, which is used in the conservation of mass equations. Typically the tortuosity is derived empirically as a fitting parameter, however this study will use the relation provided by Boudreau [44]:

$$\tau = 1 - \ln(\phi^2) = 1 - \ln(0.611^2) = 1.98 \tag{5.1.5}$$

5.1.4 Damköhler Number

The Damköhler Number as defined in Equation 2.4.9 permits the evaluation of the ratio of diffusivity through the porous medium to the reaction rate that extracts the mass from the local fluid concentration.

The characteristic length was chosen as the silica gel bead average grain radius of 0.156 cm, and the effective diffusion coefficient, D_{eff} was found using the diffusion coefficient for water vapour in air, and the porosity and tortuosity:

$$D_{eff} = \frac{\phi}{\tau} D_{WA} = \frac{0.611}{1.98} \cdot 2.532 \cdot 10^{-1} \frac{\mathrm{cm}^2}{\mathrm{s}} = 7.813 \cdot 10^{-2} \, \frac{\mathrm{cm}^2}{\mathrm{s}} \tag{5.1.6}$$

The characteristic rate of reaction (Sorption), λ_c $[\frac{1}{\mathrm{s}}]$, was taken as the empirically fitted mass transfer coefficient, α_{sf}, obtained in the preliminary sorption experiments and shown in Equation 3.3.7. Here it is substituted into Equation 2.4.9 to find the Damköhler Number as a function of the relative humidity:

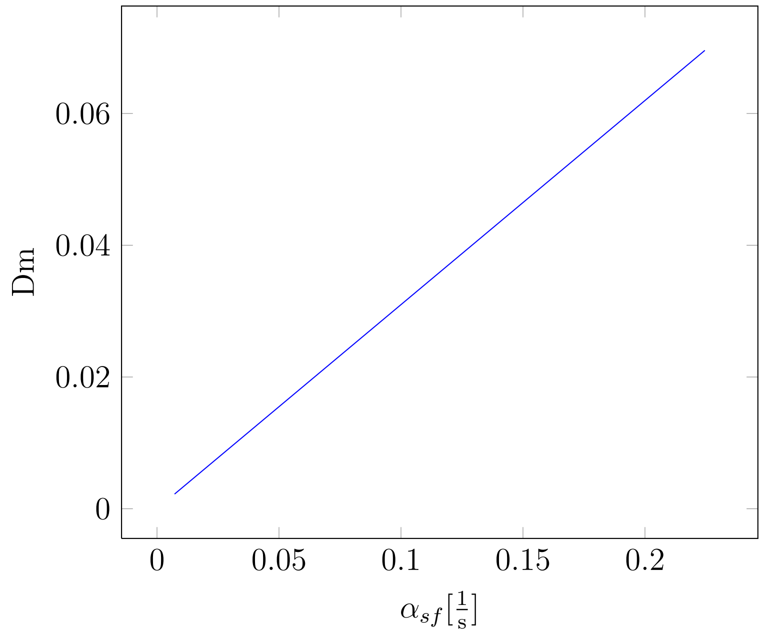

Figure 5.2: *Damköhler Number as a function of the characteristic rate of sorption over a range of bulk relative humidity from 0% to 100%*

$$\mathrm{Dm} = \frac{L_c^2/D_{eff}}{1/\lambda_c} = \frac{(0.156\mathrm{cm})^2}{\left(7.813 \cdot 10^{-2}\frac{\mathrm{cm}^2}{\mathrm{s}}\right)\left(0.072 \cdot e^{(0.0344 \cdot \mathrm{RH})}\ \frac{1}{\mathrm{s}}\right)^{-1}} \tag{5.1.7}$$

The resulting equation for Dm was plotted over the full range of relative humidity ($0\% \leq \mathrm{RH} \leq 100\%$), and the resulting range of α_{sf} (0 to 0.2) is shown in Figure 5.2. For any value of α_{sf} the Damköhler Number is much less than unity, which means that the rate of sorption is much less than the relative diffusion rate past a given silica gel grain, and the local instantaneous adsorption equilibrium assumption is not applicable. The rate of sorption will then be modelled using the kinetic rate equation with α_{sf}.

Because of the low Péclet and Damköhler numbers, the conservation equations used in the numerical model can be simplified by eliminating the advection term, and the kinetic rate equation for sorption must be used, which yields

Parameter Name	Symbol	Value	[Units]
Porosity	ϕ	0.611	[1]
Tortuosity	τ	1.98	[1]
Mass transfer coefficient	α_{sf}	$0.0072 \cdot e^{\left(0.0344 \cdot \frac{C_f}{C_{sat}}\right)}$	$\left[\frac{1}{s}\right]$
Saturation concentration at 23.7°C	C_{sat}	21.491	$\left[\frac{g}{m^3}\right]$
Langmuir coefficient	κ	88.728	$\left[\frac{m^3}{kg}\right]$
Langmuir steady state coefficient	Γ	0.426	$\left[\frac{kg}{kg}\right]$
Bulk density	ρ_{bulk}	0.824	$\left[\frac{g}{cm^3}\right]$
Effective Diffusion Coefficient	D_{eff}	$7.813 \cdot 10^{-2}$	$\left[\frac{cm^2}{s}\right]$

Table 5.1: *Conservation Equation Parameters used in Numerical Model*

the following form developed for this study:

$$\phi \frac{\partial C_f}{\partial t} = -\nabla \cdot (-D_{eff} \nabla C_f) - \rho_{bulk} \alpha_{sf} \left(\Gamma \frac{\kappa C_f}{1 + \kappa C_f} - w_s \right) \tag{5.1.8}$$

$$(1 - \phi) \frac{\partial w_s}{\partial t} = \alpha_{sf} \left(\Gamma \frac{\kappa C_f}{1 + \kappa C_f} - w_s \right) \tag{5.1.9}$$

where the associated parameters are specified in Table 5.1. It should be noted that the units are expressed as shown for clarity, however all values were converted to Meter Kilogram Second (MKS) in the numerical model for dimensional consistency.

5.2 COMSOL Geometry and Discretization

The commercial FEA package, COMSOL v4.2a, was used to create a two dimensional cross-sectional model of the diffusion sorption experiment. The conservation equations were applied to the model using the package's coefficient PDE format, and the parameters established in Table 5.1 were used as coefficients. COMSOL's MUMPS direct linear solver was used with a global scaled tolerance of 10^{-5}. The time stepping method used was BDF, with a minimum BDF order of 2, and a maximum BDF order of 5. The time-step was also limited to a maximum of 100,000 s.

5.2.1 Dimensions

The geometry was created in COMSOL by boolean addition and subtraction of primitive shapes to represent the 2D cross section of the diffusion sorption apparatus. The geometry includes the bottom source chamber, the manually operated door space, 5 cm wide channel, and top sink chamber. Only the internal area of the apparatus has been modelled, including the water source container on its sample tray. A schematic diagram showing the dimensions used in creation of the geometry can be seen in Figure 5.3.

It should be noted that the diffusion sorption experiment was setup to be one dimensional in nature, however the numerical model is constructed in 2D to illustrate the expandability of the conservation equations for future use in three dimensions. A 2D model was selected over a 3D model to minimize the solving time required.

5.2.2 Mesh Generation and Refinement

The mesh was automatically generated using COMSOL's free triangular mesh type. The elements were discretized using the Lagrangian shape function, with Quadratic element order. Four mesh refinements were made, where a single simulated variable was chosen for monitoring, and plotted against each mesh refinement to show convergence to a final value. The mesh settings for each refinement stage are shown in Table 5.2, and the four meshes used in the mesh refinement study are shown in Figure 5.4.

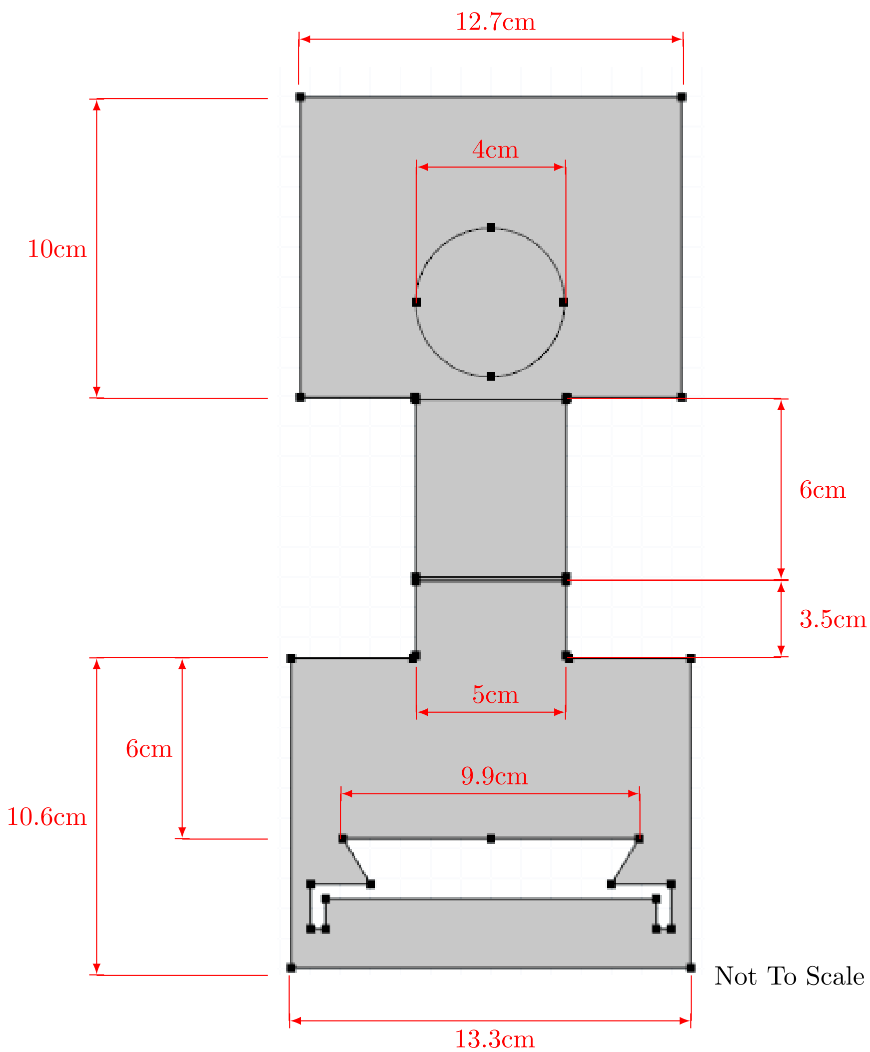

Figure 5.3: *Schematic Diagram of Diffusion Sorption Geometry in COMSOL.*

Parameter	Mesh I	Mesh I	Mesh III	Mesh IV
Maximum Element Size [cm]	1.54	1.07	0.58	0.29
Minimum Element Size [cm]	8.69E-3	3.62E-3	2.17E-3	5.8E-4
Maximum Element Growth Rate	1.3	1.25	1.2	1.1
Resolution of Curvature	0.3	0.25	0.25	0.2
Resolution of Narrow Regions	1	1	1	1
Total Number of Elements	2,364	2,962	4,592	12,689

Table 5.2: *Free Triangular Mesh Settings*

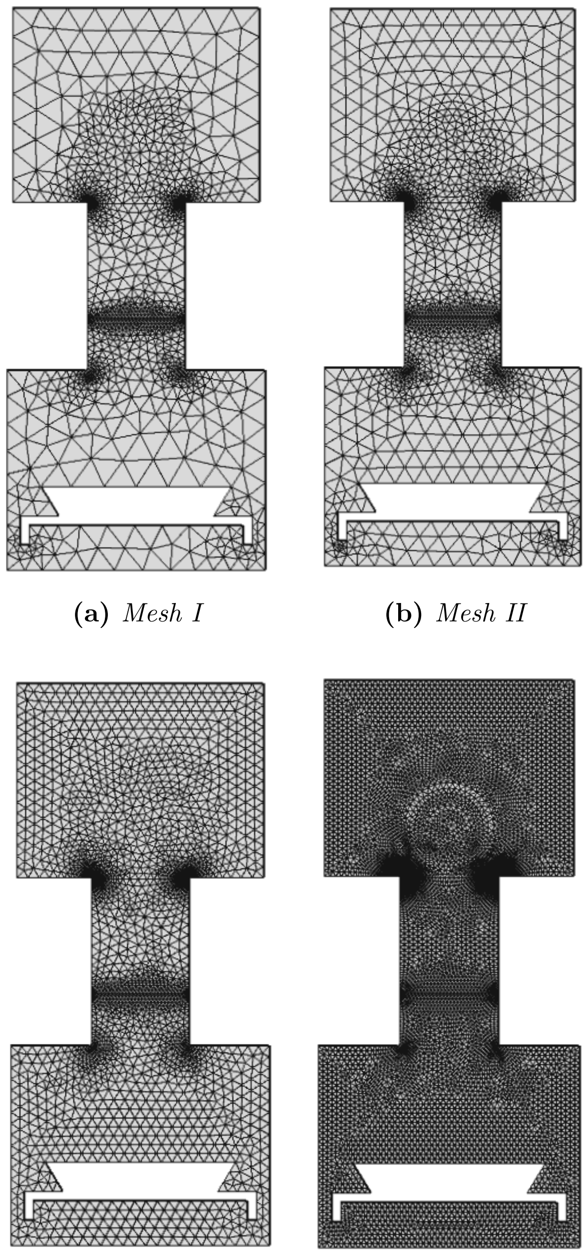

(a) *Mesh I* (b) *Mesh II*

(c) *Mesh III* (d) *Mesh IV*

Figure 5.4: *Increasing Mesh Complexity for Mesh Refinement Study*

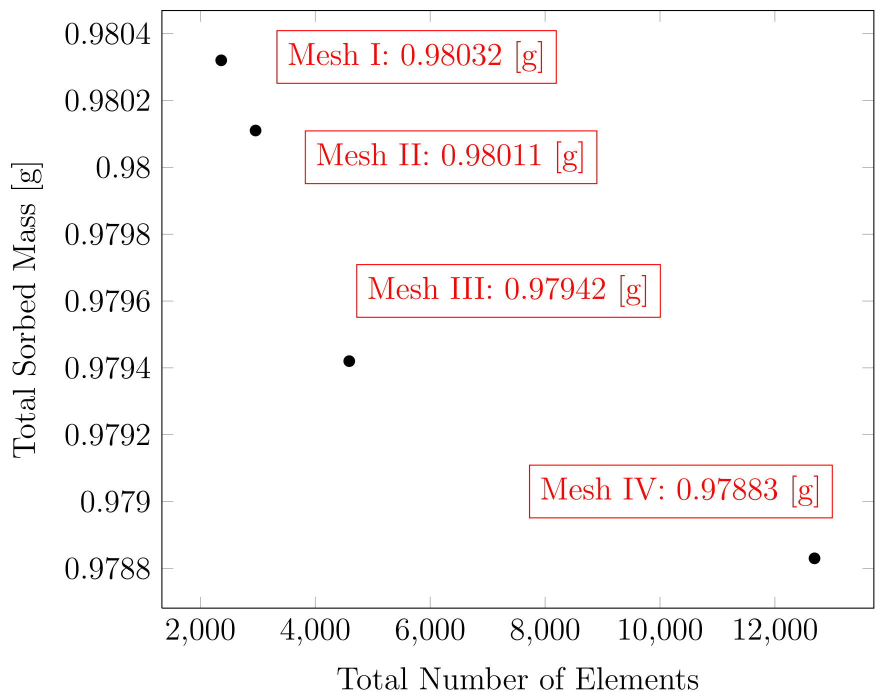

Figure 5.5: *Mesh Refinement Test: Total Sorbed Mass in Channel after Five Hours*

In this study the final sorbed mass in the channel after five hours, $\int w_s \mathrm{d}V$, was selected as the monitoring variable and integrated over the entire porous medium volume to find the total sorbed mass at the end of the simulation. The input parameters for the diffusion sorption experiment were used to simulate the first trial, and the total final sorbed mass was plotted against each mesh refinement setting as shown in Figure 5.5.

The percentage difference between the monitoring variables from Mesh III and Mesh IV can be calculated as follows:

$$\%Error = \frac{0.97942 - 0.97883}{0.97883} \cdot 100 = 0.06\% \tag{5.2.1}$$

Since the finest mesh (Mesh IV) has a very small change in the monitoring variable from the previous mesh (Mesh III), and Figure 5.5 shows a converging trend in the monitoring variable, the grid can be considered fine enough for this study so that the discretization error of the numerical model is known to be within the error introduced by all other variables. Therefore Mesh IV will be used for all numerical modelling in this study.

5.3 Boundary Conditions and Domains

To completely solve the system of partial differential equations, adequate boundary conditions are required. Dirichlet boundary conditions prescribe a known value to a given boundary, such as the water/air interface of the source container, where the partial pressure of water vapour is assumed to be in equilibrium, and thus the water vapour concentration at the boundary can be described by the saturation concentration, C_{sat}, given the temperature. For this study the temperature used to calculate the saturation concentration is the average temperature in the bottom source chamber (sensor 1) taken over the entire experiment run time: 23.8°C, which is very close to the mean room temperature of 23.7°C.

The second type of boundary condition, known as the Neumann boundary condition, prescribes a value to the normal derivative of the variable on the boundary, and is used in this work to describe a state of zero flux through the boundary such as on the outside walls of the apparatus. The schematic diagram shown in Figure 5.6 presents both the Dirichlet and Neumann type boundary conditions used in the numerical model. The prescribed boundary conditions are listed below:

- Dirichlet: $C_f = C_{sat}(23.8°\text{C}) = 21.614\ \frac{\text{g}}{\text{m}^3}$
- Neumann: $\frac{\partial C_f}{\partial \vec{n}} = 0$

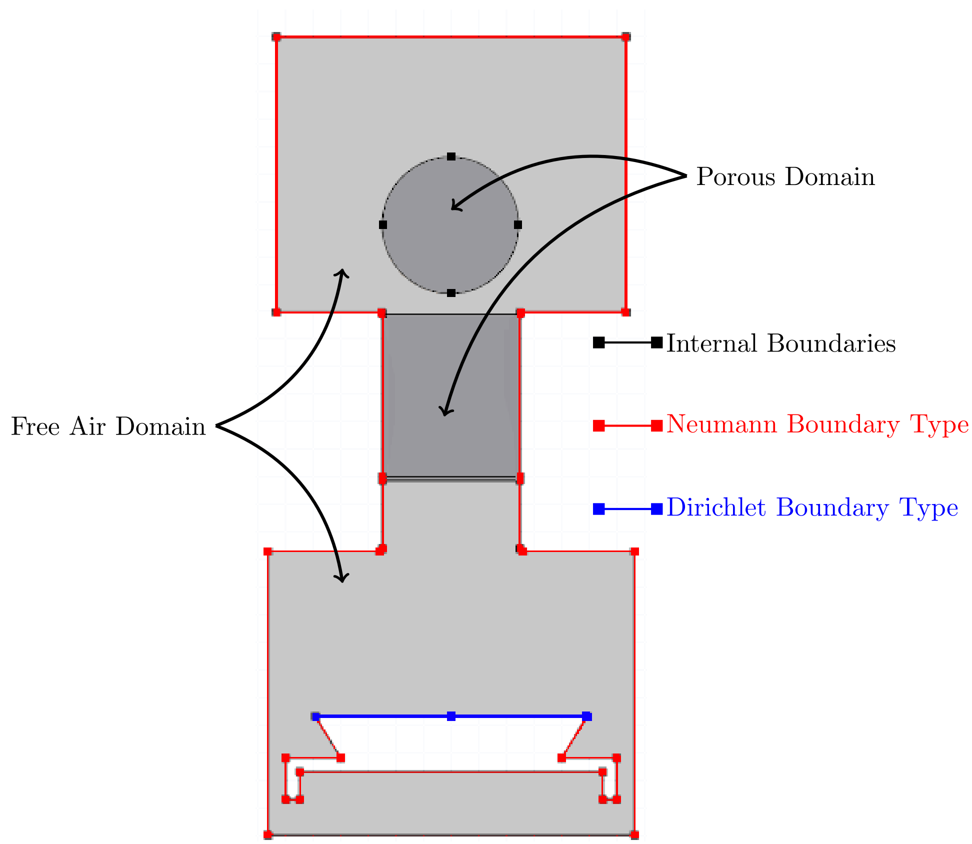

Figure 5.6: *Schematic Diagram of Boundary Conditions and Domains*

Two domain types were used in the model, where the first type is labelled in Figure 5.6 as the Porous Domain, and the conservation equations as described in Section 5.1.4 are applied to model the transport of water vapour in the porous medium. The second type, labelled as Free Air Domain, uses the same conservation equation for C_f, Equation 5.1.8, however the sorption sink term is removed, the porosity is set as 1, and the diffusion coefficient for water vapour in air, D_{WA}, is substituted for the effective diffusion coefficient, D_{eff}, yielding the following conservation equation for the Free Air Domain:

$$\frac{\partial C_f}{\partial t} = -\nabla \cdot (-D_{WA} \nabla C_f) \tag{5.3.1}$$

The adsorbed mass ratio w_s was modelled using a distributed ordinary differential equation and did not require a boundary condition. The internal boundaries between the Free Air and Porous Domains are handled automatically by COMSOL by imposing continuity of the variables across the boundaries.

5.4 Initial Conditions

To solve the system of conservation equations in time, initial conditions are required in all domains. The initial conditions apply to both conserved quantities, C_f as the concentration of water vapour in the free air and porous domains, and w_s as the adsorbed mass ratio of water vapour in the porous domain.

During the diffusion sorption experiment the bottom source chamber was allowed to reach saturation before opening of the door. The concentration was measured continuously, and was used as the initial conditions for C_f in the model. The adsorbed mass ratio w_s was assumed to be zero because the adsorbent was regenerated prior to the experiment, and any sorption of atmospheric water vapour during the filling process was assumed to be negligible.

The concentration as a function of time for all sensors inside the apparatus during Trial 1 (sensors 1 to 5) is shown in Figure 5.7, where the drop in concentration in sensor 1 indicates the opening of the manually operated door, and the beginning of the experiment. The initial conditions as measured by the sensors are recorded in Table 5.3, and were taken as the total time average for each sensor leading up to the moment the door was opened. The initial condition for the bottom chamber domain was set as 21.530 $\frac{\mathrm{g}}{\mathrm{m}^3}$, and all other domains were set as the average of sensors 2 to 5, of 0.244 $\frac{\mathrm{g}}{\mathrm{m}^3}$. The adsorbed mass ratio, w_s, was set as zero in all domains.

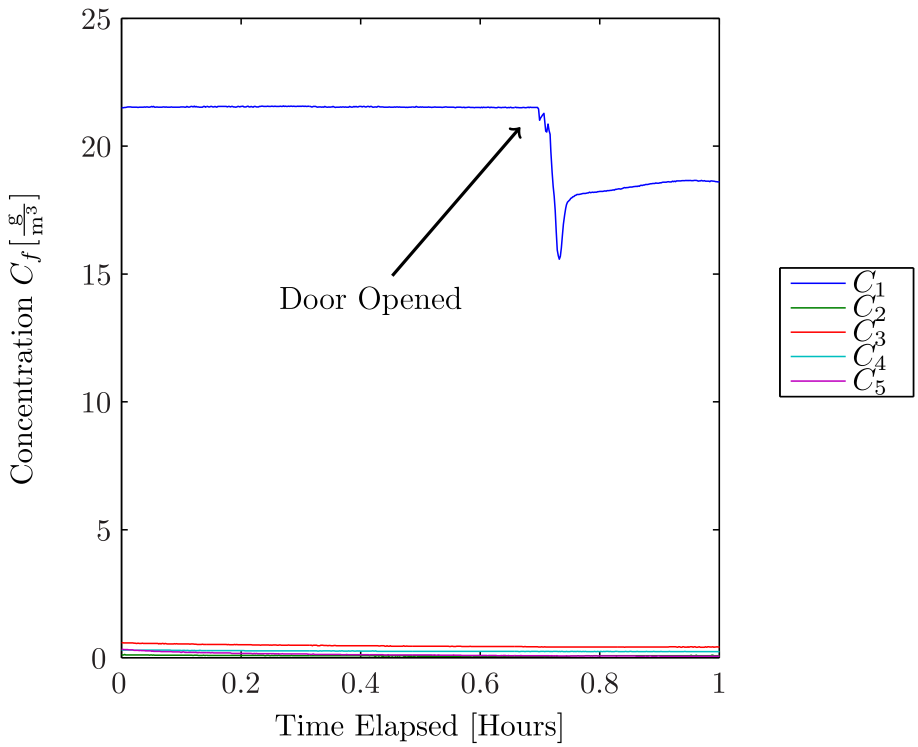

Figure 5.7: *Initial Concentration For Trial 1 Including Door Opening*

Sensor Number	Initial Concentration $[\frac{g}{m^3}]$
1	21.530
2	0.075
3	0.485
4	0.264
5	0.151

Table 5.3: *Numerical Model Initial Conditions For Trial 1*

6

Results and Discussion

This chapter describes the results of the main diffusion sorption experiment. A comparison is made between the experiment and the numerical model for the concentration over time at the various sensor locations. The repeatability of the experiment is discussed by comparing the measured data between the three trials. A sensitivity analysis is conducted for the input parameters, and finally, the sorbed mass is compared between the experiment and the model.

6.1 Concentration Tracking

The mass concentration of water vapour in the fluid phase, denoted by the variable C_f, is measured in the diffusion sorption experiment using five sensors inside the apparatus at discrete points, as previously shown in Figure 4.7. In the numerical model, probe points were used to sample the variable C_f at the same locations. The numerical model was run for the same length of simulation time as the diffusion sorption experiment (approximately fifteen days) and the probe point data was exported for comparison to the measured experimental data.

6.1.1 Comparing Trial 1 with the Numerical Model

The concentrations as a function of time from both the experiment and the numerical model are plotted in Figure 6.1. The time index of zero indicates the moment that the manually sliding door was opened. It can be seen best in Figure 5.7 that the concentration in the bottom source chamber, denoted by sensor 1, decreased as soon as the door was opened, and the water vapour began moving through the silica gel beads. In general, the concentration as function of time for the experiment, and the numerical model, agree very well. This successfully validates the numerical adsorption model and its assumptions. In the following, the discrepancies seen in Figure 6.1 will be analysed.

6.1.2 Temperature Fluctuations

The noise seen in sensor 1 in Figure 6.1 is attributed to variations in temperature observed during the experiment, and the fact that the air in the bottom chamber was at or near the saturation point with water vapour. The temperature fluctuations are also expected to cause buoyancy effects in the

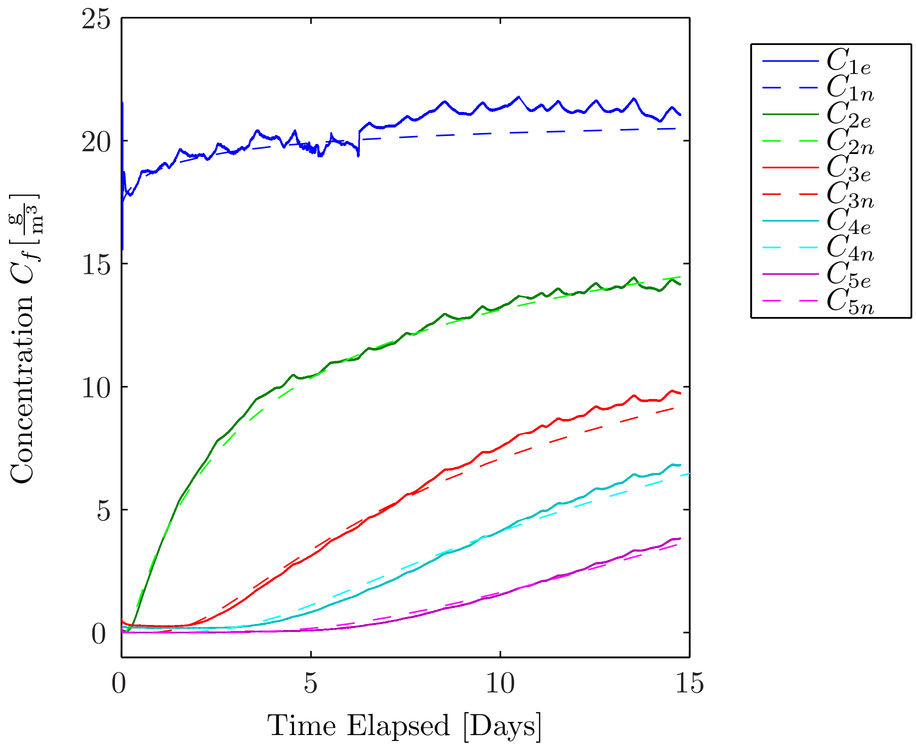

Figure 6.1: *Concentration (C_f) vs. Time Comparing Experiment (C_{ie}) to Numerical Model (C_{in}) for Each Sensor Location i*

bottom chamber, due to differences in density of the humid air. These effects were not accounted for in the numerical model and are noted as a point of further investigation. Additionally, the sensors experience larger uncertainty when measuring at the extreme ends of relative humidity, and could also be contributing to the noise and the deviation from the model.

The diffusion sorption experiment was conducted in a room insulated with 15 cm (6 in) of fibreglass batting on all sides, and with the approximate internal dimensions of 1.8m $\times$ 1.8m $\times$ 2.7m. The intent for housing the experiment in the room was to eliminate any outside influence from temperature fluctuations, however, as seen in Figure 6.1, the spikes in concentration for all sensors occur periodically and coincide with the activation of the building HVAC system in the early morning. Nonetheless, variations within the insulated room were much smaller than the ambient conditions outside the room.

The steady depression and volatility of concentration shown in sensor 1 (between days 3 to 6) coincided with a large drop in the external atmospheric temperature as found in data supplied by the campus weather station of the Earth and Atmospheric Science Department for the same time period, and shown in Figure 6.2[60].

A correlation can be seen between the temperature outside the building and the temperature in the bottom source chamber, indicating that the diffusion sorption experiment was not absolutely shielded from the external influence of temperature fluctuations outside the insulated room. The fluctuations were likely the direct cause of the building's HVAC system responding to the atmospheric temperature fluctuations. This is noted as a source of uncertainty that may be minimized in future experiments with active temperature control.

6.1.3 Repeatability

The first trial in the diffusion sorption experiment lasted for approximately 15 days. In the weeks that followed, a second and third trial were run in an effort to replicate the same results as the first trial. Trial 2 and 3 lasted approximately 10 days each due to time constraints, and the same experimental procedure was applied as in Trial 1.

The concentration versus time for sensors 1-4 has been plotted in Figures 6.3 and 6.4 where the results from each of the trials are superimposed to illustrate the repeatability of the diffusion sorption experiment.

In general the data from the three trials agree fairly well with each other, and the measurements in the bottom chamber (sensor 1) show a significant amount of noise, due to the reasons explained previously. The second trial's data, for the sensors that were located higher in the apparatus (sensor 2 to 4), tended

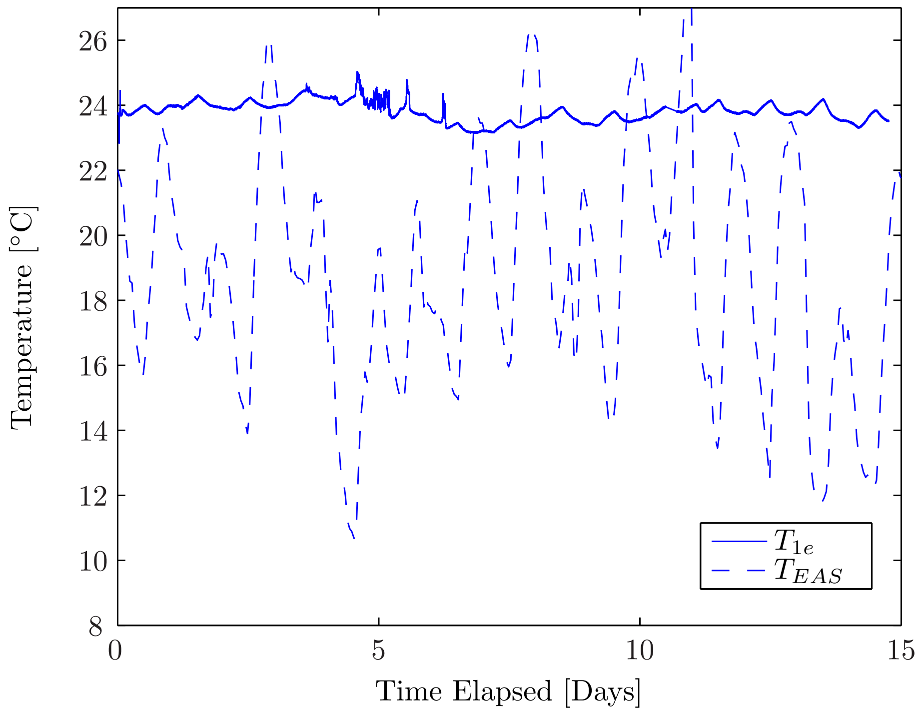

Figure 6.2: *Temperature vs. Time Comparing Trial 1, Sensor 1 (T_{1e}) to EAS Weather Station (T_{EAS})*

to diverge from the first and third trial, which is attributed to a combination of the inability to control the sensor positions exactly during setup of the experiment, and that the final bead filling height was approximately 5 mm lower than Trial 1 and 3.

Therefore, there were less silica gel beads used in the second trial, and the water vapour concentration profile increased sooner than the other two trials. It should be noted that the data acquisition from Trial 3 was interrupted between days 3-7, due to loss of power in the building where the experiment was located. The sensors were unable to record for that time period, but were restarted when the power returned.

The exact location of the sensors and bead fill height appeared to be sensitive parameters to the experiment and warranted further exploration with the numerical model. A sensitivity study has been conducted for all relevant input parameters, and is discussed in the following section.

It can be concluded from Figures 6.3 and 6.4, that the diffusion sorption experiment was repeatable and that the data from Trial 1 is not spurious. The data is then valid for comparison to the numerical model.

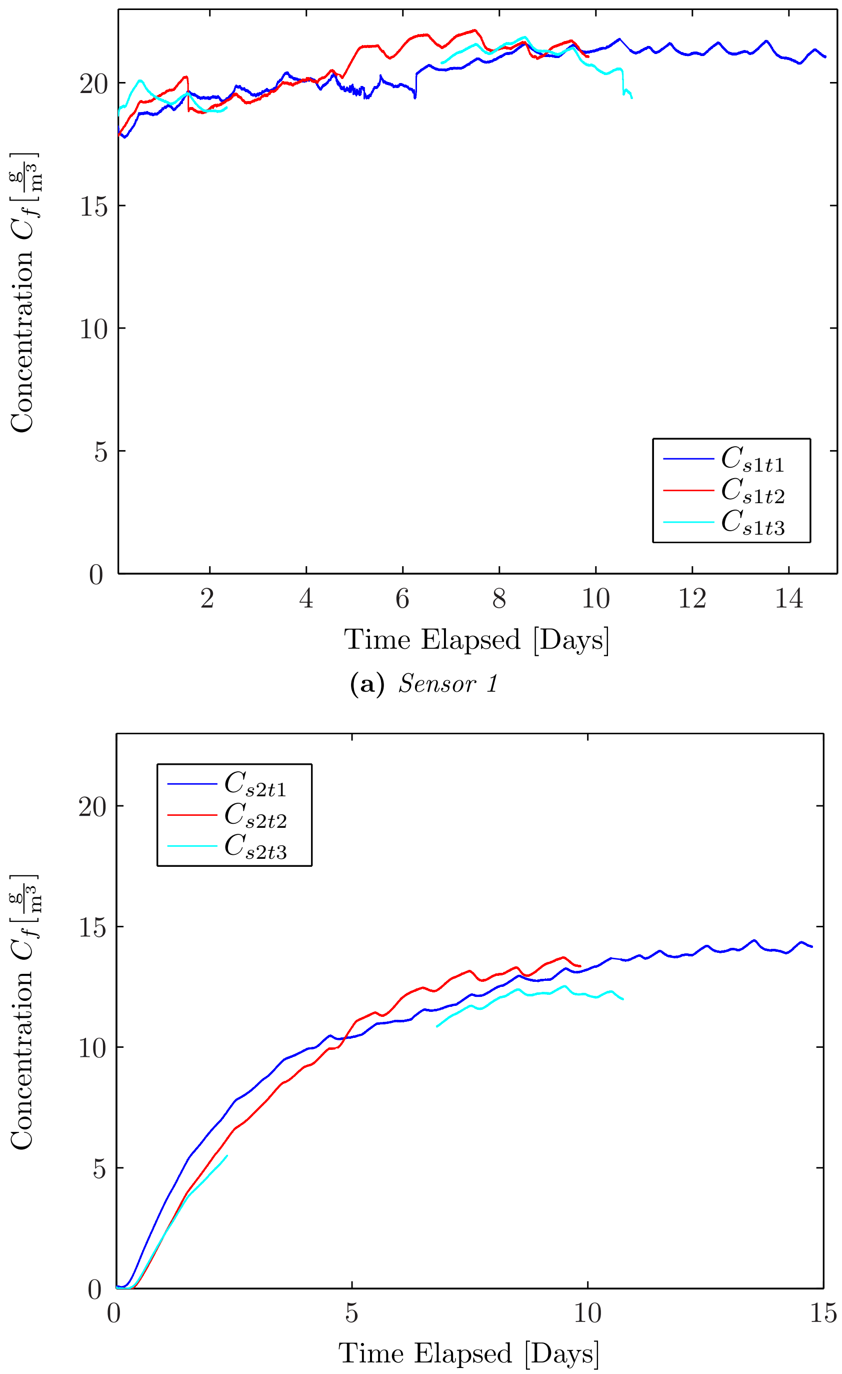

(a) *Sensor 1*

(b) *Sensor 2*

Figure 6.3: *Repeatability of Diffusion Sorption Experiment for Sensors (s) 1 & 2 in Trials (t) 1,2,3*

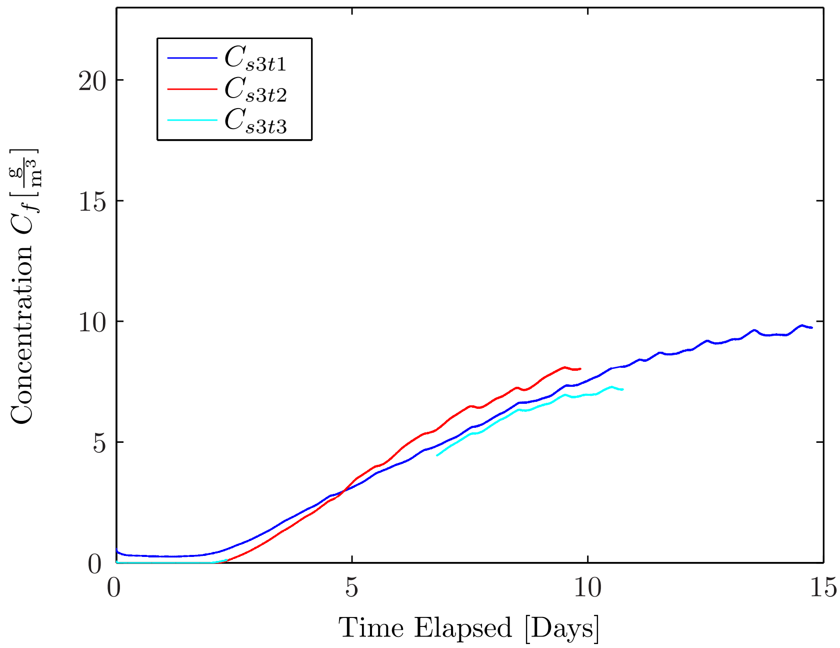

(a) *Sensor 3*

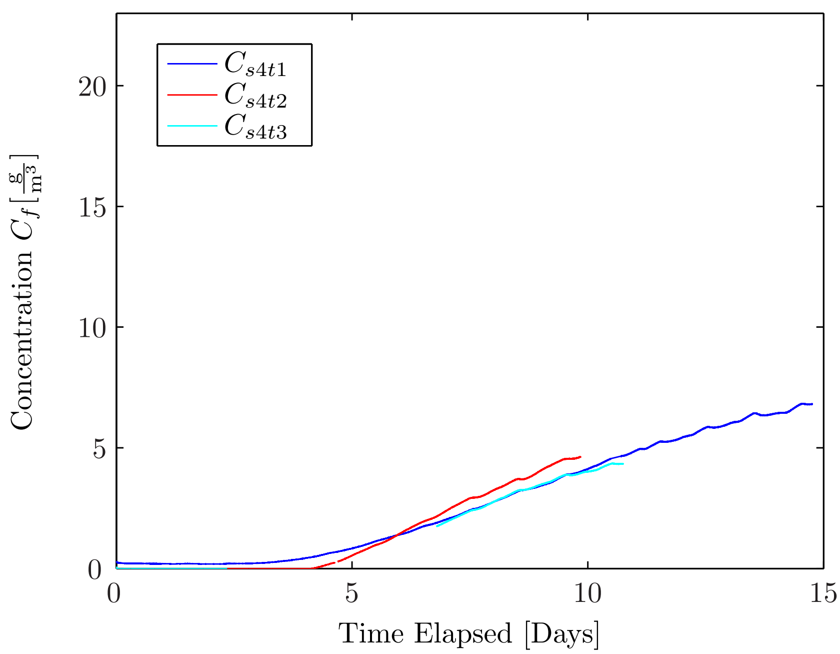

(b) *Sensor 4*

Figure 6.4: *Repeatability of Diffusion Sorption Experiment for Sensors (s) 3 & 4 in Trials (t) 1,2,3*

6.1.4 Sensitivity

It is desirable to know how the input parameters affect the numerical model, because the sensitivity of a monitored output parameter can provide insight into the behaviour of adsorption in porous media in general, and lead to conclusions about the relative importance of the parameters for use in future studies. The root mean square deviation (RMSD) of the numerical model from the experimental data was chosen as the variable for monitoring sensitivity and is defined as:

$$\mathrm{RMSD} = \sqrt{\frac{\sum_{t=1}^{n}(\hat{C}_t - C_t)^2}{n}} \tag{6.1.1}$$

where the concentration from the model, $\hat{C}_t$, is compared to the measured concentration at the same time, C_t, and n is the number of data points. The RMSD is computed for each sensor location.

The RMSD was calculated for each of the five sensors in the numerical model using the original inputs from Table 5.1 and serves as a baseline comparison for the perturbation of the parameters.

The sensitivity analysis was conducted by changing the input parameters one at a time by 10%, and the numerical model was run again using the perturbed parameter. The resulting concentration vs. time curve for each sensor is compared to the experimental data using equation 6.1.1, and the results are recorded in Table 6.1.

The total sum of the RMSD's from each sensor is shown in Table 6.1 because the sum can be compared to the value of the baseline sum to estimate the sensitivity of the parameter perturbation. The baseline total RMSD, using the original input parameters, was 1.810 $\frac{\mathrm{g}}{\mathrm{m}^3}$. All perturbations caused a worse

Parameter	[Units]	Baseline	10% Change	$\sum RMSD \frac{\mathrm{g}}{\mathrm{m}^3}$
ϕ	[1]	0.611	0.672	3.988
y_{probe}	[cm]	See Fig. 4.7	$\times 1.1$	3.833
ρ_{bulk}	$[\frac{\mathrm{g}}{\mathrm{cm}^3}]$	0.824	0.906	2.742
κ	$[\frac{\mathrm{m}^3}{\mathrm{kg}}]$	88.728	97.6	2.178
Γ	$[\frac{\mathrm{kg}}{\mathrm{kg}}]$	0.426	0.468	2.178
τ	[1]	1.98	2.18	1.998
α_{sf}	$[\frac{1}{\mathrm{s}}]$	$0.0072 \cdot e^{\left(0.0344 \cdot \frac{C_f}{C_{sat}}\right)}$	$\times 1.1$	1.661
D_{eff}	$\left[\frac{\mathrm{cm}^2}{\mathrm{s}}\right]$	$7.813 \cdot 10^{-2}$	$8.594 \cdot 10^{-2}$	1.910

Table 6.1: *Input Parameters and Sensitivity Study Results compared with the baseline RMSD of 1.81* $\frac{\mathrm{g}}{\mathrm{m}^3}$

fit of the numerical model compared to the experimental data, except for the results from α_{sf}. It can be concluded that the mass transfer coefficient as found previously, may be improved to provide a more accurate model.

The input parameters that were most sensitive to the perturbation are, in order: the porosity, the sensor location (as denoted by y_{probe}), and the bulk density. The sensor location was significantly sensitive, as the change was on the order of millimeters, which is on the scale of the sensor's form factor. It is recommended that care should be taken in future experiments to carefully control the sensor positions, or to increase the length of the porous medium channel to reduce the sensitivity of the sensor's placement.

It should be noted that the sensitivity study does not address coupled behaviour between parameters as they were perturbed one at a time. The full concentration vs. time plots for all parameter perturbations are included in Appendix H.

6.1.5 Comparing Kinetic Sorption to Local Instantaneous Equilibrium Adsorption

In Section 5.1.1, the Damköhler number was discussed, where the local instantaneous equilibrium adsorption (LIEA) assumption was shown to be invalid for this study, and a kinetic form of the conservation equations relating to adsorption was required. It can be further shown that using the LIEA assumption in the conservation equation for C_f (as in Equation 2.4.12), that the analysis of the Damköhler number was indeed correct, when compared to the kinetic equations.

In Figure 6.5, the experiment data from Trial 1, at sensor 2, is shown with the kinetic form of the conservation equations as before, with the addition of a simulation run using the LIEA conservation equation, and the same input parameters as the kinetic model. The LIEA assumption severely retards the diffusion of water vapour through the silica gel porous medium, and does not match the experimental data well as can be seen from the RMSD analysis in Figure 6.6. The LIEA assumption is thus not valid for this study and the use of the Damköhler number as a predictor is verified.

6.2 Sorbed Mass

The second variable tracked in the numerical model was the adsorbed mass ratio in the porous media, denoted by w_s, and is converted to sorbed mass by multiplying the bulk density ρ_{bulk}. The sorbed mass was also measured in the diffusion sorption experiment by measuring the 'wet' mass of the beads as quickly as possible after the experiment was shut down, and then subtracting the 'dry' mass, which was measured after baking the sample of beads from the channel in the experiment.

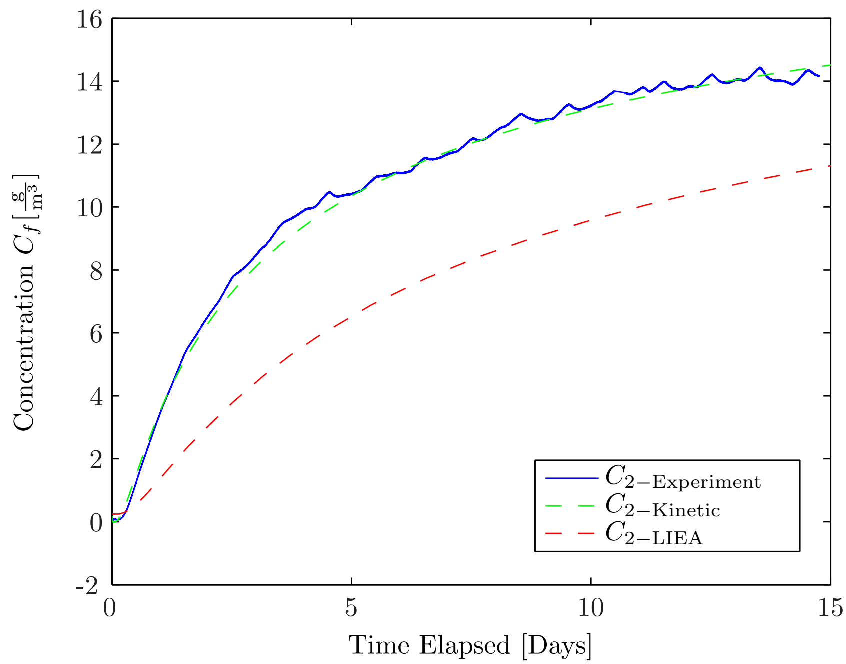

Figure 6.5: *Comparing LIEA to Kinetic Conservation Equations on Sensor 2*

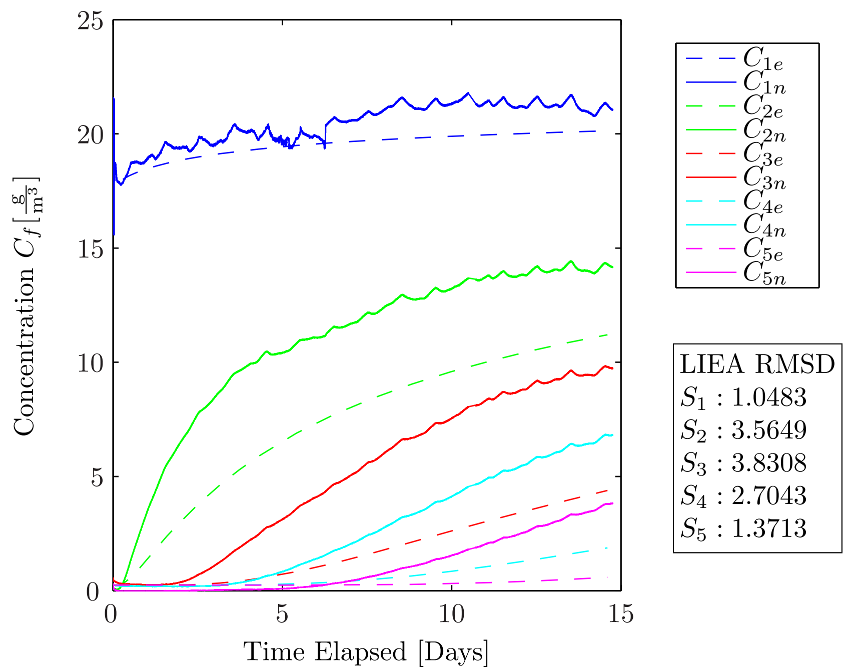

Figure 6.6: *RMSD for LIEA on Every Sensor (s) Compared to Trial 1*

6.2.1 Intermediate Sorbed Mass

The first trial of the diffusion sorption experiment had a total run time of 14.760 days, after which the mass of the silica gel beads was measured, both before and after baking. The mass difference was assumed to be the mass of water sorbed at the end time of the experiment, and is called the intermediate sorbed mass (to distinguish from the steady state sorbed mass). The measurement process neglects any de-gassing of the beads to the atmosphere prior to weighing, and also assumes that the baking process did not alter the physical structure of the beads.

The simulation time, in the numerical model of the first trial, was set to the same length of time as the diffusion sorption experiment. The concentration of adsorbed mass in the last timestep of the simulation, w_s, was then used to calculate the intermediate sorbed mass, m_{ads}, by integrating over the entire volume of the channel, and multiplying by the bulk density:

$$m_{ads} = \rho_{bulk} \left(\int w_s dV \right) \tag{6.2.1}$$

The results of the integration are compared to the measured mass in Table 6.2. The intermediate sorbed mass from the numerical model agrees to within 10% of the experiment's mass. Additionally, the intermediate masses in the second and third trials were measured, and the trials had a total run time of 9.847 and 10.748 days respectively. The numerical model was used with the same input parameters as the first trial, and the final sorbed mass was found in the same manner as Trial 1.

The intermediate sorbed mass in the second and third trial shows that the mass measurement process is repeatable, and that the simulation has better agreement for the later trials even though the input parameters used were that of Trial 1.

Trial	Wet Mass [g]	Dry Mass [g]	m_{ads} $[g]$	$\rho_{bulk}\left(\int w_s dV\right)$ [g]	% Error
1	139.190	114.379	24.811	22.695	8.528
2	129.566	111.213	18.353	19.193	-4.576
3	134.286	113.837	20.449	19.939	2.494

Table 6.2: *Intermediate Sorbed Mass Comparison*

Langmuir Equation [g]	Numerical Model [g]	% Error
34.013	34.079	-0.194

Table 6.3: *Steady State Sorbed Mass Comparison*

6.2.2 Steady State Value

The numerical model was also simulated to steady state conditions, where both the adsorbent and the free fluid were saturated with water vapour. The total sorbed mass at steady state, m_{ads-SS}, was found by integrating w_s over the volume of the channel as before, and is recorded in Table 6.3. This value can be compared to the result expected from the Langmuir equilibrium sorption equation (Eq. 2.1.2), inserting the saturation concentration used in the experiment, C_{sat}, and multiplying by the bulk density, ρ_{bulk}, and the volume, V, of the beads in the channel ($5 \times 5 \times 5.9 = 147.5$ cm^3):

$$m_{ads-SS} = \rho_{bulk}\left(\Gamma \frac{\kappa C_{sat}}{1 + \kappa C_{sat}}\right) V \tag{6.2.2}$$

The steady state sorbed mass predicted by the numerical model is less than 0.2% different than the sorbed mass found using the Langmuir equation. It can be concluded that the numerical model adequately tracks the sorbed mass both at intermediate times to within 10% of the experimental value, and that the theoretical value at steady state found from the Langmuir equation matches very well with that predicted by the numerical model.

6.2.3 Temperature Deviation

The intermediate sorbed mass was only within 10% of the experimental value. The cause of this discrepancy may be attributed in part to the use of an averaged external temperature measured in Trial 1 (23.8°C). The averaged temperature was used in the numerical model to establish the Dirichlet boundary condition at the water surface, however in reality the temperature of the water was not constant, and should have been measured directly to provide a more accurate boundary condition.

Additionally, the deviation of the temperature in the porous medium, from that used in Langmuir equilibrium sorption experiment (25°C), influenced the adsorption characteristics of the porous media. This study used an isothermal assumption in development of the conservation equations as this assumption is found to be common in literature when characterizing adsorption. However, without active temperature control the heat of adsorption altered the temperature in the porous media and changed the state of equilibrium.

The temperature deviation from 25°C in the porous medium, as measured by sensors 2-4, has been plotted in Figure 6.7. The temperature in the silica gel beads at the location of sensor 2 (entrance region) deviated 3°C initially due to the heat of adsorption, then cooled over the first five days. After which all sensors maintained a temperature deviation between 1 and 1.5°C *lower* than 25°C. According to adsorption theory, a lower temperature would increase the sorbed mass of water vapour at equilibrium, and thus the measured sorbed mass would be *higher* than that predicted by the numerical model in this work. This is indeed the case for Trial 1, as seen in Table 6.2, where the measured sorbed mass, m_{ads}, is approximately 8.5% higher than that predicted by the model.

It can be concluded that the deviation of the temperature in the porous medium from the assumed isothermal conditions has a significant effect on the time dependent sorbed mass. Actively controlling the temperature of the system to match isothermal conditions can provide closer agreement between the numerical model proposed here, and the data from the diffusion sorption experiments.

The use of an energy equation, coupled with the heat of adsorption and mass conservation equations, could provide a more accurate and realistic model for mass transport in porous media with adsorption. The sorption equilibrium equation, such as the Langmuir isotherm, would necessarily become a function of temperature, leading to a much more complex numerical model to solve. It is apparent that the local temperature plays a significant role in adsorption, and any numerical models developed to study water vapour transport during the diurnal cycle in the regolith on Mars, should include the effects of non-isothermal adsorption.

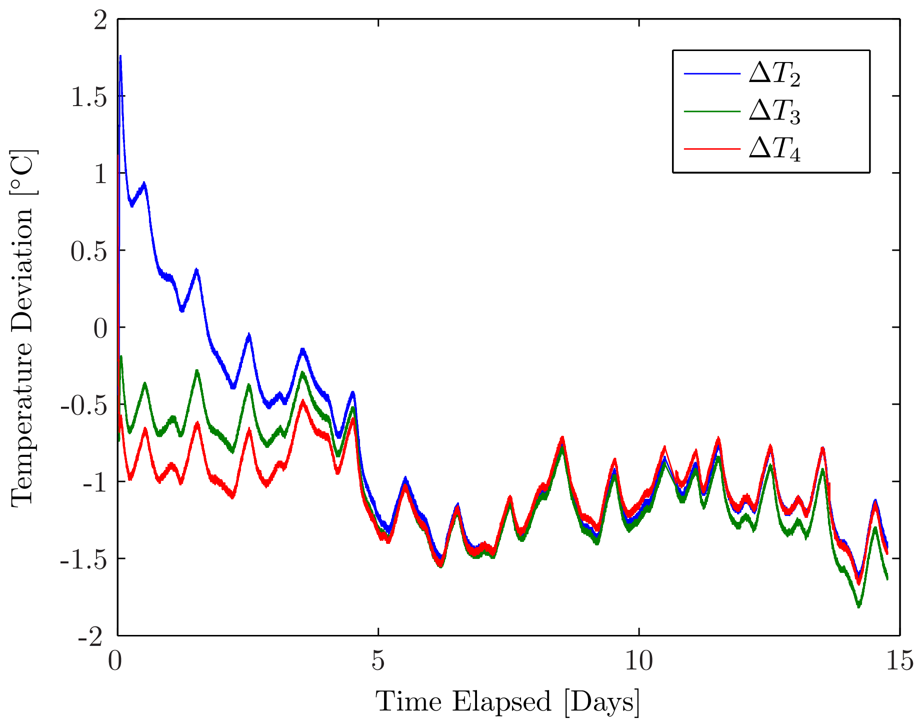

Figure 6.7: *Temperature Deviation from* 25°C *inside Porous Medium, Trial 1, Sensor i* (ΔT_i)

7

Conclusion

This chapter describes the conclusions to be drawn from the diffusion sorption experiments and the numerical model developed in this work. The deficiencies in the model are discussed, and recommendations are made for improving the experiment. Finally a discussion of future work is presented, regarding improvement of the model by adding an energy conservation equation and including the effects of temperature, and the heat of adsorption.

7.1 Experiment and Numerical Model

It is the intent of the CFD Lab, at the University of Alberta, to develop a numerical model of the transport of water vapour on the surface of Mars. The model is to include the exchange of water vapour between the subsurface water-ice sheet, and the basal atmospheric boundary layer, which passes through the porous medium known as regolith. It has been shown that the physical process known as adsorption plays a significant role in the transport and storage of water vapour in the regolith on Mars.

A numerical model of the transport of water vapour should include the effects of adsorption, and investigators associated with the study of adsorption on Mars have developed one dimensional transport equations, where they invoked the local instantaneous equilibrium adsorption assumption. Typically, the investigators have explored adsorption on geological time scales, where the local instantaneous equilibrium adsorption assumption was valid. However, the rate of adsorption can be important on much shorter time scales, such as the diurnal cycle on Mars, and is a strong function of the relative grain size, porosity, and bulk density of the medium.

The Damköhler number is a non-dimensional ratio of the rate of diffusion of mass through a porous medium, compared to the rate of adsorption of that mass. This study has shown that the Damköhler number is a useful predictor of whether the local instantaneous equilibrium adsorption assumption may be used in modelling the transport of water vapour in porous media.

For Damköhler numbers much less than unity, as found in the diffusion sorption experiment in this study, the conservation equations must use a kinetic rate of flux to model adsorption, instead of the local instantaneous equilibrium form. The latter of which predicts much slower transport of water vapour through silica gel beads when compared to the experimental data.

The numerical model developed in this study, uses the kinetic form of the conservation equations and agrees very well with the measured concentration vs. time at specified probe points. Additionally the intermediate sorbed mass of water vapour predicted in the model, agrees within 10% of measured values.

The numerical model assumed an isothermal system everywhere, and the Dirichlet boundary condition was modelled with a fixed temperature of 23.7°C. This temperature was obtained from the time averaged external temperature for the diffusion sorption experiment. In general, the concentration of water vapour above a liquid water source is sensitive to temperature. In the experiment, however, the temperature of the water was not measured, and remains a source of uncertainty in the model.

The isothermal equilibrium adsorption data for the silica gel was obtained in a sorption analyzer at 25°C. However, the measured temperature in the silica gel beads in the diffusion sorption experiment deviated from 25°C, initially it was higher due to the heat of adsorption, and later it was lower than 25°C due to the dissipation of the heat, and the cool external temperature.

The adsorbed mass at equilibrium is dependent on the temperature of the adsorbate, where a lower temperature is expected to adsorb more water vapour. The measured adsorbed mass of water vapour in the experiment was indeed higher than that predicted by the model, and a more accurate model of adsorption should include the effect of changing temperature.

The data from the sorption analyzer suggested complex behaviour in the process of sorption of water vapour on silica gel beads, that may be more accurately described with a Type IV isotherm. However, the Type I (Langmuir) isotherm was used to model the equilibrium sorption and despite the simple assumptions in Langmuir theory, the isotherm worked satisfactorily in this case.

7.1.1 Improvements to the Diffusion Sorption Experiment

The diffusion sorption experiment could be improved to reduce the uncertainty in the measured results. The point specific relative humidity and temperature as measured in the apparatus was sensitive to the sensor placement. The sensors were connected by flexible data cables that deformed when the silica gel beads were poured into the channel. A rigid wire or other suitable support structure could have been placed in the channel to mount the sensors.

Increasing the height of the channel would also reduce the sensitivity to the sensor placement, however the total run time of the diffusion sorption experiment would have increased significantly. To reduce the total run time, the cross section area of the channel could be reduced.

The concentration measured in the experiment was shown to be sensitive to the external temperature fluctuations in the building, despite being in a well insulated room. An active temperature control system, such as the one used in the calibration procedure, would eliminate any influence from external temperatures, and would also create a true isothermal system in the apparatus, if adequate thermal conductors were placed on the channel section to remove the heat of adsorption. The numerical model as developed in this work may then have a better fit to the experimental data.

Lastly, an analysis of the Péclet number showed that advection may play a role if any pressure differential exists across a porous medium. Any uncertainty due to pressure can be eliminated by the addition of a conduit between the top and bottom chamber, such as a flexible hose, which is partially filled with a liquid, such as oil or other suitable buffer. The buffer would move if any pressure gradient existed, but would not allow the passage of water vapour through the conduit.

7.2 Future Work

The adsorption of any species on an adsorbent is strongly dependent on temperature. It is also known that the isotherms generated in equilibrium sorption experiments, such as with the VTI-SA sorption analyzer, are typically very specific for a given adsorbent/adsorbate pair, at that temperature. During adsorption, the temperature of the adsorbent and the surrounding fluid will increase as the adsorbate 'condenses' or adsorbs to the surface. This heat of adsorption affects the equilibrium conditions, and should be incorporated in the adsorption model.

The heat of adsorption has been discussed in the literature[25], and it is suggested that isotherms may be extrapolated to different temperatures using the heat of adsorption, and sorption equilibrium equations derived from first principles. However, the extrapolation appears best suited for small deviations from the original isotherm temperature and doesn't account for the complex behaviour that is encountered in most porous media, such as the varying scales of pore sizes, dead end pores, where adsorption ends and condensation begins, capillary filling, neglecting changes in chemistry of the medium, or the porosity (from dissolution of the solid matrix), etc.

Due to all of these complexities, adsorption research has typically focused on empirical measurements of the specific adsorbent/adsorbate, over a range of temperatures at best. To develop an accurate model of mass transport and adsorption in the Martian regolith, the next logical step would be to obtain simulated Martian regolith such as JSC (Mars-1), or Salten Skov, and measure the porosity, bulk density, and adsorption isotherms under Martian conditions. Until these measurements can be made on actual Martian regolith, the analogous data can be used in the numerical model proposed in this work to simulate the effect of adsorption.

Finally to increase the accuracy of the model, an energy balance equation must be used to account for the heat of adsorption, and the transport of heat through the system. The energy balance would be coupled to the mass transport equation through the adsorption equilibrium (isotherm) equation.

The tracking of heat due to adsorption could play an important role in the study of the water cycle on Mars, as the possibility of liquid water becomes more likely. This is because the perchlorate salts, found at the Phoenix Mars Lander site, are known to depress the melting point of the water solution. The added heat of adsorption may be enough to keep a constant liquid layer in the rock-ice interface in the regolith, that exists through the diurnal cycles on Mars, and provide a habitable location for alien life.

References

[1] M.H. Hecht, S.P. Kounaves, R.C. Quinn, S.J. West, S.M.M. Young, D.W. Ming, D.C. Catling, B.C. Clark, W.V. Boynton, J. Hoffman, et al. Detection of perchlorate and the soluble chemistry of martian soil at the Phoenix lander site. *Science*, 325(5936):64–67, 2009.

[2] W.V. Boynton, D.W. Ming, S.P. Kounaves, S.M.M. Young, R.E. Arvidson, M.H. Hecht, J. Hoffman, P.B. Niles, D.K. Hamara, R.C. Quinn, et al. Evidence for calcium carbonate at the Mars Phoenix landing site. *Science*, 325(5936): 61–64, 2009.

[3] T.N. Titus, H.H. Kieffer, and P.R. Christensen. Exposed water ice discovered near the south pole of Mars. *Science*, 299(5609):1048–1051, 2003.

[4] P.H. Smith, L.K. Tamppari, R.E. Arvidson, D. Bass, D. Blaney, W.V. Boynton, A. Carswell, D.C. Catling, B.C. Clark, T. Duck, et al. H2o at the Phoenix landing site. *Science*, 325(5936):58–61, 2009.

[5] K.E. Williams, O.B. Toon, J.L. Heldmann, and M.T. Mellon. Ancient melting of mid-latitude snowpacks on Mars as a water source for gullies. *Icarus*, 200 (2):418–425, 2009.

[6] M.T. Mellon and R.J. Phillips. Recent gullies on Mars and the source of liquid water. *Journal of Geophysical research*, 106(E10):23165–23180, 2001.

[7] E.G. Nisbet, N.H. Sleep, et al. The habitat and nature of early life. *Nature*, 409(6823):1083–1091, 2001.

[8] L.J. Rothschild. Earth analogs for Martian life. microbes in evaporites, a new model system for life on Mars. *Icarus*, 88(1):246–260, 1990.

[9] R. Popa, A.R. Smith, R. Popa, J. Boone, and M. Fisk. Olivine-respiring bacteria isolated from the rock-ice interface in a lava-tube cave, a Mars analog environment. *Astrobiology*, 12(1):9–18, 2012.

[10] A.P. Zent, M.H. Hecht, D.R. Cobos, S.E. Wood, T.L. Hudson, S.M. Milkovich, L.P. DeFlores, and M.T. Mellon. Initial results from the thermal and electrical conductivity probe (TECP) on Phoenix. *J. Geophys. Res*, 115:E00E14, 2010.

[11] J. Zubik. Computational study of the water cycle at the surface of Mars. Master's thesis, University of Alberta, 2012.

[12] D.T.F. Möhlmann. The influence of van der Waals forces on the state of water in the shallow subsurface of Mars. *Icarus*, 195(1):131–139, 2008.

[13] F.P. Fanale and W.A. Cannon. Exchange of adsorbed H_2O and CO_2 between the regolith and atmosphere of Mars caused by changes in surface insolation. *Journal of Geophysical Research*, 79(24):3397–3402, 1974.

[14] F.P. Fanale and W.A. Cannon. Mars: CO_2 adsorption and capillary condensation on clays: significance for volatile storage and atmospheric history. *Journal of Geophysical Research*, 84(B14):8404–8414, 1979.

[15] B.M. Jakosky and C.B. Farmer. The seasonal and global behavior of water vapor in the Mars atmosphere: Complete global results of the Viking atmospheric water detector experiment. *Journal of Geophysical Research*, 87(B4): 2999–3019, 1982.

[16] B.M. Jakosky, A.P. Zent, and R.W. Zurek. The Mars water cycle: Determining the role of exchange with the regolith. *Icarus*, 130(1):87–95, 1997.

[17] P. Beck, A. Pommerol, B. Schmitt, and O. Brissaud. Kinetics of water adsorption on minerals and the breathing of the martian regolith. *Journal of Geophysical Research*, 115(E10):E10011, 2010.

[18] V. Chevrier, D.R. Ostrowski, and D.W.G. Sears. Experimental study of the sublimation of ice through an unconsolidated clay layer: Implications for the stability of ice on Mars and the possible diurnal variations in atmospheric water. *Icarus*, 196(2):459–476, 2008.

[19] K.L. Bryson, V. Chevrier, D.W.G. Sears, and R. Ulrich. Stability of ice on Mars and the water vapor diurnal cycle: Experimental study of the sublimation of ice through a fine-grained basaltic regolith. *Icarus*, 196(2):446–458, 2008.

[20] D.W.G. Sears and S.R. Moore. On laboratory simulation and the evaporation rate of water on Mars. *Geophysical research letters*, 32(16):L16202, 2005.

[21] J.D. Chittenden, V. Chevrier, L.A. Roe, K. Bryson, R. Pilgrim, and D.W.G. Sears. Experimental study of the effect of wind on the stability of water ice on Mars. *Icarus*, 196(2):477–487, 2008.

[22] I. Langmuir. The adsorption of gases on plane surfaces of glass, mica and platinum. *Journal of the American Chemical Society*, 40(9):1361–1403, 1918.

[23] S. Brunauer, P.H. Emmett, and E. Teller. Adsorption of gases in multimolecular layers. *Journal of the American Chemical Society*, 60(2):309–319, 1938.

[24] J. Bear and A.H.D. Cheng. *Modeling groundwater flow and contaminant transport*. Springer, 2010.

[25] D.D. Do. *Adsorption analysis: equilibria and kinetics*, volume 2. World Scientific, 1998.

[26] J.F. Richardson, J.M. Coulson, J.H. Harker, and J.R. Backhurst. *Chemical engineering: Particle technology and separation processes*. Coulson & Richardson's Chemical Engineering. Butterworth-Heinemann, 2002. ISBN 9780750644457.

[27] K.C. Chen. The influence of dust devils on Martian water vapour transport. Master's thesis, University of Alberta, 2011.

[28] L. Prieto. A numerical study of local water vapour transport. Master's thesis, University of Alberta, 2006.

[29] R.T. Yang. *Adsorbents: fundamentals and applications.* Wiley-Interscience, 2003.

[30] S. Brunauer, L.S. Deming, W.E. Deming, and E. Teller. On a theory of the van der Waals adsorption of gases. *Journal of the American Chemical Society*, 62(7):1723–1732, 1940.

[31] C.G.V. Burgess, D.H. Everett, S. Nuttall, et al. Adsorption hysteresis in porous materials. *Pure Appl. Chem*, 61(11):1845–1852, 1989.

[32] S. Reyes and K.F. Jensen. Estimation of effective transport coefficients in porous solids based on percolation concepts. *Chemical engineering science*, 40 (9):1723–1734, 1985.

[33] J. Rouquerol, D. Avnir, C.W. Fairbridge, D.H. Everett, J.M. Haynes, N. Pernicone, J.D.F. Ramsay, K.S.W. Sing, K.K. Unger, et al. Recommendations for the characterization of porous solids (technical report). *Pure and Applied Chemistry*, 66(8):1739–1758, 1994.

[34] D. Dollimore and G.R. Heal. An improved method for the calculation of pore size distribution from adsorption data. *Journal of Applied Chemistry*, 14(3): 109–114, 1964.

[35] C. Lastoskie, K.E Gubbins, and N. Quirke. Pore size distribution analysis of microporous carbons: a density functional theory approach. *The Journal of Physical Chemistry*, 97(18):4786–4796, 1993.

[36] T. Dogu and G. Dogu. A grain model for catalyst tortuosity. *Chemical Engineering Communications*, 103(1):1–9, 1991.

[37] C.A. León y León. New perspectives in mercury porosimetry. *Advances in Colloid and Interface Science*, 76:341–372, 1998.

[38] K. Seiferlin, P. Ehrenfreund, J. Garry, K. Gunderson, E. Hütter, G. Kargl, A. Maturilli, and J.P. Merrison. Simulating Martian regolith in the laboratory. *Planetary and Space Science*, 56(15):2009–2025, 2008.

[39] J.F. Bell, H.Y. McSween, J.A. Crisp, R.V. Morris, S.L. Murchie, N.T. Bridges, J.R. Johnson, D.T. Britt, M.P. Golombek, H.J. Moore, et al. Mineralogic and compositional properties of Martian soil and dust: Results from Mars Pathfinder. *Journal of Geophysical Research: Planets (1991–2012)*, 105(E1): 1721–1755, 2000.

[40] P. Malbrunot, D. Vidal, J. Vermesse, R. Chahine, and T.K. Bose. Adsorbent helium density measurement and its effect on adsorption isotherms at high pressure. *Langmuir*, 13(3):539–544, 1997.

[41] T. Woignier and J. Phalippou. Skeletal density of silica aerogels. *Journal of Non-Crystalline Solids*, 93(1):17–21, 1987.

[42] A. Ayral, J. Phalippou, and T. Woignier. Skeletal density of silica aerogels determined by helium pycnometry. *Journal of Materials Science*, 27(5):1166–1170, 1992.

[43] N. Epstein. On tortuosity and the tortuosity factor in flow and diffusion through porous media. *Chemical Engineering Science*, 44(3):777–779, 1989.

[44] B.P. Boudreau. The diffusive tortuosity of fine-grained unlithified sediments. *Geochimica et Cosmochimica Acta*, 60(16):3139–3142, 1996.

[45] T.L Hudson. *Growth, diffusion, and loss of subsurface ice on Mars: Experiments and models*. PhD thesis, California Institute of Technology, 2008.

[46] R.B. Bird, W.E. Stewart, and E.N. Lightfoot. *Transport phenomena*. Wiley, 2006.

[47] E.B. Arkilic, M.A. Schmidt, and K.S. Breuer. Gaseous slip flow in long microchannels. *Microelectromechanical Systems, Journal of*, 6(2):167–178, 1997.

[48] W.J. Massman. A review of the molecular diffusivities of H_2O, CO_2, CH_4, CO, O_3, SO_2, NH_3, N_2O, NO, and NO_2 in air, O_2 and N_2 near STP. *Atmospheric Environment*, 32(6):1111–1127, 1998.

[49] M. Huysmans and A. Dassargues. Review of the use of péclet numbers to determine the relative importance of advection and diffusion in low permeability environments. *Hydrogeology Journal*, 13(5-6):895–904, 2005.

[50] W.D. Carrier III. Goodbye, Hazen; hello, Kozeny-Carman. *Journal of Geotechnical and Geoenvironmental Engineering*, 129(11):1054–1056, 2003.

[51] D.W. Barr. Coefficient of permeability determined by measurable parameters. *Groundwater*, 39(3):356–361, 2001.

[52] Y. A. Cengel, M. A. Boles, and M. Kanoğlu. *Thermodynamics: an engineering approach*, volume 5. McGraw-Hill New York, 2011.

[53] R.C. Weast. *Handbook of Chemistry and Physics 53rd Edition*. Chemical Rubber Pub., 1972.

[54] A. Picard, R.S. Davis, M. Gläser, and K. Fujii. Revised formula for the density of moist air (cipm-2007). *Metrologia*, 45(2):149, 2008.

[55] X. Li, Z. Li, Q. Xia, and H. Xi. Effects of pore sizes of porous silica gels on desorption activation energy of water vapour. *Applied thermal engineering*, 27 (5):869–876, 2007.

[56] M. Bayans. Versa Laser Instructions. Personal Communication, July 2012. University of Alberta MECE Summer Student.

[57] E.A. Guggenheim. The theoretical basis of raoult's law. *Transactions of the Faraday Society*, 33:151–156, 1937.

[58] A. Wexler and S. Hasegawa. Relative humidity-temperature relationships of some saturated salt solutions in the temperature range o°C to 50°C. *Journal of Research of the National Bureau of Standards*, 53(1):19–26, 1954.

[59] J. Kestin and J.H. Whitelaw. The viscosity of dry and humid air. *International Journal of Heat and Mass Transfer*, 7(11):1245–1255, 1964.

[60] University of Alberta EAS Department. EAS Weather Station Archive. Online Database http://easweb.eas.ualberta.ca/weather_archive.php, July & August 2012. accessed July 20th 2013.

[61] P. R. Lowe and J. M. Ficke. The computation of saturation vapor pressure. Technical report, DTIC Document, 1974.

A

Appendix A: Multipycnometer Procedure and Data

The unit should be calibrated prior to taking measurements if it is not being used regularly, or the temperature in the room has changed. If the unit has not been used for a while makes sure to do at least half a dozen measurement cycles prior to recording measurements to stabilize the pressure transducer. Once calibration is completed, measuring a known volume several times to test the calibration is recommended.

1. Select the appropriate cell size for your sample and adjust toggle valves I and II accordingly. A reference chart is located on the top right corner of the lower panel on the unit.

2. For the large cell: while wearing nitrile gloves tilt the large cell on its side, and gently roll the large reference sphere in. Slide the large cell into the cell holder. Line up the holes on the sides of the large cell with the grooves on the sides of the cell holder. Close the lid.

*Vacuum - Only perform this a single time per sample/reference, after the sample/reference sphere(s) are placed in the cell holder.

3. Make sure the Gas In and Gas Out toggle valves and needle valves are closed and that the switch is on Cell. Turn on the vacuum pump and close the Connection toggle valve. Open the Gas Out toggle valve and slowly open the Gas Out needle valve. Vacuum until the analog pressure gauge reads 150 mTorr.

4. Once the appropriate pressure is reached close the Gas Out toggle valve then open the Connection toggle valve and shut off the pump.

5. To re-pressurize the system open the Gas In toggle valve and slowly open the Gas In needle valve. Close the Gas In toggle valve when the pressure read-out is slightly over 0. Open the Gas Out toggle valve and wait for the pressure read-out to stabilize. Close the Gas Out valve and zero the read-out using the Zero dial.

*Actual Calibration/Sample Run Repeat this cycle at least four times (typically ignoring the first cycle). The switch should be in the Cell position and Gas In and Gas Out toggle valves should be closed.

6. With the transducer zeroed turn the switch to Ref. Open the Gas In toggle valve and pressurize to approximately 17 PSIG (1.195 kg/cm2) using the Gas In needle valve to control the rate of pressurization. Stop the flow by closing the Gas In toggle valve.

7. Record the display reading after it has stabilized. This is the value P1 (P1 for the empty cell during the calibration runs).

8. Turn the selector valve to Cell. Record the display value after it has stabilized (DO NOT wait long to do so). This value is P2 (P2 for the empty cell during the calibration runs).

9. Vent the pressure (slowly when measuring powders) by opening the Gas Out toggle valve with the Gas Out needle valve slightly open.

10. Repeat steps 6 7 until at least three sets of measurements have been acquired.

Trial	P1	P2	$V_{ref}[cm^3]$
1	16.939	8.340	88.706
2	16.990	8.363	88.603
3	17.000	8.368	88.608
4	16.993	8.365	88.585
5	16.992	8.365	88.591
6	17.022	8.380	88.590
Average			88.595
Std. Dev.			0.010

(a) *Calibration Cell*

Trial	P'1	P'2	$V_{empty}[cm^3]$
1	17.002	6.371	148.020
2	17.002	6.368	147.959
3	17.007	6.370	147.962
4	16.994	6.365	147.929
5	17.001	6.368	147.924
6	16.990	6.364	147.919
Average			147.939
Std. Dev.			0.020

(b) *Empty Cell*

Trial	P1	P2	V_{sample} $[cm^3]$
1	17.016	6.432	2.153
2	16.993	6.426	2.252
3	16.996	6.426	2.210
4	17.001	6.427	2.178
5	17.000	6.427	2.192
6	16.998	6.428	2.256
Average			2.207
Std. Dev.			0.035
Sample Mass [g]			16.377
Density $[\frac{g}{cm^3}]$			7.421

(c) *Two Small Calibration Spheres*

Trial	P1	P2	V_{sample} $[cm^3]$
0	17.012	6.776	14.105
1	17.009	6.772	14.012
2	17.003	6.771	14.058
3	17.003	6.770	14.025
4	16.999	6.769	14.045
5	17.004	6.771	14.045
6	16.998	6.768	14.025
7	17.004	6.771	14.045
8	17.010	6.774	14.065
9	16.996	6.768	14.051
10	17.025	6.779	14.033
Average			14.041
Std. Dev.			0.016
Sample Mass [g]			29.704
Density $[\frac{g}{cm^3}]$			2.116

(d) *Silica Gel Measurement*

Table A.1: *Multipycnometer Calibration and Silica Gel Data*

B
Appendix B: Silica Gel Bulk Density Measurement Data

Test No.	m_{beads} [g]	m_{water} [g]	T_{water} [°C]	ρ_{water} [$\frac{g}{cm^3}$]	V_{cell} [cm^3]	Bulk Density ρ_{bulk} [$\frac{g}{cm^3}$]
1	87.101	105.903	18.5	0.999	106.059	0.822
2	88.668	106.202	18.5	0.999	106.358	0.837
3	87.086	105.341	18.5	0.999	105.496	0.822
4	87.037	105.348	19	0.998	105.513	0.822
5	87.15	105.615	19	0.998	105.781	0.823
6	86.331	105.681	19	0.998	105.847	0.815
7	87.464	106.137	19	0.998	106.303	0.826
8	87.014	105.702	19	0.998	105.868	0.822
9	86.699	105.767	19	0.998	105.933	0.819
10	87.789	105.808	19	0.998	105.974	0.829
Average	87.234	105.75	18.85	0.998	105.913	0.824
Std. Dev	0.637	0.286	0.242	0	0.286	0.006

Table B.1: *Silica Gel Bulk Density Measurement Data Summary*

	Dia. 1 [mm]	Dia. 2 [mm]	Dia. 3 [mm]	Mass [mg]	Volume* [cm^3]	Bead Density [$\frac{g}{cm^3}$]
	3.30	3.46	2.75	20	0.016	1.216
	3.02	3.05	2.43	15	0.012	1.280
	3.11	3.12	2.83	22	0.014	1.530
	3.31	2.79	2.27	16	0.011	1.458
	3.30	3.29	2.81	20	0.016	1.252
	3.04	3.36	2.49	17	0.013	1.277
	2.87	3.22	2.61	16	0.013	1.267
	3.13	3.07	2.81	20	0.014	1.415
	2.80	2.94	2.52	14	0.011	1.289
	3.05	3.00	2.71	16	0.013	1.232
	2.90	2.89	2.54	14	0.011	1.256
	2.77	2.78	2.51	13	0.010	1.285
	3.30	3.27	2.87	22	0.016	1.357
	3.14	3.05	2.96	20	0.015	1.347
	3.42	3.49	2.77	22	0.017	1.271
	3.21	3.24	2.82	21	0.015	1.367
	3.28	3.25	3.18	22	0.018	1.239
	3.51	3.47	2.69	22	0.017	1.282
	3.06	2.82	2.65	16	0.012	1.336
	3.46	3.50	2.99	25	0.019	1.319
	2.84	2.77	2.39	15	0.010	1.524
	3.51	3.45	3.21	28	0.020	1.376
	3.01	2.98	2.68	15	0.013	1.192
	3.56	2.95	2.45	18	0.013	1.336
	3.17	4.01	2.45	21	0.016	1.288
	3.47	3.47	2.76	22	0.017	1.264
	3.14	4.36	2.60	24	0.019	1.288
	3.50	3.46	2.92	23	0.019	1.242
	3.47	3.45	3.09	24	0.019	1.239
	3.05	3.21	2.47	15	0.013	1.185
	3.17	3.51	2.86	22	0.017	1.320
	3.64	3.76	3.22	30	0.023	1.300
	3.71	3.82	3.26	31	0.024	1.281
	2.88	3.30	2.38	16	0.012	1.351
	3.29	4.11	2.68	25	0.019	1.318
	3.43	3.62	2.65	24	0.017	1.393
	3.14	3.15	2.74	18	0.014	1.268
	3.08	3.10	2.71	18	0.014	1.329
	3.63	3.42	2.77	25	0.018	1.388
	3.90	3.56	3.13	31	0.023	1.362
	3.61	4.42	3.03	35	0.025	1.383
	3.80	3.42	2.97	26	0.020	1.286
	3.16	3.37	3.00	21	0.017	1.255
	3.59	2.76	2.25	15	0.012	1.285
	3.19	3.59	2.51	20	0.015	1.329
	3.05	3.27	2.34	16	0.012	1.309
	3.95	3.41	3.00	28	0.021	1.323
	2.99	3.47	2.52	17	0.014	1.242
	3.47	4.07	2.62	24	0.019	1.239
	3.44	3.57	2.82	23	0.018	1.268
Average	3.28	3.36	2.73	21	0.016	1.309
Std. Dev.	0.29	0.39	0.26	5	0.004	0.072

Table B.2: *Silica Gel Individual Bead Densities - 3 Axis Measurement*

* *Volume calculated using* $V = \frac{4\pi}{3}\frac{Dia.1}{2}\frac{Dia.2}{2}\frac{Dia.3}{2}$

C

Appendix C: Water Vapour Sorption Isotherm Procedure and Data

This procedure describes the experiment conducted for the VTI-SA automatic sorption analyzer. The analyzer controls the relative humidity of a nitrogen carrier gas at a specific temperature, and measures the mass change of an adsorbate in the sample tray over a range of relative humidities.

1. In preparation, the sample tray was rinsed with acetone, then de-ionized water, then with acetone again to remove any residual contaminants from previous experiments.

2. Nitrogen was made to flow inside the system to purge any foreign gases from previous experiments.

3. Source canister was filled with de-ionized water, filled to the elbow of the clear plastic tube, and hooked up to the canister.

4. Waited for the sample container to evaporate all acetone (waited until there was no more change in sample tray mass).

5. The silica gel bead sample was placed into the sample tray and left alone until the mass stabilized.

6. The silica gel bead sample was dried at 120 °C for a maximum of 120 minutes, at a rate of 1°C per minute.

7. The sample was then cooled to the selected isotherm temperature of 25°C. The dry nitrogen gas was continually flowing to ensure drying of the silica gel bead sample.

8. Relative Humidity in the nitrogen carrier gas was then increased over discrete steps to: 0.05, 0.1, 0.2, 0.3, 0.4, 0.5, 0.6, 0.7, 0.8, 0.9 %RH).

9. The mass of the sample tray was measured either every two minutes, or when a 0.001% weight change had occurred. The equilibration mass was determined when either a 0.005% weight change or less occurred between readings, or after a total of 5 minutes.

10. The equilibration points, with resulting sample mass, elapsed time, temperature, and relative humidity were recorded and logged.

Appendix C: Water Vapour Sorption Isotherm Procedure and Data

Elapsed Time [min]	Weight [mg]	Weight Change [%]	Sample Temp [°C]	Evap. Temp [°C]	RH [%]
279.1	19.989	0	25.99	22.21	0.0
639.2	20.8841	4.478	24.72	21.67	5.0
999.3	21.3935	7.026	24.69	21.88	10.0
1359.4	22.1611	10.866	24.72	21.87	20.0
1719.5	23.0354	15.24	24.67	21.97	30.0
2079.6	23.8832	19.481	24.71	21.9	40.0
2439.6	24.6081	23.108	24.68	21.92	50.0
2799.7	24.9563	24.85	24.73	21.58	60.0
3159.8	25.1429	25.784	24.69	21.88	70.0
3519.9	25.2506	26.322	24.69	21.6	80.0
3880	25.2652	26.395	24.72	21.34	90.0

Table C.1: *Equilibrated Data for Water Adsorption on Silica Gel*

VTI-SA Water Vapour Sorption Analyzer Experimental Adsorption Data for Silica Gel Beads Experiment Started: 7/16/2012 Run Started: 12:41:56

Table C.2: *VTI-SA Analyzer Water Adsorption on Silica Gel*

Elapsed Time [min]	Weight [mg]	Weight Change [%]	Sample Temp [°C]	Evap. Temp [°C]	RH [%]
0.1	20.901	0	25.86	27.64	0
0.4	20.9276	0.127	25.86	27.64	0
1.4	20.9947	0.448	25.73	27.82	0
2.4	21.0128	0.535	25.97	27.97	0
3.4	21.0221	0.579	26.67	28.07	0
4.4	21.0287	0.611	27.68	28.11	0
5.4	21.036	0.646	28.82	28.09	0
6.4	21.0468	0.698	29.98	28.05	0
7.4	21.0543	0.733	31.11	27.98	0
9.4	21.0535	0.73	33.35	27.81	0
10.4	21.0504	0.715	34.44	27.72	0
11.4	21.0465	0.696	35.52	27.61	0
12.4	21.0427	0.678	36.59	27.5	0
13.4	21.036	0.646	37.63	27.39	0
14.4	21.0246	0.591	38.66	27.28	0
15.4	21.0159	0.55	39.68	27.18	0
16.4	21.0012	0.479	40.71	27.07	0
17.4	20.9798	0.377	41.73	26.96	0
18.4	20.966	0.311	42.73	26.85	0
19.4	20.9534	0.251	43.74	26.74	0
20.4	20.9439	0.205	44.76	26.64	0
21.4	20.9338	0.157	45.8	26.54	0
22.4	20.919	0.086	46.83	26.44	0
23.4	20.8907	-0.049	47.84	26.34	0
24.4	20.8659	-0.168	48.85	26.24	0
25.4	20.8517	-0.236	49.87	26.15	0
26.4	20.8629	-0.182	50.89	26.05	0
27.4	20.8566	-0.213	51.92	25.97	0
28.4	20.8456	-0.265	52.93	25.88	0
29.4	20.8368	-0.307	53.95	25.79	0
30.4	20.8265	-0.356	54.97	25.7	0
31.4	20.8131	-0.421	55.99	25.61	0
32.4	20.7969	-0.498	57.02	25.52	0
33.4	20.7836	-0.562	58.04	25.44	0
34.4	20.7754	-0.601	59.04	25.35	0
35.4	20.7629	-0.661	60.02	25.26	0
36.4	20.748	-0.732	61.04	25.18	0
37.4	20.7314	-0.812	62.07	25.09	0
38.4	20.7131	-0.899	63.08	25.01	0
39.4	20.7005	-0.96	64.09	24.94	0
40.4	20.6861	-1.028	65.11	24.88	0

C.2 – continued from previous page

Elapsed Time [min]	Weight [mg]	Weight Change [%]	Sample Temp [°C]	Evap. Temp [°C]	RH [%]
41.4	20.6712	-1.099	66.13	24.81	0
42.4	20.6586	-1.16	67.15	24.74	0
43.4	20.6489	-1.206	68.15	24.68	0
44.4	20.6306	-1.294	69.17	24.62	0
45.4	20.6135	-1.376	70.19	24.56	0
46.4	20.6004	-1.438	71.22	24.51	0
47.4	20.5797	-1.538	72.25	24.46	0
48.4	20.5686	-1.59	73.28	24.41	0
49.4	20.5555	-1.653	74.31	24.36	0
50.4	20.5439	-1.708	75.35	24.31	0
51.4	20.5318	-1.766	76.39	24.26	0
52.4	20.5193	-1.826	77.43	24.22	0
53.4	20.5097	-1.872	78.48	24.18	0
54.4	20.4982	-1.927	79.53	24.13	0
55.4	20.4832	-1.999	80.56	24.08	0
56.4	20.4689	-2.067	81.57	24.04	0
57.4	20.4539	-2.139	82.6	23.99	0
58.4	20.4412	-2.2	83.62	23.95	0
59.4	20.4293	-2.257	84.64	23.91	0
60.4	20.4168	-2.317	85.65	23.87	0
61.4	20.4062	-2.367	86.69	23.83	0
62.4	20.3953	-2.419	87.72	23.79	0
63.4	20.386	-2.464	88.73	23.75	0
64.4	20.3779	-2.503	89.73	23.71	0
65.4	20.3688	-2.546	90.76	23.68	0
66.4	20.3563	-2.606	91.76	23.65	0
67.4	20.3453	-2.659	92.78	23.62	0
68.4	20.3354	-2.706	93.81	23.59	0
69.4	20.3239	-2.761	94.85	23.55	0
70.4	20.3145	-2.806	95.88	23.52	0
71.4	20.3053	-2.85	96.92	23.49	0
72.4	20.2975	-2.888	97.97	23.46	0
73.4	20.2876	-2.935	99.01	23.43	0
74.4	20.2808	-2.967	100.04	23.41	0
75.4	20.2729	-3.005	101.07	23.38	0
76.4	20.2605	-3.065	102.08	23.36	0
77.4	20.2505	-3.112	103.11	23.33	0
78.4	20.2429	-3.149	104.15	23.31	0
79.4	20.2359	-3.182	105.18	23.29	0
80.4	20.2302	-3.21	106.2	23.27	0
81.4	20.2239	-3.239	107.23	23.25	0
82.4	20.2158	-3.278	108.25	23.23	0
83.4	20.2099	-3.306	109.27	23.21	0
84.4	20.202	-3.344	110.3	23.19	0
85.4	20.1975	-3.366	111.34	23.18	0
86.4	20.1923	-3.391	112.37	23.16	0
87.4	20.1876	-3.413	113.39	23.15	0
88.4	20.1819	-3.44	114.43	23.13	0
89.4	20.1744	-3.476	115.46	23.12	0
90.4	20.1693	-3.501	116.48	23.1	0
91.4	20.1623	-3.534	117.5	23.09	0
92.4	20.1551	-3.569	118.73	23.08	0
93.4	20.1402	-3.64	120.71	23.07	0
94.4	20.128	-3.699	122.17	23.06	0
95.4	20.1171	-3.75	122.86	23.05	0
96.4	20.1125	-3.772	123.09	23.03	0
97.4	20.1	-3.832	123.07	23.02	0
98.4	20.0973	-3.845	122.94	23.02	0
99.4	20.0921	-3.87	122.78	23.01	0
100.4	20.0945	-3.859	122.61	23	0
102.4	20.097	-3.847	122.4	22.99	0
103.4	20.091	-3.875	122.34	22.98	0
104.4	20.0879	-3.89	122.28	22.97	0
105.4	20.0851	-3.903	122.23	22.97	0
107.4	20.0805	-3.926	122.23	22.96	0
109.4	20.0795	-3.93	122.26	22.95	0
111.4	20.0735	-3.959	122.28	22.94	0
113.5	20.0734	-3.96	122.29	22.93	0
114.4	20.0679	-3.986	122.32	22.93	0
116.4	20.0702	-3.975	122.35	22.93	0
117.4	20.0648	-4.001	122.35	22.93	0
119.4	20.0625	-4.012	122.38	22.92	0
121.5	20.0609	-4.019	122.42	22.91	0
123.4	20.0574	-4.036	122.44	22.91	0
125.4	20.0562	-4.042	122.42	22.9	0

C.2 – continued from previous page

Elapsed Time [min]	Weight [mg]	Weight Change [%]	Sample Temp [°C]	Evap. Temp [°C]	RH [%]
127.4	20.0527	-4.059	122.47	22.9	0
129.4	20.0501	-4.071	122.52	22.9	0
131.4	20.0477	-4.083	122.51	22.9	0
133.4	20.0456	-4.093	122.52	22.89	0
135.4	20.0422	-4.109	122.53	22.9	0
137.4	20.0426	-4.107	122.57	22.89	0
139.4	20.0417	-4.111	122.58	22.89	0
141.4	20.0384	-4.127	122.6	22.89	0
143.4	20.037	-4.134	122.61	22.89	0
145.4	20.0372	-4.133	122.62	22.89	0
147.5	20.0355	-4.141	122.62	22.89	0
149.4	20.0327	-4.154	122.64	22.89	0
151.5	20.0319	-4.158	122.63	22.89	0
153.6	20.0316	-4.16	122.62	22.88	0
155.7	20.0305	-4.165	122.63	22.89	0
157.7	20.0293	-4.171	122.65	22.89	0
159.7	20.0279	-4.177	122.63	22.89	0
161.7	20.0269	-4.182	122.62	22.89	0
163.7	20.0261	-4.186	122.62	22.89	0
165.8	20.0257	-4.188	122.64	22.89	0
167.8	20.0238	-4.197	122.66	22.89	0
169.8	20.0232	-4.2	122.65	22.89	0
171.9	20.0237	-4.198	122.65	22.89	0
173.4	20.0204	-4.213	122.66	22.89	0
175.4	20.0192	-4.219	122.67	22.89	0
177.4	20.0182	-4.224	122.66	22.89	0
179.4	20.0181	-4.224	122.68	22.89	0
181.5	20.0166	-4.232	122.67	22.89	0
183.5	20.0186	-4.222	122.66	22.89	0
184.4	20.0157	-4.236	122.66	22.89	0
186.5	20.0154	-4.237	122.67	22.89	0
188.5	20.0161	-4.234	122.68	22.9	0
190.6	20.0144	-4.242	122.67	22.9	0
192.6	20.0134	-4.247	122.67	22.9	0
194.7	20.0135	-4.246	122.66	22.9	0
196.7	20.0138	-4.245	122.66	22.9	0
198.8	20.0125	-4.251	122.66	22.9	0
200.9	20.012	-4.254	122.66	22.91	0
203	20.011	-4.258	122.66	22.91	0
205.1	20.0103	-4.262	122.69	22.91	0
207.1	20.0102	-4.262	122.69	22.92	0
209.1	20.0098	-4.264	122.7	22.92	0
211.1	20.0083	-4.271	122.69	22.92	0
213.1	20.0081	-4.272	119.87	22.92	5
214.4	20.0008	-4.307	116.85	22.92	5
215.4	19.9941	-4.339	113.85	22.92	5
216.4	19.9902	-4.358	110.94	22.92	5
217.4	19.9876	-4.37	108.13	22.91	5
219.4	19.9918	-4.35	102.69	22.91	5
220.4	19.9881	-4.368	100.04	22.91	5
222.4	19.9877	-4.37	94.97	22.9	5
224.4	19.9903	-4.357	90.23	22.89	5
226.4	19.9893	-4.362	85.77	22.88	5
227.4	19.9829	-4.393	83.63	22.87	5
228.4	19.9857	-4.38	81.55	22.87	5
229.4	19.9881	-4.368	79.53	22.86	5
231.4	19.969	-4.459	75.67	22.85	5
232.4	19.964	-4.483	73.82	22.84	5
233.4	19.9693	-4.458	72.03	22.84	5
234.4	19.9718	-4.446	70.29	22.83	5
236.4	19.9728	-4.441	66.95	22.81	5
238.4	19.9742	-4.434	63.81	22.79	5
240.4	19.9737	-4.437	60.83	22.77	5
242.4	19.9704	-4.453	58.02	22.74	5
243.4	19.9751	-4.43	56.68	22.73	5
244.4	19.9808	-4.403	55.37	22.72	5
246.4	19.9837	-4.389	52.85	22.69	5
248.4	19.985	-4.383	50.47	22.67	5
250.5	19.9865	-4.376	48.21	22.64	5
252.5	19.9854	-4.381	46.08	22.61	5
254.6	19.9839	-4.388	43.57	22.58	5
256.4	19.9861	-4.377	42.14	22.56	5
258.4	19.9848	-4.384	40.32	22.53	5
260.5	19.9852	-4.382	38.59	22.5	5
262.5	19.9841	-4.387	36.95	22.48	5

C.2 – continued from previous page

Elapsed Time [min]	Weight [mg]	Weight Change [%]	Sample Temp [°C]	Evap. Temp [°C]	RH [%]
264.4	19.9863	-4.376	35.39	22.45	5
266.5	19.987	-4.373	33.93	22.41	5
268.6	19.9871	-4.373	32.19	22.38	5
270.7	19.9878	-4.369	30.87	22.35	5
272.7	19.9884	-4.367	29.63	22.31	5
274.7	19.9881	-4.368	28.45	22.29	5
276.8	19.9889	-4.364	27.31	22.26	5
278.8	19.989	-4.363	26.25	22.22	5
280.5	19.9689	-4.46	25.42	22.19	5
281.5	19.989	-4.363	24.92	22.17	5
282.5	20.0031	-4.296	24.41	22.16	5
284.6	20.0047	-4.288	24.12	22.13	5
286.5	20.0078	-4.274	24.25	22.13	5
287.5	20.0143	-4.243	24.36	22.13	5
288.5	20.0185	-4.222	24.45	22.13	5
290.5	20.021	-4.21	24.56	22.12	5
292.5	20.0224	-4.204	24.64	22.13	5
293.5	20.0199	-4.216	24.66	22.13	5
294.5	20.0222	-4.204	24.66	22.13	5
295.5	20.0187	-4.221	24.67	22.13	5
296.5	20.0232	-4.2	24.67	22.13	5
297.5	20.0184	-4.223	24.69	22.13	5
298.5	20.015	-4.239	24.71	22.14	5
299.5	20.0214	-4.209	24.72	22.14	5
300.5	20.0257	-4.188	24.71	22.14	5
301.5	20.0305	-4.165	24.7	22.14	5
302.5	20.0329	-4.153	24.69	22.14	5
303.5	20.0391	-4.124	24.7	22.13	5
304.5	20.0415	-4.112	24.7	22.13	5
306.5	20.0462	-4.09	24.69	22.13	5
308.5	20.051	-4.067	24.68	22.12	5
309.5	20.0548	-4.049	24.66	22.12	5
310.5	20.0593	-4.027	24.65	22.12	5
311.5	20.0619	-4.015	24.64	22.12	5
313.5	20.0648	-4.001	24.68	22.1	5
314.5	20.0686	-3.983	24.7	22.09	5
315.5	20.0729	-3.962	24.71	22.07	5
316.5	20.0767	-3.944	24.71	22.06	5
317.5	20.0804	-3.926	24.71	22.05	5
318.5	20.084	-3.909	24.71	22.04	5
319.5	20.0875	-3.892	24.71	22.04	5
320.5	20.0925	-3.868	24.72	22.03	5
322.5	20.0975	-3.844	24.73	22.01	5
323.5	20.1006	-3.83	24.71	22	5
324.5	20.1061	-3.803	24.7	22	5
325.5	20.1097	-3.786	24.7	21.99	5
327.5	20.1183	-3.745	24.73	21.98	5
329.5	20.1226	-3.724	24.69	21.96	5
330.5	20.1273	-3.702	24.68	21.96	5
331.5	20.1312	-3.683	24.67	21.96	5
332.5	20.1346	-3.667	24.68	21.95	5
333.5	20.1403	-3.64	24.69	21.94	5
334.5	20.1427	-3.628	24.72	21.94	5
335.5	20.1456	-3.614	24.75	21.93	5
336.5	20.1502	-3.592	24.74	21.92	5
337.5	20.1549	-3.57	24.74	21.92	5
338.5	20.1591	-3.55	24.74	21.92	5
339.5	20.1656	-3.518	24.71	21.92	5
341.5	20.1711	-3.492	24.68	21.9	5
343.5	20.1774	-3.462	24.72	21.9	5
344.5	20.182	-3.44	24.74	21.89	5
345.5	20.1866	-3.418	24.75	21.88	5
346.5	20.1912	-3.396	24.74	21.87	5
347.5	20.1943	-3.381	24.74	21.87	5
348.5	20.1986	-3.361	24.72	21.86	5
349.5	20.2043	-3.333	24.7	21.86	5
350.5	20.2071	-3.32	24.71	21.85	5
351.5	20.2128	-3.293	24.73	21.84	5
352.5	20.2165	-3.275	24.72	21.84	5
353.5	20.2205	-3.256	24.71	21.83	5
354.5	20.2241	-3.239	24.71	21.83	5
355.5	20.2296	-3.213	24.71	21.82	5
356.5	20.2341	-3.191	24.71	21.81	5
357.5	20.2385	-3.17	24.7	21.81	5
358.5	20.2425	-3.15	24.7	21.81	5

C.2 – continued from previous page

Elapsed Time [min]	Weight [mg]	Weight Change [%]	Sample Temp [°C]	Evap. Temp [°C]	RH [%]
359.5	20.2465	-3.131	24.71	21.81	5
360.5	20.2504	-3.113	24.71	21.8	5
361.5	20.2557	-3.087	24.72	21.79	5
362.5	20.2599	-3.067	24.71	21.78	5
363.5	20.2647	-3.045	24.71	21.78	5
364.5	20.2698	-3.02	24.72	21.78	5
365.5	20.2731	-3.004	24.72	21.78	5
366.5	20.2758	-2.991	24.72	21.77	5
367.5	20.2814	-2.964	24.72	21.77	5
368.5	20.2869	-2.938	24.73	21.76	5
369.5	20.2898	-2.924	24.72	21.76	5
370.5	20.2939	-2.905	24.71	21.76	5
371.5	20.2979	-2.886	24.72	21.76	5
372.5	20.3015	-2.868	24.71	21.76	5
373.5	20.3059	-2.847	24.7	21.76	5
374.5	20.3089	-2.833	24.71	21.76	5
375.5	20.3137	-2.81	24.71	21.75	5
376.5	20.3185	-2.787	24.72	21.76	5
377.5	20.323	-2.766	24.71	21.75	5
378.5	20.3277	-2.743	24.69	21.75	5
379.5	20.3311	-2.727	24.69	21.75	5
380.5	20.3351	-2.708	24.7	21.74	5
381.5	20.339	-2.689	24.69	21.74	5
382.5	20.3435	-2.667	24.7	21.74	5
383.5	20.3484	-2.644	24.7	21.74	5
384.5	20.3513	-2.63	24.69	21.73	5
385.5	20.3559	-2.608	24.68	21.73	5
386.5	20.3609	-2.584	24.68	21.72	5
387.5	20.3645	-2.567	24.68	21.72	5
388.5	20.3675	-2.552	24.68	21.71	5
389.5	20.3706	-2.538	24.7	21.72	5
390.5	20.3757	-2.514	24.71	21.72	5
391.5	20.3796	-2.495	24.71	21.71	5
392.5	20.383	-2.479	24.71	21.71	5
393.5	20.3867	-2.461	24.72	21.7	5
394.5	20.3909	-2.441	24.73	21.7	5
395.5	20.3949	-2.422	24.73	21.7	5
396.5	20.3976	-2.408	24.73	21.7	5
397.5	20.4028	-2.384	24.72	21.69	5
398.5	20.4063	-2.367	24.73	21.69	5
399.5	20.4101	-2.349	24.72	21.68	5
400.5	20.4131	-2.334	24.7	21.67	5
401.5	20.4179	-2.312	24.71	21.67	5
402.5	20.4212	-2.296	24.72	21.68	5
403.5	20.4255	-2.275	24.72	21.68	5
404.5	20.4292	-2.257	24.73	21.68	5
405.5	20.432	-2.244	24.75	21.68	5
406.5	20.4365	-2.222	24.76	21.68	5
407.5	20.4408	-2.202	24.74	21.67	5
408.5	20.444	-2.186	24.72	21.68	5
409.5	20.4477	-2.169	24.71	21.68	5
410.5	20.4511	-2.152	24.72	21.68	5
411.5	20.4553	-2.132	24.72	21.68	5
412.5	20.4581	-2.119	24.73	21.68	5
413.5	20.462	-2.101	24.73	21.69	5
414.5	20.4667	-2.078	24.71	21.69	5
415.5	20.4701	-2.062	24.69	21.69	5
416.5	20.4737	-2.044	24.69	21.68	5
417.5	20.4763	-2.032	24.69	21.68	5
418.5	20.4801	-2.014	24.69	21.68	5
419.5	20.4834	-1.998	24.7	21.68	5
420.5	20.4862	-1.985	24.7	21.69	5
421.5	20.4894	-1.969	24.71	21.69	5
422.5	20.4931	-1.952	24.71	21.7	5
423.5	20.4979	-1.929	24.71	21.69	5
425.5	20.5026	-1.906	24.71	21.68	5
426.5	20.5062	-1.889	24.72	21.68	5
427.5	20.5093	-1.874	24.72	21.68	5
428.5	20.5143	-1.85	24.72	21.68	5
430.5	20.52	-1.823	24.74	21.69	5
431.5	20.523	-1.809	24.74	21.68	5
432.5	20.5257	-1.796	24.72	21.67	5
433.5	20.5284	-1.783	24.73	21.67	5
434.5	20.5329	-1.761	24.72	21.68	5
435.5	20.5353	-1.75	24.7	21.68	5

C.2 – continued from previous page

Elapsed Time [min]	Weight [mg]	Weight Change [%]	Sample Temp [°C]	Evap. Temp [°C]	RH [%]
436.5	20.5401	-1.727	24.71	21.68	5
437.5	20.5424	-1.716	24.72	21.68	5
438.5	20.5466	-1.696	24.71	21.68	5
439.5	20.5497	-1.681	24.71	21.68	5
441.5	20.5546	-1.657	24.71	21.69	5
442.5	20.5587	-1.638	24.71	21.68	5
443.5	20.5624	-1.62	24.72	21.68	5
445.5	20.5678	-1.594	24.7	21.68	5
447.5	20.5735	-1.567	24.71	21.7	5
448.5	20.5767	-1.552	24.71	21.71	5
449.5	20.5792	-1.54	24.71	21.71	5
450.5	20.5817	-1.528	24.72	21.7	5
451.5	20.5856	-1.509	24.72	21.69	5
452.5	20.5878	-1.498	24.72	21.69	5
453.5	20.5913	-1.482	24.73	21.7	5
454.5	20.594	-1.469	24.74	21.7	5
455.5	20.5964	-1.457	24.74	21.7	5
456.5	20.5996	-1.442	24.73	21.71	5
458.5	20.605	-1.416	24.72	21.71	5
459.5	20.6088	-1.398	24.71	21.7	5
461.5	20.6126	-1.38	24.73	21.7	5
462.5	20.6162	-1.363	24.73	21.7	5
464.5	20.6214	-1.338	24.73	21.7	5
466.5	20.6267	-1.312	24.74	21.71	5
467.5	20.629	-1.302	24.73	21.72	5
469.5	20.6341	-1.277	24.71	21.71	5
470.5	20.6373	-1.262	24.72	21.7	5
471.5	20.6395	-1.251	24.73	21.7	5
472.5	20.6421	-1.239	24.71	21.69	5
473.5	20.6446	-1.227	24.7	21.7	5
475.5	20.6499	-1.202	24.72	21.7	5
476.5	20.6521	-1.191	24.73	21.7	5
478.5	20.656	-1.172	24.74	21.71	5
480.5	20.6604	-1.151	24.73	21.71	5
481.5	20.6628	-1.14	24.74	21.7	5
482.5	20.6654	-1.127	24.75	21.7	5
483.5	20.6675	-1.117	24.75	21.69	5
484.5	20.6703	-1.104	24.74	21.69	5
485.5	20.6727	-1.092	24.74	21.69	5
486.5	20.6754	-1.079	24.74	21.7	5
487.5	20.6776	-1.069	24.73	21.7	5
489.5	20.6821	-1.048	24.74	21.7	5
490.5	20.6848	-1.034	24.73	21.7	5
492.5	20.6894	-1.013	24.73	21.69	5
494.5	20.6935	-0.993	24.75	21.68	5
496.5	20.6975	-0.974	24.74	21.68	5
498.5	20.7022	-0.951	24.75	21.68	5
500.5	20.7061	-0.932	24.75	21.69	5
502.5	20.7103	-0.912	24.74	21.68	5
503.5	20.7136	-0.897	24.75	21.68	5
505.5	20.7169	-0.881	24.75	21.67	5
506.5	20.7195	-0.868	24.75	21.67	5
508.5	20.7235	-0.849	24.75	21.68	5
510.5	20.7273	-0.831	24.74	21.68	5
511.5	20.7298	-0.819	24.74	21.68	5
513.5	20.7322	-0.808	24.71	21.69	5
514.5	20.7348	-0.795	24.69	21.68	5
516.5	20.7383	-0.779	24.72	21.66	5
518.5	20.7431	-0.756	24.75	21.66	5
520.5	20.7466	-0.739	24.74	21.66	5
522.5	20.7497	-0.724	24.69	21.66	5
523.5	20.7524	-0.711	24.67	21.66	5
525.5	20.7563	-0.692	24.69	21.66	5
527.5	20.7598	-0.676	24.72	21.67	5
529.5	20.7622	-0.664	24.72	21.65	5
530.5	20.7646	-0.653	24.72	21.64	5
532.5	20.7686	-0.634	24.72	21.64	5
534.5	20.7724	-0.615	24.73	21.65	5
536.5	20.7754	-0.601	24.72	21.65	5
538.5	20.7784	-0.587	24.74	21.66	5
540.5	20.7819	-0.57	24.73	21.68	5
542.5	20.7831	-0.564	24.73	21.67	5
543.5	20.7855	-0.553	24.73	21.66	5
545.5	20.7878	-0.542	24.72	21.65	5
547.5	20.7917	-0.523	24.73	21.66	5

C.2 – continued from previous page

Elapsed Time [min]	Weight [mg]	Weight Change [%]	Sample Temp [°C]	Evap. Temp [°C]	RH [%]
549.5	20.7945	-0.509	24.74	21.66	5
551.6	20.7959	-0.503	24.72	21.66	5
553.5	20.7992	-0.487	24.68	21.68	5
555.5	20.8028	-0.47	24.7	21.69	5
557.5	20.8047	-0.461	24.72	21.68	5
559.5	20.8082	-0.444	24.71	21.67	5
561.5	20.8098	-0.436	24.75	21.67	5
562.5	20.812	-0.426	24.76	21.67	5
564.5	20.8142	-0.415	24.75	21.68	5
566.5	20.8162	-0.406	24.72	21.69	5
568.5	20.8197	-0.389	24.71	21.7	5
570.5	20.8216	-0.38	24.74	21.7	5
572.5	20.825	-0.364	24.72	21.69	5
574.5	20.8278	-0.35	24.68	21.68	5
575.5	20.8306	-0.337	24.7	21.68	5
577.5	20.8316	-0.332	24.72	21.68	5
579.5	20.8328	-0.326	24.72	21.69	5
581.5	20.8363	-0.31	24.73	21.7	5
583.6	20.8377	-0.303	24.73	21.7	5
585.6	20.8395	-0.294	24.74	21.71	5
586.5	20.8419	-0.283	24.73	21.72	5
588.5	20.8433	-0.276	24.72	21.71	5
590.5	20.845	-0.268	24.73	21.69	5
592.6	20.8468	-0.26	24.74	21.7	5
593.5	20.8495	-0.247	24.73	21.71	5
595.5	20.8512	-0.238	24.73	21.71	5
597.6	20.851	-0.239	24.73	21.71	5
598.5	20.8538	-0.226	24.73	21.71	5
600.5	20.8562	-0.214	24.73	21.73	5
602.5	20.8582	-0.205	24.74	21.73	5
604.5	20.8591	-0.201	24.76	21.72	5
606.5	20.8616	-0.189	24.73	21.71	5
608.5	20.8629	-0.182	24.74	21.7	5
610.5	20.8648	-0.173	24.74	21.7	5
612.6	20.8659	-0.168	24.68	21.7	5
614.5	20.8683	-0.157	24.68	21.71	5
616.5	20.8689	-0.154	24.7	21.71	5
618.5	20.8707	-0.145	24.72	21.72	5
620.6	20.871	-0.144	24.75	21.7	5
621.5	20.8733	-0.133	24.75	21.69	5
623.6	20.8744	-0.128	24.74	21.68	5
625.6	20.8758	-0.121	24.74	21.67	5
627.6	20.8764	-0.118	24.77	21.69	5
629.7	20.8783	-0.109	24.78	21.69	5
631.5	20.8804	-0.098	24.75	21.69	5
633.5	20.8814	-0.094	24.75	21.7	5
635.5	20.8827	-0.088	24.74	21.7	5
637.5	20.8825	-0.088	24.72	21.68	5
639.5	20.8853	-0.075	24.72	21.67	10
640.5	20.8878	-0.063	24.72	21.66	10
641.5	20.8916	-0.045	24.73	21.65	10
642.5	20.8955	-0.026	24.74	21.65	10
643.5	20.9011	0.001	24.76	21.65	10
644.5	20.907	0.028	24.75	21.65	10
645.5	20.9136	0.06	24.74	21.65	10
646.5	20.9202	0.092	24.74	21.65	10
647.5	20.9262	0.12	24.74	21.65	10
648.5	20.9325	0.151	24.75	21.65	10
649.5	20.9377	0.175	24.74	21.64	10
650.5	20.9433	0.202	24.74	21.65	10
651.5	20.9496	0.233	24.75	21.65	10
652.5	20.9565	0.265	24.75	21.65	10
653.5	20.9621	0.292	24.74	21.65	10
654.5	20.9666	0.314	24.76	21.65	10
655.5	20.972	0.34	24.75	21.65	10
656.5	20.977	0.364	24.75	21.65	10
657.5	20.9817	0.386	24.76	21.64	10
658.5	20.989	0.421	24.75	21.63	10
659.5	20.9957	0.453	24.75	21.63	10
660.5	20.9998	0.472	24.74	21.62	10
661.5	21.0035	0.49	24.74	21.62	10
662.5	21.009	0.517	24.75	21.62	10
663.5	21.0142	0.542	24.74	21.63	10
664.5	21.0195	0.567	24.74	21.64	10
665.5	21.0233	0.585	24.73	21.64	10

C.2 – continued from previous page

Elapsed Time [min]	Weight [mg]	Weight Change [%]	Sample Temp [°C]	Evap. Temp [°C]	RH [%]
666.5	21.028	0.607	24.72	21.65	10
667.5	21.033	0.632	24.73	21.65	10
668.5	21.0378	0.654	24.74	21.65	10
669.5	21.0422	0.675	24.75	21.66	10
670.5	21.047	0.698	24.75	21.67	10
671.5	21.0502	0.714	24.74	21.67	10
672.5	21.0548	0.736	24.75	21.68	10
673.5	21.0574	0.748	24.74	21.68	10
674.5	21.0608	0.765	24.74	21.68	10
675.5	21.0663	0.791	24.75	21.69	10
676.5	21.0718	0.817	24.76	21.7	10
677.5	21.0743	0.829	24.74	21.7	10
678.5	21.0769	0.841	24.73	21.71	10
679.5	21.081	0.861	24.74	21.71	10
680.5	21.0858	0.884	24.75	21.71	10
681.5	21.0894	0.901	24.77	21.71	10
682.5	21.0926	0.916	24.77	21.72	10
683.5	21.097	0.938	24.76	21.73	10
684.5	21.1011	0.957	24.75	21.73	10
685.5	21.105	0.976	24.73	21.73	10
686.5	21.1077	0.989	24.7	21.73	10
687.5	21.111	1.005	24.69	21.73	10
688.5	21.1134	1.016	24.71	21.74	10
689.5	21.1186	1.041	24.73	21.75	10
690.5	21.1218	1.057	24.73	21.75	10
691.5	21.1256	1.075	24.74	21.75	10
692.5	21.1292	1.092	24.74	21.76	10
693.5	21.1327	1.109	24.74	21.75	10
694.5	21.1355	1.122	24.74	21.75	10
695.5	21.1385	1.136	24.74	21.76	10
696.5	21.1409	1.148	24.73	21.77	10
697.5	21.145	1.167	24.73	21.77	10
698.5	21.1474	1.179	24.74	21.77	10
699.5	21.1502	1.192	24.74	21.76	10
700.5	21.1538	1.209	24.73	21.77	10
701.5	21.156	1.22	24.73	21.77	10
702.5	21.1603	1.24	24.71	21.78	10
703.5	21.1634	1.255	24.71	21.78	10
704.5	21.1661	1.268	24.7	21.78	10
705.5	21.169	1.282	24.69	21.78	10
706.5	21.1718	1.295	24.69	21.77	10
708.5	21.1764	1.318	24.71	21.78	10
709.5	21.1791	1.33	24.71	21.79	10
710.5	21.1822	1.345	24.72	21.79	10
711.5	21.1897	1.381	24.73	21.79	10
712.5	21.1874	1.37	24.73	21.78	10
713.5	21.1901	1.383	24.71	21.79	10
714.5	21.1924	1.394	24.68	21.8	10
715.5	21.1951	1.407	24.67	21.8	10
717.5	21.2002	1.432	24.7	21.8	10
719.5	21.2054	1.456	24.73	21.8	10
720.5	21.2077	1.467	24.73	21.81	10
721.5	21.2102	1.479	24.72	21.81	10
723.5	21.2129	1.492	24.7	21.81	10
724.5	21.2162	1.508	24.69	21.81	10
726.5	21.221	1.531	24.71	21.82	10
727.5	21.2236	1.543	24.72	21.82	10
728.5	21.2262	1.556	24.73	21.83	10
729.5	21.229	1.569	24.73	21.83	10
731.5	21.2313	1.58	24.71	21.83	10
733.5	21.2352	1.599	24.73	21.84	10
734.5	21.2379	1.612	24.74	21.84	10
735.5	21.2409	1.626	24.71	21.84	10
737.5	21.2429	1.636	24.7	21.84	10
738.5	21.2459	1.65	24.71	21.84	10
740.5	21.2505	1.672	24.72	21.85	10
742.5	21.2537	1.687	24.73	21.85	10
744.5	21.2568	1.702	24.73	21.85	10
746.5	21.2591	1.713	24.75	21.86	10
747.5	21.2615	1.725	24.74	21.86	10
749.5	21.2648	1.74	24.75	21.86	10
751.5	21.2678	1.755	24.72	21.86	10
752.5	21.27	1.766	24.73	21.87	10
754.5	21.273	1.78	24.73	21.87	10
756.5	21.2764	1.796	24.7	21.86	10

C.2 – continued from previous page

Elapsed Time [min]	Weight [mg]	Weight Change [%]	Sample Temp [°C]	Evap. Temp [°C]	RH [%]
758.5	21.2782	1.804	24.66	21.87	10
760.5	21.2828	1.827	24.7	21.87	10
762.5	21.2841	1.833	24.71	21.87	10
764.5	21.2871	1.847	24.72	21.87	10
765.5	21.2894	1.858	24.73	21.86	10
767.5	21.2924	1.873	24.72	21.84	10
769.6	21.2927	1.874	24.74	21.82	10
771.5	21.2967	1.893	24.71	21.82	10
773.5	21.3006	1.912	24.68	21.82	10
775.6	21.3014	1.916	24.73	21.81	10
777.6	21.3025	1.921	24.72	21.81	10
779.5	21.3055	1.935	24.72	21.82	10
781.5	21.3079	1.947	24.68	21.81	10
783.5	21.3084	1.949	24.67	21.81	10
785.5	21.311	1.962	24.7	21.82	10
786.5	21.3134	1.973	24.71	21.82	10
788.5	21.3149	1.98	24.71	21.82	10
790.6	21.3163	1.987	24.71	21.82	10
792.5	21.3185	1.997	24.7	21.83	10
794.5	21.3207	2.008	24.69	21.82	10
796.5	21.3218	2.013	24.68	21.82	10
797.5	21.3241	2.024	24.68	21.83	10
799.6	21.3239	2.023	24.69	21.83	10
801.5	21.3271	2.039	24.7	21.82	10
803.5	21.3284	2.045	24.69	21.83	10
805.6	21.3302	2.054	24.7	21.83	10
807.6	21.3309	2.057	24.71	21.83	10
809.6	21.3329	2.066	24.71	21.82	10
811.5	21.3352	2.077	24.72	21.83	10
813.5	21.3359	2.081	24.71	21.83	10
815.5	21.3368	2.085	24.71	21.83	10
817.5	21.3391	2.096	24.71	21.84	10
819.5	21.3417	2.108	24.71	21.83	10
821.6	21.3412	2.106	24.71	21.83	10
823.5	21.3436	2.118	24.67	21.84	10
825.6	21.3446	2.122	24.7	21.84	10
827.6	21.3454	2.126	24.71	21.83	10
829.6	21.3463	2.131	24.72	21.84	10
831.6	21.3471	2.134	24.72	21.84	10
833.5	21.3496	2.146	24.72	21.84	10
835.6	21.3496	2.146	24.7	21.84	10
837.6	21.3514	2.155	24.72	21.85	10
839.6	21.3524	2.16	24.72	21.84	10
841.6	21.3519	2.157	24.72	21.84	10
843.5	21.3542	2.168	24.67	21.85	10
845.5	21.3561	2.177	24.65	21.85	10
847.5	21.3553	2.173	24.7	21.85	10
849.6	21.3567	2.18	24.73	21.85	10
851.6	21.3584	2.188	24.72	21.85	10
853.7	21.3573	2.183	24.69	21.85	10
855.8	21.358	2.187	24.69	21.85	10
857.5	21.3605	2.199	24.69	21.85	10
859.5	21.3618	2.205	24.69	21.85	10
861.5	21.3606	2.199	24.68	21.84	10
863.5	21.3632	2.211	24.7	21.85	10
865.5	21.363	2.21	24.7	21.85	10
867.6	21.3629	2.21	24.65	21.85	10
869.6	21.3646	2.218	24.67	21.86	10
871.7	21.3657	2.223	24.69	21.85	10
873.8	21.3657	2.223	24.7	21.85	10
875.9	21.3659	2.224	24.71	21.86	10
878	21.3677	2.233	24.72	21.86	10
880.1	21.3674	2.231	24.73	21.86	10
882.1	21.3669	2.229	24.71	21.87	10
884.2	21.369	2.239	24.71	21.87	10
886.3	21.3698	2.243	24.7	21.86	10
888.3	21.37	2.244	24.67	21.87	10
890.4	21.3708	2.248	24.71	21.87	10
892.4	21.3706	2.247	24.68	21.87	10
894.5	21.3723	2.255	24.65	21.87	10
895.5	21.3744	2.265	24.66	21.87	10
897.6	21.3748	2.267	24.68	21.87	10
899.6	21.3756	2.27	24.71	21.87	10
901.6	21.3747	2.266	24.71	21.88	10
903.7	21.3762	2.273	24.7	21.87	10

C.2 – continued from previous page

Elapsed Time [min]	Weight [mg]	Weight Change [%]	Sample Temp [°C]	Evap. Temp [°C]	RH [%]
905.7	21.3764	2.275	24.7	21.87	10
907.8	21.3765	2.275	24.69	21.87	10
909.8	21.3771	2.278	24.67	21.87	10
911.8	21.3789	2.286	24.7	21.87	10
913.8	21.379	2.287	24.72	21.87	10
915.9	21.3796	2.29	24.72	21.87	10
917.9	21.3803	2.293	24.68	21.87	10
920	21.3802	2.293	24.65	21.86	10
922.1	21.3811	2.297	24.68	21.87	10
924.1	21.3821	2.302	24.68	21.87	10
926.1	21.3806	2.295	24.69	21.87	10
928.1	21.3815	2.299	24.69	21.88	10
929.5	21.3836	2.309	24.7	21.87	10
931.6	21.3826	2.304	24.68	21.87	10
933.6	21.3833	2.307	24.68	21.88	10
935.7	21.3834	2.308	24.69	21.88	10
937.7	21.3846	2.314	24.68	21.87	10
939.7	21.3846	2.314	24.7	21.87	10
941.8	21.3856	2.318	24.71	21.88	10
943.8	21.385	2.316	24.69	21.88	10
945.8	21.3844	2.313	24.69	21.87	10
947.8	21.3848	2.315	24.7	21.88	10
949.5	21.3873	2.327	24.68	21.88	10
951.5	21.3863	2.322	24.67	21.87	10
953.6	21.3874	2.327	24.67	21.88	10
955.6	21.3881	2.33	24.68	21.88	10
957.5	21.3859	2.32	24.7	21.88	10
959.5	21.3865	2.323	24.66	21.88	10
961.5	21.389	2.335	24.67	21.88	10
963.6	21.3897	2.338	24.68	21.88	10
965.6	21.3881	2.331	24.66	21.88	10
967.7	21.3892	2.335	24.68	21.88	10
969.7	21.3899	2.339	24.69	21.88	10
971.7	21.389	2.334	24.71	21.88	10
973.7	21.3908	2.344	24.71	21.89	10
975.8	21.3899	2.339	24.66	21.88	10
977.9	21.3891	2.335	24.7	21.88	10
979.9	21.3909	2.344	24.69	21.88	10
981.9	21.3921	2.35	24.69	21.88	10
983.9	21.3906	2.343	24.68	21.88	10
985.5	21.3929	2.353	24.7	21.88	10
987.6	21.3926	2.352	24.71	21.88	10
989.6	21.3927	2.353	24.71	21.88	10
990.5	21.3902	2.34	24.72	21.88	10
992.5	21.3927	2.352	24.68	21.88	10
994.5	21.3936	2.357	24.67	21.88	10
996.5	21.3912	2.345	24.69	21.87	10
998.5	21.3935	2.356	24.7	21.88	10
1000.5	21.3937	2.357	24.69	21.88	20
1001.5	21.4029	2.401	24.69	21.87	20
1002.5	21.4101	2.436	24.69	21.87	20
1003.5	21.4218	2.491	24.69	21.86	20
1004.5	21.4336	2.548	24.68	21.87	20
1005.5	21.4473	2.614	24.68	21.86	20
1006.5	21.4599	2.674	24.69	21.86	20
1007.5	21.4706	2.725	24.69	21.86	20
1008.5	21.4817	2.778	24.69	21.85	20
1009.5	21.492	2.827	24.69	21.85	20
1010.5	21.504	2.885	24.67	21.85	20
1011.5	21.5133	2.929	24.64	21.85	20
1012.5	21.5284	3.002	24.64	21.85	20
1013.5	21.5404	3.059	24.66	21.85	20
1014.5	21.5477	3.094	24.67	21.85	20
1015.5	21.5573	3.14	24.69	21.84	20
1016.5	21.5654	3.179	24.7	21.84	20
1017.5	21.5751	3.225	24.71	21.84	20
1018.5	21.5845	3.27	24.7	21.84	20
1019.5	21.5944	3.318	24.7	21.84	20
1020.5	21.6032	3.359	24.7	21.84	20
1021.5	21.6121	3.402	24.7	21.84	20
1022.5	21.624	3.459	24.69	21.83	20
1023.5	21.6283	3.48	24.69	21.83	20
1024.5	21.6359	3.516	24.69	21.84	20
1025.5	21.644	3.555	24.69	21.84	20
1026.5	21.6539	3.602	24.71	21.84	20

C.2 – continued from previous page

Elapsed Time [min]	Weight [mg]	Weight Change [%]	Sample Temp [°C]	Evap. Temp [°C]	RH [%]
1027.5	21.6709	3.684	24.71	21.83	20
1029.5	21.6774	3.714	24.72	21.82	20
1030.5	21.6866	3.759	24.71	21.82	20
1031.5	21.6947	3.798	24.72	21.83	20
1032.5	21.7003	3.824	24.71	21.83	20
1033.5	21.7073	3.858	24.71	21.83	20
1034.5	21.7192	3.914	24.71	21.83	20
1035.5	21.7236	3.936	24.69	21.82	20
1036.5	21.7297	3.965	24.66	21.82	20
1037.5	21.7359	3.994	24.65	21.82	20
1038.5	21.7423	4.025	24.67	21.82	20
1039.5	21.7484	4.054	24.68	21.82	20
1040.5	21.7553	4.087	24.68	21.82	20
1041.5	21.7619	4.119	24.68	21.82	20
1042.5	21.7667	4.142	24.68	21.81	20
1043.5	21.7726	4.17	24.68	21.82	20
1044.5	21.7779	4.196	24.69	21.82	20
1045.5	21.7836	4.223	24.69	21.82	20
1046.5	21.7889	4.248	24.69	21.82	20
1047.5	21.7946	4.275	24.69	21.82	20
1048.5	21.7996	4.299	24.69	21.82	20
1049.5	21.8054	4.327	24.68	21.81	20
1050.5	21.8113	4.355	24.69	21.82	20
1051.5	21.817	4.382	24.7	21.82	20
1052.5	21.8214	4.404	24.7	21.82	20
1053.5	21.8264	4.427	24.7	21.82	20
1054.5	21.8324	4.456	24.7	21.82	20
1055.5	21.8375	4.48	24.7	21.81	20
1056.5	21.8413	4.499	24.71	21.82	20
1057.5	21.8468	4.525	24.72	21.82	20
1058.5	21.8531	4.555	24.72	21.82	20
1059.5	21.8572	4.575	24.73	21.82	20
1060.5	21.8609	4.592	24.74	21.81	20
1061.5	21.8666	4.62	24.75	21.81	20
1062.5	21.8701	4.636	24.75	21.81	20
1063.5	21.8738	4.654	24.72	21.81	20
1064.5	21.8777	4.673	24.7	21.81	20
1065.5	21.881	4.689	24.71	21.81	20
1066.5	21.8864	4.715	24.71	21.81	20
1067.5	21.8895	4.73	24.71	21.8	20
1068.5	21.8927	4.745	24.71	21.8	20
1069.5	21.8976	4.768	24.72	21.8	20
1070.5	21.9012	4.785	24.72	21.81	20
1071.5	21.9051	4.804	24.72	21.81	20
1072.5	21.9082	4.819	24.72	21.8	20
1073.5	21.9121	4.837	24.72	21.8	20
1074.5	21.9154	4.853	24.72	21.79	20
1075.5	21.9179	4.865	24.73	21.79	20
1076.5	21.9218	4.884	24.74	21.79	20
1077.5	21.9263	4.905	24.74	21.8	20
1078.5	21.9296	4.921	24.74	21.79	20
1079.5	21.9333	4.939	24.71	21.79	20
1080.5	21.9363	4.953	24.7	21.79	20
1081.5	21.939	4.966	24.7	21.78	20
1083.5	21.945	4.995	24.71	21.79	20
1084.5	21.9487	5.012	24.71	21.79	20
1085.5	21.9512	5.025	24.72	21.78	20
1086.5	21.9547	5.041	24.72	21.78	20
1088.5	21.9586	5.06	24.72	21.78	20
1089.5	21.961	5.071	24.71	21.78	20
1090.5	21.9644	5.088	24.71	21.78	20
1091.5	21.9678	5.104	24.72	21.79	20
1092.5	21.9703	5.116	24.73	21.78	20
1093.5	21.9733	5.13	24.73	21.78	20
1095.5	21.9773	5.149	24.71	21.78	20
1096.5	21.9808	5.166	24.71	21.78	20
1097.5	21.9837	5.18	24.71	21.78	20
1098.5	21.9863	5.192	24.68	21.78	20
1099.5	21.9891	5.206	24.68	21.78	20
1101.5	21.9937	5.228	24.69	21.77	20
1102.5	21.996	5.239	24.69	21.78	20
1103.5	21.9988	5.252	24.69	21.78	20
1104.5	22.0009	5.262	24.69	21.78	20
1105.5	22.004	5.277	24.69	21.78	20
1106.5	22.0064	5.289	24.7	21.78	20

C.2 – continued from previous page

Elapsed Time [min]	Weight [mg]	Weight Change [%]	Sample Temp [°C]	Evap. Temp [°C]	RH [%]
1107.5	22.0085	5.299	24.7	21.78	20
1108.5	22.0108	5.31	24.71	21.78	20
1110.5	22.0133	5.322	24.7	21.78	20
1111.5	22.0161	5.335	24.7	21.78	20
1113.5	22.0211	5.359	24.7	21.79	20
1115.5	22.0239	5.372	24.69	21.79	20
1117.5	22.0282	5.393	24.67	21.79	20
1119.5	22.031	5.406	24.69	21.8	20
1121.5	22.0343	5.422	24.7	21.8	20
1122.5	22.0372	5.436	24.68	21.79	20
1124.5	22.0383	5.441	24.69	21.79	20
1125.5	22.0409	5.454	24.68	21.8	20
1126.5	22.0457	5.477	24.69	21.8	20
1128.5	22.0464	5.48	24.7	21.8	20
1130.5	22.0515	5.505	24.69	21.79	20
1132.5	22.0549	5.521	24.7	21.8	20
1134.5	22.0585	5.538	24.67	21.8	20
1136.5	22.0607	5.549	24.68	21.8	20
1138.5	22.062	5.555	24.68	21.79	20
1139.5	22.0644	5.566	24.69	21.79	20
1141.5	22.0685	5.586	24.7	21.79	20
1143.6	22.0689	5.588	24.7	21.79	20
1145.6	22.0706	5.596	24.7	21.78	20
1147.5	22.0743	5.613	24.71	21.79	20
1149.6	22.0746	5.615	24.69	21.78	20
1150.5	22.0804	5.643	24.69	21.78	20
1151.5	22.0775	5.629	24.69	21.78	20
1153.5	22.0764	5.624	24.69	21.78	20
1154.5	22.079	5.636	24.68	21.79	20
1156.5	22.0816	5.649	24.67	21.78	20
1158.5	22.0856	5.668	24.67	21.78	20
1160.6	22.0858	5.669	24.66	21.77	20
1162.5	22.0882	5.68	24.68	21.78	20
1163.5	22.0905	5.691	24.69	21.78	20
1165.6	22.0919	5.698	24.7	21.77	20
1167.6	22.0919	5.698	24.67	21.77	20
1169.5	22.0942	5.708	24.68	21.78	20
1171.5	22.0981	5.728	24.69	21.78	20
1173.5	22.0979	5.726	24.7	21.78	20
1175.6	22.0979	5.727	24.7	21.78	20
1176.5	22.1005	5.739	24.69	21.79	20
1178.5	22.1017	5.745	24.67	21.79	20
1180.5	22.1051	5.761	24.69	21.78	20
1181.5	22.1026	5.749	24.68	21.78	20
1183.6	22.1042	5.757	24.68	21.79	20
1185.5	22.107	5.77	24.69	21.79	20
1187.5	22.1072	5.771	24.7	21.78	20
1189.5	22.1079	5.774	24.69	21.78	20
1191.5	22.1206	5.835	24.7	21.79	20
1192.5	22.1107	5.788	24.71	21.79	20
1194.6	22.1115	5.791	24.74	21.79	20
1196.6	22.1122	5.795	24.69	21.79	20
1198.5	22.1156	5.811	24.7	21.8	20
1200.5	22.1162	5.814	24.7	21.8	20
1202.5	22.1182	5.824	24.71	21.8	20
1204.5	22.1254	5.858	24.71	21.8	20
1205.5	22.119	5.828	24.71	21.8	20
1207.5	22.1234	5.848	24.7	21.8	20
1208.5	22.1192	5.828	24.7	21.8	20
1210.5	22.1206	5.835	24.7	21.8	20
1212.6	22.1209	5.836	24.7	21.81	20
1214.6	22.122	5.842	24.67	21.8	20
1216.5	22.1242	5.852	24.67	21.8	20
1218.5	22.1235	5.849	24.69	21.81	20
1220.5	22.145	5.952	24.7	21.81	20
1221.5	22.1289	5.875	24.7	21.81	20
1222.5	22.1262	5.862	24.71	21.81	20
1224.5	22.1272	5.866	24.71	21.8	20
1225.5	22.1315	5.887	24.71	21.81	20
1226.5	22.1356	5.907	24.71	21.82	20
1227.5	22.1288	5.874	24.72	21.81	20
1229.5	22.1331	5.895	24.71	21.8	20
1230.5	22.1309	5.884	24.71	21.8	20
1232.6	22.1308	5.884	24.7	21.81	20
1234.6	22.13	5.88	24.69	21.81	20

C.2 – continued from previous page

Elapsed Time [min]	Weight [mg]	Weight Change [%]	Sample Temp [°C]	Evap. Temp [°C]	RH [%]
1236.6	22.1299	5.879	24.69	21.8	20
1238.6	22.1312	5.886	24.7	21.8	20
1240.7	22.1325	5.892	24.71	21.8	20
1242.5	22.1346	5.902	24.7	21.8	20
1244.5	22.1354	5.906	24.69	21.79	20
1246.5	22.1365	5.911	24.69	21.8	20
1248.6	22.1369	5.913	24.68	21.8	20
1250.6	22.1375	5.916	24.69	21.79	20
1252.6	22.1371	5.914	24.69	21.8	20
1254.7	22.1385	5.921	24.69	21.79	20
1256.7	22.1383	5.919	24.7	21.79	20
1258.5	22.1407	5.931	24.69	21.78	20
1260.5	22.1408	5.932	24.69	21.79	20
1261.5	22.146	5.957	24.69	21.78	20
1262.5	22.1493	5.973	24.68	21.78	20
1263.5	22.1428	5.941	24.68	21.77	20
1265.5	22.1425	5.94	24.7	21.77	20
1267.5	22.1423	5.939	24.7	21.77	20
1269.5	22.1497	5.974	24.7	21.77	20
1270.5	22.1439	5.947	24.71	21.76	20
1272.5	22.1427	5.941	24.73	21.76	20
1274.5	22.1439	5.947	24.71	21.77	20
1276.5	22.1435	5.945	24.7	21.77	20
1278.5	22.1434	5.944	24.69	21.77	20
1280.5	22.1453	5.953	24.68	21.77	20
1282.6	22.1442	5.948	24.68	21.77	20
1284.6	22.1458	5.956	24.68	21.76	20
1286.6	22.1458	5.956	24.69	21.77	20
1288.6	22.1459	5.956	24.68	21.77	20
1290.6	22.1456	5.955	24.69	21.77	20
1292.6	22.1465	5.959	24.69	21.77	20
1294.7	22.1474	5.963	24.7	21.78	20
1296.5	22.1506	5.978	24.67	21.77	20
1298.5	22.1504	5.978	24.68	21.77	20
1300.5	22.1511	5.981	24.7	21.78	20
1302.5	22.1501	5.976	24.71	21.78	20
1303.5	22.1572	6.01	24.69	21.78	20
1305.5	22.1504	5.978	24.7	21.78	20
1307.6	22.1517	5.984	24.7	21.79	20
1309.6	22.1515	5.983	24.7	21.79	20
1311.6	22.1518	5.985	24.68	21.78	20
1313.6	22.1526	5.988	24.7	21.79	20
1315.5	22.1619	6.033	24.69	21.79	20
1316.5	22.1576	6.012	24.68	21.8	20
1317.5	22.1524	5.987	24.68	21.8	20
1319.5	22.1533	5.991	24.69	21.8	20
1321.5	22.1538	5.994	24.69	21.81	20
1323.5	22.1542	5.996	24.69	21.81	20
1325.6	22.1555	6.002	24.67	21.81	20
1327.6	22.1539	5.994	24.69	21.82	20
1328.5	22.1573	6.01	24.69	21.82	20
1329.5	22.1551	6	24.68	21.82	20
1331.6	22.1539	5.994	24.7	21.82	20
1333.6	22.155	5.999	24.69	21.82	20
1335.6	22.1558	6.004	24.68	21.82	20
1337.6	22.1555	6.002	24.67	21.83	20
1339.6	22.1549	5.999	24.69	21.84	20
1341.6	22.1567	6.008	24.7	21.85	20
1343.6	22.1577	6.013	24.71	21.85	20
1345.6	22.1574	6.011	24.7	21.86	20
1347.7	22.1576	6.012	24.69	21.86	20
1349.8	22.159	6.019	24.7	21.85	20
1351.8	22.1595	6.021	24.7	21.86	20
1353.9	22.1592	6.02	24.68	21.87	20
1355.9	22.1603	6.025	24.7	21.86	20
1357.9	22.16	6.024	24.73	21.86	20
1360	22.1606	6.026	24.71	21.88	30
1361.5	22.1696	6.07	24.72	21.87	30
1362.5	22.1816	6.127	24.72	21.86	30
1363.5	22.1942	6.187	24.7	21.86	30
1364.5	22.2082	6.254	24.67	21.86	30
1365.5	22.22	6.311	24.66	21.86	30
1366.5	22.2334	6.375	24.66	21.86	30
1367.5	22.2469	6.439	24.66	21.86	30
1368.5	22.2583	6.494	24.67	21.86	30

C.2 – continued from previous page

Elapsed Time [min]	Weight [mg]	Weight Change [%]	Sample Temp [°C]	Evap. Temp [°C]	RH [%]
1369.5	22.2712	6.556	24.68	21.86	30
1370.5	22.2841	6.617	24.69	21.85	30
1371.5	22.2971	6.679	24.7	21.86	30
1372.5	22.3074	6.729	24.71	21.86	30
1373.5	22.3183	6.781	24.7	21.86	30
1374.5	22.3309	6.841	24.7	21.86	30
1375.5	22.3408	6.888	24.71	21.86	30
1376.5	22.3528	6.946	24.71	21.86	30
1377.5	22.3629	6.994	24.71	21.86	30
1378.5	22.3749	7.052	24.7	21.87	30
1379.5	22.3857	7.103	24.69	21.87	30
1380.5	22.3957	7.151	24.68	21.87	30
1381.5	22.4052	7.197	24.68	21.87	30
1382.5	22.4138	7.238	24.68	21.87	30
1383.5	22.4224	7.279	24.68	21.86	30
1384.5	22.433	7.33	24.67	21.87	30
1385.5	22.4429	7.377	24.67	21.87	30
1386.5	22.4525	7.423	24.68	21.87	30
1387.5	22.4618	7.468	24.68	21.87	30
1388.5	22.4709	7.511	24.67	21.87	30
1389.5	22.4794	7.552	24.67	21.87	30
1390.5	22.4877	7.591	24.68	21.87	30
1391.5	22.4953	7.628	24.69	21.87	30
1392.5	22.505	7.674	24.7	21.87	30
1393.5	22.5129	7.712	24.69	21.88	30
1394.5	22.5199	7.745	24.68	21.87	30
1395.5	22.5278	7.783	24.68	21.87	30
1396.5	22.5354	7.819	24.68	21.87	30
1397.5	22.5405	7.844	24.68	21.87	30
1398.5	22.5508	7.893	24.68	21.87	30
1399.5	22.5573	7.924	24.68	21.87	30
1400.5	22.5658	7.965	24.69	21.88	30
1401.5	22.5718	7.994	24.69	21.88	30
1402.5	22.5786	8.027	24.69	21.88	30
1403.5	22.5846	8.055	24.69	21.87	30
1404.5	22.5902	8.082	24.7	21.87	30
1405.5	22.5987	8.122	24.72	21.88	30
1406.5	22.6046	8.151	24.73	21.88	30
1407.5	22.611	8.181	24.73	21.88	30
1408.5	22.6179	8.214	24.71	21.88	30
1409.5	22.6245	8.246	24.7	21.88	30
1410.5	22.6292	8.268	24.69	21.87	30
1411.5	22.6399	8.32	24.69	21.87	30
1413.5	22.6465	8.351	24.69	21.88	30
1414.5	22.6538	8.386	24.69	21.88	30
1415.5	22.6606	8.419	24.7	21.88	30
1416.5	22.6645	8.437	24.72	21.88	30
1417.5	22.6693	8.46	24.72	21.88	30
1418.5	22.6747	8.486	24.71	21.88	30
1419.5	22.6797	8.51	24.71	21.89	30
1420.5	22.6836	8.529	24.71	21.89	30
1421.5	22.6889	8.554	24.71	21.88	30
1422.5	22.6942	8.579	24.7	21.88	30
1423.5	22.7007	8.611	24.69	21.88	30
1424.5	22.7037	8.625	24.7	21.88	30
1425.5	22.7087	8.649	24.71	21.89	30
1426.5	22.7125	8.667	24.72	21.89	30
1427.5	22.7159	8.683	24.72	21.9	30
1428.5	22.7204	8.705	24.72	21.89	30
1429.5	22.7253	8.728	24.72	21.89	30
1430.5	22.7397	8.797	24.73	21.89	30
1431.5	22.7371	8.785	24.72	21.89	30
1432.5	22.7406	8.801	24.68	21.9	30
1433.5	22.7449	8.822	24.66	21.9	30
1434.5	22.7506	8.849	24.67	21.9	30
1436.5	22.7566	8.878	24.7	21.89	30
1437.5	22.7599	8.894	24.71	21.89	30
1438.5	22.7641	8.914	24.69	21.89	30
1439.5	22.7689	8.937	24.7	21.89	30
1440.5	22.7718	8.951	24.69	21.89	30
1441.5	22.7766	8.974	24.69	21.89	30
1442.5	22.7808	8.994	24.67	21.89	30
1443.5	22.7844	9.011	24.65	21.89	30
1444.5	22.7877	9.027	24.67	21.89	30
1445.5	22.791	9.043	24.7	21.89	30

C.2 – continued from previous page

Elapsed Time [min]	Weight [mg]	Weight Change [%]	Sample Temp [°C]	Evap. Temp [°C]	RH [%]
1446.5	22.7947	9.06	24.7	21.9	30
1447.5	22.7982	9.077	24.7	21.9	30
1448.5	22.8027	9.099	24.71	21.9	30
1449.5	22.8057	9.113	24.71	21.89	30
1450.5	22.8086	9.127	24.71	21.89	30
1451.5	22.8123	9.144	24.7	21.89	30
1452.5	22.8155	9.16	24.7	21.89	30
1453.5	22.8187	9.175	24.71	21.89	30
1454.5	22.8223	9.192	24.73	21.89	30
1455.5	22.8246	9.203	24.71	21.89	30
1456.5	22.8276	9.218	24.69	21.88	30
1457.5	22.8297	9.228	24.67	21.88	30
1458.5	22.8329	9.243	24.67	21.88	30
1459.5	22.8356	9.256	24.68	21.88	30
1460.5	22.8384	9.27	24.68	21.88	30
1461.5	22.8417	9.285	24.68	21.88	30
1462.5	22.844	9.296	24.69	21.88	30
1463.5	22.8479	9.315	24.69	21.88	30
1465.5	22.8521	9.335	24.7	21.89	30
1467.5	22.8572	9.359	24.7	21.89	30
1469.5	22.8621	9.383	24.68	21.89	30
1471.5	22.8667	9.405	24.69	21.89	30
1472.5	22.8696	9.419	24.69	21.89	30
1474.5	22.8741	9.44	24.72	21.89	30
1475.5	22.8768	9.453	24.71	21.88	30
1477.5	22.8793	9.465	24.7	21.9	30
1478.5	22.8817	9.477	24.69	21.9	30
1479.5	22.8842	9.488	24.68	21.9	30
1481.5	22.8876	9.505	24.69	21.89	30
1483.5	22.8916	9.524	24.71	21.9	30
1484.5	22.8937	9.534	24.71	21.9	30
1485.5	22.8958	9.544	24.72	21.9	30
1487.6	22.897	9.55	24.72	21.89	30
1488.5	22.8993	9.561	24.71	21.89	30
1490.5	22.9032	9.58	24.7	21.9	30
1492.5	22.9066	9.596	24.69	21.9	30
1493.5	22.9095	9.61	24.69	21.9	30
1495.6	22.9098	9.611	24.69	21.9	30
1497.5	22.9149	9.635	24.69	21.91	30
1499.5	22.9157	9.639	24.65	21.91	30
1500.5	22.9184	9.652	24.65	21.91	30
1502.5	22.9206	9.663	24.67	21.91	30
1503.5	22.9237	9.677	24.67	21.91	30
1505.5	22.9239	9.678	24.68	21.92	30
1507.5	22.9265	9.691	24.68	21.92	30
1508.5	22.9291	9.703	24.69	21.92	30
1510.5	22.9347	9.73	24.7	21.92	30
1511.5	22.9322	9.718	24.69	21.93	30
1512.5	22.9349	9.731	24.7	21.94	30
1514.5	22.9384	9.748	24.68	21.93	30
1516.5	22.9405	9.758	24.69	21.93	30
1518.5	22.9439	9.774	24.69	21.94	30
1520.5	22.9461	9.785	24.68	21.94	30
1522.5	22.955	9.827	24.68	21.94	30
1523.5	22.9501	9.804	24.7	21.94	30
1525.5	22.953	9.817	24.7	21.96	30
1527.5	22.9553	9.829	24.69	21.94	30
1529.6	22.9562	9.833	24.69	21.94	30
1531.5	22.9596	9.849	24.69	21.94	30
1533.6	22.9606	9.854	24.68	21.94	30
1534.5	22.9628	9.865	24.68	21.94	30
1536.6	22.964	9.87	24.69	21.94	30
1538.6	22.965	9.875	24.7	21.95	30
1540.5	22.9681	9.89	24.69	21.95	30
1542.5	22.9687	9.893	24.69	21.94	30
1544.5	22.972	9.908	24.68	21.95	30
1545.5	22.9745	9.921	24.69	21.95	30
1546.5	22.9826	9.959	24.69	21.95	30
1547.5	22.9741	9.918	24.68	21.95	30
1549.5	22.9744	9.92	24.69	21.95	30
1551.5	22.9776	9.935	24.68	21.96	30
1553.5	22.9785	9.94	24.69	21.96	30
1555.6	22.9798	9.946	24.7	21.96	30
1557.6	22.9819	9.956	24.69	21.97	30
1559.6	22.9831	9.962	24.69	21.96	30

C.2 – continued from previous page

Elapsed Time [min]	Weight [mg]	Weight Change [%]	Sample Temp [°C]	Evap. Temp [°C]	RH [%]
1561.6	22.9845	9.968	24.68	21.96	30
1563.7	22.9858	9.975	24.65	21.95	30
1565.7	22.9861	9.976	24.67	21.95	30
1567.7	22.9879	9.985	24.67	21.95	30
1569.7	22.9886	9.988	24.68	21.94	30
1571.7	22.989	9.99	24.67	21.95	30
1573.5	22.9913	10.001	24.67	21.95	30
1575.6	22.9923	10.005	24.67	21.95	30
1577.6	22.9936	10.012	24.67	21.95	30
1579.6	22.9954	10.021	24.69	21.97	30
1581.7	22.9967	10.027	24.69	21.97	30
1583.7	22.9985	10.035	24.69	21.98	30
1585.8	22.9996	10.041	24.67	21.98	30
1587.9	23.0006	10.045	24.68	21.98	30
1589.5	23.0027	10.055	24.68	21.95	30
1591.5	23.0144	10.112	24.66	21.95	30
1592.5	23.0038	10.061	24.66	21.96	30
1594.5	23.0051	10.067	24.68	21.97	30
1596.6	23.0052	10.068	24.68	21.96	30
1597.5	23.0093	10.087	24.68	21.96	30
1599.5	23.0077	10.079	24.67	21.96	30
1601.6	23.0083	10.082	24.67	21.96	30
1603.6	23.0083	10.082	24.68	21.96	30
1605.6	23.0099	10.09	24.68	21.96	30
1606.5	23.0135	10.107	24.68	21.96	30
1607.5	23.0097	10.089	24.69	21.97	30
1609.5	23.0098	10.089	24.68	21.97	30
1611.5	23.0133	10.106	24.67	21.96	30
1613.5	23.0124	10.102	24.68	21.97	30
1615.6	23.0138	10.108	24.66	21.97	30
1617.6	23.0148	10.113	24.65	21.97	30
1619.5	23.0182	10.129	24.65	21.98	30
1621.6	23.0178	10.128	24.67	21.98	30
1623.5	23.0199	10.138	24.65	21.97	30
1624.5	23.026	10.167	24.65	21.97	30
1625.5	23.0205	10.141	24.65	21.98	30
1627.5	23.0205	10.141	24.66	21.98	30
1629.5	23.0208	10.142	24.65	21.98	30
1631.5	23.0221	10.148	24.64	21.98	30
1633.6	23.0229	10.152	24.67	21.99	30
1635.6	23.0238	10.157	24.68	21.98	30
1637.7	23.0244	10.159	24.68	21.97	30
1639.7	23.0237	10.156	24.66	21.98	30
1641.8	23.0229	10.152	24.66	21.98	30
1643.5	23.0263	10.168	24.65	21.98	30
1645.5	23.0266	10.17	24.65	21.99	30
1647.6	23.0254	10.164	24.67	21.99	30
1649.6	23.0257	10.166	24.67	21.99	30
1651.7	23.0264	10.169	24.66	22	30
1653.5	23.024	10.157	24.67	22	30
1655.6	23.0243	10.159	24.68	22	30
1657.6	23.0242	10.158	24.68	22	30
1659.6	23.0224	10.15	24.67	22	30
1660.5	23.0246	10.16	24.66	22	30
1662.5	23.0229	10.152	24.67	22	30
1664.5	23.0254	10.164	24.66	22	30
1666.5	23.0238	10.156	24.67	22.02	30
1668.5	23.0254	10.164	24.67	22.02	30
1670.6	23.0256	10.165	24.66	22.01	30
1672.6	23.0269	10.171	24.68	22.01	30
1674.6	23.0268	10.171	24.67	22.02	30
1676.6	23.0275	10.174	24.63	22	30
1678.6	23.0286	10.179	24.67	21.99	30
1680.6	23.0288	10.18	24.69	21.99	30
1681.5	23.032	10.195	24.69	21.99	30
1683.5	23.0306	10.189	24.69	21.98	30
1685.5	23.0317	10.194	24.69	21.98	30
1687.6	23.0327	10.199	24.66	21.98	30
1689.6	23.0341	10.206	24.68	21.98	30
1691.6	23.0333	10.202	24.69	21.97	30
1693.6	23.0335	10.203	24.67	21.98	30
1695.7	23.0326	10.199	24.64	21.98	30
1697.8	23.0327	10.199	24.68	21.98	30
1699.8	23.0328	10.2	24.69	21.97	30
1701.9	23.0337	10.204	24.7	21.98	30

C.2 – continued from previous page

Elapsed Time [min]	Weight [mg]	Weight Change [%]	Sample Temp [°C]	Evap. Temp [°C]	RH [%]
1704	23.0327	10.199	24.7	21.97	30
1706	23.033	10.201	24.7	21.97	30
1708.1	23.0333	10.202	24.7	21.96	30
1710.1	23.0331	10.201	24.71	21.97	30
1712.1	23.0324	10.198	24.68	21.97	30
1714.2	23.0343	10.206	24.64	21.96	30
1716.2	23.0356	10.213	24.66	21.97	30
1718.3	23.0354	10.212	24.68	21.97	30
1720.3	23.0354	10.212	24.66	21.96	40
1721.5	23.045	10.258	24.65	21.96	40
1722.5	23.056	10.31	24.67	21.97	40
1723.5	23.0705	10.38	24.68	21.97	40
1724.5	23.0833	10.441	24.67	21.97	40
1725.5	23.096	10.502	24.64	21.96	40
1726.5	23.1098	10.568	24.64	21.95	40
1727.5	23.1284	10.657	24.65	21.95	40
1728.5	23.1386	10.705	24.66	21.95	40
1729.5	23.1499	10.76	24.66	21.95	40
1730.5	23.1631	10.823	24.64	21.95	40
1731.5	23.174	10.875	24.65	21.95	40
1732.5	23.1878	10.941	24.67	21.95	40
1733.5	23.1995	10.997	24.67	21.95	40
1734.5	23.2099	11.047	24.64	21.95	40
1735.5	23.2223	11.106	24.66	21.95	40
1736.5	23.2344	11.164	24.68	21.95	40
1737.5	23.2467	11.223	24.69	21.95	40
1738.5	23.2594	11.284	24.7	21.95	40
1739.5	23.2732	11.35	24.67	21.95	40
1740.5	23.2808	11.386	24.66	21.95	40
1741.5	23.2908	11.434	24.68	21.95	40
1742.5	23.3003	11.479	24.69	21.95	40
1743.5	23.3092	11.522	24.7	21.95	40
1744.5	23.318	11.564	24.71	21.95	40
1745.5	23.3335	11.638	24.69	21.95	40
1746.5	23.3404	11.671	24.66	21.95	40
1747.5	23.3509	11.721	24.64	21.95	40
1748.5	23.3589	11.76	24.66	21.95	40
1749.5	23.3683	11.805	24.68	21.94	40
1750.5	23.3767	11.845	24.69	21.94	40
1751.5	23.3847	11.883	24.69	21.94	40
1752.5	23.4002	11.957	24.7	21.95	40
1753.5	23.4038	11.974	24.7	21.95	40
1754.5	23.4127	12.017	24.68	21.94	40
1755.5	23.4192	12.048	24.65	21.94	40
1756.5	23.4344	12.121	24.66	21.94	40
1758.5	23.4419	12.157	24.7	21.93	40
1759.5	23.4496	12.194	24.7	21.93	40
1760.5	23.4561	12.225	24.69	21.93	40
1761.5	23.4647	12.266	24.66	21.93	40
1762.5	23.472	12.301	24.67	21.93	40
1763.5	23.4786	12.332	24.69	21.93	40
1764.5	23.4852	12.364	24.69	21.92	40
1765.5	23.4915	12.394	24.7	21.92	40
1766.5	23.4981	12.426	24.69	21.93	40
1767.5	23.5105	12.485	24.66	21.93	40
1769.5	23.519	12.525	24.68	21.93	40
1770.5	23.5246	12.552	24.7	21.92	40
1771.5	23.5294	12.576	24.7	21.92	40
1772.5	23.5415	12.634	24.7	21.92	40
1773.5	23.5443	12.647	24.69	21.92	40
1774.5	23.547	12.66	24.69	21.92	40
1775.5	23.5532	12.689	24.69	21.99	40
1776.5	23.5574	12.709	24.7	22.06	40
1777.5	23.5685	12.763	24.72	22.11	40
1778.5	23.5772	12.804	24.72	22.08	40
1779.5	23.5824	12.829	24.7	22.06	40
1780.5	23.5849	12.841	24.7	22.05	40
1781.5	23.5884	12.858	24.7	22.05	40
1782.5	23.5954	12.891	24.67	22.04	40
1783.5	23.6021	12.923	24.65	22.04	40
1784.5	23.6061	12.942	24.66	22.03	40
1785.5	23.6111	12.966	24.69	22.03	40
1786.5	23.6148	12.984	24.69	22.02	40
1787.5	23.619	13.004	24.7	22.02	40
1788.5	23.6228	13.022	24.71	22.02	40

C.2 – continued from previous page

Elapsed Time [min]	Weight [mg]	Weight Change [%]	Sample Temp [°C]	Evap. Temp [°C]	RH [%]
1789.5	23.6293	13.054	24.7	22.01	40
1790.5	23.635	13.081	24.67	22.01	40
1791.5	23.6384	13.097	24.65	22.01	40
1792.5	23.6412	13.11	24.65	22.01	40
1793.5	23.6478	13.142	24.68	22.01	40
1795.5	23.6558	13.18	24.69	22	40
1796.5	23.6615	13.207	24.68	22	40
1797.5	23.6646	13.222	24.68	21.99	40
1798.5	23.6698	13.247	24.68	21.99	40
1799.5	23.6719	13.257	24.67	21.99	40
1801.5	23.6748	13.271	24.62	21.99	40
1802.5	23.6777	13.285	24.62	22	40
1803.5	23.6877	13.333	24.64	22	40
1805.5	23.6926	13.356	24.68	21.99	40
1807.6	23.6935	13.36	24.7	21.98	40
1808.5	23.6979	13.382	24.7	21.98	40
1809.5	23.7019	13.401	24.7	21.98	40
1810.5	23.7047	13.414	24.69	21.98	40
1811.5	23.712	13.449	24.68	21.98	40
1813.5	23.7189	13.482	24.69	21.98	40
1814.5	23.7168	13.472	24.69	21.98	40
1816.5	23.7195	13.485	24.67	21.99	40
1817.5	23.726	13.516	24.65	21.99	40
1818.5	23.7301	13.536	24.64	21.98	40
1819.5	23.7353	13.56	24.66	21.98	40
1821.5	23.7367	13.567	24.68	21.97	40
1823.5	23.7411	13.588	24.7	21.98	40
1824.5	23.7439	13.602	24.68	21.98	40
1825.5	23.746	13.612	24.64	21.98	40
1826.5	23.7489	13.626	24.62	21.99	40
1828.5	23.7516	13.638	24.67	21.99	40
1829.5	23.7547	13.653	24.68	21.99	40
1830.5	23.7569	13.664	24.69	21.98	40
1831.5	23.7599	13.678	24.69	21.98	40
1833.5	23.7653	13.704	24.69	21.98	40
1835.5	23.7674	13.714	24.68	21.98	40
1836.5	23.7695	13.724	24.67	21.97	40
1838.5	23.7724	13.738	24.69	21.98	40
1840.5	23.7774	13.762	24.65	21.99	40
1842.6	23.7786	13.768	24.67	21.98	40
1844.5	23.7812	13.78	24.7	21.99	40
1845.5	23.785	13.798	24.7	21.99	40
1847.5	23.789	13.818	24.65	21.99	40
1849.5	23.7924	13.834	24.7	21.99	40
1851.5	23.7957	13.849	24.72	21.99	40
1853.5	23.8012	13.876	24.68	21.99	40
1855.5	23.8022	13.881	24.68	21.99	40
1857.5	23.8044	13.891	24.68	21.99	40
1859.5	23.8076	13.907	24.67	21.99	40
1861.5	23.8123	13.929	24.69	21.99	40
1863.5	23.8143	13.938	24.71	21.98	40
1865.5	23.8162	13.947	24.71	21.97	40
1867.5	23.8171	13.952	24.66	21.95	40
1869.5	23.8203	13.967	24.67	21.95	40
1871.5	23.8212	13.971	24.69	21.96	40
1873.5	23.8243	13.986	24.68	21.97	40
1875.5	23.8257	13.993	24.69	21.97	40
1877.6	23.8271	14	24.66	21.97	40
1879.6	23.8285	14.006	24.62	21.98	40
1881.5	23.8319	14.023	24.61	21.98	40
1883.5	23.8334	14.03	24.65	21.98	40
1885.5	23.834	14.033	24.68	21.97	40
1887.5	23.8369	14.047	24.67	21.97	40
1888.5	23.8395	14.059	24.67	21.97	40
1890.5	23.841	14.066	24.66	21.97	40
1892.6	23.8418	14.07	24.68	21.97	40
1894.6	23.8431	14.076	24.63	21.97	40
1895.5	23.8456	14.088	24.63	21.97	40
1897.6	23.8469	14.094	24.67	21.97	40
1899.6	23.8474	14.097	24.7	21.97	40
1901.7	23.8485	14.102	24.69	21.97	40
1903.5	23.8511	14.115	24.65	21.97	40
1905.5	23.8524	14.121	24.68	21.96	40
1907.6	23.8527	14.122	24.7	21.96	40
1909.6	23.8544	14.13	24.65	21.96	40

C.2 – continued from previous page

Elapsed Time [min]	Weight [mg]	Weight Change [%]	Sample Temp [°C]	Evap. Temp [°C]	RH [%]
1911.6	23.8555	14.136	24.68	21.96	40
1913.6	23.8553	14.134	24.67	21.96	40
1915.7	23.8564	14.14	24.68	21.96	40
1917.5	23.8593	14.154	24.7	21.96	40
1919.6	23.8579	14.147	24.7	21.95	40
1921.6	23.8578	14.147	24.67	21.96	40
1923.6	23.8579	14.147	24.63	21.95	40
1925.6	23.8591	14.153	24.69	21.95	40
1927.6	23.8585	14.15	24.68	21.95	40
1929.6	23.8569	14.142	24.71	21.95	40
1930.5	23.8591	14.153	24.71	21.95	40
1932.5	23.8613	14.164	24.7	21.95	40
1934.6	23.8601	14.158	24.67	21.94	40
1936.6	23.8613	14.164	24.71	21.95	40
1938.6	23.8624	14.169	24.69	21.95	40
1940.6	23.8631	14.172	24.69	21.94	40
1942.7	23.8629	14.171	24.69	21.95	40
1944.8	23.8631	14.172	24.7	21.95	40
1946.9	23.8623	14.168	24.69	21.95	40
1948.9	23.8642	14.177	24.66	21.95	40
1951	23.8659	14.185	24.69	21.95	40
1953.1	23.8664	14.188	24.72	21.95	40
1955.1	23.8663	14.187	24.71	21.94	40
1957.1	23.8672	14.192	24.72	21.95	40
1959.1	23.868	14.196	24.67	21.95	40
1961.1	23.8685	14.198	24.71	21.94	40
1963.1	23.8685	14.198	24.72	21.94	40
1965.1	23.8705	14.208	24.71	21.94	40
1967.1	23.8704	14.207	24.68	21.94	40
1969.1	23.8696	14.203	24.67	21.94	40
1971.2	23.8701	14.205	24.69	21.94	40
1973.3	23.8706	14.208	24.7	21.94	40
1975.3	23.8699	14.205	24.69	21.94	40
1977.3	23.871	14.21	24.69	21.94	40
1979.4	23.8705	14.207	24.69	21.94	40
1981.4	23.8718	14.214	24.67	21.94	40
1983.4	23.8705	14.207	24.68	21.93	40
1985.4	23.8702	14.206	24.67	21.94	40
1987.5	23.872	14.215	24.66	21.94	40
1989.6	23.8719	14.214	24.67	21.94	40
1991.6	23.8715	14.212	24.68	21.94	40
1993.6	23.8731	14.22	24.65	21.94	40
1995.7	23.8734	14.221	24.65	21.94	40
1997.7	23.8722	14.216	24.68	21.93	40
1999.8	23.8731	14.22	24.68	21.94	40
2001.5	23.876	14.234	24.66	21.94	40
2003.6	23.8752	14.23	24.68	21.93	40
2005.6	23.8747	14.227	24.7	21.93	40
2007.7	23.8764	14.236	24.69	21.93	40
2009.7	23.8755	14.231	24.68	21.93	40
2011.7	23.8743	14.226	24.7	21.93	40
2013.7	23.8757	14.232	24.7	21.94	40
2015.8	23.8763	14.235	24.7	21.93	40
2017.8	23.8762	14.235	24.69	21.93	40
2019.8	23.8757	14.232	24.72	21.93	40
2021.5	23.8781	14.244	24.7	21.93	40
2023.5	23.8759	14.233	24.66	21.93	40
2025.5	23.8751	14.229	24.68	21.93	40
2027.5	23.8781	14.244	24.73	21.93	40
2029.6	23.8775	14.241	24.71	21.93	40
2031.6	23.8772	14.239	24.68	21.92	40
2033.6	23.8778	14.242	24.69	21.93	40
2035.6	23.8793	14.25	24.71	21.92	40
2037.7	23.8783	14.245	24.73	21.92	40
2039.8	23.8773	14.24	24.67	21.92	40
2041.8	23.8788	14.247	24.68	21.92	40
2043.8	23.8796	14.251	24.7	21.92	40
2045.9	23.8787	14.246	24.71	21.92	40
2047.9	23.8794	14.25	24.66	21.92	40
2049.9	23.8796	14.251	24.66	21.92	40
2052	23.8788	14.247	24.69	21.91	40
2054	23.8792	14.249	24.72	21.92	40
2054.5	23.8814	14.259	24.71	21.92	40
2056.5	23.8826	14.265	24.68	21.92	40
2058.6	23.8812	14.259	24.7	21.92	40

C.2 – continued from previous page

Elapsed Time [min]	Weight [mg]	Weight Change [%]	Sample Temp [°C]	Evap. Temp [°C]	RH [%]
2060.6	23.8815	14.26	24.71	21.92	40
2062.6	23.8834	14.269	24.66	21.92	40
2064.6	23.8845	14.274	24.68	21.92	40
2066.6	23.8836	14.27	24.71	21.92	40
2068.6	23.8849	14.276	24.7	21.91	40
2070.6	23.8839	14.272	24.68	21.91	40
2072.7	23.8835	14.27	24.7	21.91	40
2074.8	23.8826	14.265	24.72	21.91	40
2076.5	23.8853	14.278	24.7	21.91	40
2078.5	23.8825	14.265	24.68	21.9	40
2080.6	23.8825	14.265	24.72	21.9	50
2081.5	23.89	14.301	24.72	21.9	50
2082.5	23.9023	14.359	24.74	21.91	50
2083.5	23.9158	14.424	24.76	21.9	50
2084.5	23.9292	14.488	24.76	21.9	50
2085.5	23.9409	14.544	24.76	21.9	50
2086.5	23.9541	14.607	24.74	21.9	50
2087.5	23.9692	14.679	24.71	21.9	50
2088.5	23.9821	14.741	24.68	21.9	50
2089.5	23.9949	14.803	24.67	21.9	50
2090.5	24.0068	14.859	24.69	21.9	50
2091.5	24.0186	14.916	24.7	21.89	50
2092.5	24.0313	14.976	24.7	21.89	50
2093.5	24.0427	15.031	24.71	21.89	50
2094.5	24.0563	15.096	24.72	21.9	50
2095.5	24.0672	15.148	24.72	21.9	50
2096.5	24.0803	15.211	24.71	21.89	50
2097.5	24.0908	15.261	24.69	21.89	50
2098.5	24.1021	15.316	24.67	21.89	50
2099.5	24.113	15.368	24.7	21.89	50
2100.5	24.1213	15.407	24.72	21.89	50
2101.5	24.1342	15.469	24.72	21.89	50
2102.5	24.146	15.525	24.73	21.89	50
2103.5	24.1552	15.57	24.73	21.89	50
2104.5	24.1644	15.613	24.73	21.89	50
2105.5	24.1729	15.654	24.74	21.88	50
2106.5	24.1829	15.702	24.75	21.89	50
2107.5	24.1926	15.748	24.74	21.88	50
2108.5	24.2024	15.795	24.72	21.88	50
2109.5	24.2123	15.843	24.7	21.88	50
2110.5	24.2188	15.874	24.71	21.88	50
2111.5	24.227	15.913	24.72	21.88	50
2112.5	24.2346	15.95	24.69	21.88	50
2113.5	24.2447	15.998	24.66	21.88	50
2114.5	24.2531	16.038	24.64	21.88	50
2115.5	24.2622	16.082	24.66	21.88	50
2116.5	24.2686	16.112	24.68	21.88	50
2117.5	24.2755	16.145	24.7	21.88	50
2118.5	24.2839	16.185	24.7	21.87	50
2119.5	24.2916	16.222	24.7	21.88	50
2120.5	24.2992	16.258	24.7	21.88	50
2121.5	24.3059	16.29	24.71	21.88	50
2122.5	24.3136	16.327	24.71	21.88	50
2123.5	24.3204	16.36	24.69	21.88	50
2124.5	24.3252	16.383	24.7	21.87	50
2125.5	24.332	16.415	24.71	21.88	50
2126.5	24.3377	16.443	24.72	21.88	50
2127.5	24.3438	16.472	24.71	21.88	50
2128.5	24.3486	16.495	24.7	21.87	50
2129.5	24.3538	16.52	24.7	21.87	50
2130.5	24.3591	16.545	24.72	21.87	50
2131.5	24.3673	16.584	24.72	21.87	50
2132.5	24.3706	16.6	24.73	21.87	50
2133.5	24.3776	16.633	24.72	21.87	50
2134.5	24.3821	16.655	24.69	21.87	50
2135.5	24.3868	16.677	24.65	21.87	50
2136.5	24.3917	16.701	24.66	21.87	50
2138.5	24.3976	16.729	24.7	21.87	50
2139.5	24.4022	16.751	24.72	21.87	50
2140.5	24.4072	16.775	24.72	21.87	50
2141.5	24.412	16.798	24.73	21.86	50
2142.5	24.4169	16.822	24.73	21.86	50
2143.5	24.4208	16.84	24.73	21.86	50
2144.5	24.4249	16.86	24.71	21.86	50
2145.5	24.4276	16.873	24.71	21.86	50

C.2 – continued from previous page

Elapsed Time [min]	Weight [mg]	Weight Change [%]	Sample Temp [°C]	Evap. Temp [°C]	RH [%]
2146.5	24.4322	16.895	24.71	21.86	50
2148.5	24.4379	16.922	24.7	21.86	50
2149.5	24.4401	16.933	24.7	21.86	50
2150.5	24.445	16.956	24.71	21.86	50
2151.5	24.449	16.975	24.71	21.86	50
2152.5	24.4517	16.988	24.7	21.86	50
2154.5	24.4577	17.017	24.71	21.86	50
2155.5	24.4602	17.029	24.7	21.86	50
2156.5	24.4629	17.042	24.7	21.85	50
2157.5	24.4654	17.054	24.7	21.86	50
2159.5	24.4706	17.078	24.71	21.86	50
2160.5	24.4737	17.093	24.7	21.86	50
2161.5	24.4762	17.105	24.7	21.86	50
2162.5	24.4798	17.123	24.69	21.86	50
2164.5	24.483	17.138	24.69	21.86	50
2165.5	24.4863	17.154	24.69	21.87	50
2167.5	24.4903	17.173	24.68	21.87	50
2169.5	24.4928	17.185	24.71	21.87	50
2170.5	24.4967	17.203	24.72	21.88	50
2171.5	24.5008	17.223	24.72	21.88	50
2172.5	24.5037	17.237	24.7	21.88	50
2173.5	24.5062	17.249	24.7	21.88	50
2175.5	24.5072	17.254	24.7	21.88	50
2176.5	24.5096	17.265	24.71	21.89	50
2177.5	24.5123	17.278	24.71	21.89	50
2178.5	24.515	17.291	24.71	21.9	50
2179.5	24.5195	17.312	24.71	21.9	50
2181.5	24.5226	17.327	24.69	21.9	50
2183.5	24.526	17.343	24.69	21.9	50
2185.5	24.531	17.367	24.71	21.9	50
2187.5	24.5335	17.379	24.7	21.9	50
2189.5	24.5347	17.385	24.71	21.9	50
2191.5	24.5396	17.408	24.73	21.91	50
2193.5	24.5417	17.418	24.73	21.91	50
2195.5	24.5438	17.429	24.71	21.91	50
2197.5	24.5466	17.442	24.71	21.92	50
2199.5	24.5491	17.454	24.72	21.92	50
2201.6	24.5509	17.463	24.71	21.91	50
2203.6	24.5526	17.471	24.72	21.92	50
2204.5	24.5548	17.481	24.71	21.92	50
2206.5	24.5575	17.494	24.72	21.91	50
2208.5	24.5573	17.493	24.75	21.91	50
2209.5	24.5595	17.504	24.75	21.91	50
2211.5	24.5605	17.509	24.74	21.91	50
2213.5	24.5633	17.522	24.73	21.91	50
2215.5	24.5627	17.519	24.72	21.9	50
2217.5	24.5644	17.528	24.73	21.91	50
2219.5	24.5667	17.538	24.73	21.91	50
2221.5	24.567	17.54	24.73	21.91	50
2223.6	24.5676	17.543	24.74	21.91	50
2225.6	24.5693	17.551	24.75	21.91	50
2227.5	24.5714	17.561	24.73	21.91	50
2229.5	24.571	17.559	24.66	21.9	50
2231.5	24.5707	17.557	24.67	21.91	50
2233.6	24.5722	17.565	24.71	21.91	50
2234.5	24.575	17.578	24.72	21.91	50
2236.5	24.5735	17.571	24.72	21.91	50
2238.5	24.5751	17.579	24.73	21.91	50
2240.6	24.5759	17.582	24.71	21.91	50
2242.6	24.5758	17.582	24.72	21.91	50
2244.6	24.5764	17.585	24.72	21.91	50
2246.7	24.5778	17.592	24.71	21.91	50
2247.5	24.5799	17.602	24.71	21.91	50
2249.6	24.5795	17.6	24.7	21.91	50
2251.6	24.5807	17.606	24.69	21.92	50
2253.5	24.5831	17.617	24.71	21.92	50
2255.5	24.5829	17.616	24.73	21.91	50
2257.5	24.5829	17.616	24.75	21.92	50
2259.6	24.5842	17.622	24.7	21.92	50
2261.6	24.584	17.621	24.69	21.92	50
2263.6	24.5848	17.625	24.64	21.91	50
2265.6	24.5861	17.631	24.69	21.92	50
2267.6	24.5864	17.633	24.71	21.92	50
2269.7	24.5868	17.635	24.72	21.91	50
2271.7	24.5868	17.634	24.65	21.92	50

C.2 – continued from previous page

Elapsed Time [min]	Weight [mg]	Weight Change [%]	Sample Temp [°C]	Evap. Temp [°C]	RH [%]
2273.7	24.5881	17.641	24.69	21.92	50
2275.8	24.5889	17.644	24.72	21.91	50
2277.9	24.5886	17.643	24.71	21.91	50
2279.9	24.5886	17.643	24.71	21.92	50
2282	24.5899	17.649	24.69	21.92	50
2284.1	24.5885	17.643	24.66	21.92	50
2286.1	24.5886	17.643	24.73	21.93	50
2288.1	24.5892	17.646	24.74	21.92	50
2290.1	24.5883	17.642	24.72	21.92	50
2292.2	24.5894	17.647	24.66	21.93	50
2294.2	24.5902	17.651	24.69	21.92	50
2296.3	24.5894	17.647	24.69	21.92	50
2298.3	24.5879	17.64	24.69	21.92	50
2300.4	24.5877	17.639	24.7	21.92	50
2302.4	24.5893	17.646	24.71	21.92	50
2304.4	24.5894	17.647	24.69	21.92	50
2304.5	24.5923	17.661	24.69	21.92	50
2306.5	24.5919	17.659	24.72	21.92	50
2308.6	24.5916	17.657	24.68	21.92	50
2310.6	24.5928	17.663	24.64	21.92	50
2312.6	24.5917	17.658	24.67	21.92	50
2314.5	24.5941	17.67	24.7	21.92	50
2316.5	24.5935	17.667	24.68	21.92	50
2318.5	24.5948	17.673	24.69	21.91	50
2320.6	24.596	17.678	24.67	21.92	50
2322.6	24.5953	17.675	24.7	21.92	50
2324.6	24.5947	17.672	24.71	21.91	50
2326.6	24.5962	17.679	24.66	21.92	50
2328.5	24.5986	17.691	24.69	21.92	50
2330.5	24.5944	17.671	24.68	21.91	50
2332.5	24.5938	17.668	24.67	21.91	50
2334.5	24.5952	17.675	24.68	21.92	50
2336.5	24.5965	17.681	24.72	21.91	50
2338.5	24.5978	17.687	24.68	21.91	50
2340.6	24.5988	17.692	24.68	21.92	50
2342.6	24.5971	17.684	24.7	21.92	50
2344.6	24.5965	17.681	24.68	21.91	50
2346.6	24.5969	17.683	24.7	21.92	50
2348.7	24.5975	17.685	24.68	21.92	50
2350.8	24.5972	17.684	24.67	21.91	50
2352.5	24.5995	17.695	24.69	21.92	50
2354.5	24.6011	17.703	24.69	21.92	50
2356.5	24.5997	17.696	24.66	21.91	50
2358.6	24.5997	17.696	24.66	21.91	50
2360.6	24.6017	17.706	24.72	21.91	50
2362.6	24.6007	17.701	24.71	21.91	50
2364.6	24.5994	17.695	24.69	21.91	50
2366.7	24.5975	17.686	24.67	21.92	50
2368.5	24.6008	17.702	24.68	21.92	50
2370.6	24.6015	17.705	24.7	21.91	50
2372.6	24.6007	17.701	24.67	21.91	50
2373.5	24.5984	17.69	24.68	21.92	50
2375.5	24.5987	17.691	24.69	21.92	50
2377.6	24.599	17.693	24.67	21.92	50
2379.6	24.5994	17.695	24.7	21.91	50
2381.7	24.5985	17.691	24.69	21.93	50
2383.5	24.6013	17.704	24.65	21.93	50
2385.6	24.6003	17.699	24.67	21.92	50
2387.6	24.5989	17.692	24.71	21.92	50
2389.6	24.6005	17.7	24.7	21.92	50
2391.7	24.5997	17.696	24.71	21.92	50
2393.8	24.5992	17.694	24.68	21.92	50
2395.9	24.6	17.698	24.68	21.92	50
2398	24.6016	17.705	24.69	21.92	50
2400.1	24.6004	17.7	24.71	21.91	50
2402.1	24.6002	17.699	24.65	21.92	50
2403.5	24.6025	17.71	24.66	21.92	50
2405.6	24.6018	17.706	24.68	21.91	50
2407.6	24.6009	17.702	24.7	21.92	50
2409.7	24.6018	17.706	24.64	21.92	50
2411.7	24.6038	17.716	24.68	21.91	50
2412.5	24.6014	17.704	24.68	21.91	50
2414.5	24.6019	17.707	24.66	21.91	50
2416.6	24.6023	17.709	24.68	21.91	50
2418.6	24.6016	17.705	24.67	21.91	50

C.2 – continued from previous page

Elapsed Time [min]	Weight [mg]	Weight Change [%]	Sample Temp [°C]	Evap. Temp [°C]	RH [%]
2420.6	24.6013	17.704	24.7	21.91	50
2422.6	24.6033	17.714	24.69	21.91	50
2424.7	24.6046	17.72	24.67	21.91	50
2426.7	24.6036	17.715	24.69	21.91	50
2428.8	24.6034	17.714	24.69	21.91	50
2430.5	24.6058	17.725	24.7	21.92	50
2432.6	24.6046	17.72	24.69	21.91	50
2434.6	24.6051	17.722	24.67	21.91	50
2436.6	24.6059	17.726	24.71	21.92	50
2438.7	24.6072	17.732	24.7	21.92	50
2440.7	24.6089	17.74	24.69	21.91	60
2441.5	24.615	17.769	24.7	21.91	60
2442.5	24.6306	17.844	24.71	21.91	60
2443.5	24.6458	17.917	24.71	21.92	60
2444.5	24.6592	17.981	24.72	21.91	60
2445.5	24.6733	18.048	24.72	21.91	60
2446.5	24.686	18.109	24.7	21.91	60
2447.5	24.6965	18.159	24.68	21.9	60
2448.5	24.71	18.224	24.7	21.9	60
2449.5	24.7206	18.275	24.72	21.9	60
2450.5	24.7337	18.337	24.72	21.9	60
2451.5	24.7461	18.397	24.71	21.9	60
2452.5	24.7564	18.446	24.71	21.9	60
2453.5	24.7665	18.494	24.71	21.9	60
2454.5	24.7766	18.543	24.69	21.89	60
2455.5	24.7857	18.586	24.66	21.89	60
2456.5	24.796	18.636	24.65	21.89	60
2457.5	24.8057	18.682	24.67	21.9	60
2458.5	24.8148	18.726	24.7	21.9	60
2459.5	24.823	18.765	24.72	21.9	60
2460.5	24.8301	18.798	24.74	21.9	60
2461.5	24.8384	18.838	24.73	21.89	60
2462.5	24.8453	18.871	24.71	21.89	60
2463.5	24.8524	18.905	24.72	21.89	60
2464.5	24.8595	18.939	24.72	21.9	60
2465.5	24.8686	18.983	24.72	21.9	60
2466.5	24.8748	19.013	24.72	21.9	60
2467.5	24.8793	19.034	24.71	21.89	60
2468.5	24.8853	19.063	24.72	21.89	60
2469.5	24.8906	19.088	24.72	21.89	60
2470.5	24.8954	19.111	24.72	21.89	60
2471.5	24.9007	19.136	24.72	21.9	60
2472.5	24.9062	19.163	24.72	21.9	60
2473.5	24.9113	19.187	24.71	21.9	60
2474.5	24.9153	19.206	24.71	21.89	60
2475.5	24.9192	19.225	24.72	21.89	60
2476.5	24.9225	19.241	24.72	21.89	60
2477.5	24.9255	19.255	24.7	21.9	60
2478.5	24.9304	19.278	24.71	21.9	60
2479.5	24.9346	19.299	24.71	21.9	60
2480.5	24.9385	19.317	24.7	21.9	60
2481.5	24.9411	19.33	24.71	21.89	60
2482.5	24.9448	19.347	24.71	21.89	60
2484.5	24.9496	19.37	24.71	21.9	60
2485.5	24.953	19.387	24.71	21.9	60
2487.5	24.9546	19.394	24.71	21.89	60
2488.5	24.9587	19.414	24.71	21.89	60
2490.5	24.9618	19.428	24.71	21.88	60
2491.5	24.9641	19.44	24.72	21.89	60
2492.5	24.9676	19.456	24.72	21.88	60
2494.6	24.969	19.463	24.73	21.88	60
2495.5	24.9712	19.474	24.73	21.88	60
2497.6	24.973	19.482	24.74	21.87	60
2499.5	24.9763	19.498	24.74	21.88	60
2501.5	24.9774	19.503	24.74	21.87	60
2503.6	24.9783	19.507	24.71	21.86	60
2505.6	24.9802	19.517	24.71	21.87	60
2507.6	24.9811	19.521	24.69	21.87	60
2509.6	24.9817	19.524	24.71	21.86	60
2511.7	24.9818	19.524	24.74	21.87	60
2513.5	24.9847	19.538	24.73	21.86	60
2515.6	24.9834	19.532	24.72	21.86	60
2517.6	24.9855	19.542	24.72	21.86	60
2519.6	24.9871	19.55	24.73	21.85	60
2521.6	24.9861	19.545	24.7	21.85	60

C.2 – continued from previous page

Elapsed Time [min]	Weight [mg]	Weight Change [%]	Sample Temp [°C]	Evap. Temp [°C]	RH [%]
2523.6	24.9864	19.546	24.7	21.85	60
2525.6	24.9885	19.556	24.71	21.85	60
2527.7	24.9867	19.548	24.69	21.84	60
2529.7	24.9866	19.547	24.69	21.84	60
2531.7	24.9856	19.543	24.71	21.85	60
2533.8	24.9876	19.552	24.71	21.84	60
2535.8	24.9871	19.55	24.7	21.83	60
2536.5	24.9849	19.539	24.71	21.84	60
2538.5	24.986	19.544	24.72	21.84	60
2540.6	24.9868	19.548	24.71	21.84	60
2542.6	24.987	19.549	24.7	21.84	60
2544.6	24.9874	19.551	24.69	21.84	60
2546.5	24.9851	19.54	24.7	21.85	60
2548.6	24.9861	19.545	24.71	21.86	60
2550.6	24.987	19.549	24.69	21.86	60
2551.5	24.9891	19.559	24.68	21.87	60
2553.5	24.9864	19.546	24.7	21.87	60
2554.5	24.9888	19.558	24.71	21.87	60
2556.6	24.9902	19.564	24.7	21.88	60
2557.5	24.9928	19.577	24.7	21.88	60
2559.6	24.993	19.578	24.71	21.89	60
2561.6	24.9927	19.577	24.7	21.89	60
2563.7	24.9929	19.578	24.71	21.91	60
2565.7	24.9948	19.587	24.68	21.91	60
2567.8	24.9939	19.582	24.7	21.91	60
2569.5	24.996	19.592	24.7	21.91	60
2571.6	24.9953	19.589	24.71	21.91	60
2573.6	24.9963	19.594	24.69	21.93	60
2575.6	24.9979	19.601	24.64	21.93	60
2577.6	24.9977	19.601	24.66	21.93	60
2579.7	24.9987	19.605	24.69	21.93	60
2581.7	25	19.611	24.69	21.94	60
2583.8	25.0018	19.62	24.67	21.94	60
2585.9	25.0023	19.622	24.68	21.94	60
2587.9	25.0014	19.618	24.68	21.94	60
2590	25.0025	19.623	24.68	21.95	60
2592	25.0025	19.623	24.63	21.95	60
2594	25.0028	19.625	24.66	21.95	60
2596	25.0016	19.619	24.68	21.96	60
2596.5	25.0041	19.631	24.68	21.96	60
2598.6	25.0033	19.627	24.68	21.96	60
2600.6	25.0033	19.627	24.68	21.95	60
2602.7	25.0032	19.627	24.68	21.95	60
2604.8	25.004	19.631	24.69	21.96	60
2606.8	25.0044	19.632	24.69	21.96	60
2608.8	25.0055	19.638	24.68	21.96	60
2610.9	25.0042	19.631	24.68	21.96	60
2613	25.0027	19.624	24.69	21.96	60
2615	25.0019	19.621	24.69	21.96	60
2617.1	25.0035	19.628	24.69	21.96	60
2619.1	25.0017	19.619	24.69	21.95	60
2621.1	25.0027	19.624	24.7	21.94	60
2623.2	25.0043	19.632	24.71	21.95	60
2625.2	25.0048	19.634	24.7	21.94	60
2627.2	25.0028	19.625	24.69	21.94	60
2629.3	25.0027	19.624	24.7	21.96	60
2631.3	25.0047	19.634	24.7	21.96	60
2633.4	25.0039	19.63	24.69	21.96	60
2633.5	25.0063	19.642	24.69	21.96	60
2635.5	25.0025	19.623	24.7	21.95	60
2637.5	25.0048	19.634	24.7	21.96	60
2639.5	25.0061	19.64	24.7	21.97	60
2641.5	25.0049	19.635	24.69	21.97	60
2643.5	25.0025	19.623	24.7	21.96	60
2645.5	25.0052	19.636	24.69	21.96	60
2647.5	25.0024	19.623	24.69	21.97	60
2649.5	25.0045	19.633	24.69	21.97	60
2651.5	25.0008	19.615	24.7	21.96	60
2653.5	24.9979	19.601	24.7	21.97	60
2654.5	25.0009	19.616	24.71	21.97	60
2656.5	25.0037	19.629	24.69	21.97	60
2658.5	25.0019	19.621	24.71	21.97	60
2660.5	25.0022	19.622	24.68	21.96	60
2662.5	25.0024	19.623	24.68	21.96	60
2663.5	25.0001	19.612	24.69	21.96	60

C.2 – continued from previous page

Elapsed Time [min]	Weight [mg]	Weight Change [%]	Sample Temp [°C]	Evap. Temp [°C]	RH [%]
2665.5	24.9967	19.595	24.69	21.95	60
2667.5	24.9965	19.595	24.69	21.95	60
2669.6	24.9971	19.598	24.7	21.96	60
2671.5	24.9995	19.609	24.68	21.96	60
2673.6	25	19.612	24.69	21.96	60
2675.6	25.0015	19.619	24.69	21.95	60
2677.6	25.0002	19.612	24.69	21.95	60
2679.7	24.9999	19.611	24.68	21.94	60
2681.7	24.9993	19.608	24.69	21.93	60
2683.8	24.9984	19.604	24.69	21.93	60
2685.8	24.9979	19.601	24.69	21.92	60
2687.9	24.9983	19.603	24.69	21.91	60
2688.5	24.9958	19.591	24.69	21.91	60
2690.5	24.9935	19.58	24.72	21.91	60
2692.6	24.9917	19.572	24.74	21.9	60
2694.6	24.9932	19.579	24.73	21.89	60
2696.6	24.9918	19.572	24.71	21.89	60
2698.7	24.9916	19.571	24.7	21.88	60
2700.5	24.9887	19.557	24.71	21.87	60
2702.5	24.9885	19.556	24.71	21.86	60
2704.6	24.9871	19.55	24.69	21.85	60
2706.6	24.9868	19.548	24.69	21.84	60
2708.6	24.9851	19.54	24.7	21.83	60
2710.6	24.9839	19.534	24.71	21.82	60
2712.6	24.9848	19.539	24.72	21.82	60
2714.6	24.9841	19.535	24.72	21.8	60
2715.5	24.982	19.525	24.73	21.79	60
2716.5	24.979	19.511	24.73	21.79	60
2718.5	24.9794	19.513	24.72	21.78	60
2720.5	24.9793	19.512	24.71	21.77	60
2721.5	24.9755	19.494	24.71	21.76	60
2722.5	24.9781	19.507	24.72	21.76	60
2724.5	24.978	19.506	24.73	21.74	60
2725.5	24.9757	19.495	24.73	21.73	60
2726.5	24.9725	19.48	24.73	21.73	60
2728.5	24.969	19.463	24.74	21.71	60
2730.6	24.967	19.454	24.74	21.7	60
2731.5	24.9701	19.468	24.73	21.7	60
2732.5	24.9736	19.485	24.73	21.69	60
2734.5	24.973	19.482	24.74	21.69	60
2736.5	24.9678	19.458	24.76	21.67	60
2738.6	24.9677	19.457	24.76	21.67	60
2739.5	24.97	19.468	24.77	21.66	60
2741.6	24.9691	19.463	24.76	21.65	60
2742.5	24.9715	19.475	24.75	21.65	60
2743.5	24.9666	19.451	24.75	21.64	60
2744.5	24.9702	19.469	24.75	21.64	60
2745.5	24.9657	19.447	24.75	21.64	60
2747.5	24.9653	19.446	24.72	21.64	60
2749.6	24.964	19.439	24.71	21.63	60
2751.5	24.9663	19.45	24.72	21.63	60
2752.5	24.9635	19.437	24.74	21.63	60
2753.5	24.9657	19.448	24.74	21.63	60
2754.5	24.9635	19.437	24.75	21.63	60
2755.5	24.9667	19.452	24.75	21.63	60
2756.5	24.9638	19.438	24.76	21.63	60
2758.5	24.9636	19.437	24.74	21.62	60
2760.6	24.9629	19.434	24.73	21.62	60
2762.6	24.9629	19.434	24.72	21.62	60
2764.6	24.9609	19.424	24.73	21.62	60
2766.5	24.9586	19.413	24.73	21.61	60
2768.5	24.9606	19.423	24.72	21.61	60
2770.6	24.9607	19.423	24.73	21.6	60
2772.6	24.9604	19.422	24.74	21.61	60
2773.5	24.9625	19.432	24.74	21.6	60
2774.5	24.9587	19.414	24.74	21.6	60
2776.5	24.9606	19.423	24.75	21.6	60
2778.5	24.9609	19.424	24.75	21.6	60
2780.5	24.958	19.411	24.73	21.59	60
2782.5	24.9611	19.425	24.7	21.59	60
2783.5	24.9566	19.404	24.7	21.59	60
2785.5	24.9544	19.393	24.69	21.58	60
2786.5	24.9573	19.407	24.7	21.58	60
2788.5	24.9557	19.4	24.7	21.58	60
2790.6	24.9569	19.405	24.71	21.58	60

C.2 – continued from previous page

Elapsed Time [min]	Weight [mg]	Weight Change [%]	Sample Temp [°C]	Evap. Temp [°C]	RH [%]
2792.6	24.958	19.41	24.7	21.59	60
2794.6	24.9562	19.402	24.71	21.58	60
2796.6	24.9565	19.403	24.71	21.58	60
2798.7	24.9559	19.4	24.72	21.58	60
2800.5	24.9587	19.414	24.73	21.58	70
2801.5	24.971	19.472	24.74	21.58	70
2802.5	24.984	19.535	24.73	21.58	70
2803.5	24.9954	19.589	24.74	21.58	70
2804.5	25.01	19.659	24.75	21.57	70
2805.5	25.0208	19.711	24.76	21.57	70
2806.5	25.0325	19.767	24.77	21.57	70
2807.5	25.0436	19.82	24.78	21.57	70
2808.5	25.0525	19.863	24.77	21.57	70
2809.5	25.061	19.903	24.73	21.56	70
2810.5	25.0697	19.945	24.72	21.56	70
2811.5	25.0783	19.986	24.73	21.56	70
2812.5	25.0836	20.011	24.74	21.56	70
2813.5	25.0904	20.044	24.73	21.56	70
2814.5	25.0949	20.066	24.72	21.56	70
2815.5	25.0992	20.086	24.72	21.56	70
2816.5	25.1045	20.111	24.71	21.56	70
2818.5	25.112	20.147	24.7	21.55	70
2820.5	25.115	20.162	24.72	21.55	70
2821.5	25.1186	20.179	24.73	21.56	70
2823.5	25.1227	20.198	24.74	21.57	70
2824.5	25.1258	20.213	24.74	21.57	70
2826.6	25.1253	20.211	24.73	21.57	70
2827.5	25.1285	20.226	24.7	21.57	70
2829.6	25.129	20.228	24.68	21.57	70
2831.6	25.1283	20.225	24.69	21.58	70
2833.6	25.1302	20.235	24.71	21.58	70
2834.5	25.1276	20.222	24.71	21.58	70
2836.5	25.128	20.224	24.72	21.58	70
2838.5	25.1265	20.217	24.73	21.59	70
2840.6	25.1264	20.216	24.72	21.59	70
2842.6	25.1264	20.216	24.7	21.6	70
2844.6	25.1244	20.207	24.71	21.6	70
2845.5	25.1267	20.218	24.7	21.61	70
2846.5	25.1236	20.203	24.7	21.61	70
2848.6	25.1241	20.205	24.71	21.61	70
2850.6	25.1228	20.199	24.74	21.62	70
2852.6	25.1224	20.197	24.74	21.62	70
2854.7	25.1226	20.198	24.75	21.62	70
2856.7	25.122	20.195	24.72	21.63	70
2858.7	25.1216	20.193	24.72	21.64	70
2860.8	25.121	20.19	24.74	21.65	70
2862.8	25.12	20.185	24.75	21.66	70
2864.8	25.1218	20.194	24.73	21.67	70
2865.5	25.1194	20.183	24.73	21.67	70
2867.5	25.1213	20.192	24.73	21.68	70
2868.5	25.1183	20.177	24.73	21.68	70
2870.5	25.1216	20.193	24.73	21.69	70
2872.5	25.1206	20.188	24.71	21.7	70
2873.5	25.1233	20.201	24.71	21.7	70
2875.5	25.1196	20.184	24.71	21.7	70
2877.5	25.1205	20.188	24.71	21.7	70
2879.6	25.1223	20.196	24.7	21.71	70
2881.6	25.1223	20.196	24.71	21.72	70
2883.6	25.1211	20.191	24.7	21.72	70
2885.5	25.1242	20.206	24.71	21.73	70
2887.6	25.1242	20.205	24.72	21.74	70
2889.6	25.1243	20.206	24.72	21.74	70
2891.6	25.1236	20.203	24.7	21.74	70
2893.7	25.1246	20.208	24.71	21.75	70
2895.8	25.1244	20.207	24.72	21.75	70
2897.9	25.1235	20.202	24.72	21.75	70
2899.5	25.1267	20.218	24.72	21.76	70
2901.5	25.1254	20.212	24.73	21.76	70
2903.5	25.1243	20.206	24.73	21.76	70
2905.6	25.1238	20.204	24.72	21.76	70
2907.5	25.126	20.214	24.69	21.77	70
2909.5	25.1256	20.212	24.7	21.77	70
2911.5	25.1247	20.208	24.72	21.77	70
2913.6	25.1248	20.208	24.72	21.77	70
2915.6	25.1257	20.213	24.75	21.78	70

C.2 – continued from previous page

Elapsed Time [min]	Weight [mg]	Weight Change [%]	Sample Temp [°C]	Evap. Temp [°C]	RH [%]
2917.6	25.125	20.209	24.74	21.77	70
2919.6	25.1266	20.217	24.75	21.77	70
2921.6	25.1264	20.216	24.73	21.77	70
2923.6	25.1266	20.217	24.71	21.77	70
2924.5	25.1287	20.227	24.72	21.77	70
2925.5	25.1266	20.217	24.72	21.77	70
2927.5	25.1266	20.217	24.72	21.78	70
2929.6	25.1273	20.221	24.73	21.79	70
2931.6	25.1272	20.22	24.74	21.79	70
2933.6	25.1278	20.223	24.74	21.79	70
2935.6	25.1285	20.226	24.74	21.8	70
2937.6	25.1284	20.226	24.73	21.8	70
2939.6	25.1271	20.22	24.74	21.8	70
2941.6	25.1278	20.223	24.74	21.8	70
2943.7	25.1271	20.219	24.68	21.81	70
2945.7	25.1287	20.227	24.71	21.81	70
2947.7	25.1294	20.23	24.73	21.81	70
2949.8	25.1281	20.224	24.74	21.81	70
2951.9	25.1283	20.225	24.76	21.81	70
2953.9	25.1288	20.228	24.73	21.81	70
2955.9	25.1285	20.226	24.73	21.81	70
2958	25.1294	20.23	24.74	21.81	70
2959.5	25.1315	20.241	24.75	21.82	70
2961.6	25.1312	20.239	24.72	21.83	70
2963.6	25.1305	20.236	24.7	21.83	70
2965.6	25.1305	20.236	24.74	21.84	70
2967.6	25.1307	20.237	24.71	21.84	70
2969.6	25.1325	20.245	24.68	21.83	70
2971.5	25.1301	20.234	24.71	21.83	70
2972.5	25.1324	20.245	24.74	21.83	70
2974.5	25.1317	20.242	24.73	21.83	70
2976.6	25.1335	20.25	24.73	21.83	70
2978.5	25.1309	20.238	24.7	21.83	70
2980.5	25.1314	20.24	24.67	21.83	70
2982.6	25.1303	20.235	24.71	21.83	70
2984.6	25.1313	20.24	24.72	21.83	70
2986.6	25.1313	20.24	24.73	21.84	70
2988.6	25.132	20.243	24.73	21.84	70
2990.6	25.133	20.248	24.71	21.84	70
2992.6	25.1328	20.247	24.66	21.84	70
2994.6	25.1331	20.248	24.66	21.84	70
2996.6	25.1327	20.246	24.71	21.84	70
2998.6	25.1344	20.255	24.73	21.84	70
3000.6	25.1335	20.25	24.72	21.85	70
3002.6	25.1337	20.251	24.68	21.85	70
3004.6	25.1348	20.256	24.68	21.85	70
3006.7	25.1366	20.265	24.71	21.85	70
3008.8	25.136	20.262	24.7	21.84	70
3010.8	25.1356	20.26	24.72	21.84	70
3012.9	25.135	20.257	24.69	21.83	70
3014.9	25.1351	20.258	24.72	21.83	70
3017	25.1355	20.26	24.75	21.82	70
3019.1	25.1353	20.259	24.73	21.83	70
3021.1	25.1358	20.261	24.72	21.82	70
3023.1	25.1354	20.259	24.73	21.82	70
3025.1	25.1352	20.258	24.72	21.81	70
3027.1	25.134	20.253	24.73	21.8	70
3028.5	25.1363	20.264	24.74	21.8	70
3030.6	25.1365	20.265	24.74	21.79	70
3032.6	25.1355	20.26	24.73	21.79	70
3034.5	25.1334	20.249	24.71	21.79	70
3036.5	25.1356	20.26	24.67	21.79	70
3038.6	25.1369	20.266	24.7	21.79	70
3040.6	25.1357	20.261	24.7	21.79	70
3042.6	25.1351	20.258	24.68	21.79	70
3044.6	25.1371	20.267	24.71	21.79	70
3046.7	25.1363	20.264	24.7	21.79	70
3048.7	25.1349	20.257	24.65	21.79	70
3050.8	25.1367	20.265	24.66	21.79	70
3052.9	25.1368	20.266	24.69	21.79	70
3054.9	25.1354	20.259	24.7	21.79	70
3057	25.1357	20.261	24.67	21.8	70
3059.1	25.1374	20.269	24.7	21.8	70
3060.5	25.1352	20.258	24.72	21.79	70
3062.5	25.1351	20.258	24.69	21.8	70

C.2 – continued from previous page

Elapsed Time [min]	Weight [mg]	Weight Change [%]	Sample Temp [°C]	Evap. Temp [°C]	RH [%]
3064.6	25.135	20.257	24.65	21.8	70
3066.6	25.1357	20.26	24.69	21.8	70
3068.6	25.1368	20.266	24.71	21.8	70
3070.7	25.1369	20.266	24.71	21.8	70
3072.7	25.1368	20.266	24.73	21.8	70
3074.7	25.1361	20.262	24.71	21.81	70
3076.8	25.1367	20.266	24.72	21.81	70
3078.9	25.1358	20.261	24.71	21.81	70
3081	25.1374	20.269	24.72	21.81	70
3083	25.1372	20.268	24.73	21.81	70
3085	25.1372	20.268	24.75	21.82	70
3087.1	25.1359	20.261	24.72	21.82	70
3089.1	25.1369	20.266	24.66	21.82	70
3091.1	25.1382	20.273	24.66	21.82	70
3093.1	25.1378	20.271	24.69	21.82	70
3095.1	25.1379	20.271	24.71	21.83	70
3097.2	25.1395	20.279	24.73	21.83	70
3099.2	25.139	20.276	24.74	21.82	70
3101.3	25.1382	20.273	24.73	21.82	70
3103.3	25.1386	20.275	24.71	21.82	70
3105.3	25.1385	20.274	24.72	21.82	70
3107.4	25.1382	20.273	24.73	21.82	70
3109.5	25.1395	20.279	24.7	21.82	70
3111.5	25.1386	20.275	24.7	21.82	70
3113.5	25.1396	20.279	24.69	21.82	70
3115.6	25.1402	20.282	24.72	21.82	70
3117.6	25.1411	20.286	24.68	21.82	70
3119.6	25.1405	20.284	24.73	21.82	70
3121.7	25.1409	20.286	24.73	21.83	70
3123.7	25.1409	20.286	24.68	21.83	70
3125.7	25.1408	20.285	24.67	21.83	70
3127.8	25.1413	20.288	24.72	21.84	70
3129.8	25.1413	20.287	24.74	21.84	70
3131.8	25.1408	20.285	24.72	21.83	70
3133.8	25.1406	20.284	24.73	21.83	70
3135.9	25.1402	20.282	24.72	21.84	70
3138	25.1391	20.277	24.72	21.84	70
3140	25.1388	20.276	24.68	21.84	70
3142	25.1405	20.284	24.67	21.84	70
3144.1	25.1397	20.28	24.71	21.84	70
3146.1	25.1406	20.284	24.71	21.84	70
3148.2	25.1412	20.287	24.72	21.85	70
3150.2	25.1419	20.29	24.7	21.85	70
3152.3	25.1404	20.283	24.68	21.86	70
3154.4	25.1409	20.286	24.68	21.86	70
3156.4	25.1421	20.291	24.69	21.88	70
3158.5	25.1434	20.297	24.69	21.88	70
3160.6	25.1422	20.292	24.7	21.88	80
3161.5	25.1444	20.302	24.7	21.88	80
3162.5	25.151	20.334	24.71	21.88	80
3163.5	25.1582	20.368	24.72	21.89	80
3164.5	25.1657	20.404	24.71	21.89	80
3165.5	25.1701	20.425	24.69	21.89	80
3166.5	25.1749	20.448	24.69	21.89	80
3167.5	25.1806	20.476	24.7	21.89	80
3168.5	25.1856	20.5	24.7	21.89	80
3169.5	25.1923	20.532	24.7	21.89	80
3171.5	25.197	20.554	24.69	21.9	80
3172.5	25.204	20.588	24.7	21.9	80
3173.5	25.207	20.602	24.71	21.9	80
3175.5	25.2104	20.618	24.72	21.9	80
3177.5	25.2136	20.634	24.73	21.9	80
3179.5	25.2163	20.646	24.7	21.9	80
3180.5	25.2194	20.661	24.69	21.9	80
3182.6	25.219	20.659	24.7	21.9	80
3184.5	25.2235	20.681	24.71	21.89	80
3186.6	25.2216	20.672	24.7	21.9	80
3188.6	25.2231	20.679	24.72	21.9	80
3190.6	25.2242	20.684	24.71	21.89	80
3192.6	25.2232	20.679	24.69	21.88	80
3194.7	25.2244	20.685	24.71	21.89	80
3196.5	25.2265	20.695	24.71	21.89	80
3198.5	25.2281	20.703	24.71	21.89	80
3200.5	25.2261	20.693	24.72	21.89	80
3202.6	25.2276	20.701	24.72	21.9	80

C.2 – continued from previous page

Elapsed Time [min]	Weight [mg]	Weight Change [%]	Sample Temp [°C]	Evap. Temp [°C]	RH [%]
3204.6	25.2278	20.701	24.7	21.9	80
3206.6	25.2286	20.705	24.7	21.9	80
3208.6	25.228	20.702	24.71	21.9	80
3210.6	25.2293	20.709	24.71	21.91	80
3212.6	25.2287	20.706	24.7	21.91	80
3214.5	25.2316	20.72	24.7	21.9	80
3215.5	25.2383	20.751	24.69	21.9	80
3217.5	25.2308	20.716	24.71	21.9	80
3218.5	25.2411	20.765	24.71	21.98	80
3220.5	25.2417	20.768	24.73	21.99	80
3222.5	25.2468	20.792	24.73	21.98	80
3224.5	25.2488	20.802	24.72	21.97	80
3226.5	25.2505	20.81	24.72	21.97	80
3228.5	25.2515	20.815	24.71	21.95	80
3230.6	25.2523	20.818	24.68	21.94	80
3232.6	25.253	20.822	24.7	21.94	80
3234.6	25.2537	20.825	24.69	21.93	80
3236.6	25.255	20.831	24.65	21.92	80
3238.6	25.2564	20.838	24.62	21.91	80
3240.6	25.2569	20.841	24.68	21.9	80
3241.5	25.2546	20.829	24.69	21.9	80
3243.5	25.2527	20.82	24.69	21.89	80
3245.6	25.2533	20.823	24.68	21.89	80
3247.6	25.2539	20.826	24.69	21.88	80
3249.6	25.2518	20.816	24.69	21.88	80
3251.6	25.2511	20.813	24.68	21.87	80
3253.7	25.2515	20.815	24.7	21.86	80
3255.7	25.251	20.812	24.68	21.85	80
3257.7	25.2505	20.81	24.64	21.84	80
3259.8	25.2512	20.813	24.67	21.84	80
3261.8	25.2513	20.814	24.69	21.83	80
3263.8	25.2506	20.81	24.68	21.82	80
3265.8	25.2505	20.81	24.69	21.82	80
3267.8	25.2507	20.811	24.68	21.82	80
3269.8	25.2512	20.813	24.7	21.81	80
3271.5	25.2487	20.801	24.68	21.81	80
3273.5	25.249	20.803	24.64	21.8	80
3275.6	25.2484	20.8	24.68	21.81	80
3277.6	25.2491	20.803	24.69	21.8	80
3279.6	25.2479	20.798	24.68	21.8	80
3281.6	25.248	20.798	24.69	21.79	80
3283.6	25.2484	20.8	24.71	21.79	80
3285.7	25.2475	20.796	24.68	21.79	80
3287.7	25.2476	20.796	24.64	21.78	80
3289.7	25.2478	20.797	24.69	21.78	80
3291.8	25.2481	20.798	24.7	21.78	80
3293.8	25.2472	20.794	24.65	21.77	80
3295.9	25.2477	20.796	24.63	21.77	80
3298	25.2474	20.795	24.67	21.77	80
3299.5	25.2495	20.805	24.69	21.77	80
3301.5	25.2485	20.8	24.69	21.77	80
3303.6	25.2495	20.805	24.65	21.77	80
3305.6	25.2496	20.806	24.7	21.76	80
3307.6	25.25	20.808	24.68	21.76	80
3309.6	25.2499	20.807	24.65	21.76	80
3311.6	25.25	20.808	24.69	21.76	80
3313.6	25.25	20.808	24.65	21.76	80
3315.6	25.2488	20.802	24.62	21.76	80
3317.6	25.2482	20.799	24.67	21.76	80
3319.7	25.2488	20.802	24.7	21.75	80
3321.7	25.2493	20.804	24.71	21.75	80
3323.7	25.2477	20.797	24.7	21.74	80
3325.8	25.2481	20.799	24.71	21.74	80
3327.8	25.249	20.803	24.73	21.74	80
3329.8	25.25	20.808	24.7	21.74	80
3331.9	25.2488	20.802	24.68	21.73	80
3334	25.2493	20.804	24.7	21.73	80
3336.1	25.2497	20.806	24.7	21.73	80
3336.5	25.2469	20.793	24.68	21.73	80
3338.6	25.2478	20.797	24.67	21.72	80
3340.6	25.2475	20.796	24.69	21.72	80
3342.6	25.2487	20.801	24.66	21.72	80
3344.6	25.2485	20.8	24.62	21.72	80
3346.6	25.2487	20.801	24.64	21.71	80
3348.6	25.2491	20.803	24.67	21.71	80

C.2 – continued from previous page

Elapsed Time [min]	Weight [mg]	Weight Change [%]	Sample Temp [°C]	Evap. Temp [°C]	RH [%]
3350.6	25.2491	20.803	24.67	21.71	80
3352.6	25.2491	20.803	24.66	21.71	80
3354.7	25.25	20.807	24.68	21.71	80
3356.8	25.25	20.807	24.7	21.7	80
3358.8	25.2494	20.805	24.69	21.69	80
3360.5	25.2472	20.794	24.68	21.69	80
3362.6	25.249	20.803	24.62	21.69	80
3364.6	25.2485	20.8	24.65	21.69	80
3366.6	25.2483	20.8	24.67	21.68	80
3368.6	25.2482	20.799	24.64	21.68	80
3370.7	25.2501	20.808	24.67	21.67	80
3372.8	25.2487	20.801	24.67	21.67	80
3374.8	25.2472	20.794	24.68	21.66	80
3376.8	25.2479	20.797	24.68	21.66	80
3378.9	25.2476	20.796	24.65	21.66	80
3381	25.2481	20.799	24.65	21.66	80
3383	25.2489	20.802	24.69	21.66	80
3385.1	25.2471	20.794	24.69	21.66	80
3387.1	25.2483	20.799	24.67	21.65	80
3389.1	25.2485	20.8	24.67	21.64	80
3391.1	25.2485	20.8	24.62	21.64	80
3393.2	25.2479	20.798	24.65	21.64	80
3395.3	25.2495	20.805	24.64	21.64	80
3397.3	25.2478	20.797	24.67	21.64	80
3399.4	25.2497	20.806	24.71	21.65	80
3401.4	25.2488	20.802	24.69	21.65	80
3403.5	25.2498	20.806	24.67	21.65	80
3405.6	25.2486	20.801	24.69	21.65	80
3407.6	25.2492	20.804	24.63	21.65	80
3409.7	25.2488	20.802	24.65	21.65	80
3411.7	25.25	20.808	24.62	21.65	80
3413.7	25.2483	20.799	24.67	21.65	80
3415.5	25.2514	20.814	24.7	21.65	80
3417.5	25.2493	20.804	24.69	21.65	80
3419.6	25.2494	20.805	24.69	21.65	80
3421.6	25.2488	20.802	24.68	21.65	80
3423.6	25.2491	20.803	24.69	21.65	80
3425.6	25.2483	20.799	24.67	21.65	80
3427.6	25.2487	20.802	24.66	21.65	80
3429.6	25.2502	20.808	24.7	21.65	80
3431.6	25.2485	20.8	24.7	21.65	80
3433.7	25.248	20.798	24.67	21.65	80
3435.7	25.2499	20.807	24.66	21.66	80
3437.8	25.2495	20.805	24.7	21.66	80
3439.9	25.2499	20.807	24.7	21.66	80
3441.9	25.2493	20.804	24.67	21.66	80
3443.9	25.2496	20.806	24.65	21.66	80
3445.9	25.2497	20.806	24.68	21.66	80
3448	25.2484	20.8	24.68	21.66	80
3450	25.2486	20.801	24.7	21.66	80
3452	25.2494	20.805	24.72	21.66	80
3454.1	25.2487	20.801	24.67	21.66	80
3456.1	25.2487	20.801	24.67	21.66	80
3458.1	25.2485	20.8	24.7	21.66	80
3460.1	25.2484	20.8	24.71	21.66	80
3462.2	25.2483	20.799	24.71	21.65	80
3464.3	25.2487	20.801	24.66	21.66	80
3466.4	25.2496	20.806	24.62	21.65	80
3468.4	25.2502	20.809	24.66	21.65	80
3470.4	25.2488	20.802	24.67	21.65	80
3472.4	25.2503	20.809	24.67	21.66	80
3474.4	25.2509	20.812	24.64	21.66	80
3476.5	25.2501	20.808	24.68	21.66	80
3478.5	25.2505	20.81	24.67	21.67	80
3480.5	25.2505	20.81	24.64	21.66	80
3482.6	25.2509	20.812	24.69	21.66	80
3484.6	25.2505	20.81	24.67	21.65	80
3486.6	25.2516	20.815	24.66	21.65	80
3488.6	25.251	20.812	24.62	21.65	80
3490.7	25.249	20.803	24.66	21.64	80
3492.7	25.2502	20.808	24.69	21.65	80
3494.5	25.2529	20.821	24.68	21.64	80
3495.5	25.2507	20.811	24.65	21.64	80
3497.5	25.251	20.812	24.64	21.64	80
3499.5	25.2509	20.812	24.66	21.64	80

C.2 – continued from previous page

Elapsed Time [min]	Weight [mg]	Weight Change [%]	Sample Temp [°C]	Evap. Temp [°C]	RH [%]
3501.5	25.2509	20.812	24.68	21.64	80
3503.6	25.2491	20.803	24.68	21.63	80
3505.6	25.2486	20.801	24.69	21.63	80
3507.6	25.2492	20.804	24.65	21.62	80
3509.6	25.2496	20.805	24.66	21.62	80
3511.6	25.2489	20.802	24.68	21.61	80
3513.7	25.2501	20.808	24.68	21.61	80
3515.7	25.251	20.812	24.68	21.61	80
3517.7	25.2495	20.805	24.68	21.6	80
3519.7	25.2506	20.811	24.69	21.6	80
3520.5	25.2528	20.821	24.69	21.6	90
3522.5	25.2524	20.819	24.69	21.57	90
3523.5	25.2556	20.834	24.65	21.55	90
3524.5	25.2588	20.849	24.63	21.53	90
3526.6	25.2592	20.851	24.65	21.5	90
3527.5	25.2614	20.862	24.66	21.49	90
3528.5	25.265	20.879	24.67	21.48	90
3530.5	25.2661	20.885	24.68	21.46	90
3532.5	25.269	20.898	24.67	21.44	90
3534.6	25.2687	20.897	24.67	21.43	90
3536.6	25.2678	20.893	24.67	21.41	90
3538.6	25.2685	20.896	24.67	21.4	90
3540.6	25.2698	20.902	24.66	21.39	90
3541.5	25.2676	20.892	24.67	21.39	90
3543.5	25.2665	20.886	24.69	21.38	90
3544.5	25.2688	20.897	24.69	21.38	90
3546.5	25.2679	20.893	24.68	21.37	90
3548.6	25.2689	20.898	24.7	21.36	90
3550.5	25.2666	20.887	24.67	21.36	90
3552.5	25.2664	20.886	24.66	21.35	90
3554.6	25.2659	20.884	24.68	21.34	90
3556.6	25.2666	20.887	24.69	21.33	90
3558.6	25.267	20.889	24.7	21.33	90
3560.6	25.2673	20.89	24.69	21.33	90
3562.6	25.2668	20.888	24.68	21.33	90
3564.7	25.2664	20.886	24.69	21.32	90
3566.8	25.2673	20.89	24.69	21.32	90
3568.8	25.2665	20.886	24.68	21.31	90
3570.8	25.2678	20.893	24.69	21.29	90
3572.9	25.2673	20.89	24.68	21.27	90
3574.5	25.2643	20.876	24.68	21.26	90
3576.5	25.2663	20.886	24.7	21.25	90
3578.5	25.2668	20.888	24.69	21.25	90
3580.5	25.2647	20.878	24.7	21.24	90
3582.5	25.2637	20.873	24.7	21.24	90
3583.5	25.2666	20.887	24.71	21.23	90
3585.5	25.2671	20.889	24.72	21.23	90
3587.6	25.2652	20.88	24.73	21.23	90
3589.6	25.2645	20.877	24.71	21.23	90
3591.6	25.2635	20.872	24.69	21.23	90
3593.7	25.2624	20.867	24.72	21.23	90
3595.5	25.2648	20.878	24.7	21.23	90
3597.6	25.2651	20.88	24.71	21.23	90
3599.6	25.2633	20.871	24.71	21.22	90
3601.6	25.2641	20.875	24.7	21.23	90
3603.6	25.2642	20.876	24.7	21.23	90
3605.7	25.2638	20.874	24.71	21.22	90
3607.7	25.2644	20.876	24.72	21.22	90
3609.8	25.2652	20.88	24.72	21.22	90
3611.8	25.2637	20.873	24.7	21.21	90
3613.9	25.2652	20.88	24.71	21.21	90
3615.9	25.2651	20.88	24.7	21.21	90
3618	25.2658	20.883	24.69	21.2	90
3620	25.2641	20.875	24.72	21.2	90
3622.1	25.2643	20.876	24.72	21.2	90
3623.5	25.2666	20.887	24.71	21.2	90
3625.5	25.2647	20.878	24.71	21.19	90
3627.5	25.2652	20.88	24.71	21.18	90
3629.5	25.2646	20.877	24.71	21.19	90
3631.6	25.2635	20.872	24.68	21.17	90
3633.6	25.2643	20.876	24.71	21.16	90
3635.6	25.2643	20.876	24.72	21.15	90
3637.5	25.2615	20.862	24.72	21.15	90
3639.5	25.263	20.87	24.72	21.14	90
3641.6	25.2645	20.877	24.71	21.14	90

C.2 – continued from previous page

Elapsed Time [min]	Weight [mg]	Weight Change [%]	Sample Temp [°C]	Evap. Temp [°C]	RH [%]
3642.5	25.2618	20.864	24.71	21.13	90
3644.6	25.2623	20.866	24.68	21.13	90
3646.6	25.262	20.865	24.67	21.12	90
3648.6	25.2619	20.865	24.7	21.11	90
3650.6	25.2625	20.867	24.71	21.11	90
3652.7	25.2616	20.863	24.69	21.1	90
3654.7	25.2617	20.863	24.74	21.1	90
3655.5	25.2595	20.853	24.74	21.1	90
3657.5	25.2605	20.858	24.75	21.1	90
3659.5	25.2602	20.856	24.71	21.1	90
3661.6	25.2596	20.853	24.67	21.1	90
3663.6	25.2611	20.86	24.72	21.1	90
3665.6	25.2599	20.855	24.71	21.09	90
3667.7	25.2605	20.858	24.71	21.09	90
3669.7	25.2611	20.861	24.7	21.09	90
3671.7	25.2602	20.856	24.72	21.09	90
3673.8	25.2617	20.864	24.73	21.09	90
3675.9	25.2599	20.855	24.73	21.09	90
3677.5	25.2624	20.867	24.72	21.09	90
3679.5	25.2612	20.861	24.67	21.09	90
3681.6	25.2605	20.858	24.71	21.08	90
3683.6	25.2607	20.859	24.73	21.08	90
3685.7	25.2614	20.862	24.74	21.08	90
3686.5	25.2591	20.851	24.73	21.08	90
3688.5	25.2611	20.86	24.73	21.07	90
3690.6	25.2602	20.856	24.74	21.07	90
3691.5	25.2579	20.845	24.74	21.07	90
3693.5	25.2605	20.858	24.69	21.07	90
3695.6	25.2616	20.863	24.73	21.07	90
3697.6	25.2609	20.86	24.75	21.06	90
3698.5	25.2588	20.85	24.76	21.06	90
3700.6	25.2588	20.849	24.71	21.07	90
3702.6	25.2586	20.849	24.72	21.07	90
3704.7	25.2574	20.843	24.73	21.07	90
3706.5	25.2601	20.856	24.72	21.07	90
3708.6	25.2594	20.852	24.72	21.07	90
3710.6	25.2588	20.85	24.72	21.08	90
3712.7	25.2606	20.858	24.73	21.08	90
3714.7	25.2596	20.853	24.72	21.08	90
3716.7	25.2599	20.855	24.7	21.08	90
3718.7	25.2593	20.852	24.73	21.09	90
3719.5	25.2617	20.863	24.74	21.09	90
3721.5	25.2593	20.852	24.74	21.08	90
3723.5	25.2589	20.85	24.74	21.09	90
3725.6	25.2603	20.857	24.73	21.09	90
3727.6	25.2596	20.853	24.72	21.09	90
3729.6	25.2603	20.857	24.74	21.09	90
3731.6	25.2613	20.862	24.73	21.09	90
3733.5	25.2589	20.85	24.74	21.1	90
3735.6	25.2595	20.853	24.69	21.1	90
3737.5	25.2619	20.864	24.7	21.11	90
3739.6	25.2623	20.867	24.72	21.11	90
3741.6	25.2621	20.865	24.71	21.12	90
3743.5	25.2655	20.882	24.7	21.12	90
3744.5	25.2629	20.869	24.7	21.13	90
3746.5	25.2616	20.863	24.69	21.13	90
3748.5	25.2631	20.87	24.7	21.13	90
3750.6	25.2651	20.88	24.68	21.14	90
3752.6	25.2648	20.878	24.65	21.13	90
3754.7	25.2647	20.878	24.68	21.15	90
3756.7	25.2659	20.884	24.69	21.14	90
3758.7	25.2643	20.876	24.66	21.13	90
3760.7	25.2642	20.876	24.69	21.13	90
3762.8	25.2655	20.882	24.7	21.13	90
3764.9	25.2642	20.875	24.72	21.12	90
3766.5	25.2666	20.887	24.73	21.13	90
3768.6	25.2648	20.878	24.72	21.12	90
3770.5	25.2618	20.864	24.67	21.11	90
3772.5	25.2636	20.873	24.7	21.12	90
3774.5	25.2646	20.878	24.71	21.12	90
3776.6	25.2631	20.87	24.71	21.11	90
3778.6	25.263	20.87	24.72	21.11	90
3780.6	25.2645	20.877	24.69	21.1	90
3782.6	25.2627	20.869	24.71	21.1	90
3784.7	25.2634	20.871	24.69	21.1	90

C.2 – continued from previous page

Elapsed Time [min]	Weight [mg]	Weight Change [%]	Sample Temp [°C]	Evap. Temp [°C]	RH [%]
3786.7	25.2647	20.878	24.69	21.1	90
3788.8	25.2634	20.872	24.71	21.09	90
3790.8	25.2639	20.874	24.71	21.09	90
3792.8	25.2652	20.88	24.68	21.1	90
3794.5	25.2621	20.865	24.69	21.1	90
3796.6	25.2641	20.875	24.69	21.1	90
3798.5	25.2663	20.886	24.71	21.1	90
3799.5	25.2641	20.875	24.72	21.1	90
3801.6	25.2636	20.873	24.67	21.11	90
3803.6	25.2628	20.869	24.69	21.11	90
3805.5	25.2652	20.88	24.72	21.11	90
3807.5	25.2636	20.872	24.74	21.11	90
3809.6	25.2655	20.882	24.74	21.12	90
3811.6	25.2656	20.882	24.72	21.12	90
3812.5	25.2633	20.871	24.73	21.12	90
3814.6	25.2643	20.876	24.72	21.13	90
3816.6	25.2659	20.884	24.68	21.14	90
3818.6	25.2664	20.886	24.73	21.14	90
3820.6	25.2656	20.882	24.74	21.14	90
3822.5	25.2689	20.898	24.7	21.15	90
3824.5	25.2665	20.886	24.68	21.15	90
3826.5	25.2682	20.895	24.73	21.15	90
3828.5	25.2698	20.902	24.71	21.16	90
3830.6	25.2684	20.895	24.71	21.14	90
3832.6	25.2671	20.889	24.68	21.16	90
3834.6	25.2684	20.896	24.7	21.17	90
3836.7	25.2681	20.894	24.67	21.17	90
3837.5	25.2651	20.88	24.66	21.17	90
3839.5	25.2636	20.873	24.69	21.17	90
3841.5	25.2674	20.891	24.71	21.18	90
3843.6	25.2677	20.892	24.72	21.19	90
3845.6	25.2698	20.902	24.73	21.2	90
3847.6	25.2684	20.896	24.74	21.22	90
3849.6	25.2673	20.89	24.69	21.22	90
3851.6	25.2687	20.897	24.72	21.23	90
3852.5	25.264	20.874	24.73	21.23	90
3854.5	25.2614	20.862	24.74	21.22	90
3856.6	25.2623	20.866	24.74	21.22	90
3858.6	25.2619	20.864	24.74	21.23	90
3859.5	25.2641	20.875	24.74	21.24	90
3861.5	25.2637	20.873	24.74	21.24	90
3863.5	25.2647	20.878	24.74	21.25	90
3865.5	25.264	20.875	24.74	21.26	90
3867.6	25.2632	20.871	24.73	21.27	90
3869.6	25.2636	20.873	24.73	21.28	90
3871.6	25.2648	20.878	24.69	21.29	90
3873.7	25.2642	20.875	24.7	21.3	90
3875.7	25.2622	20.866	24.72	21.31	90
3876.5	25.265	20.88	24.72	21.32	90
3878.5	25.2646	20.878	24.74	21.33	90

VTI-SA Sorption Graph

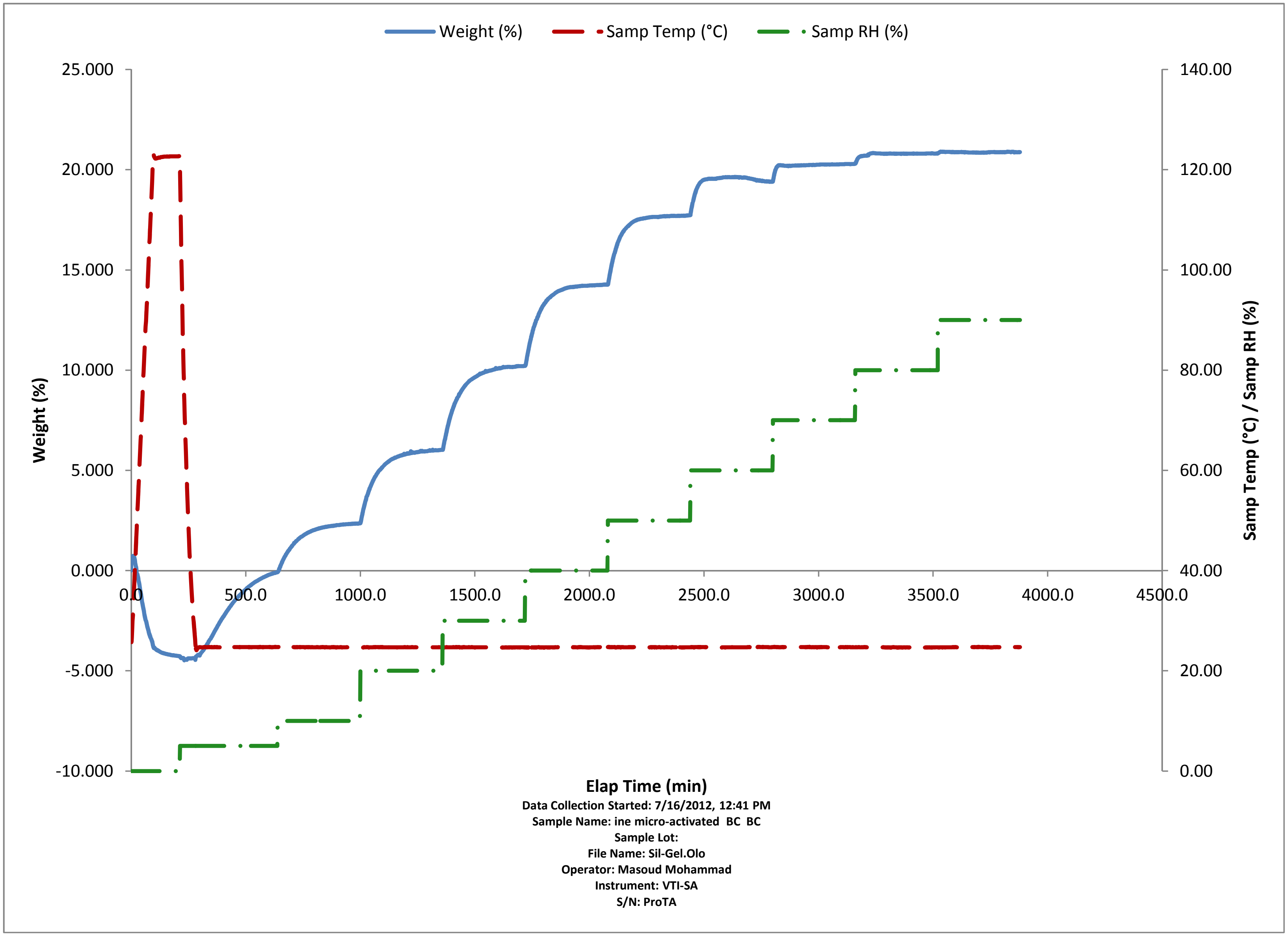

VTI Corporation. {Wt-RH-Temp Sil-Gel-lo-1}. 7/25/2013

D

Appendix D: Mass Transfer Coefficient Plots and Data

This appendix contains all the data, plots, and linear regression for the mass transfer coefficient at all RH intervals using the VTI-SA Sorption Analyzer for Water Vapour on Silica Gel at 25°C.

Table D.1: *VTI-SA Analyzer Silica Gel Mass vs. Time at 25°C 5-10%RH*

Time Stamp [min]	Weight [mg]	Weight Change [%]	Time Elapsed [min]	$ln(1-\frac{m_t}{m_f})$
639	20.885	-0.075	0	0.0000
640	20.888	-0.063	1	-0.0050
641	20.892	-0.045	2	-0.0125
642	20.896	-0.026	3	-0.0204
643	20.901	0.001	4	-0.0318
644	20.907	0.028	5	-0.0437
645	20.914	0.060	6	-0.0575
646	20.920	0.092	7	-0.0715
647	20.926	0.120	8	-0.0842
648	20.933	0.151	9	-0.0978
649	20.938	0.175	10	-0.1091
650	20.943	0.202	11	-0.1216
651	20.950	0.233	12	-0.1357
652	20.956	0.265	13	-0.1513
653	20.962	0.292	14	-0.1643
654	20.967	0.314	15	-0.1748
655	20.972	0.340	16	-0.1875
656	20.977	0.364	17	-0.1995
657	20.982	0.386	18	-0.2108
658	20.989	0.421	19	-0.2287
659	20.996	0.453	20	-0.2455
660	21.000	0.472	21	-0.2558
661	21.004	0.490	22	-0.2654
662	21.009	0.517	23	-0.2796
663	21.014	0.542	24	-0.2933
664	21.019	0.567	25	-0.3073
665	21.023	0.585	26	-0.3176
666	21.028	0.607	27	-0.3303
667	21.033	0.632	28	-0.3443
668	21.038	0.654	29	-0.3576
669	21.042	0.675	30	-0.3700
670	21.047	0.698	31	-0.3839
671	21.050	0.714	32	-0.3932
672	21.055	0.736	33	-0.4067
673	21.057	0.748	34	-0.4146
674	21.061	0.765	35	-0.4247
675	21.066	0.791	36	-0.4415
676	21.072	0.817	37	-0.4586
677	21.074	0.829	38	-0.4662
678	21.077	0.841	39	-0.4744
679	21.081	0.861	40	-0.4874
680	21.086	0.884	41	-0.5029
681	21.089	0.901	42	-0.5149
682	21.093	0.916	43	-0.5253
683	21.097	0.938	44	-0.5404

D.1 – continued from previous page

Time Stamp [min]	Weight [mg]	Weight Change [%]	Time Elapsed [min]	$ln(1-\frac{m_t}{m_f})$
684	21.101	0.957	45	-0.5542
685	21.105	0.976	46	-0.5677
686	21.108	0.989	47	-0.5771
687	21.111	1.005	48	-0.5887
688	21.113	1.016	49	-0.5973
689	21.119	1.041	50	-0.6162
690	21.122	1.057	51	-0.6280
691	21.126	1.075	52	-0.6420
692	21.129	1.092	53	-0.6554
693	21.133	1.109	54	-0.6691
694	21.135	1.122	55	-0.6796
695	21.138	1.136	56	-0.6914
696	21.141	1.148	57	-0.7012
697	21.145	1.167	58	-0.7173
698	21.147	1.179	59	-0.7274
699	21.150	1.192	60	-0.7384
700	21.154	1.209	61	-0.7535
701	21.156	1.220	62	-0.7630
702	21.160	1.240	63	-0.7811
703	21.163	1.255	64	-0.7946
704	21.166	1.268	65	-0.8066
705	21.169	1.282	66	-0.8195
706	21.172	1.295	67	-0.8319
708	21.176	1.318	69	-0.8530
709	21.179	1.330	70	-0.8654
710	21.182	1.345	71	-0.8804
711	21.190	1.381	72	-0.9165
712	21.187	1.370	73	-0.9050
713	21.190	1.383	74	-0.9183
714	21.192	1.394	75	-0.9300
715	21.195	1.407	76	-0.9434
717	21.200	1.432	78	-0.9699
719	21.205	1.456	80	-0.9971
720	21.208	1.467	81	-1.0094
721	21.210	1.479	82	-1.0232
723	21.213	1.492	84	-1.0380
724	21.216	1.508	85	-1.0568
726	21.221	1.531	87	-1.0839
727	21.224	1.543	88	-1.0993
728	21.226	1.556	89	-1.1146
729	21.229	1.569	90	-1.1321
731	21.231	1.580	92	-1.1457
733	21.235	1.599	94	-1.1706
734	21.238	1.612	95	-1.1876
735	21.241	1.626	96	-1.2075
737	21.243	1.636	98	-1.2208
738	21.246	1.650	99	-1.2407
740	21.251	1.672	101	-1.2731
742	21.254	1.687	103	-1.2954
744	21.257	1.702	105	-1.3177
746	21.259	1.713	107	-1.3356
747	21.261	1.725	108	-1.3532
749	21.265	1.740	110	-1.3787
751	21.268	1.755	112	-1.4029
752	21.270	1.766	113	-1.4206
754	21.273	1.780	115	-1.4454
756	21.276	1.796	117	-1.4737
758	21.278	1.804	119	-1.4893
760	21.283	1.827	121	-1.5305
762	21.284	1.833	123	-1.5423
764	21.287	1.847	125	-1.5704
765	21.289	1.858	126	-1.5925
767	21.292	1.873	128	-1.6223
770	21.293	1.874	130	-1.6252
771	21.297	1.893	132	-1.6664
773	21.301	1.912	134	-1.7077
776	21.301	1.916	136	-1.7165
778	21.303	1.921	138	-1.7288
779	21.305	1.935	140	-1.7619
781	21.308	1.947	142	-1.7902
783	21.308	1.949	144	-1.7964
785	21.311	1.962	146	-1.8279
786	21.313	1.973	147	-1.8574
788	21.315	1.980	149	-1.8761

D.1 – continued from previous page

Time Stamp [min]	Weight [mg]	Weight Change [%]	Time Elapsed [min]	$ln(1-\frac{m_t}{m_f})$
791	21.316	1.987	151	-1.8949
792	21.319	1.997	153	-1.9240
794	21.321	2.008	155	-1.9541
796	21.322	2.013	157	-1.9693
797	21.324	2.024	158	-2.0021
800	21.324	2.023	160	-1.9992
801	21.327	2.039	162	-2.0476
803	21.328	2.045	164	-2.0666
806	21.330	2.054	166	-2.0964
808	21.331	2.057	168	-2.1080
810	21.333	2.066	170	-2.1395
811	21.335	2.077	172	-2.1794
813	21.336	2.081	174	-2.1923
815	21.337	2.085	176	-2.2083
817	21.339	2.096	178	-2.2501
819	21.342	2.108	180	-2.2996
822	21.341	2.106	182	-2.2902
823	21.344	2.118	184	-2.3384
826	21.345	2.122	186	-2.3580
828	21.345	2.126	188	-2.3741
830	21.346	2.131	190	-2.3951
832	21.347	2.134	192	-2.4111
833	21.350	2.146	194	-2.4683
836	21.350	2.146	196	-2.4676
838	21.351	2.155	198	-2.5111
840	21.352	2.160	200	-2.5366
842	21.352	2.157	202	-2.5238
843	21.354	2.168	204	-2.5807
845	21.356	2.177	206	-2.6314
847	21.355	2.173	208	-2.6102
850	21.357	2.180	210	-2.6489
852	21.358	2.188	212	-2.6984
854	21.357	2.183	214	-2.6671
856	21.358	2.187	216	-2.6863
857	21.361	2.199	218	-2.7624
859	21.362	2.205	220	-2.8017
861	21.361	2.199	222	-2.7655
863	21.363	2.211	224	-2.8499
865	21.363	2.210	226	-2.8414
868	21.363	2.210	228	-2.8380
870	21.365	2.218	230	-2.8964
872	21.366	2.223	232	-2.9364
874	21.366	2.223	234	-2.9364
876	21.366	2.224	236	-2.9458
878	21.368	2.233	239	-3.0163
880	21.367	2.231	241	-3.0023
882	21.367	2.229	243	-2.9840
884	21.369	2.239	245	-3.0672
886	21.370	2.243	247	-3.1038
888	21.370	2.244	249	-3.1112
890	21.371	2.248	251	-3.1480
892	21.371	2.247	253	-3.1396
894	21.372	2.255	255	-3.2202
895	21.374	2.265	256	-3.3295
898	21.375	2.267	258	-3.3490
900	21.376	2.270	260	-3.3949
902	21.375	2.266	262	-3.3453
904	21.376	2.273	264	-3.4298
906	21.376	2.275	266	-3.4482
908	21.376	2.275	268	-3.4513
910	21.377	2.278	270	-3.4894
912	21.379	2.286	272	-3.6105
914	21.379	2.287	274	-3.6203
916	21.380	2.290	276	-3.6642
918	21.380	2.293	278	-3.7209
920	21.380	2.293	281	-3.7155
922	21.381	2.297	283	-3.7852
924	21.382	2.302	285	-3.8762
926	21.381	2.295	287	-3.7456
928	21.382	2.299	289	-3.8253
929	21.384	2.309	290	-4.0357
932	21.383	2.304	292	-3.9281
934	21.383	2.307	294	-3.9956
936	21.383	2.308	296	-4.0099

D.1 – continued from previous page

Time Stamp [min]	Weight [mg]	Weight Change [%]	Time Elapsed [min]	$ln(1-\frac{m_t}{m_f})$
938	21.385	2.314	298	-4.1477
940	21.385	2.314	300	-4.1517
942	21.386	2.318	302	-4.2808
944	21.385	2.316	304	-4.2009
946	21.384	2.313	306	-4.1311
948	21.385	2.315	308	-4.1752
949	21.387	2.327	310	-4.5708
951	21.386	2.322	312	-4.3965
954	21.387	2.327	314	-4.5770
956	21.388	2.330	316	-4.7286
957	21.386	2.320	318	-4.3222
959	21.386	2.323	320	-4.4181
961	21.389	2.335	322	-4.9666
964	21.390	2.338	324	-5.1641
966	21.388	2.331	326	-4.7324
968	21.389	2.335	328	-4.9957
970	21.390	2.339	330	-5.2606
972	21.389	2.334	332	-4.9390
974	21.391	2.344	334	-5.6690
976	21.390	2.339	336	-5.2356
978	21.389	2.335	338	-4.9907
980	21.391	2.344	340	-5.7378
982	21.392	2.350	342	-6.9900
984	21.391	2.343	344	-5.5607

Table D.2: *VTI-SA Analyzer Silica Gel Mass vs. Time at 25°C 10-20%RH*

Time Stamp [min]	Weight [mg]	Weight Change [%]	Time Elapsed [min]	$ln(1-\frac{m_t}{m_f})$
1000	21.394	2.357	0	0.0000
1001	21.403	2.401	1	-0.0121
1002	21.410	2.436	2	-0.0216
1003	21.422	2.491	3	-0.0372
1004	21.434	2.548	4	-0.0533
1005	21.447	2.614	5	-0.0724
1006	21.460	2.674	6	-0.0901
1007	21.471	2.725	7	-0.1055
1008	21.482	2.778	8	-0.1217
1009	21.492	2.827	9	-0.1369
1010	21.504	2.885	10	-0.1550
1011	21.513	2.929	11	-0.1692
1012	21.528	3.002	12	-0.1928
1013	21.540	3.059	13	-0.2119
1014	21.548	3.094	14	-0.2238
1015	21.557	3.140	15	-0.2396
1016	21.565	3.179	16	-0.2531
1017	21.575	3.225	17	-0.2695
1018	21.584	3.270	18	-0.2855
1019	21.594	3.318	19	-0.3029
1020	21.603	3.359	20	-0.3184
1021	21.612	3.402	21	-0.3345
1022	21.624	3.459	22	-0.3563
1023	21.628	3.480	23	-0.3645
1024	21.636	3.516	24	-0.3787
1025	21.644	3.555	25	-0.3942
1026	21.654	3.602	26	-0.4135
1027	21.671	3.684	27	-0.4477
1029	21.677	3.714	29	-0.4609
1030	21.687	3.759	30	-0.4801
1031	21.695	3.798	31	-0.4974
1032	21.700	3.824	32	-0.5095
1033	21.707	3.858	33	-0.5248
1034	21.719	3.914	34	-0.5511
1035	21.724	3.936	35	-0.5612
1036	21.730	3.965	36	-0.5752
1037	21.736	3.994	37	-0.5896
1038	21.742	4.025	38	-0.6048
1039	21.748	4.054	39	-0.6194
1040	21.755	4.087	40	-0.6363
1041	21.762	4.119	41	-0.6527
1042	21.767	4.142	42	-0.6647

D.2 – continued from previous page

Time Stamp [min]	Weight [mg]	Weight Change [%]	Time Elapsed [min]	$ln(1-\frac{m_t}{m_f})$
1043	21.773	4.170	43	-0.6797
1044	21.778	4.196	44	-0.6935
1045	21.784	4.223	45	-0.7084
1046	21.789	4.248	46	-0.7226
1047	21.795	4.275	47	-0.7379
1048	21.800	4.299	48	-0.7516
1049	21.805	4.327	49	-0.7679
1050	21.811	4.355	50	-0.7844
1051	21.817	4.382	51	-0.8007
1052	21.821	4.404	52	-0.8137
1053	21.826	4.427	53	-0.8284
1054	21.832	4.456	54	-0.8464
1055	21.837	4.480	55	-0.8621
1056	21.841	4.499	56	-0.8739
1057	21.847	4.525	57	-0.8912
1058	21.853	4.555	58	-0.9115
1059	21.857	4.575	59	-0.9249
1060	21.861	4.592	60	-0.9369
1061	21.867	4.620	61	-0.9562
1062	21.870	4.636	62	-0.9680
1063	21.874	4.654	63	-0.9808
1064	21.878	4.673	64	-0.9945
1065	21.881	4.689	65	-1.0061
1066	21.886	4.715	66	-1.0255
1067	21.890	4.730	67	-1.0370
1068	21.893	4.745	68	-1.0487
1069	21.898	4.768	69	-1.0670
1070	21.901	4.785	70	-1.0808
1071	21.905	4.804	71	-1.0958
1072	21.908	4.819	72	-1.1080
1073	21.912	4.837	73	-1.1233
1074	21.915	4.853	74	-1.1367
1075	21.918	4.865	75	-1.1468
1076	21.922	4.884	76	-1.1630
1077	21.926	4.905	77	-1.1818
1078	21.930	4.921	78	-1.1962
1079	21.933	4.939	79	-1.2120
1080	21.936	4.953	80	-1.2254
1081	21.939	4.966	81	-1.2375
1083	21.945	4.995	83	-1.2645
1084	21.949	5.012	84	-1.2817
1085	21.951	5.025	85	-1.2938
1086	21.955	5.041	86	-1.3104
1088	21.959	5.060	88	-1.3293
1089	21.961	5.071	89	-1.3412
1090	21.964	5.088	90	-1.3584
1091	21.968	5.104	91	-1.3760
1092	21.970	5.116	92	-1.3885
1093	21.973	5.130	93	-1.4044
1095	21.977	5.149	95	-1.4258
1096	21.981	5.166	96	-1.4452
1097	21.984	5.180	97	-1.4615
1098	21.986	5.192	98	-1.4759
1099	21.989	5.206	99	-1.4919
1101	21.994	5.228	101	-1.5192
1102	21.996	5.239	102	-1.5331
1103	21.999	5.252	103	-1.5496
1104	22.001	5.262	104	-1.5627
1105	22.004	5.277	105	-1.5825
1106	22.006	5.289	106	-1.5974
1107	22.008	5.299	107	-1.6110
1108	22.011	5.310	108	-1.6260
1110	22.013	5.322	110	-1.6431
1111	22.016	5.335	111	-1.6616
1113	22.021	5.359	113	-1.6969
1115	22.024	5.372	115	-1.7168
1117	22.028	5.393	117	-1.7489
1119	22.031	5.406	119	-1.7696
1121	22.034	5.422	121	-1.7949
1122	22.037	5.436	122	-1.8181
1124	22.038	5.441	124	-1.8274
1125	22.041	5.454	125	-1.8487
1126	22.046	5.477	126	-1.8889
1128	22.046	5.480	128	-1.8948

D.2 – continued from previous page

Time Stamp [min]	Weight [mg]	Weight Change [%]	Time Elapsed [min]	$ln(1-\frac{m_t}{m_f})$
1130	22.052	5.505	130	-1.9402
1132	22.055	5.521	132	-1.9715
1134	22.059	5.538	134	-2.0061
1136	22.061	5.549	136	-2.0273
1138	22.062	5.555	138	-2.0397
1139	22.064	5.566	139	-2.0640
1141	22.068	5.586	141	-2.1070
1144	22.069	5.588	143	-2.1120
1146	22.071	5.596	145	-2.1297
1147	22.074	5.613	147	-2.1711
1150	22.075	5.615	149	-2.1753
1150	22.080	5.643	150	-2.2436
1151	22.077	5.629	151	-2.2083
1153	22.076	5.624	153	-2.1959
1154	22.079	5.636	154	-2.2260
1156	22.082	5.649	156	-2.2591
1158	22.086	5.668	158	-2.3098
1161	22.086	5.669	160	-2.3124
1162	22.088	5.680	162	-2.3447
1163	22.091	5.691	163	-2.3762
1166	22.092	5.698	165	-2.3958
1168	22.092	5.698	167	-2.3955
1169	22.094	5.708	169	-2.4285
1171	22.098	5.728	171	-2.4891
1173	22.098	5.726	173	-2.4854
1176	22.098	5.727	175	-2.4862
1176	22.101	5.739	176	-2.5277
1178	22.102	5.745	178	-2.5472
1180	22.105	5.761	180	-2.6045
1181	22.103	5.749	181	-2.5617
1184	22.104	5.757	183	-2.5896
1185	22.107	5.770	185	-2.6379
1187	22.107	5.771	187	-2.6431
1189	22.108	5.774	189	-2.6557
1191	22.121	5.835	191	-2.9228
1192	22.111	5.788	192	-2.7090
1195	22.111	5.791	194	-2.7237
1197	22.112	5.795	196	-2.7377
1198	22.116	5.811	198	-2.8085
1200	22.116	5.814	200	-2.8220
1202	22.118	5.824	202	-2.8678
1204	22.125	5.858	204	-3.0476
1205	22.119	5.828	205	-2.8867
1207	22.123	5.848	207	-2.9925
1208	22.119	5.828	208	-2.8903
1210	22.121	5.835	210	-2.9240
1213	22.121	5.836	212	-2.9309
1215	22.122	5.842	214	-2.9585
1216	22.124	5.852	216	-3.0144
1218	22.124	5.849	218	-2.9973
1220	22.145	5.952	220	-3.8186
1221	22.129	5.875	221	-3.1470
1222	22.126	5.862	222	-3.0693
1224	22.127	5.866	224	-3.0968
1225	22.131	5.887	225	-3.2296
1226	22.136	5.907	226	-3.3738
1227	22.129	5.874	227	-3.1450
1229	22.133	5.895	229	-3.2842
1230	22.131	5.884	230	-3.2116
1233	22.131	5.884	232	-3.2058
1235	22.130	5.880	234	-3.1820
1237	22.130	5.879	236	-3.1783
1239	22.131	5.886	238	-3.2198
1241	22.132	5.892	240	-3.2619
1242	22.135	5.902	242	-3.3395
1244	22.135	5.906	244	-3.3688
1246	22.136	5.911	246	-3.4092
1249	22.137	5.913	248	-3.4251
1251	22.137	5.916	250	-3.4494
1253	22.137	5.914	252	-3.4325
1255	22.138	5.921	254	-3.4913
1257	22.138	5.919	256	-3.4814
1258	22.141	5.931	258	-3.5900
1260	22.141	5.932	260	-3.5964

D.2 – continued from previous page

Time Stamp [min]	Weight [mg]	Weight Change [%]	Time Elapsed [min]	$ln(1-\frac{m_t}{m_f})$
1261	22.146	5.957	261	-3.8818
1262	22.149	5.973	262	-4.1143
1263	22.143	5.941	263	-3.6961
1265	22.142	5.940	265	-3.6787
1267	22.142	5.939	267	-3.6711
1269	22.150	5.974	269	-4.1452
1270	22.144	5.947	270	-3.7545
1272	22.143	5.941	272	-3.6918
1274	22.144	5.947	274	-3.7545
1276	22.144	5.945	276	-3.7335
1278	22.143	5.944	278	-3.7281
1280	22.145	5.953	280	-3.8346
1283	22.144	5.948	282	-3.7741
1285	22.146	5.956	284	-3.8662
1287	22.146	5.956	286	-3.8662
1289	22.146	5.956	288	-3.8703
1291	22.146	5.955	290	-3.8549
1293	22.147	5.959	292	-3.9139
1295	22.147	5.963	294	-3.9710
1296	22.151	5.978	296	-4.2176
1298	22.150	5.978	298	-4.2074
1300	22.151	5.981	300	-4.2644
1302	22.150	5.976	302	-4.1773
1303	22.157	6.010	303	-5.1072
1305	22.150	5.978	305	-4.2074
1308	22.152	5.984	307	-4.3280
1310	22.152	5.983	309	-4.3053
1312	22.152	5.985	311	-4.3380
1314	22.153	5.988	313	-4.4210
1316	22.158	6.012	316	-5.1928
1317	22.152	5.987	317	-4.3945
1319	22.153	5.991	319	-4.4940
1321	22.154	5.994	321	-4.5561
1323	22.154	5.996	323	-4.6026
1326	22.155	6.002	325	-4.7849
1328	22.154	5.994	327	-4.5644
1328	22.157	6.010	328	-5.1142
1329	22.155	6.000	329	-4.7269
1332	22.154	5.994	331	-4.5687
1334	22.155	5.999	333	-4.7099
1336	22.156	6.004	335	-4.8411
1338	22.155	6.002	337	-4.7876
1340	22.155	5.999	339	-4.6957
1342	22.157	6.008	341	-4.9984
1344	22.158	6.013	343	-5.2208
1346	22.157	6.011	345	-5.1435
1348	22.158	6.012	347	-5.1812
1350	22.159	6.019	349	-5.5731
1352	22.160	6.021	351	-5.7962

Table D.3: *VTI-SA Analyzer Silica Gel Mass vs. Time at 25°C 20-30%RH*

Time Stamp [min]	Weight [mg]	Weight Change [%]	Time Elapsed [min]	$ln(1-\frac{m_t}{m_f})$
1360	22.161	6.026	0	0.0000
1361	22.170	6.070	1	-0.0104
1362	22.182	6.127	3	-0.0243
1363	22.194	6.187	3	-0.0392
1364	22.208	6.254	4	-0.0561
1365	22.220	6.311	6	-0.0704
1366	22.233	6.375	6	-0.0870
1367	22.247	6.439	7	-0.1041
1368	22.258	6.494	9	-0.1186
1369	22.271	6.556	9	-0.1355
1370	22.284	6.617	11	-0.1524
1371	22.297	6.679	12	-0.1699
1372	22.307	6.729	12	-0.1840
1373	22.318	6.781	14	-0.1991
1374	22.331	6.841	15	-0.2168
1375	22.341	6.888	15	-0.2310
1376	22.353	6.946	17	-0.2485

D.3 – continued from previous page

Time Stamp [min]	Weight [mg]	Weight Change [%]	Time Elapsed [min]	$ln(1 - \frac{m_t}{m_f})$
1377	22.363	6.994	17	-0.2634
1378	22.375	7.052	18	-0.2814
1379	22.386	7.103	19	-0.2980
1380	22.396	7.151	20	-0.3136
1381	22.405	7.197	21	-0.3286
1382	22.414	7.238	22	-0.3422
1383	22.422	7.279	23	-0.3562
1384	22.433	7.330	24	-0.3736
1385	22.443	7.377	26	-0.3902
1386	22.452	7.423	27	-0.4066
1387	22.462	7.468	27	-0.4229
1388	22.471	7.511	28	-0.4388
1389	22.479	7.552	30	-0.4539
1390	22.488	7.591	30	-0.4691
1391	22.495	7.628	31	-0.4831
1392	22.505	7.674	32	-0.5012
1393	22.513	7.712	33	-0.5163
1394	22.520	7.745	34	-0.5298
1395	22.528	7.783	35	-0.5452
1396	22.535	7.819	37	-0.5603
1397	22.540	7.844	37	-0.5706
1398	22.551	7.893	38	-0.5917
1399	22.557	7.924	39	-0.6052
1400	22.566	7.965	40	-0.6232
1401	22.572	7.994	41	-0.6361
1402	22.579	8.027	42	-0.6511
1403	22.585	8.055	43	-0.6642
1404	22.590	8.082	45	-0.6767
1405	22.599	8.122	45	-0.6960
1406	22.605	8.151	47	-0.7097
1407	22.611	8.181	47	-0.7247
1408	22.618	8.214	49	-0.7411
1409	22.624	8.246	50	-0.7571
1410	22.629	8.268	50	-0.7686
1411	22.640	8.320	51	-0.7955
1413	22.646	8.351	54	-0.8123
1414	22.654	8.386	54	-0.8313
1415	22.661	8.419	55	-0.8494
1416	22.665	8.437	56	-0.8600
1417	22.669	8.460	58	-0.8729
1418	22.675	8.486	58	-0.8880
1419	22.680	8.510	59	-0.9018
1420	22.684	8.529	60	-0.9128
1421	22.689	8.554	61	-0.9281
1422	22.694	8.579	62	-0.9435
1423	22.701	8.611	63	-0.9629
1424	22.704	8.625	64	-0.9720
1425	22.709	8.649	66	-0.9871
1426	22.713	8.667	66	-0.9990
1427	22.716	8.683	68	-1.0096
1428	22.720	8.705	69	-1.0239
1429	22.725	8.728	69	-1.0396
1430	22.740	8.797	70	-1.0871
1431	22.737	8.785	71	-1.0786
1432	22.741	8.801	72	-1.0901
1433	22.745	8.822	74	-1.1051
1434	22.751	8.849	74	-1.1248
1436	22.757	8.878	76	-1.1462
1437	22.760	8.894	77	-1.1583
1438	22.764	8.914	79	-1.1737
1439	22.769	8.937	79	-1.1916
1440	22.772	8.951	80	-1.2026
1441	22.777	8.974	82	-1.2211
1442	22.781	8.994	82	-1.2376
1443	22.784	9.011	84	-1.2517
1444	22.788	9.027	85	-1.2650
1445	22.791	9.043	85	-1.2787
1446	22.795	9.060	86	-1.2940
1447	22.798	9.077	87	-1.3086
1448	22.803	9.099	88	-1.3281
1449	22.806	9.113	89	-1.3408
1450	22.809	9.127	91	-1.3537
1451	22.812	9.144	91	-1.3701
1452	22.815	9.160	92	-1.3847

D.3 – continued from previous page

Time Stamp [min]	Weight [mg]	Weight Change [%]	Time Elapsed [min]	$ln(1-\frac{m_t}{m_f})$
1453	22.819	9.175	94	-1.3995
1454	22.822	9.192	94	-1.4164
1455	22.825	9.203	96	-1.4272
1456	22.828	9.218	96	-1.4415
1457	22.830	9.228	98	-1.4519
1458	22.833	9.243	98	-1.4678
1459	22.836	9.256	100	-1.4809
1460	22.838	9.270	101	-1.4956
1461	22.842	9.285	102	-1.5123
1462	22.844	9.296	103	-1.5243
1463	22.848	9.315	104	-1.5448
1465	22.852	9.335	106	-1.5676
1467	22.857	9.359	108	-1.5964
1469	22.862	9.383	110	-1.6242
1471	22.867	9.405	112	-1.6513
1472	22.870	9.419	113	-1.6691
1474	22.874	9.440	115	-1.6965
1475	22.877	9.453	116	-1.7136
1477	22.879	9.465	118	-1.7295
1478	22.882	9.477	119	-1.7453
1479	22.884	9.488	120	-1.7616
1481	22.888	9.505	122	-1.7846
1483	22.892	9.524	124	-1.8119
1484	22.894	9.534	125	-1.8268
1485	22.896	9.544	126	-1.8419
1488	22.897	9.550	128	-1.8508
1488	22.899	9.561	129	-1.8681
1490	22.903	9.580	131	-1.8974
1492	22.907	9.596	133	-1.9234
1493	22.910	9.610	134	-1.9466
1496	22.910	9.611	136	-1.9487
1497	22.915	9.635	138	-1.9905
1499	22.916	9.639	140	-1.9975
1500	22.918	9.652	141	-2.0203
1502	22.921	9.663	143	-2.0395
1503	22.924	9.677	144	-2.0668
1505	22.924	9.678	146	-2.0688
1507	22.926	9.691	148	-2.0923
1508	22.929	9.703	149	-2.1175
1510	22.935	9.730	151	-2.1717
1511	22.932	9.718	152	-2.1474
1512	22.935	9.731	153	-2.1741
1514	22.938	9.748	155	-2.2096
1516	22.941	9.758	157	-2.2319
1518	22.944	9.774	159	-2.2685
1520	22.946	9.785	161	-2.2937
1522	22.955	9.827	163	-2.3993
1523	22.950	9.804	164	-2.3403
1525	22.953	9.817	166	-2.3746
1527	22.955	9.829	168	-2.4041
1530	22.956	9.833	170	-2.4158
1531	22.960	9.849	172	-2.4601
1534	22.961	9.854	174	-2.4729
1534	22.963	9.865	175	-2.5035
1537	22.964	9.870	177	-2.5209
1539	22.965	9.875	179	-2.5353
1540	22.968	9.890	181	-2.5803
1542	22.969	9.893	183	-2.5897
1544	22.972	9.908	185	-2.6410
1545	22.975	9.921	186	-2.6828
1546	22.983	9.959	187	-2.8279
1547	22.974	9.918	188	-2.6751
1549	22.974	9.920	190	-2.6814
1551	22.978	9.935	192	-2.7347
1553	22.979	9.940	194	-2.7521
1556	22.980	9.946	196	-2.7758
1558	22.982	9.956	198	-2.8148
1560	22.983	9.962	200	-2.8373
1562	22.985	9.968	202	-2.8654
1564	22.986	9.975	204	-2.8929
1566	22.986	9.976	206	-2.8977
1568	22.988	9.985	208	-2.9369
1570	22.989	9.988	210	-2.9524
1572	22.989	9.990	212	-2.9609

D.3 – continued from previous page

Time Stamp [min]	Weight [mg]	Weight Change [%]	Time Elapsed [min]	$ln(1-\frac{m_t}{m_f})$
1573	22.991	10.001	214	-3.0115
1576	22.992	10.005	216	-3.0347
1578	22.994	10.012	218	-3.0673
1580	22.995	10.021	220	-3.1130
1582	22.997	10.027	222	-3.1471
1584	22.998	10.035	224	-3.1948
1586	23.000	10.041	226	-3.2269
1588	23.001	10.045	228	-3.2557
1589	23.003	10.055	230	-3.3201
1591	23.014	10.112	232	-3.7853
1592	23.004	10.061	233	-3.3556
1594	23.005	10.067	235	-3.3985
1597	23.005	10.068	237	-3.4048
1597	23.009	10.087	238	-3.5558
1599	23.008	10.079	240	-3.4943
1602	23.008	10.082	242	-3.5146
1604	23.008	10.082	244	-3.5146
1606	23.010	10.090	246	-3.5802
1606	23.013	10.107	247	-3.7377
1607	23.010	10.089	248	-3.5706
1609	23.010	10.089	250	-3.5747
1611	23.013	10.106	252	-3.7289
1613	23.012	10.102	254	-3.6877
1616	23.014	10.108	256	-3.7515
1618	23.015	10.113	258	-3.8057
1619	23.018	10.129	260	-3.9929
1622	23.018	10.128	262	-3.9713
1623	23.020	10.138	264	-4.1101
1624	23.026	10.167	265	-4.6645
1625	23.021	10.141	266	-4.1528
1627	23.021	10.141	268	-4.1528
1629	23.021	10.142	270	-4.1761
1631	23.022	10.148	272	-4.2767
1634	23.023	10.152	274	-4.3450
1636	23.024	10.157	276	-4.4276
1638	23.024	10.159	278	-4.4818
1640	23.024	10.156	280	-4.4165
1642	23.023	10.152	282	-4.3435
1643	23.026	10.168	284	-4.6953
1645	23.027	10.170	286	-4.7313
1648	23.025	10.164	288	-4.5960
1650	23.026	10.166	290	-4.6287
1652	23.026	10.169	292	-4.7121
1653	23.024	10.157	294	-4.4438
1656	23.024	10.159	296	-4.4784
1658	23.024	10.158	298	-4.4601
1660	23.022	10.150	300	-4.3004
1660	23.025	10.160	301	-4.5005
1662	23.023	10.152	303	-4.3406
1664	23.025	10.164	305	-4.5940
1666	23.024	10.156	307	-4.4245
1668	23.025	10.164	309	-4.5960
1671	23.026	10.165	311	-4.6170
1673	23.027	10.171	313	-4.7712
1675	23.027	10.171	315	-4.7599
1677	23.027	10.174	317	-4.8533
1679	23.029	10.179	319	-5.0321
1681	23.029	10.180	321	-5.0769
1681	23.032	10.195	322	-5.9397
1683	23.031	10.189	324	-5.4685
1685	23.032	10.194	326	-5.8494
1688	23.033	10.199	328	-6.3026
1690	23.034	10.206	330	-8.7863
1692	23.033	10.202	332	-6.8063
1694	23.033	10.203	334	-6.9757
1696	23.033	10.199	336	-6.2919
1698	23.033	10.199	338	-6.3552
1700	23.033	10.200	340	-6.4120
1702	23.034	10.204	342	-7.3112
1704	23.033	10.199	344	-6.3452
1706	23.033	10.201	346	-6.5624
1708	23.033	10.202	348	-6.8404
1710	23.033	10.201	350	-6.6479
1712	23.032	10.198	352	-6.1482

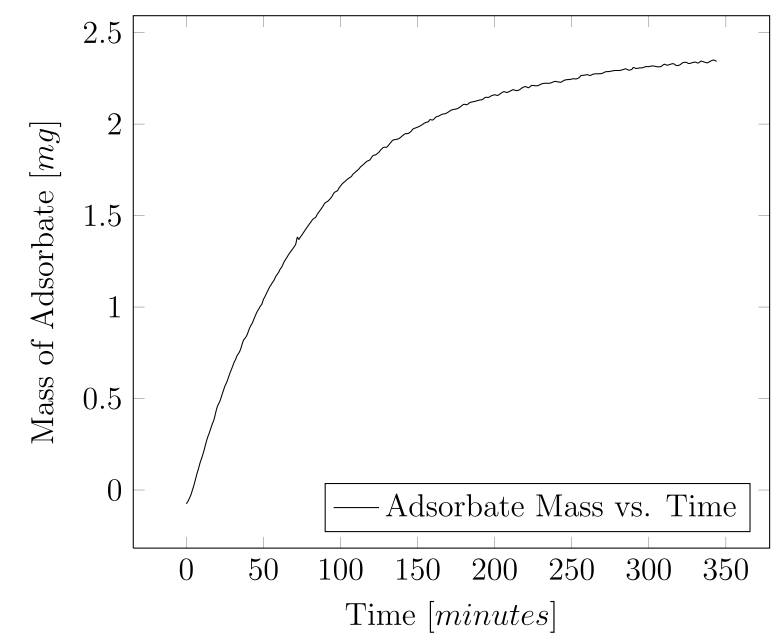

(a) *Mass vs. Time*

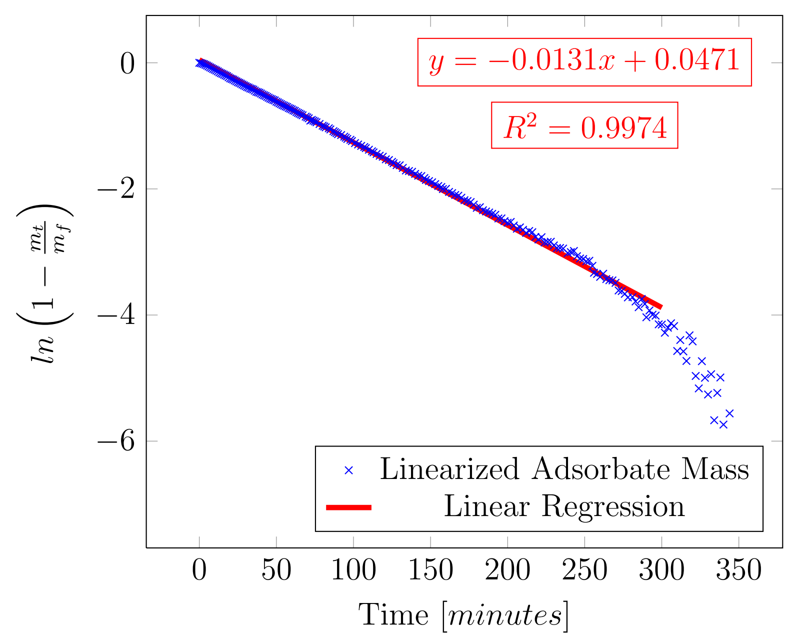

(b) *Linearized Mass vs. Time*

Figure D.1: *Adsorbate Mass vs. Time for Increment of Relative Humidity from 5% to 10%*

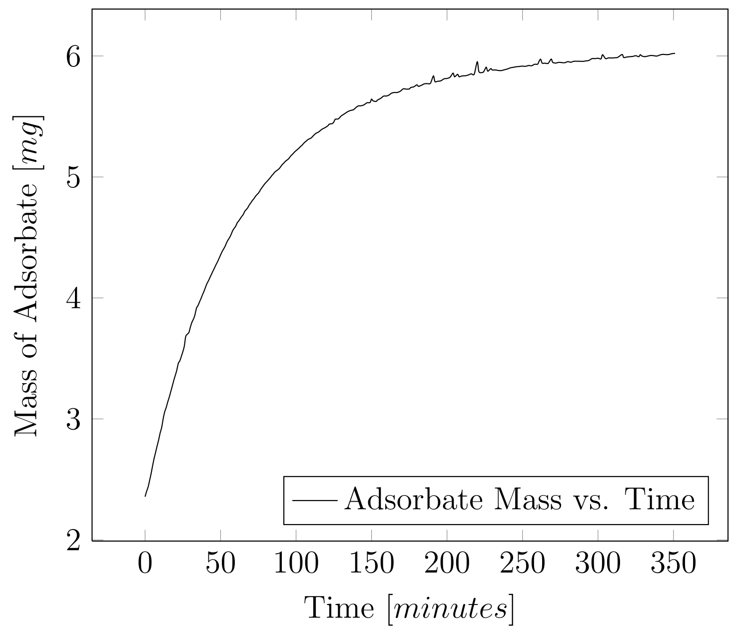

(a) *Mass vs. Time*

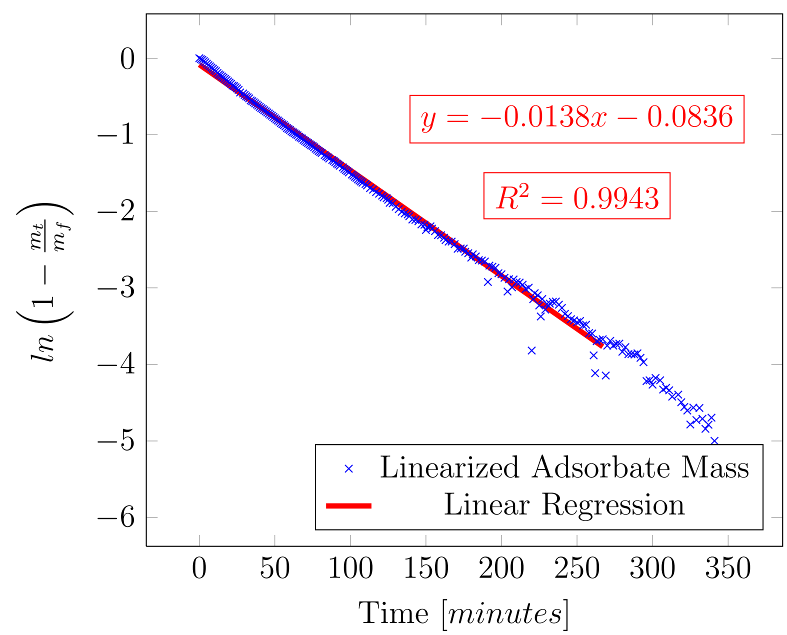

(b) *Linearized Mass vs. Time*

Figure D.2: *Adsorbate Mass vs. Time for Increment of Relative Humidity from 10% to 20%*

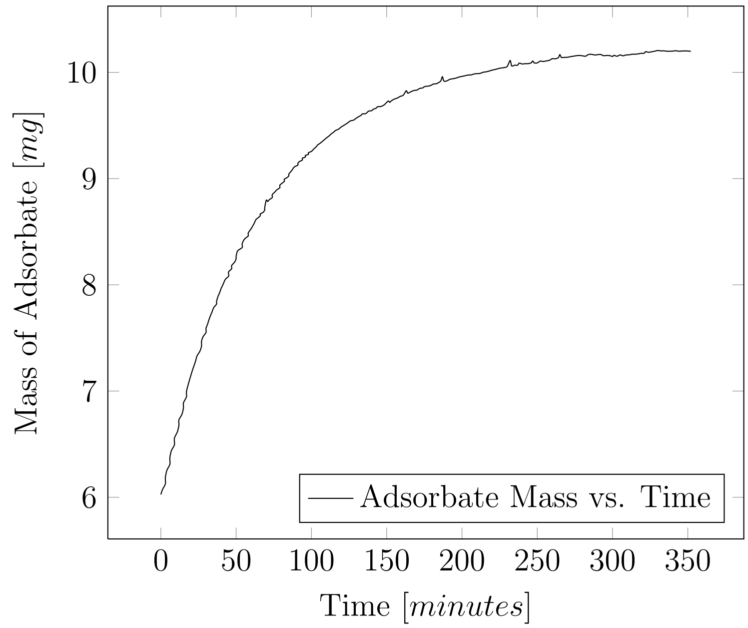

(a) *Mass vs. Time*

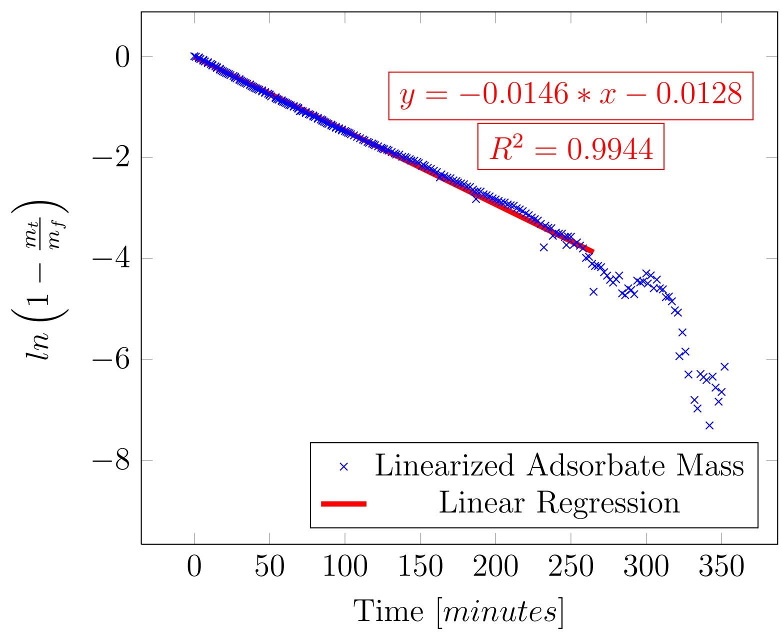

(b) *Linearized Mass vs. Time*

Figure D.3: *Adsorbate Mass vs. Time for Increment of Relative Humidity from 20% to 30%*

Table D.4: *VTI-SA Analyzer Silica Gel Mass vs. Time at 25°C 30-40%RH*

Time Stamp [min]	Weight [mg]	Weight Change [%]	Time Elapsed [min]	$ln(1-\frac{m_t}{m_f})$
1720	23.035	10.212	0	0.0000
1721	23.045	10.258	1	-0.0114
1722	23.056	10.310	2	-0.0245
1723	23.071	10.380	3	-0.0423
1724	23.083	10.441	4	-0.0581
1725	23.096	10.502	5	-0.0740
1726	23.110	10.568	6	-0.0917
1727	23.128	10.657	7	-0.1159
1728	23.139	10.705	8	-0.1295
1729	23.150	10.760	9	-0.1447
1730	23.163	10.823	10	-0.1629
1731	23.174	10.875	11	-0.1780
1732	23.188	10.941	12	-0.1977
1733	23.200	10.997	13	-0.2147
1734	23.210	11.047	14	-0.2299
1735	23.222	11.106	15	-0.2485
1736	23.234	11.164	16	-0.2669
1737	23.247	11.223	17	-0.2859
1738	23.259	11.284	18	-0.3061
1739	23.273	11.350	19	-0.3284
1740	23.281	11.386	20	-0.3408
1741	23.291	11.434	21	-0.3575
1742	23.300	11.479	22	-0.3737
1743	23.309	11.522	23	-0.3891
1744	23.318	11.564	24	-0.4044
1745	23.333	11.638	25	-0.4321
1746	23.340	11.671	26	-0.4448
1747	23.351	11.721	27	-0.4642
1748	23.359	11.760	28	-0.4794
1749	23.368	11.805	29	-0.4974
1750	23.377	11.845	30	-0.5138
1751	23.385	11.883	31	-0.5297
1752	23.400	11.957	32	-0.5611
1753	23.404	11.974	33	-0.5685
1754	23.413	12.017	34	-0.5871
1755	23.419	12.048	35	-0.6010
1756	23.434	12.121	36	-0.6343
1758	23.442	12.157	38	-0.6512
1759	23.450	12.194	39	-0.6686
1760	23.456	12.225	40	-0.6836
1761	23.465	12.266	41	-0.7039
1762	23.472	12.301	42	-0.7215
1763	23.479	12.332	43	-0.7375
1764	23.485	12.364	44	-0.7539
1765	23.492	12.394	45	-0.7699
1766	23.498	12.426	46	-0.7867
1767	23.511	12.485	47	-0.8194
1769	23.519	12.525	49	-0.8422
1770	23.525	12.552	50	-0.8577
1771	23.529	12.576	51	-0.8712
1772	23.542	12.634	52	-0.9059
1773	23.544	12.647	53	-0.9139
1774	23.547	12.660	54	-0.9219
1775	23.553	12.689	55	-0.9404
1776	23.557	12.709	56	-0.9530
1777	23.569	12.763	57	-0.9877
1778	23.577	12.804	58	-1.0154
1779	23.582	12.829	59	-1.0324
1780	23.585	12.841	60	-1.0409
1781	23.588	12.858	61	-1.0526
1782	23.595	12.891	62	-1.0763
1783	23.602	12.923	63	-1.0998
1784	23.606	12.942	64	-1.1142
1785	23.611	12.966	65	-1.1321
1786	23.615	12.984	66	-1.1460
1787	23.619	13.004	67	-1.1614
1788	23.623	13.022	68	-1.1760
1789	23.629	13.054	69	-1.2011
1790	23.635	13.081	70	-1.2236
1791	23.638	13.097	71	-1.2373
1792	23.641	13.110	72	-1.2486
1793	23.648	13.142	73	-1.2760
1795	23.656	13.180	75	-1.3104
1796	23.661	13.207	76	-1.3356

D.4 – continued from previous page

Time Stamp [min]	Weight [mg]	Weight Change [%]	Time Elapsed [min]	$ln(1-\frac{m_t}{m_f})$
1797	23.665	13.222	77	-1.3494
1798	23.670	13.247	78	-1.3736
1799	23.672	13.257	79	-1.3834
1801	23.675	13.271	81	-1.3969
1802	23.678	13.285	82	-1.4109
1803	23.688	13.333	83	-1.4603
1805	23.693	13.356	85	-1.4853
1808	23.693	13.360	87	-1.4900
1808	23.698	13.382	88	-1.5135
1809	23.702	13.401	89	-1.5350
1810	23.705	13.414	90	-1.5505
1811	23.712	13.449	91	-1.5921
1813	23.719	13.482	93	-1.6324
1814	23.717	13.472	94	-1.6198
1816	23.719	13.485	96	-1.6362
1817	23.726	13.516	97	-1.6765
1818	23.730	13.536	98	-1.7025
1819	23.735	13.560	99	-1.7364
1821	23.737	13.567	101	-1.7457
1823	23.741	13.588	103	-1.7765
1824	23.744	13.602	104	-1.7958
1825	23.746	13.612	105	-1.8110
1826	23.749	13.626	106	-1.8319
1828	23.752	13.638	108	-1.8518
1829	23.755	13.653	109	-1.8753
1830	23.757	13.664	110	-1.8926
1831	23.760	13.678	111	-1.9162
1833	23.765	13.704	113	-1.9605
1835	23.767	13.714	115	-1.9781
1836	23.770	13.724	116	-1.9961
1838	23.772	13.738	118	-2.0220
1840	23.777	13.762	120	-2.0667
1843	23.779	13.768	122	-2.0786
1844	23.781	13.780	124	-2.1033
1845	23.785	13.798	125	-2.1400
1847	23.789	13.818	127	-2.1814
1849	23.792	13.834	129	-2.2178
1851	23.796	13.849	131	-2.2534
1853	23.801	13.876	133	-2.3168
1855	23.802	13.881	135	-2.3290
1857	23.804	13.891	137	-2.3564
1859	23.808	13.907	139	-2.3972
1861	23.812	13.929	141	-2.4590
1863	23.814	13.938	143	-2.4869
1865	23.816	13.947	145	-2.5140
1867	23.817	13.952	147	-2.5281
1869	23.820	13.967	149	-2.5765
1871	23.821	13.971	151	-2.5900
1873	23.824	13.986	153	-2.6401
1875	23.826	13.993	155	-2.6637
1878	23.827	14.000	157	-2.6877
1880	23.828	14.006	159	-2.7113
1881	23.832	14.023	161	-2.7744
1883	23.833	14.030	163	-2.8031
1885	23.834	14.033	165	-2.8138
1887	23.837	14.047	167	-2.8738
1888	23.840	14.059	168	-2.9295
1890	23.841	14.066	170	-2.9612
1893	23.842	14.070	172	-2.9811
1895	23.843	14.076	174	-3.0110
1895	23.846	14.088	175	-3.0735
1898	23.847	14.094	177	-3.1067
1900	23.847	14.097	179	-3.1195
1902	23.848	14.102	181	-3.1487
1903	23.851	14.115	183	-3.2247
1905	23.852	14.121	185	-3.2634
1908	23.853	14.122	187	-3.2712
1910	23.854	14.130	189	-3.3259
1912	23.855	14.136	191	-3.3626
1914	23.855	14.134	193	-3.3552
1916	23.856	14.140	195	-3.3930
1917	23.859	14.154	197	-3.5021
1920	23.858	14.147	199	-3.4482
1922	23.858	14.147	201	-3.4451

D.4 – continued from previous page

Time Stamp [min]	Weight [mg]	Weight Change [%]	Time Elapsed [min]	$ln(1-\frac{m_t}{m_f})$
1924	23.858	14.147	203	-3.4470
1926	23.859	14.153	205	-3.4937
1928	23.858	14.150	207	-3.4701
1930	23.857	14.142	209	-3.4131
1930	23.859	14.153	210	-3.4943
1932	23.861	14.164	212	-3.5842
1935	23.860	14.158	214	-3.5345
1937	23.861	14.164	216	-3.5842
1939	23.862	14.169	218	-3.6326
1941	23.863	14.172	220	-3.6612
1943	23.863	14.171	222	-3.6522
1945	23.863	14.172	225	-3.6635
1947	23.862	14.168	227	-3.6245
1949	23.864	14.177	229	-3.7153
1951	23.866	14.185	231	-3.7994
1953	23.866	14.188	233	-3.8243
1955	23.866	14.187	235	-3.8197
1957	23.867	14.192	237	-3.8701
1959	23.868	14.196	239	-3.9184
1961	23.869	14.198	241	-3.9474
1963	23.868	14.198	243	-3.9453
1965	23.871	14.208	245	-4.0786
1967	23.870	14.207	247	-4.0671
1969	23.870	14.203	249	-4.0135
1971	23.870	14.205	251	-4.0489
1973	23.871	14.208	253	-4.0810
1975	23.870	14.205	255	-4.0378
1977	23.871	14.210	257	-4.1104
1979	23.870	14.207	259	-4.0762
1981	23.872	14.214	261	-4.1708
1983	23.871	14.207	263	-4.0763
1985	23.870	14.206	265	-4.0535
1987	23.872	14.215	267	-4.1875
1990	23.872	14.214	269	-4.1784
1992	23.871	14.212	271	-4.1445
1994	23.873	14.220	273	-4.2738
1996	23.873	14.221	275	-4.2966
1998	23.872	14.216	277	-4.2057
2000	23.873	14.220	280	-4.2752
2001	23.876	14.234	281	-4.5550
2004	23.875	14.230	283	-4.4709
2006	23.875	14.227	285	-4.4207
2008	23.876	14.236	287	-4.6047
2010	23.875	14.231	289	-4.4969
2012	23.874	14.226	291	-4.3870
2014	23.876	14.232	293	-4.5256
2016	23.876	14.235	296	-4.5871
2018	23.876	14.235	298	-4.5775
2020	23.876	14.232	300	-4.5202
2021	23.878	14.244	301	-4.8326
2023	23.876	14.233	303	-4.5419
2025	23.875	14.229	305	-4.4572
2027	23.878	14.244	307	-4.8230
2030	23.877	14.241	309	-4.7364
2032	23.877	14.239	311	-4.6970
2034	23.878	14.242	313	-4.7847
2036	23.879	14.250	315	-5.0250
2038	23.878	14.245	317	-4.8603
2040	23.877	14.240	320	-4.7079
2042	23.879	14.247	322	-4.9308
2044	23.880	14.251	324	-5.0801
2046	23.879	14.246	326	-4.9096
2048	23.879	14.250	328	-5.0281
2050	23.880	14.251	330	-5.0769
2052	23.879	14.247	332	-4.9336
2054	23.879	14.249	334	-4.9954
2054	23.881	14.259	334	-5.4827
2056	23.883	14.265	336	-5.8976
2059	23.881	14.259	338	-5.4316
2061	23.881	14.260	340	-5.5062
2063	23.883	14.269	342	-6.3513
2065	23.885	14.274	344	-7.6644
2067	23.884	14.270	346	-6.4831

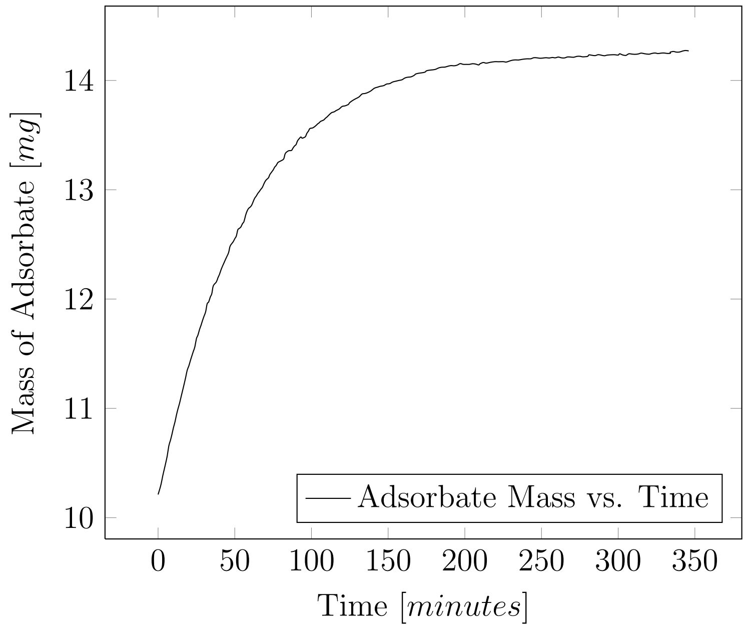

(a) *Mass vs. Time*

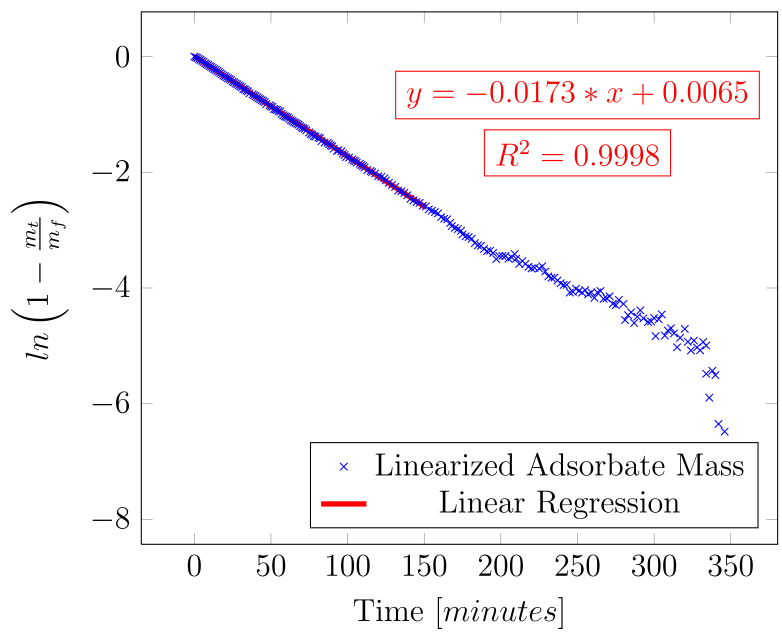

(b) *Linearized Mass vs. Time*

Figure D.4: *Adsorbate Mass vs. Time for Increment of Relative Humidity from 30% to 40%*

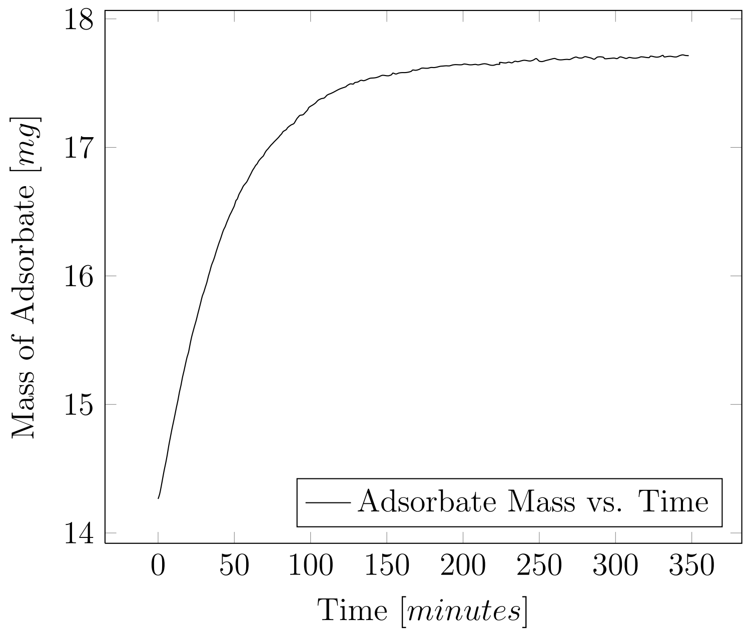

(a) *Mass vs. Time*

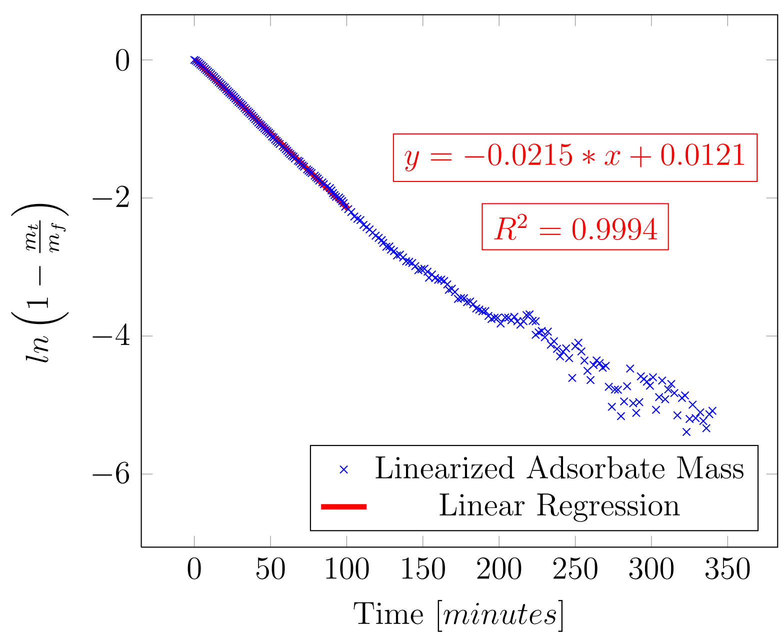

(b) *Linearized Mass vs. Time*

Figure D.5: *Adsorbate Mass vs. Time for Increment of Relative Humidity from 40% to 50%*

Table D.5: *VTI-SA Analyzer Silica Gel Mass vs. Time at 25°C 40-50%RH*

Time Stamp [min]	Weight [mg]	Weight Change [%]	Time Elapsed [min]	$ln(1-\frac{m_t}{m_f})$
2081	23.882	14.265	0	0
2081	23.89	14.301	1	-0.0105
2082	23.902	14.359	2	-0.0277
2083	23.916	14.424	3	-0.0471
2084	23.929	14.488	4	-0.0667
2085	23.941	14.544	5	-0.0842
2086	23.954	14.607	6	-0.1042
2087	23.969	14.679	7	-0.1276
2088	23.982	14.741	8	-0.1482
2089	23.995	14.803	9	-0.1689
2090	24.007	14.859	10	-0.1885
2091	24.019	14.916	11	-0.2085
2092	24.031	14.976	12	-0.2302
2093	24.043	15.031	13	-0.2503
2094	24.056	15.096	14	-0.2748
2095	24.067	15.148	15	-0.2948
2096	24.08	15.211	16	-0.3194
2097	24.091	15.261	17	-0.3397
2098	24.102	15.316	18	-0.3619
2099	24.113	15.368	19	-0.3837
2100	24.121	15.407	20	-0.4008
2101	24.134	15.469	21	-0.4276
2102	24.146	15.525	22	-0.4529
2103	24.155	15.57	23	-0.4733
2104	24.164	15.613	24	-0.4937
2105	24.173	15.654	25	-0.5133
2106	24.183	15.702	26	-0.5367
2107	24.193	15.748	27	-0.5598
2108	24.202	15.795	28	-0.5839
2109	24.212	15.843	29	-0.6088
2110	24.219	15.874	30	-0.6255
2111	24.227	15.913	31	-0.6468
2112	24.235	15.95	32	-0.6672
2113	24.245	15.998	33	-0.6947
2114	24.253	16.038	34	-0.7183
2115	24.262	16.082	35	-0.7444
2116	24.269	16.112	36	-0.7632
2117	24.275	16.145	37	-0.7837
2118	24.284	16.185	38	-0.8095
2119	24.292	16.222	39	-0.8339
2120	24.299	16.258	40	-0.8582
2121	24.306	16.29	41	-0.8803
2122	24.314	16.327	42	-0.9063
2123	24.32	16.36	43	-0.93
2124	24.325	16.383	44	-0.9468
2125	24.332	16.415	45	-0.9713
2126	24.338	16.443	46	-0.9925
2127	24.344	16.472	47	-1.0154
2128	24.349	16.495	48	-1.0337
2129	24.354	16.52	49	-1.0542
2130	24.359	16.545	50	-1.0757
2131	24.367	16.584	51	-1.1092
2132	24.371	16.6	52	-1.1231
2133	24.378	16.633	53	-1.1534
2134	24.382	16.655	54	-1.1735
2135	24.387	16.677	55	-1.1945
2136	24.392	16.701	56	-1.2173
2138	24.398	16.729	58	-1.2452
2139	24.402	16.751	59	-1.2675
2140	24.407	16.775	60	-1.2926
2141	24.412	16.798	61	-1.3171
2142	24.417	16.822	62	-1.3427
2143	24.421	16.84	63	-1.3632
2144	24.425	16.86	64	-1.3856
2145	24.428	16.873	65	-1.4007
2146	24.432	16.895	66	-1.4271
2148	24.438	16.922	68	-1.4605
2149	24.44	16.933	69	-1.4737
2150	24.445	16.956	70	-1.5037
2151	24.449	16.975	71	-1.5287
2152	24.452	16.988	72	-1.5459
2154	24.458	17.017	74	-1.5857
2155	24.46	17.029	75	-1.603
2156	24.463	17.042	76	-1.6215

D.5 – continued from previous page

Time Stamp [min]	Weight [mg]	Weight Change [%]	Time Elapsed [min]	$ln(1-\frac{m_t}{m_f})$
2157	24.465	17.054	77	-1.6391
2159	24.471	17.078	79	-1.6768
2160	24.474	17.093	80	-1.7002
2161	24.476	17.105	81	-1.7193
2162	24.48	17.123	82	-1.7476
2164	24.483	17.138	84	-1.7736
2165	24.486	17.154	85	-1.8004
2167	24.49	17.173	87	-1.8344
2169	24.493	17.185	89	-1.8568
2170	24.497	17.203	90	-1.8911
2171	24.501	17.223	91	-1.9296
2172	24.504	17.237	92	-1.9581
2173	24.506	17.249	93	-1.9824
2175	24.507	17.254	95	-1.9931
2176	24.51	17.265	96	-2.0171
2177	24.512	17.278	97	-2.0455
2178	24.515	17.291	98	-2.0752
2179	24.519	17.312	99	-2.1256
2181	24.523	17.327	101	-2.1622
2183	24.526	17.343	103	-2.2039
2185	24.531	17.367	105	-2.2686
2187	24.533	17.379	107	-2.3021
2189	24.535	17.385	109	-2.3198
2191	24.54	17.408	111	-2.3902
2193	24.542	17.418	113	-2.4224
2195	24.544	17.429	115	-2.4557
2197	24.547	17.442	117	-2.5029
2199	24.549	17.454	119	-2.5464
2202	24.551	17.463	121	-2.578
2204	24.553	17.471	123	-2.6098
2204	24.555	17.481	124	-2.6514
2206	24.558	17.494	126	-2.7068
2208	24.557	17.493	128	-2.7023
2209	24.559	17.504	129	-2.7484
2211	24.561	17.509	131	-2.7702
2213	24.563	17.522	133	-2.8332
2215	24.563	17.519	135	-2.8203
2217	24.564	17.528	137	-2.8614
2219	24.567	17.538	139	-2.9169
2221	24.567	17.54	141	-2.9246
2224	24.568	17.543	143	-2.9419
2226	24.569	17.551	145	-2.987
2227	24.571	17.561	147	-3.0463
2229	24.571	17.559	149	-3.0333
2231	24.571	17.557	151	-3.0247
2234	24.572	17.565	153	-3.0689
2234	24.575	17.578	154	-3.1553
2236	24.573	17.571	156	-3.1083
2238	24.575	17.579	158	-3.1601
2241	24.576	17.582	160	-3.1849
2243	24.576	17.582	162	-3.1832
2245	24.576	17.585	164	-3.2023
2247	24.578	17.592	166	-3.2523
2247	24.58	17.602	167	-3.3303
2250	24.58	17.6	169	-3.3149
2252	24.581	17.606	171	-3.3623
2253	24.583	17.617	173	-3.4623
2255	24.583	17.616	175	-3.4512
2257	24.583	17.616	177	-3.4513
2260	24.584	17.622	179	-3.5096
2262	24.584	17.621	181	-3.5004
2264	24.585	17.625	183	-3.5393
2266	24.586	17.631	185	-3.6008
2268	24.586	17.633	187	-3.6177
2270	24.587	17.635	189	-3.6412
2272	24.587	17.634	191	-3.6376
2274	24.588	17.641	193	-3.7094
2276	24.589	17.644	195	-3.7537
2278	24.589	17.643	197	-3.7351
2280	24.589	17.643	199	-3.736
2282	24.59	17.649	201	-3.8186
2284	24.588	17.643	204	-3.7313
2286	24.589	17.643	206	-3.7351
2288	24.589	17.646	208	-3.7715

D.5 – continued from previous page

Time Stamp [min]	Weight [mg]	Weight Change [%]	Time Elapsed [min]	$ln(1-\frac{m_t}{m_f})$
2290	24.588	17.642	210	-3.7216
2292	24.589	17.647	212	-3.7866
2294	24.59	17.651	214	-3.8356
2296	24.589	17.647	216	-3.7856
2298	24.588	17.64	218	-3.6972
2300	24.588	17.639	220	-3.6871
2302	24.589	17.646	222	-3.7795
2304	24.589	17.647	224	-3.7866
2304	24.592	17.661	224	-3.9824
2306	24.592	17.659	226	-3.9483
2309	24.592	17.657	228	-3.9271
2311	24.593	17.663	230	-4.0177
2313	24.592	17.658	232	-3.9365
2314	24.594	17.67	234	-4.1258
2316	24.594	17.667	236	-4.0756
2318	24.595	17.673	238	-4.186
2321	24.596	17.678	240	-4.2949
2323	24.595	17.675	242	-4.2278
2325	24.595	17.672	244	-4.1786
2327	24.596	17.679	246	-4.3205
2328	24.599	17.691	248	-4.6076
2330	24.594	17.671	250	-4.1489
2332	24.594	17.668	252	-4.0976
2334	24.595	17.675	254	-4.2231
2336	24.597	17.681	256	-4.3557
2338	24.598	17.687	258	-4.5045
2341	24.599	17.692	260	-4.6379
2343	24.597	17.684	262	-4.4206
2345	24.597	17.681	264	-4.3538
2347	24.597	17.683	266	-4.3923
2349	24.597	17.685	268	-4.4597
2351	24.597	17.684	270	-4.4323
2352	24.599	17.695	272	-4.7355
2354	24.601	17.703	274	-5.0258
2356	24.6	17.696	276	-4.7756
2359	24.6	17.696	278	-4.7784
2361	24.602	17.706	280	-5.1611
2363	24.601	17.701	282	-4.9482
2365	24.599	17.695	284	-4.7277
2367	24.598	17.686	286	-4.4716
2368	24.601	17.702	288	-4.9746
2371	24.601	17.705	290	-5.114
2373	24.601	17.701	292	-4.9579
2373	24.598	17.69	293	-4.5846
2375	24.599	17.691	295	-4.6239
2378	24.599	17.693	297	-4.6622
2380	24.599	17.695	299	-4.72
2382	24.599	17.691	301	-4.5984
2383	24.601	17.704	303	-5.0689
2386	24.6	17.699	305	-4.8852
2388	24.599	17.692	307	-4.6453
2390	24.601	17.7	309	-4.9164
2392	24.6	17.696	311	-4.7731
2394	24.599	17.694	313	-4.6943
2396	24.6	17.698	315	-4.8263
2398	24.602	17.705	317	-5.1488
2400	24.6	17.7	320	-4.8975
2402	24.6	17.699	322	-4.8611
2403	24.603	17.71	323	-5.39
2406	24.602	17.706	325	-5.2019
2408	24.601	17.702	327	-4.9946
2410	24.602	17.706	329	-5.1896
2412	24.604	17.716	331	-5.8912
2412	24.601	17.704	332	-5.1061
2414	24.602	17.707	334	-5.2316
2417	24.602	17.709	336	-5.336
2419	24.602	17.705	338	-5.1334
2421	24.601	17.704	340	-5.0837
2423	24.603	17.714	342	-5.6812
2425	24.605	17.72	344	-6.4162
2427	24.604	17.715	346	-5.8036
2429	24.603	17.714	348	-5.7015

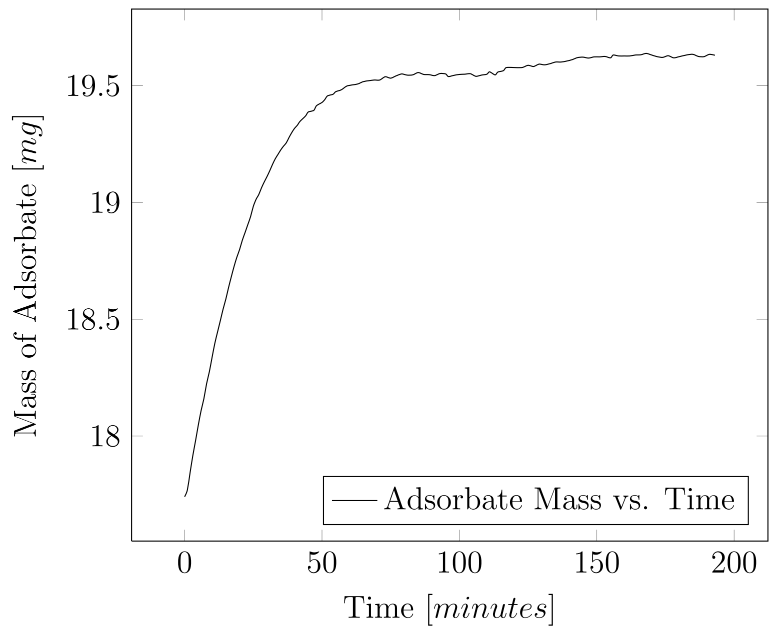

(a) *Mass vs. Time*

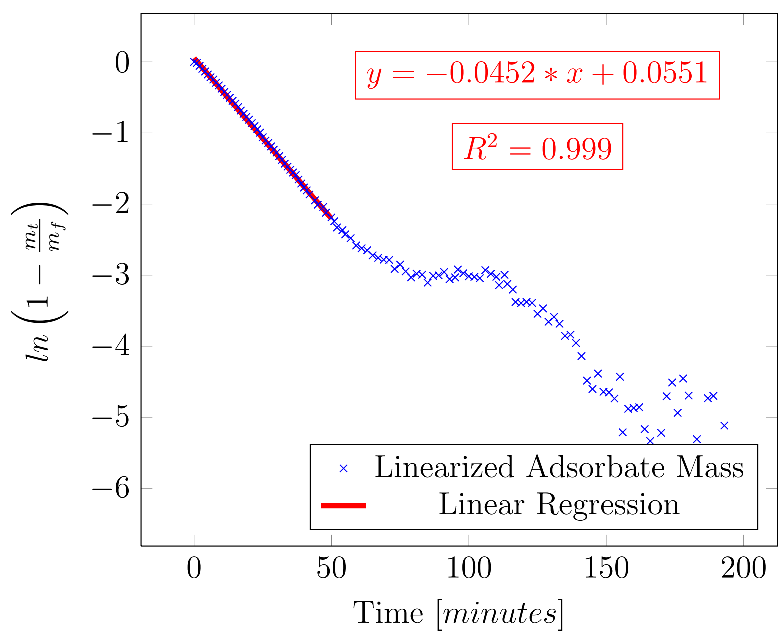

(b) *Linearized Mass vs. Time*

Figure D.6: *Adsorbate Mass vs. Time for Increment of Relative Humidity from 50% to 60%*

Table D.6: *VTI-SA Analyzer Silica Gel Mass vs. Time at 25°C 50-60%RH*

Time Stamp [min]	Weight [mg]	Weight Change [%]	Time Elapsed [min]	$ln(1-\frac{m_t}{m_f})$
2441	24.609	17.74	0	0
2441	24.615	17.769	1	-0.0153
2442	24.631	17.844	2	-0.0561
2443	24.646	17.917	3	-0.0975
2444	24.659	17.981	4	-0.1353
2445	24.673	18.048	5	-0.1766
2446	24.686	18.109	6	-0.2156
2447	24.696	18.159	7	-0.2489
2448	24.71	18.224	8	-0.2935
2449	24.721	18.275	9	-0.3301
2450	24.734	18.337	10	-0.3769
2451	24.746	18.397	11	-0.4235
2452	24.756	18.446	12	-0.4639
2453	24.766	18.494	13	-0.5049
2454	24.777	18.543	14	-0.5482
2455	24.786	18.586	15	-0.5884
2456	24.796	18.636	16	-0.6366
2457	24.806	18.682	17	-0.6836
2458	24.815	18.726	18	-0.7302
2459	24.823	18.765	19	-0.7739
2460	24.83	18.798	20	-0.8131
2461	24.838	18.838	21	-0.8618
2462	24.845	18.871	22	-0.9032
2463	24.852	18.905	23	-0.9487
2464	24.859	18.939	24	-0.9956
2465	24.869	18.983	25	-1.0599
2466	24.875	19.013	26	-1.1062
2467	24.879	19.034	27	-1.1407
2468	24.885	19.063	28	-1.1891
2469	24.891	19.088	29	-1.2336
2470	24.895	19.111	30	-1.2764
2471	24.901	19.136	31	-1.3252
2472	24.906	19.163	32	-1.3787
2473	24.911	19.187	33	-1.4313
2474	24.915	19.206	34	-1.4735
2475	24.919	19.225	35	-1.5182
2476	24.923	19.241	36	-1.5564
2477	24.925	19.255	37	-1.5927
2478	24.93	19.278	38	-1.6552
2479	24.935	19.299	39	-1.7124
2480	24.938	19.317	40	-1.7678
2481	24.941	19.33	41	-1.8074
2482	24.945	19.347	42	-1.8656
2484	24.95	19.37	44	-1.9477
2485	24.953	19.387	45	-2.0092
2487	24.955	19.394	47	-2.0401
2488	24.959	19.414	48	-2.1217
2490	24.962	19.428	50	-2.1883
2491	24.964	19.44	51	-2.2432
2492	24.968	19.456	52	-2.3295
2495	24.969	19.463	54	-2.3667
2495	24.971	19.474	55	-2.4276
2498	24.973	19.482	57	-2.4803
2499	24.976	19.498	59	-2.5836
2501	24.977	19.503	61	-2.6222
2504	24.978	19.507	63	-2.6509
2506	24.98	19.517	65	-2.7217
2508	24.981	19.521	67	-2.7567
2510	24.982	19.524	69	-2.7822
2512	24.982	19.524	71	-2.7862
2513	24.985	19.538	73	-2.9129
2516	24.983	19.532	75	-2.8522
2518	24.985	19.542	77	-2.9475
2520	24.987	19.55	79	-3.0317
2522	24.986	19.545	81	-2.98
2524	24.986	19.546	83	-2.9949
2526	24.989	19.556	85	-3.1057
2528	24.987	19.548	87	-3.0102
2530	24.987	19.547	89	-3.0034
2532	24.986	19.543	91	-2.9564
2534	24.988	19.552	93	-3.0573
2536	24.987	19.55	95	-3.0317
2536	24.985	19.539	96	-2.9214
2538	24.986	19.544	98	-2.9742

D.6 – continued from previous page

Time Stamp [min]	Weight [mg]	Weight Change [%]	Time Elapsed [min]	$ln(1-\frac{m_t}{m_f})$
2541	24.987	19.548	100	-3.0162
2543	24.987	19.549	102	-3.0247
2545	24.987	19.551	104	-3.0431
2546	24.985	19.54	106	-2.9301
2549	24.986	19.545	108	-2.9816
2551	24.987	19.549	110	-3.0238
2551	24.989	19.559	111	-3.1409
2553	24.986	19.546	113	-2.9958
2554	24.989	19.558	114	-3.1246
2557	24.99	19.564	116	-3.203
2557	24.993	19.577	117	-3.3785
2560	24.993	19.578	119	-3.3934
2562	24.993	19.577	121	-3.3772
2564	24.993	19.578	123	-3.3908
2566	24.995	19.587	125	-3.5439
2568	24.994	19.582	127	-3.4686
2569	24.996	19.592	129	-3.6559
2572	24.995	19.589	131	-3.5884
2574	24.996	19.594	133	-3.684
2576	24.998	19.601	135	-3.8546
2578	24.998	19.601	137	-3.8371
2580	24.999	19.605	139	-3.9546
2582	25	19.611	141	-4.1389
2584	25.002	19.62	143	-4.4843
2586	25.002	19.622	145	-4.6025
2588	25.001	19.618	147	-4.3856
2590	25.002	19.623	149	-4.641
2592	25.003	19.623	151	-4.65
2594	25.003	19.625	153	-4.7365
2596	25.002	19.619	155	-4.4301
2596	25.004	19.631	156	-5.2116
2599	25.003	19.627	158	-4.8805
2601	25.003	19.627	160	-4.8698
2603	25.003	19.627	162	-4.8586
2605	25.004	19.631	164	-5.1669
2607	25.004	19.632	166	-5.3342
2609	25.005	19.638	168	-6.1878
2611	25.004	19.631	170	-5.2196
2613	25.003	19.624	172	-4.7042
2615	25.002	19.621	174	-4.511
2617	25.003	19.628	176	-4.9377
2619	25.002	19.619	178	-4.455
2621	25.003	19.624	180	-4.6947
2623	25.004	19.632	183	-5.3086
2625	25.005	19.634	185	-5.5686
2627	25.003	19.625	187	-4.7321
2629	25.003	19.624	189	-4.6994
2631	25.005	19.634	191	-5.5462
2633	25.004	19.63	193	-5.1168

Table D.7: *VTI-SA Analyzer Silica Gel Mass vs. Time at 25°C 60-70%RH*

Time Stamp [min]	Weight [mg]	Weight Change [%]	Time Elapsed [min]	$ln(1-\frac{m_t}{m_f})$
2800	24.959	19.414	0	0
2801	24.971	19.472	1	-0.0743
2802	24.984	19.535	2	-0.1598
2803	24.995	19.589	3	-0.2408
2804	25.01	19.659	4	-0.3556
2805	25.021	19.711	5	-0.4494
2806	25.032	19.767	6	-0.5625
2807	25.044	19.82	7	-0.6836
2808	25.053	19.863	8	-0.792
2809	25.061	19.903	9	-0.9079
2810	25.07	19.945	10	-1.042
2811	25.078	19.986	11	-1.1946
2812	25.084	20.011	12	-1.3029
2813	25.09	20.044	13	-1.4589
2814	25.095	20.066	14	-1.5805
2815	25.099	20.086	15	-1.7093
2816	25.105	20.111	16	-1.8977

D.7 – continued from previous page

Time Stamp [min]	Weight [mg]	Weight Change [%]	Time Elapsed [min]	$ln(1-\frac{m_t}{m_f})$
2818	25.112	20.147	18	-2.2435
2820	25.115	20.162	20	-2.4202
2821	25.119	20.179	21	-2.6925
2823	25.123	20.198	23	-3.1254
2824	25.126	20.213	24	-3.6482
2827	25.125	20.211	26	-3.5522
2827	25.128	20.226	27	-4.5946
2830	25.129	20.228	29	-4.8952
2832	25.128	20.225	31	-4.4774
2834	25.128	20.222	34	-4.1887
2836	25.128	20.224	36	-4.3337
2838	25.127	20.217	38	-3.8406
2841	25.126	20.216	40	-3.7882
2843	25.126	20.216	42	-3.801
2845	25.124	20.207	44	-3.384
2845	25.127	20.218	45	-3.8921
2846	25.124	20.203	46	-3.2504
2849	25.124	20.205	48	-3.3282
2851	25.123	20.199	50	-3.141

Table D.8: *VTI-SA Analyzer Silica Gel Mass vs. Time at 25°C 70-80%RH*

Time Stamp [min]	Weight [mg]	Weight Change [%]	Time Elapsed [min]	$ln(1-\frac{m_t}{m_f})$
3161	25.142	20.292	0	0
3161	25.144	20.302	1	-0.022
3162	25.151	20.334	2	-0.093
3163	25.158	20.368	3	-0.1762
3164	25.166	20.404	4	-0.2708
3165	25.17	20.425	5	-0.3314
3166	25.175	20.448	6	-0.4011
3167	25.181	20.476	7	-0.492
3168	25.186	20.5	8	-0.5786
3169	25.192	20.532	9	-0.7067
3171	25.197	20.554	11	-0.8073
3172	25.204	20.588	12	-0.9811
3173	25.207	20.602	13	-1.0654
3175	25.21	20.618	15	-1.1712
3177	25.214	20.634	17	-1.282
3179	25.216	20.646	19	-1.385
3180	25.219	20.661	20	-1.5165
3183	25.219	20.659	22	-1.4982
3184	25.223	20.681	24	-1.7268
3187	25.222	20.672	26	-1.6234
3189	25.223	20.679	28	-1.7044
3191	25.224	20.684	30	-1.7665
3193	25.223	20.679	32	-1.7071
3195	25.224	20.685	34	-1.7794
3196	25.227	20.695	36	-1.9162
3198	25.228	20.703	38	-2.0301
3200	25.226	20.693	40	-1.8879
3203	25.228	20.701	42	-1.996
3205	25.228	20.701	44	-2.0073
3207	25.229	20.705	46	-2.0668
3209	25.228	20.702	48	-2.025
3211	25.229	20.709	50	-2.13
3213	25.229	20.706	52	-2.0775
3214	25.232	20.72	54	-2.3477
3215	25.238	20.751	55	-3.5581
3217	25.231	20.716	57	-2.2665

Table D.9: *VTI-SA Analyzer Silica Gel Mass vs. Time at 25°C 80-90%RH*

Time Stamp [min]	Weight [mg]	Weight Change [%]	Time Elapsed [min]	$ln(1-\frac{m_t}{m_f})$
3520	25.253	20.821	0	0
3522	25.252	20.819	2	0.0252

D.9 – continued from previous page

Time Stamp [min]	Weight [mg]	Weight Change [%]	Time Elapsed [min]	$ln(1-\frac{m_t}{m_f})$
3523	25.256	20.834	3	-0.1814
3524	25.259	20.849	4	-0.4312
3527	25.259	20.851	6	-0.4682
3527	25.261	20.862	7	-0.7079
3528	25.265	20.879	8	-1.267
3530	25.266	20.885	10	-1.5285
3532	25.269	20.898	12	-3.0351
3535	25.269	20.897	14	-2.7681
3537	25.268	20.893	16	-2.156
3539	25.269	20.896	18	-2.5825
3541	25.268	20.892	21	-2.0364
3543	25.266	20.886	23	-1.6332
3544	25.269	20.897	24	-2.799
3546	25.268	20.893	26	-2.2077
3549	25.269	20.898	28	-2.9939
3550	25.267	20.887	30	-1.6588
3552	25.266	20.886	32	-1.5987
3555	25.266	20.884	34	-1.4711
3557	25.267	20.887	36	-1.6797
3559	25.267	20.889	38	-1.8205
3561	25.267	20.89	40	-1.9089
3563	25.267	20.888	42	-1.7393
3565	25.266	20.886	44	-1.6229
3567	25.267	20.89	46	-1.9157
3569	25.267	20.886	48	-1.6384
3571	25.268	20.893	50	-2.1226
3573	25.267	20.89	52	-1.8961
3574	25.264	20.876	54	-1.1336
3576	25.266	20.886	56	-1.5937
3578	25.267	20.888	58	-1.7502
3580	25.265	20.878	60	-1.2063
3582	25.264	20.873	62	-1.0212
3583	25.267	20.887	63	-1.6535
3585	25.267	20.889	65	-1.8267

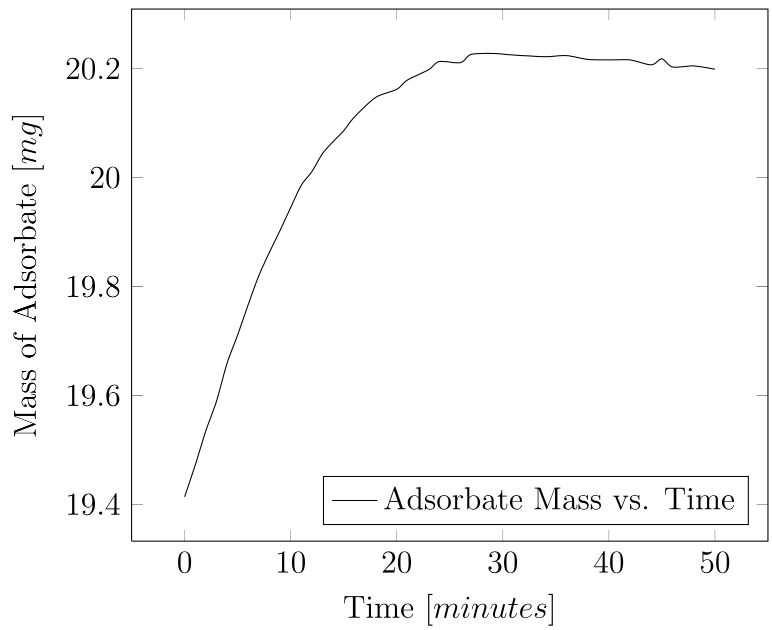

(a) *Mass vs. Time*

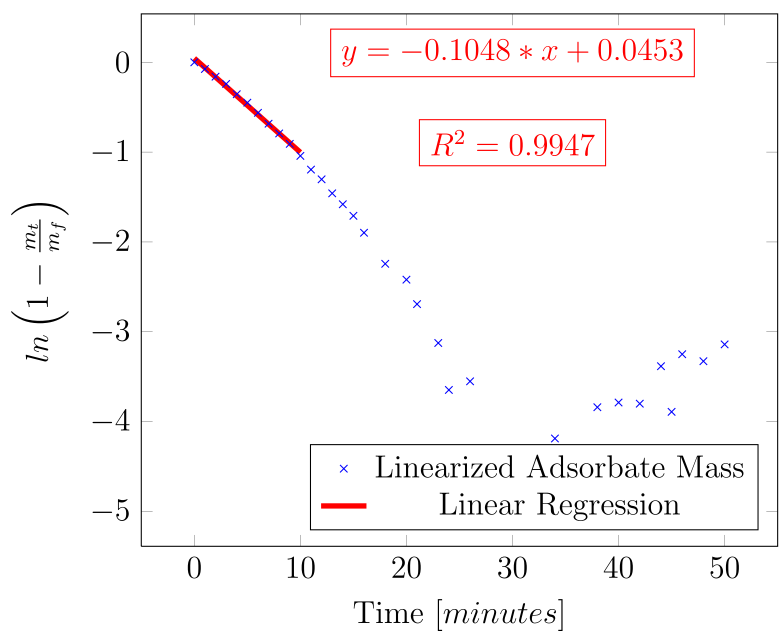

(b) *Linearized Mass vs. Time*

Figure D.7: *Adsorbate Mass vs. Time for Increment of Relative Humidity from 60% to 70%*

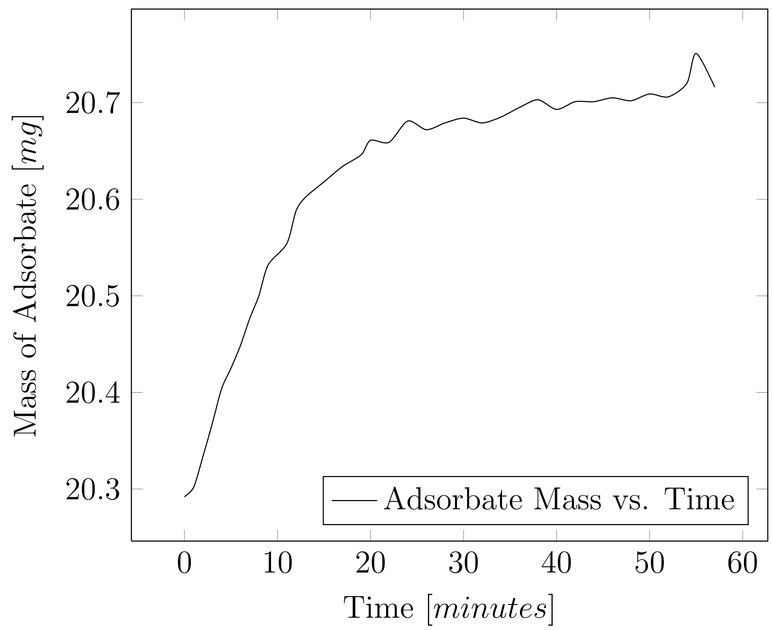

(a) *Mass vs. Time*

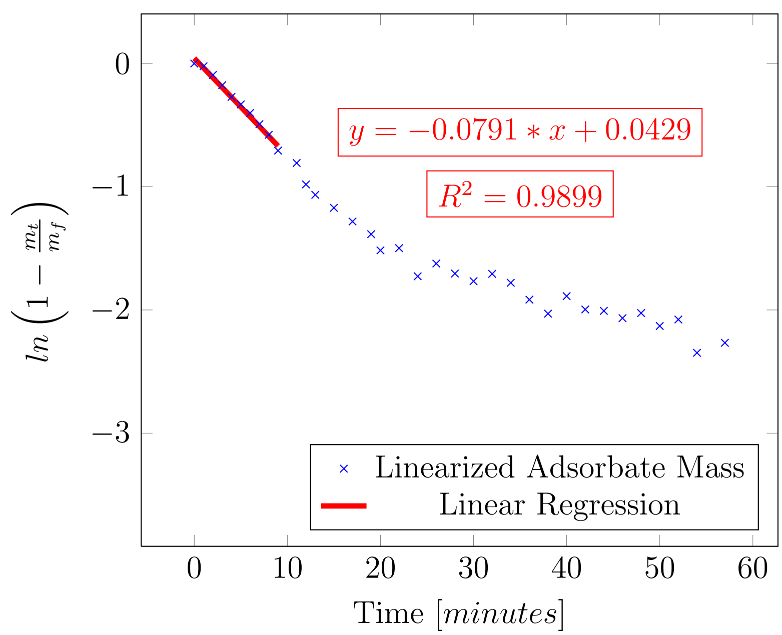

(b) *Linearized Mass vs. Time*

Figure D.8: *Adsorbate Mass vs. Time for Increment of Relative Humidity from 70% to 80%*

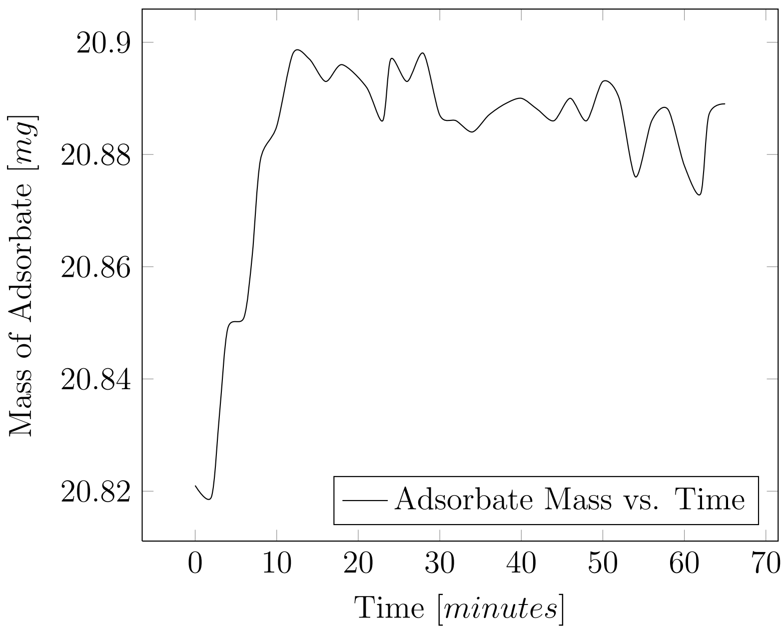

(a) *Mass vs. Time*

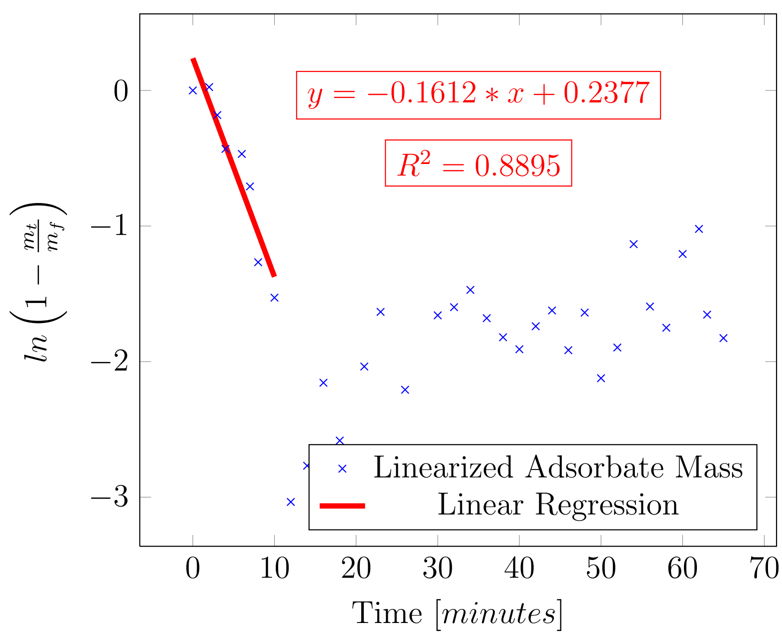

(b) *Linearized Mass vs. Time*

Figure D.9: *Adsorbate Mass vs. Time for Increment of Relative Humidity from 80% to 90%*

E

Appendix E: Solidworks CAD Drawings

This section contains the 2D drawing files used for guiding the laser are included for all parts of the diffusion-sorption apparatus.

- Solidworks 2D CAD drawings used in Versa Laser Cutter

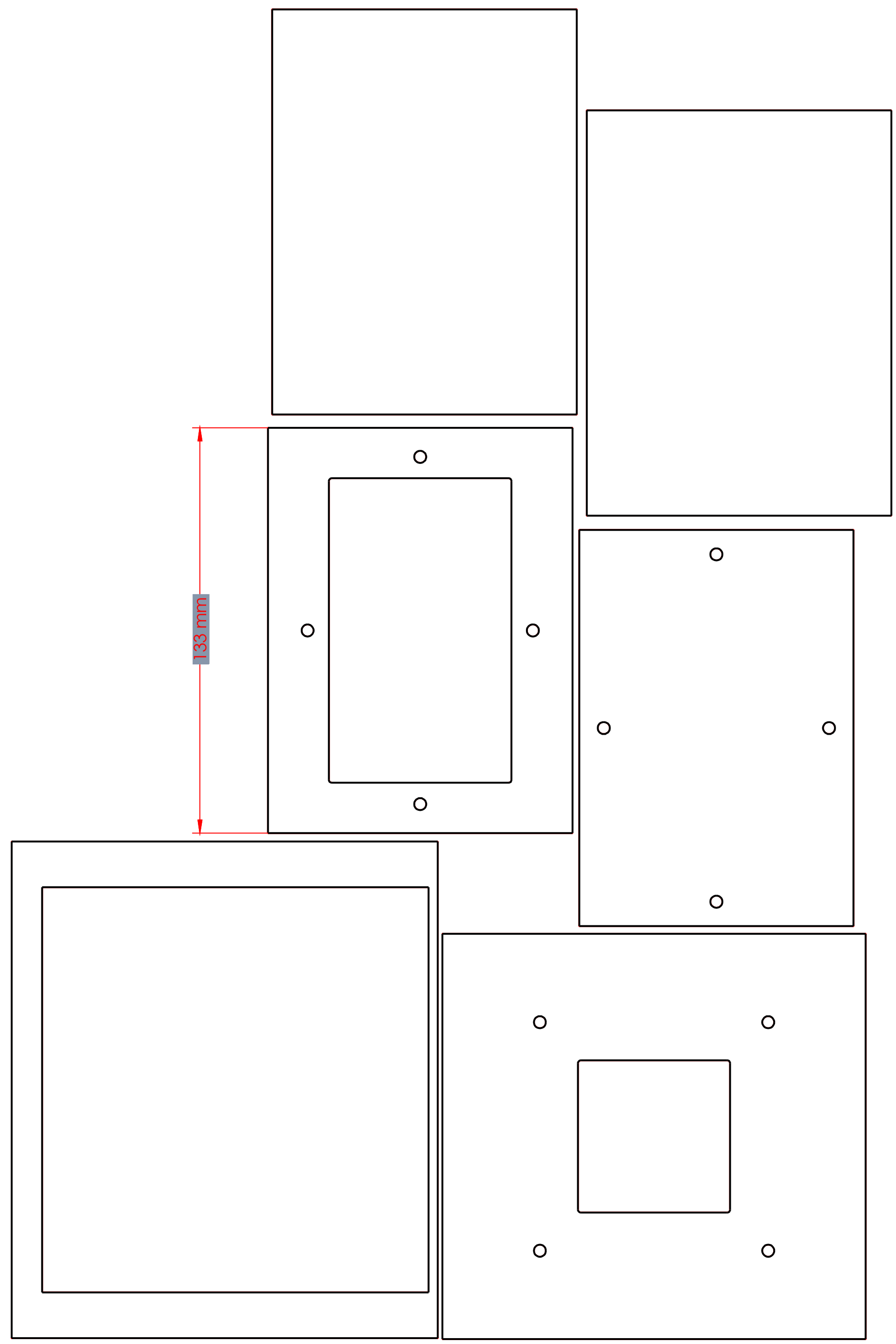

Bottom Chamber Drawing

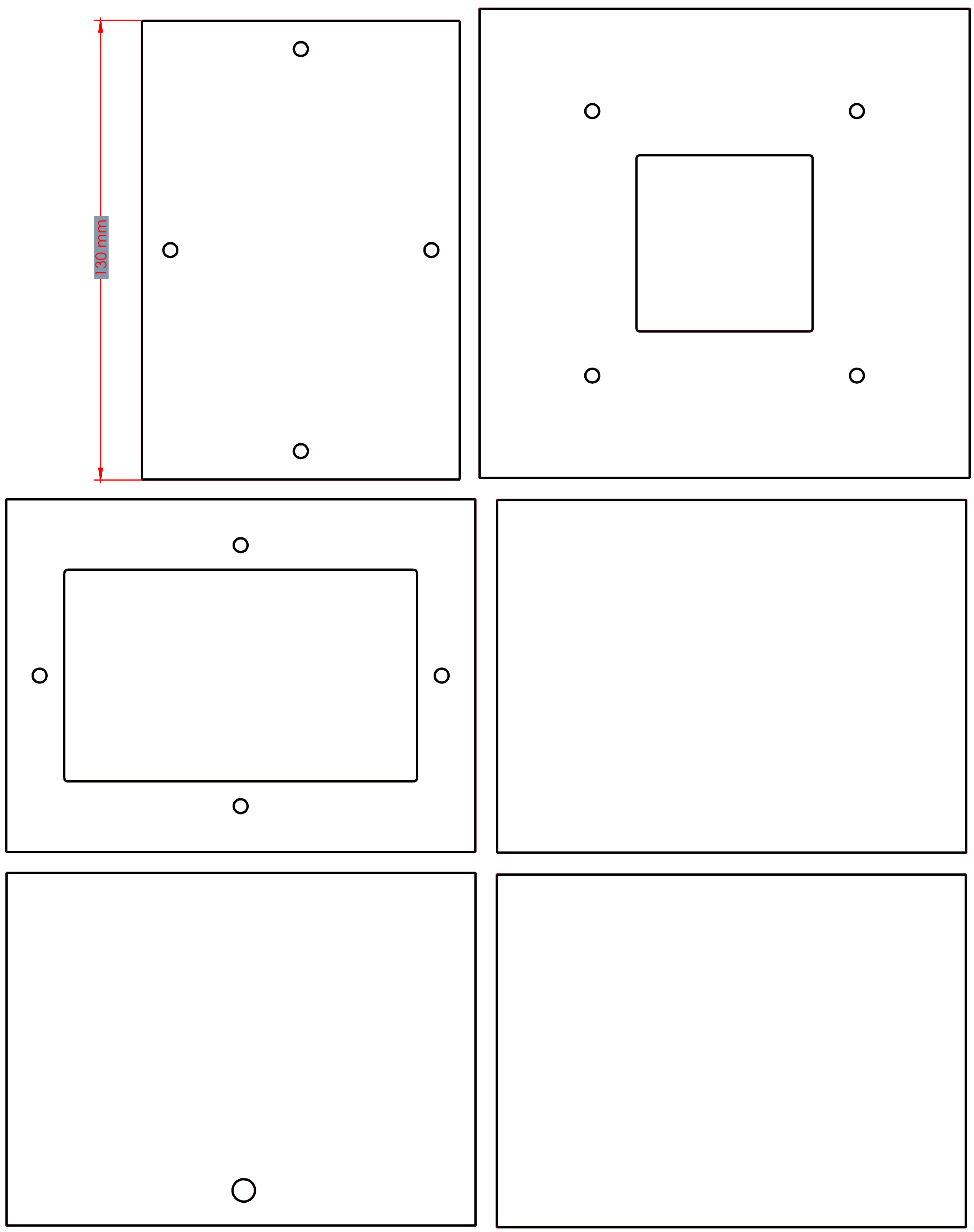

Top Chamber Drawing

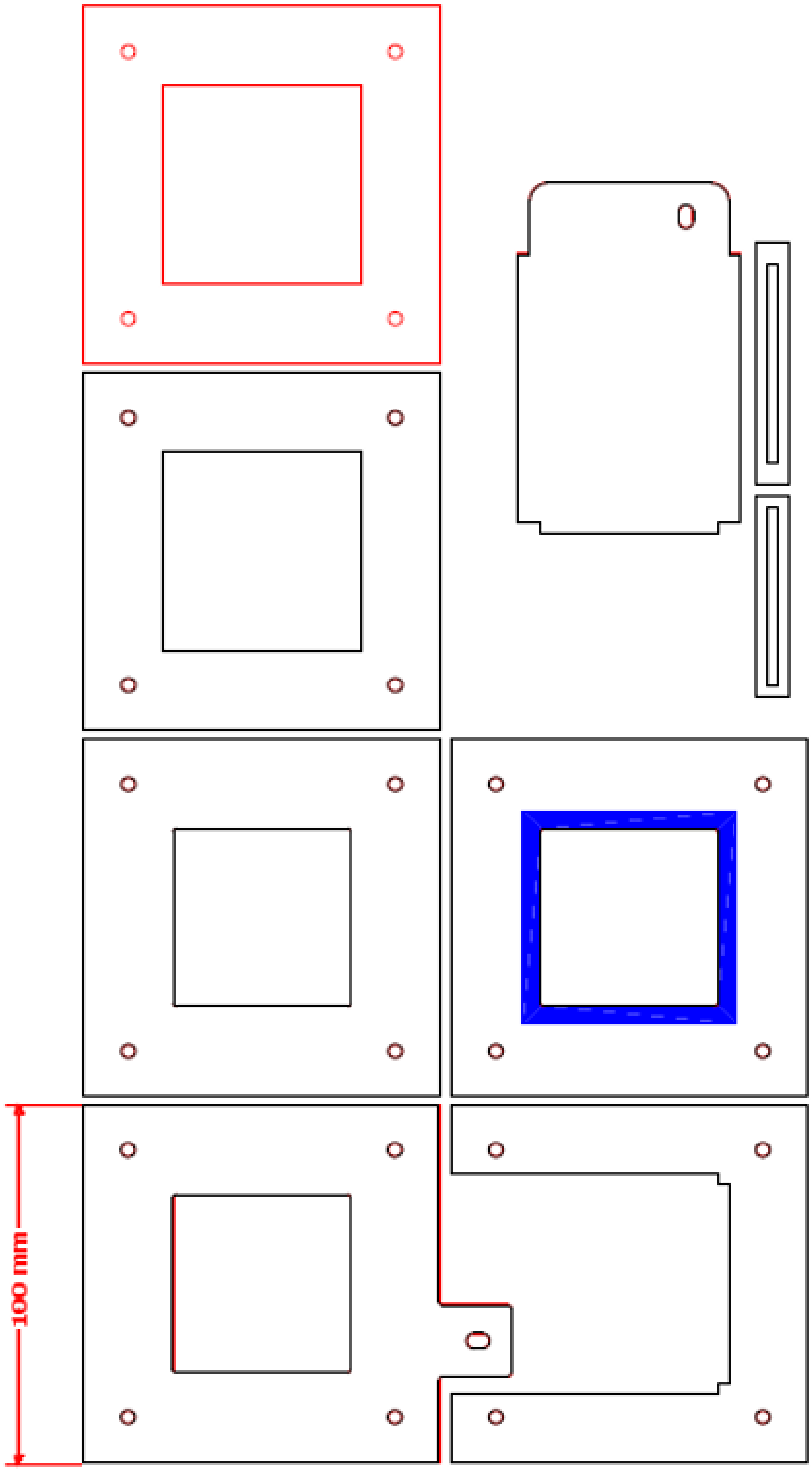

Manual Sliding Door Drawing

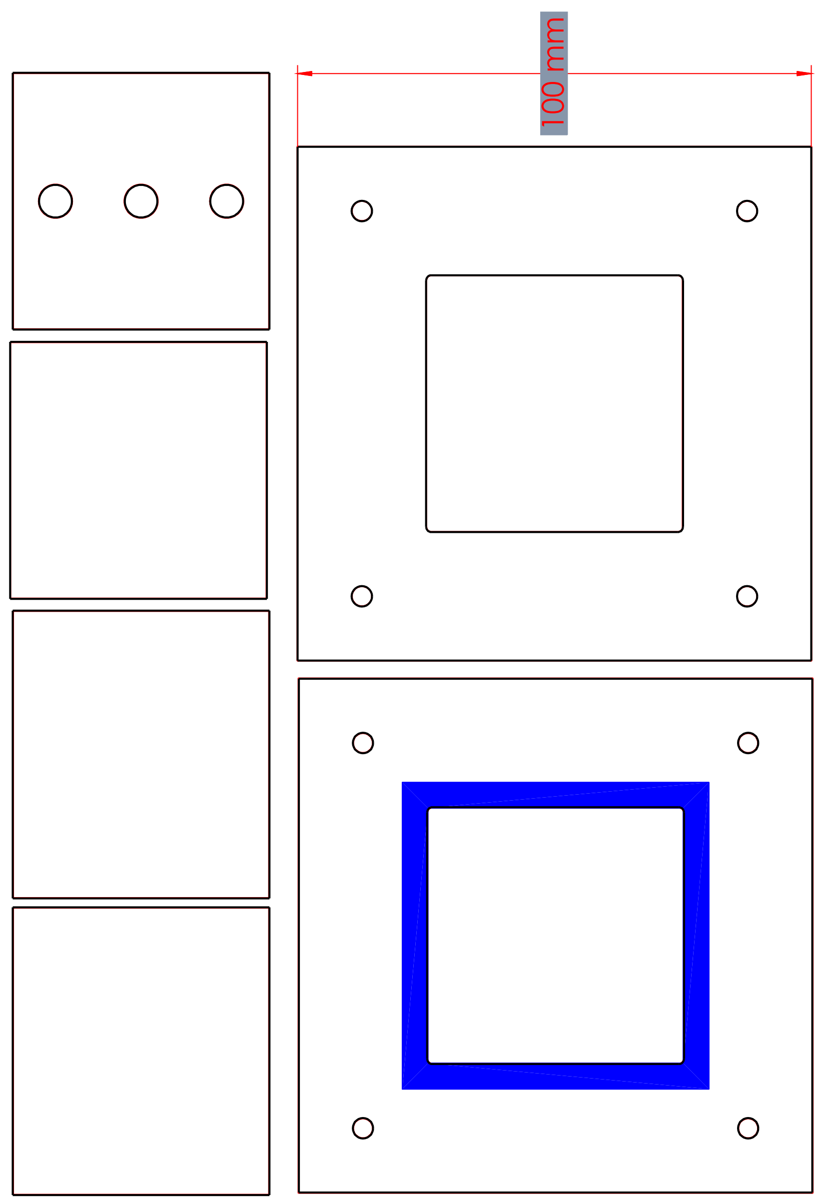

Porous Media Channel Drawing

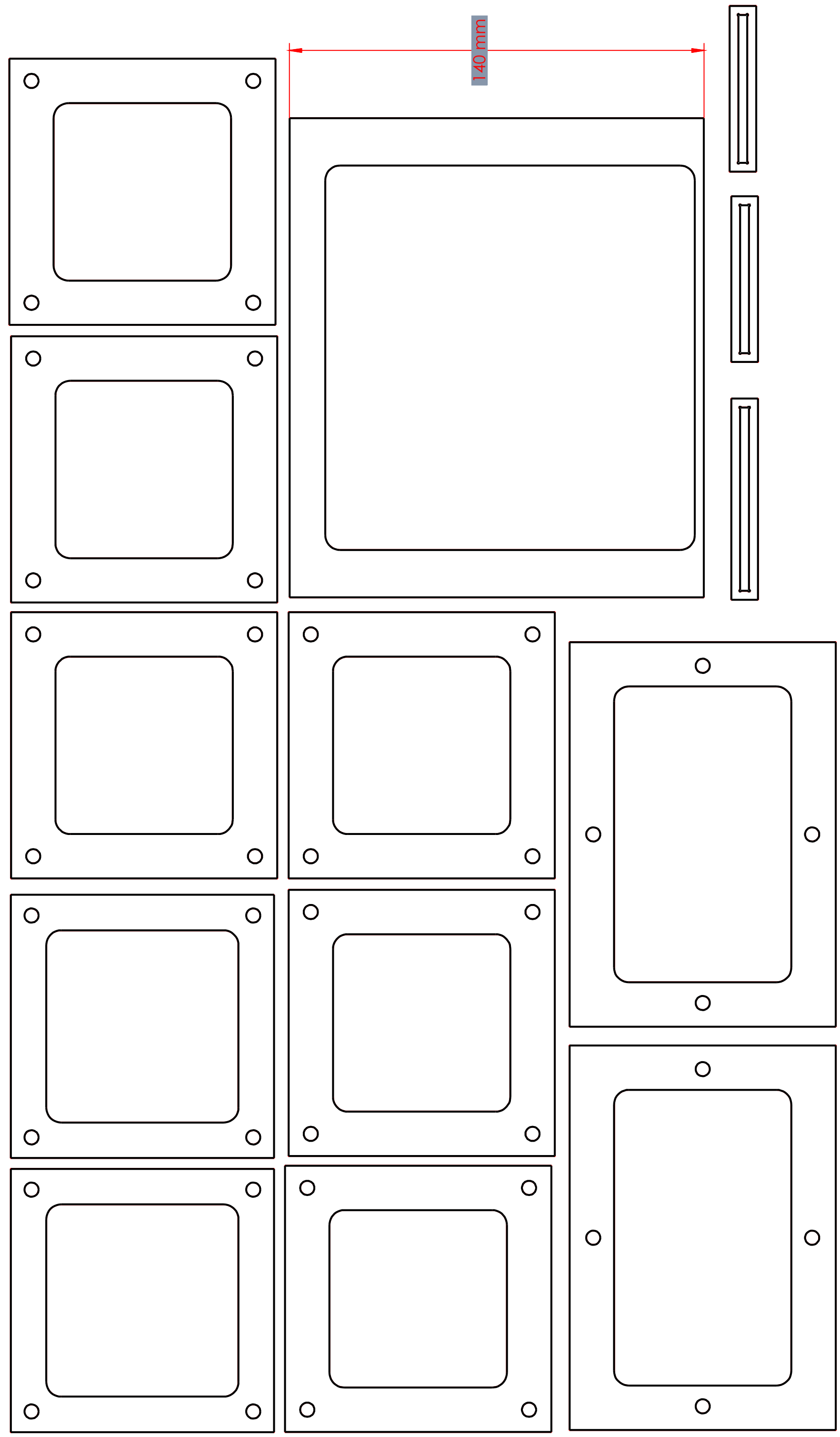
140 mm

F

Appendix F: Sensor Calibration

This section contains the calibration data for each Sensirion SHT˜75 Relative Humidity and Temperature sensor.

- Measured Temperatures and Relative Humidity Values
- Steady state plots for all sensors, for each flask ingredient showing that equilibrium had been reached.

Flask Contents	RH at 25°C	T1	T2	T3	T4	T5	T6	T7
Dessicated	0	25.345	25.253	25.436	25.409	25.171	25.458	25.401
Lithium Chloride	11.30 ± 0.27	25.246	25.255	25.448	25.332	25.172	25.466	25.368
Potassium Carbonate	43.16 ± 0.39	25.400	25.241	25.455	25.390	25.205	25.526	25.417
Sodium Chloride	75.29 ± 0.12	25.505	25.485	25.579	25.534	25.493	25.598	25.545
Pure Distilled Water	100	25.776	25.258	25.472	25.288	25.129	25.591	25.534

Table F.1: *Averaged Temperatures During Calibration*

Flask Contents	RH at 25°C	RH1	RH2	RH3	RH4	RH5	RH6	RH7
Dessicated	0	0.171	0.305	0.732	-0.277	0.451	0.866	1.520
Lithium Chloride	11.30 ± 0.27	14.188	13.863	14.280	13.282	13.636	14.444	14.388
Potassium Carbonate	43.16 ± 0.39	45.922	45.677	45.877	44.808	45.193	45.721	44.808
Sodium Chloride	75.29 ± 0.12	73.976	73.738	74.419	73.529	73.455	74.279	73.383
Pure Distilled Water	100	97.455	100.197	99.433	98.315	99.756	98.064	97.368

Table F.2: *Averaged Relative Humidities During Calibration*

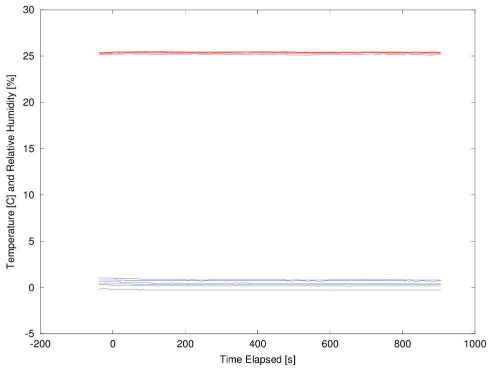

(a) *Zero RH (Dessicated)*

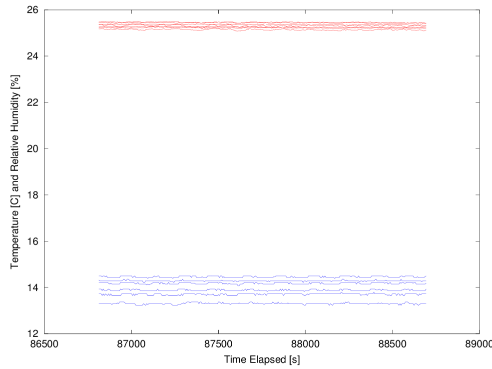

(b) *Lithium Chloride*

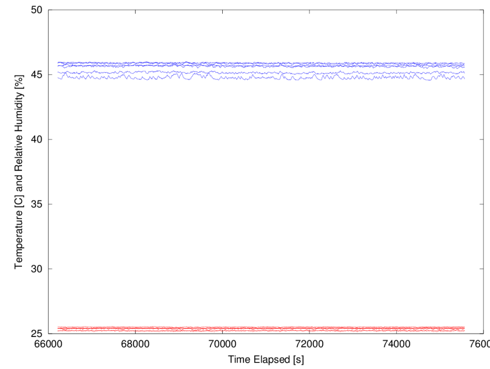

(c) *Potassium Carbonate*

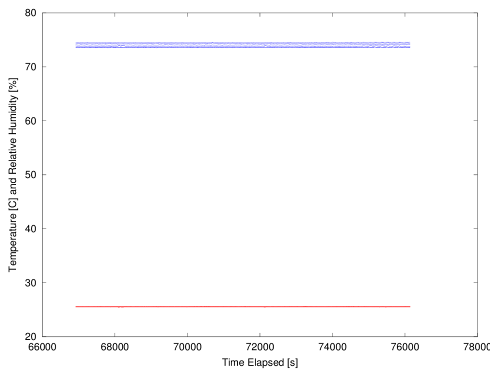

(d) *Sodium Chloride*

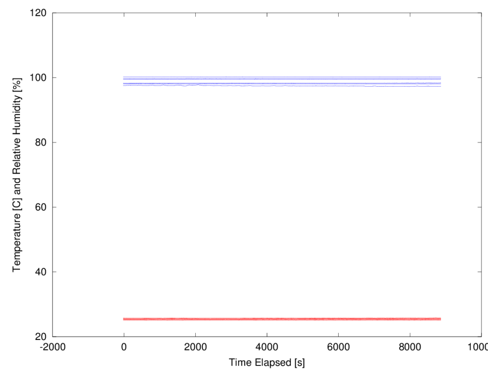

(e) *Pure Distilled Water*

Figure F.1: *Plots of Temperature and Relative Humidity for each flask contents and all sensors Red: Temperature, Blue: Relative Humidity*

G

Appendix G: Mathematical Derivations

This section contains any mathematical derivations used in the main thesis.

- Density of water vapour in air using CIPM-2007 method of Picard et al. [54]
- Comparitive method by Lowe and Ficke [61] to calculate Saturation Pressure of Water Vapour in Air.
- An Error analysis on the Sensirion SHT-75 Relative Humidity and Temperature Sensors using method of Lowe and Ficke [61].

Calculation of mass concentration of water vapour in air given T,P, and RH.
Reference: Picard et al. doi:10.1088/0026-1394/45/2/004
This method is applicable in the range of 600 hPa to 1100 hPa, and 15 C to 27 C.

Defining Coefficients:

$a\_0 := 1.58123 \cdot 10^{-6} \, \frac{K}{Pa}$

$a\_1 := -2.9331 \cdot 10^{-8} \, \frac{1}{Pa}$

$a\_2 := 1.1043 \cdot 10^{-10} \, \frac{1}{K \cdot Pa}$

$b\_0 := 5.707 \cdot 10^{-6} \, \frac{K}{Pa}$

$b\_1 := -2.051 \cdot 10^{-8} \, \frac{1}{Pa}$

$c\_0 := 1.9898 \cdot 10^{-4} \, \frac{K}{Pa}$

$c\_1 := -2.376 \cdot 10^{-6} \, \frac{1}{Pa}$

$d := 1.83 \cdot 10^{-11} \, \frac{K^2}{Pa^2}$

$e\_c := -0.765 \cdot 10^{-8} \, \frac{K^2}{Pa^2}$

$A := 1.2378847 \cdot 10^{-5} \, \frac{1}{K^2}$

$B := -1.9121316 \cdot 10^{-2} \, \frac{1}{K}$

$C := 33.93711047$

$D := -6.3431645 \cdot 10^{3} \, K$

$alpha := 1.00062$

$beta := 3.14 \cdot 10^{-8} \, \frac{1}{Pa}$

$gamma := 5.6 \cdot 10^{-7}$

Define the Pressure (Pa), Temperature (K), and RH (0<RH<1) of moist air:

$P := 101325 \, Pa$

$T\_c := 25$

$T := (T\_c) \, °C \qquad T = 298.15 \, K$

$RH := 1$

The partial pressure is:

$p\_v := 1 \, Pa \cdot e^{\left(A \cdot T^2 + B \cdot T + C + \frac{D}{T}\right)} \qquad p\_v = \left(3.17 \cdot 10^{3}\right) Pa$

The Enhancement Factor f is:

$f := alpha + beta \cdot P + gamma \cdot (T\_c)^2 \qquad f = 1.004$

Mole fraction of vapour x_v:

$$x\_v := RH \cdot f \cdot \frac{p\_v}{P} \qquad x\_v = 0.031$$

Compressibility Factor Z:

$$Z := 1 - \frac{P}{T}\left(a\_0 + a\_1 \cdot T + a\_2 \cdot T^2 + (b\_0 + b\_1 \cdot T) \cdot x\_v + (c\_0 + c\_1 \cdot T) \cdot x\_v^2\right) + \frac{P^2}{T^2}\left(d + e\_c \cdot x\_v^2\right)$$

$$Z = 0.999$$

Total Density of humid air:

$$M\_v := 18.01528 \ \frac{gm}{mol} \qquad M\_a := 28.96546 \ \frac{gm}{mol}$$

$$R\_u := 8.314472 \ \frac{J}{mol \cdot K}$$

$$rho\_air := P \cdot \frac{M\_a}{Z \cdot R\_u \cdot T}\left(1 - x\_v \cdot \left(1 - \frac{M\_v}{M\_a}\right)\right) \qquad rho\_air = 1.171 \ \frac{kg}{m^3}$$

Mass Concentration rho_vap:

$$rho\_vap := \frac{M\_v \cdot P}{R\_u \cdot T} \cdot x\_v \qquad rho\_vap = 23.131 \ \frac{gm}{m^3}$$

Alternately, using the ideal gas law assuming Z = 1:

$$rho\_vapideal := M\_v \cdot \frac{p\_v}{R\_u \cdot T} \qquad rho\_vapideal = 23.035 \ \frac{gm}{m^3}$$

$$PercentError := \frac{(rho\_vap - rho\_vapideal)}{rho\_vap} \cdot 100 \qquad PercentError = 0.413$$

A calculation for the concentration of water vapour given temperature and relative humidity:
Reference: Lowe and Ficke 1974. - The computation of saturation vapour pressure

The constants that are known:

$M_{H2O} := 18.0153 \, \frac{gm}{mol}$

$R_u := 8.314 \, \frac{m^3 \, Pa}{K \cdot mol}$

$mbar := Pa \cdot 100$

Under the given conditions:

$T := 25$

$T_K := T \, °C$

$T_K = 298.15 \, K$

$RH := 100\%$

The partial pressure of water vapour at a given temperature by Lowe et al. Corresponds to a relative humidity of 100% at the given temperature:

Where the constants ai are given as:

$a_0 := 6.107799961$

$a_1 := 4.436518521 \cdot 10^{-1}$

$a_2 := 1.428945805 \cdot 10^{-2}$

$a_3 := 2.650648471 \cdot 10^{-4}$

$a_4 := 3.031240396 \cdot 10^{-6}$

$a_5 := 2.034080948 \cdot 10^{-8}$

$a_6 := 6.136820929 \cdot 10^{-11}$

Lowe's equation for partial pressure of water vapour:

$$e(T) := \left(a_0 + T \cdot \left(a_1 + T \cdot \left(a_2 + T \cdot \left(a_3 + T \cdot \left(a_4 + T \cdot \left(a_5 + T \cdot a_6\right)\right)\right)\right)\right)\right) \, mbar$$

The concentration of water vapour may be found from the ideal gas law and the partial pressure of water vapour for a given relative humidity and temperature:

$$Concentration(RH, e) := e \cdot RH \cdot \frac{M_{H2O}}{R_u \cdot T_K}$$

The partial pressure and thus the concentration may be found, seen in the solution below:

$$eval := e(T) = \left(3.167 \cdot 10^3\right) \, Pa$$

$$Concentration(RH, eval) = 23.016 \, \frac{gm}{m^3}$$

An estimate of the error propogation may be made using the error in the temperature and relative humidity sensors (Sensiron model SHT-75) taken from the 2011 datasheet:

$$ErrorT := 0.3\ K$$
$$ErrorRH := 1.8\%$$

The derivative of the vapour pressure with respect to temperature may be explicitly stated as:

$$manuale.DT(T) := \left(a_1 + 2 \cdot T \cdot a_2 + 3 \cdot T^2 \cdot a_3 + 4 \cdot T^3 \cdot a_4 + 5 \cdot T^4 \cdot a_5 + 6 \cdot T^5 \cdot a_6\right) \frac{mbar}{K}$$

$$manuale.DT(T) = 188.79\ \frac{Pa}{K}$$

Or implicitly defined using MathCAD:

$$Pvap.DT := \frac{d}{dT} e(T)\ \frac{1}{\Delta°C} = 188.79\ \frac{kg}{m \cdot s^2 \cdot K}$$

The error in the vapour pressure may be taken as:

$$ErrorVap := \sqrt{Pvap.DT^2 \cdot ErrorT^2} = 56.637\ Pa$$

The partial derivatives with respect to Temperature, Relative Humidity, and vapour pressure may be solved explicitly and implicitly with MathCAD:

$$Conc.DRH := \frac{d}{dRH} Concentration(RH, eval) = 23.016\ \frac{gm}{m^3}$$

$$Conc.DRH.explicit := eval \cdot \frac{M_{H2O}}{R_u \cdot T_K} = 23.016\ \frac{gm}{m^3}$$

$$Conc.De := RH \cdot \frac{M_{H2O}}{R_u \cdot T_K} = \left(7.268 \cdot 10^{-6}\right)\ \frac{s^2}{m^2}$$

$$Conc.DT := \frac{Pvap.DT \cdot RH \cdot \frac{M_{H2O}}{R_u} \cdot T_K - eval \cdot RH \cdot \frac{M_{H2O}}{R_u}}{T_K^{\,2}} = 0.001\ \frac{kg}{m^3 \cdot K}$$

The partial derivatives and errors may be combined to find the total propogated error in the concentration using the SHT75 sensors:

$$ErrorConc := \sqrt{\left(Conc.DT^2 \cdot ErrorT^2\right) + \left(Conc.DRH^2 \cdot ErrorRH^2\right) + \left(Conc.De^2 \cdot ErrorVap^2\right)}$$

$$ErrorConc = 0.701\ \frac{gm}{m^3}$$

H

Appendix H: Sensitivity Study

This section contains the plots from the sensitivity study created using COMSOL and custom MATLAB code.

- ► Plots for Input Parameters

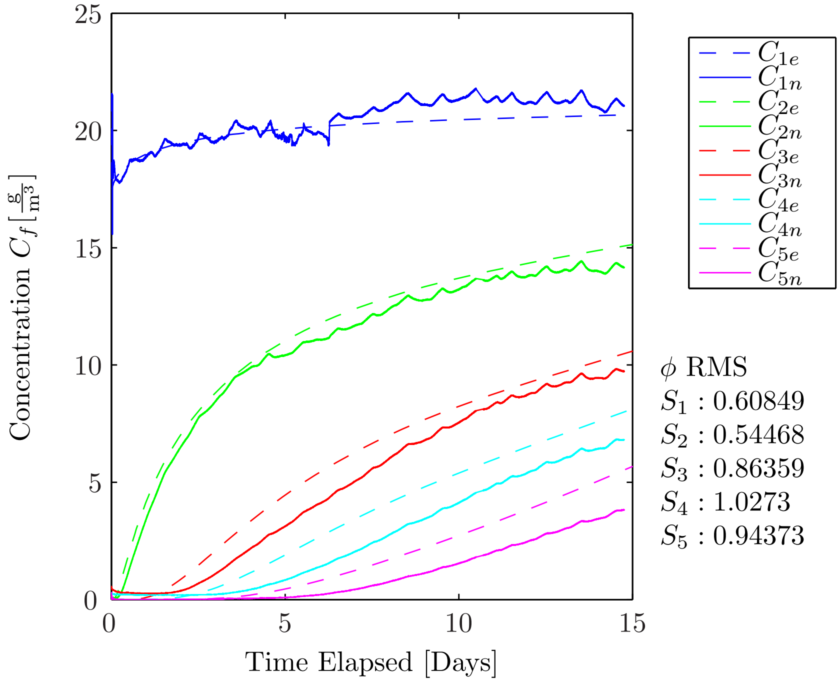

(a) *Porosity* $\phi = 0.672$

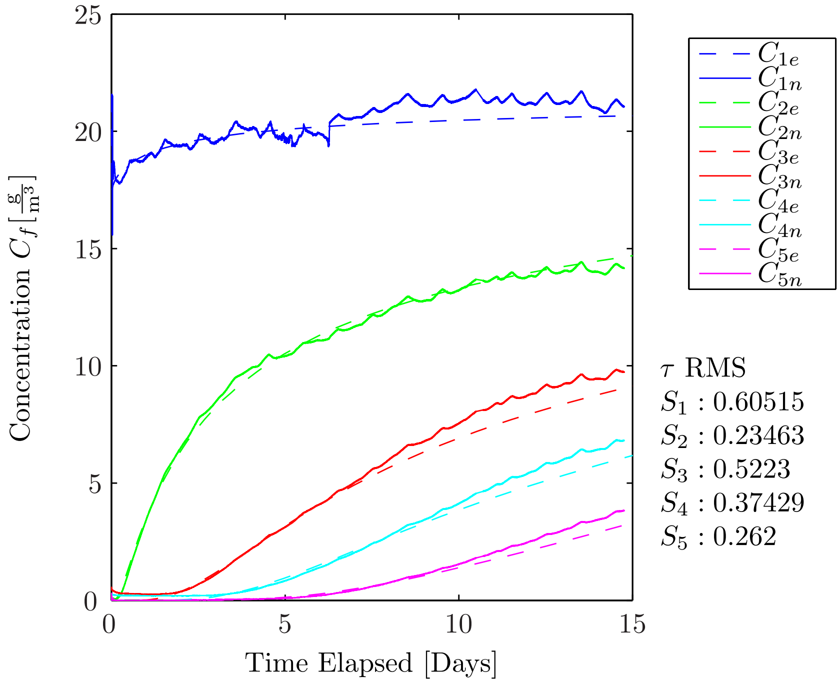

(b) *Tortuosity* $\tau = 2.18$

Figure H.1: *Sensitivity Study for all Sensors (s) 3 compared to Trial (t) 1*

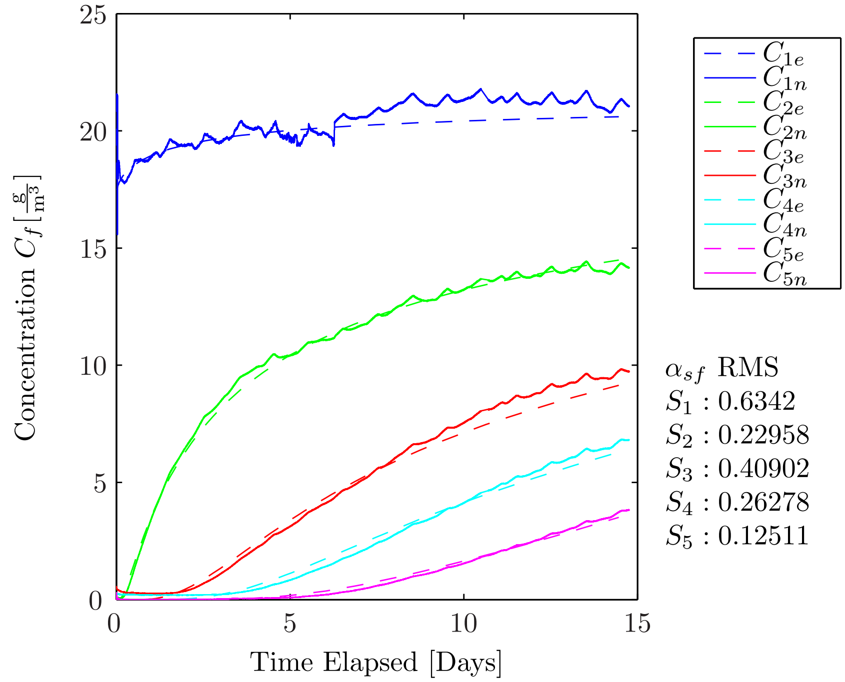

(c) *Mass Transfer Coefficient* $\alpha_{sf} = 0.0079 \times e^{0.0344*\mathrm{RH}}$

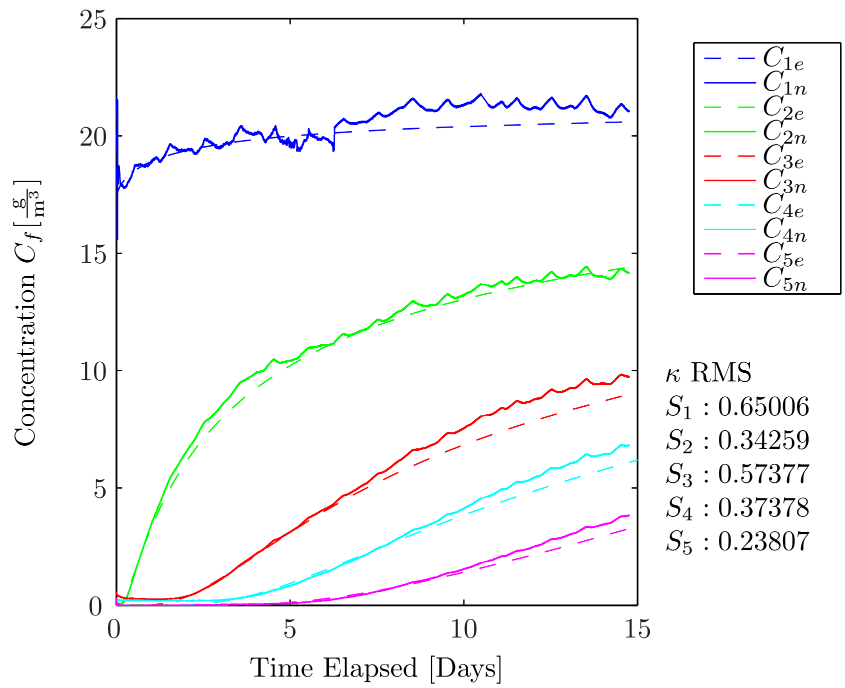

(d) *Langmuir Coeff.* $\kappa = 97.6$

Figure H.1: *Sensitivity Study for all Sensors (s) 3 compared to Trial (t) 1*

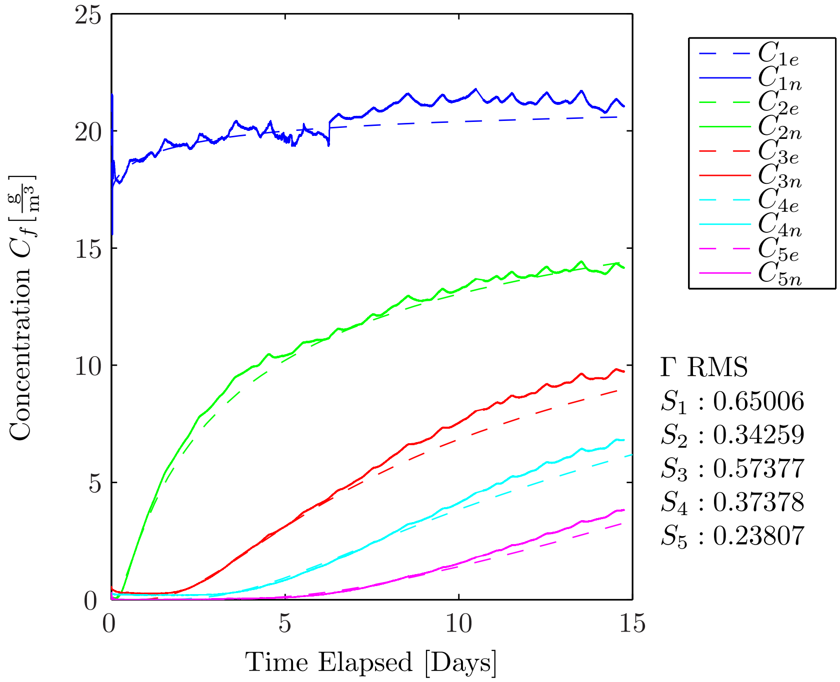

(e) *Langmuir Coeff.* $\Gamma = 0.468$

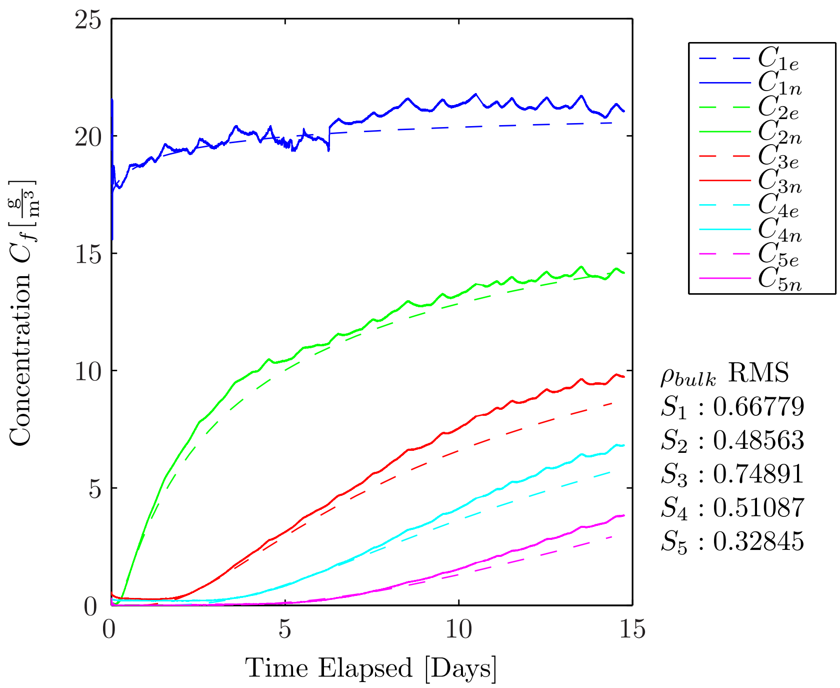

(f) *Bulk Density* $\rho_{bulk} = 0.906$

Figure H.1: *Sensitivity Study for all Sensors (s) 3 compared to Trial (t) 1*

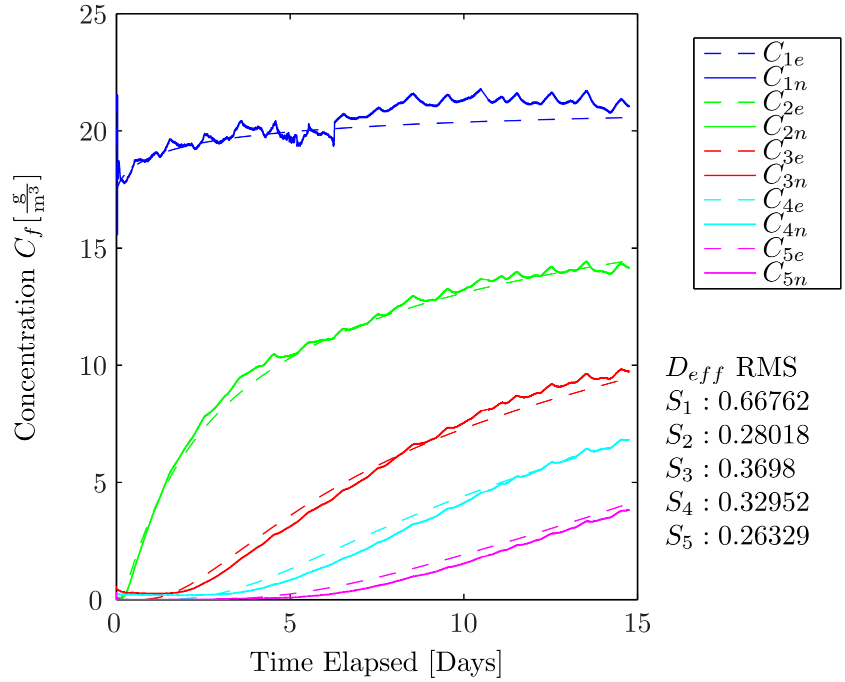

(g) *Effective Diffusion Coeff.* $D_{eff} = 8.594E - 2$

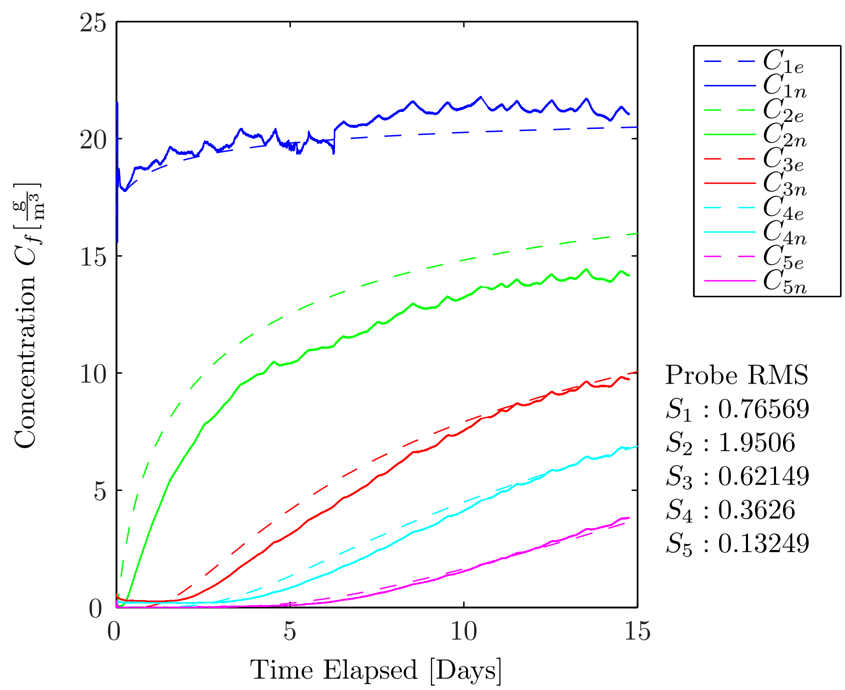

(h) *Probe Location* $y_{probe} = y_{probe} \times 1.1$

Figure H.1: *Sensitivity Study for all Sensors (s) 3 compared to Trial (t) 1*